A Formulation of Multidimensional Growth Models for the Assessment and Forecast of Technology Attributes

A Thesis
Presented to
The Academic Faculty

by

Travis W. Danner

In Partial Fulfillment
of the Requirements for the Degree
Doctor of Philosophy

School of Aerospace Engineering
Georgia Institute of Technology
August, 2006

A Formulation of Multidimensional Growth Models for the Assessment and Forecast of Technology Attributes

Approved by:

Professor Dimitri Mavris
Committee Chair
School of Aerospace Engineering
Georgia Institute of Technology

Professor Alan Porter
School of Industrial and
Systems Engineering
Georgia Institute of Technology

Professor Daniel Schrage
School of Aerospace Engineering
Georgia Institute of Technology

Dr. Michelle Kirby
School of Aerospace Engineering
Georgia Institute of Technology

Dr. Gary Seng
Aeronautics Division
NASA Glenn Research Center

Date Approved: 05 July 2006

Dedicated to

Biederman.

ACKNOWLEDGMENTS

After years of thinking about propulsion technology development and in recent months thinking of little else, it is an effort—though a pleasant one—to remember the world that extends beyond this document and its development. As I think of the many people, books, and experiences that have influenced my thinking over the years, I am conscious of numerous contributions and numerous debts. I realize that there are many contributions—recent and long ago, direct and indirect—that either escape my memory or my ability to understand and express them. Yet I am grateful for the good they and their bearers have brought to me and to my work.

Professor Dimitri Mavris first suggested to me the need for a quantitative method for assessing the technology potential of complex systems and forecasting their potential development. I am grateful to him for encouraging me to develop such a model and for advising that work. I am also grateful for a highly knowledgeable and energetic dissertation committee. I am grateful to Professors Daniel Schrage and Alan Porter for their suggested improvements to my discussions and demonstration that have strengthened my arguments. Dr. Michelle Kirby has offered countless suggestions over the years as her door has always been open. Dr. Gary Seng of the NASA Glenn Research Center graciously agreed to participate in the project despite the distance involved, and I particularly appreciated his perspective regarding the practical application of multidimensional growth models.

Thanks go to all my colleagues and friends at the Aerospace Systems Design Laboratory: including Jimmy Tai, Jorge de Luis, Tom Ender, Rob McDonald, Brian German, Andrew Frits, and many others. Few questions, small or great, go unanswered for very long around here. In particular, thank you, Andrew Frits, for your

feedback on my dissertation and for encouraging me to set a date and make it happen. Thank you, Brian German, for also taking the time to read and comment on my dissertation. And most of all, thank you both for humoring me long after having heard more than you ever wanted to know about multidimensional growth models.

I also owe many thanks to Jennifer Mauss for here editorial assistance. She read a late draft of the work and offered helpful suggestions regarding matters of grammar, style, and punctuation.

To the Georgia Tech Navigators and particularly Donnie Hoover I am grateful for an extraordinary friendship that has provided me with constant fellowship and support. My parents, Bill and Raye Danner, have devoted countless hours to my growth and happiness in all matters of life. Thank you, Mom and Dad. I respect and appreciate you far more than you know. And finally, I have the deepest gratitude for Rachel, who married me despite the unfinished dissertation on my desk and whose acceptance, care, and patience has helped me maintain both a sense of humor and perspective.

TABLE OF CONTENTS

LIST OF TABLES

LIST OF FIGURES

NOMENCLATURE

a	growth curve shift parameter
a_o	ambient acoustic velocity
α	confidence level
b	growth curve shape parameter
β	model coefficient
BPR	Bypass Ratio
c	ellipsoid major axis
c_p	specific heat at constant pressure
dB	total takeoff noise
DEA	Data Envelopment Analysis
dy	rate of change of growth curve
E	Energy
EE_{cl}	Expected Uncertainty at a Specified Confidence Level
EINOx	Nitrogen Oxide Emissions Index
Ex	Exergy
Fg	Thrust
FPR	Fan Pressure Ratio
g	gravity
$gamma$	ratio of specific heats
ghp	gas horsepower
h	mass specific enthalphy
h^o	methalpy
HPC	High Pressure Compressor

HPT	High Pressure Turbine
k	constant of proportionality
L	Capability Limit
LPC	Low Pressure Compressor
LPT	Low Pressure Turbine
M	fixed level of the state of the art
$\dot{m}$	mass flow rate
m_dot	mass flow
MDGM	Multidimensional Growth Model
MRL	Manufacturing Readiness Level
n	number of capability dimensions
NPD	New Product Development
OPR	Overall Pressure Ratio
P	Pressure
P_{t3}	Combustor Inlet Pressure
PDR	Point of Diminishing Returns
$\dot{Q}_o$	rate of heat transfer
S	Entropy
s	mass specific entropy
$\dot{S}_{gen}$	Rate Of Entropy Generation
SFC	Specific Fuel Consumption
σ	distribution standard deviation
SoA	State of the Art
t	time
T	Temperature
T/W	Thrust-to-Weight Ratio of Engine
T_{t3}	Combustor Inlet Total Temperature

T_{t4}	Turbine Inlet Total Temperature
TIF	Technology Impact Forecasting
TRL	Technology Readiness Level
TWR	Thrust-to-Weight Ratio of Aircraft
V	Velocity
V_j	Exhaust Jet Velocity
$\dot{W}$	Rate Of Work Production
y	metric capability level
y_o	initial metric capability level
z	altitude

Subscripts

t	time
o	ambient condition
$pred$	predicted
$real$	real or actual
cl	confidence level
sfc	specific fuel consumption
fg	thrust
ei	nitrogen oxide emissions index
db	total takeoff noise

SUMMARY

Developing technology systems requires all manner of investment—engineering talent, prototypes, test facilities, and more. Even for simple design problems the investment can be substantial; for complex technology systems, the development costs can be staggering. The profitability of a corporation in a technology-driven industry is crucially dependent on maximizing the effectiveness of research and development investment. Decision-makers charged with allocation of this investment are forced to choose between the further evolution of existing technologies and the pursuit of revolutionary technologies. At risk on the one hand is excessive investment in an evolutionary technology which has only limited availability for further improvement. On the other hand, the pursuit of a revolutionary technology may mean abandoning momentum and the potential for substantial evolutionary improvement resulting from the years of accumulated knowledge. The informed answer to this question, evolutionary or revolutionary, requires knowledge of the expected rate of improvement and the potential a technology offers for further improvement. This research is dedicated to formulating the assessment and forecasting tools necessary to acquire this knowledge.

The same physical laws and principles that enable the development and improvement of specific technologies also limit the ultimate capability of those technologies. Researchers have long used this concept as the foundation for modeling technological advancement through extrapolation by analogy to biological growth models. These models are employed to depict technology development as it asymptotically approaches limits established by the fundamental principles on which the technological

approach is based. This has proven an effective and accurate approach to modeling and forecasting simple single-attribute technologies. With increased system complexity and the introduction of multiple system objectives, however, the usefulness of this modeling technique begins to diminish.

With the introduction of multiple objectives, researchers often abandon technology growth models for scoring models and technology frontiers. While both approaches possess advantages over current growth models for the assessment of multi-objective technologies, each lacks a necessary dimension for comprehensive technology assessment. By collapsing multiple system metrics into a single, non-intuitive technology measure, scoring models provide a succinct framework for multi-objective technology assessment and forecasting. Yet, with no consideration of physical limits, scoring models provide no insight as to the feasibility of a particular combination of system capabilities. They only indicate that a given combination of system capabilities yields a particular score. Conversely, technology frontiers are constructed with the distinct objective of providing insight into the feasibility of system capability combinations. Yet again, upper limits to overall system performance are ignored. Furthermore, the data required to forecast subsequent technology frontiers is often inhibitive.

In an attempt to reincorporate the fundamental nature of technology advancement as bound by physical principles, researchers have sought to normalize multi-objective systems whereby the variability of a single system objective is eliminated as a result of changes in the remaining objectives. This drastically limits the applicability of the resulting technology model because it is only applicable for a single setting of all other system attributes. Attempts to maintain the interaction between the growth curves of each technical objective of a complex system have thus far been limited to qualitative and subjective consideration.

This research proposes the formulation of multidimensional growth models as an approach to simulating the advancement of multi-objective technologies towards

their upper limits. Multidimensional growth models were formulated by noticing and exploiting the correlation between technology growth models and technology frontiers. Both are frontiers in actuality. The technology growth curve is a frontier between capability levels of a single attribute and time, while a technology frontier is a frontier between the capability levels of two or more attributes. Multidimensional growth models are formulated by exploiting the mathematical significance of this correlation. The result is a model that can capture both the interaction between multiple system attributes and their expected rates of improvement over time. The fundamental nature of technology development is maintained, and interdependent growth curves are generated for each system metric with minimal data requirements. Being founded on the basic nature of technology advancement, relative to physical limits, the availability for further improvement can be determined for a single metric relative to other system measures of merit. A by-product of this modeling approach is a single n-dimensional technology frontier linking all n system attributes with time. This provides an environment capable of forecasting future system capability in the form of advancing technology frontiers.

The ability of a multidimensional growth model to capture the expected improvement of a specific technological approach is dependent on accurately identifying the physical limitations to each pertinent attribute. This research investigates two potential approaches to identifying those physical limits, a physics-based approach and a regression-based approach. The regression-based approach has found limited acceptance among forecasters, although it does show potential for estimating upper limits with a specified degree of uncertainty. Forecasters have long favored physics-based approaches for establishing the upper limit to unidimensional growth models. The task of accurately identifying upper limits has become increasingly difficult with the extension of growth models into multiple dimensions. A lone researcher may be able to identify the physical limitation to a single attribute of a simple system; however, as

system complexity and the number of attributes increases, the attention of researchers from multiple fields of study is required. Thus, limit identification is itself an area of research and development requiring some level of investment. Whether estimated by physics or regression-based approaches, predicted limits will always have some degree of uncertainty. This research takes the approach of quantifying the impact of that uncertainty on model forecasts rather than heavily endorsing a single technique to limit identification.

In addition to formulating the multidimensional growth model, this research provides a systematic procedure for applying that model to specific technology architectures. Researchers and decision-makers are able to investigate the potential for additional improvement within that technology architecture and to estimate the expected cost of each incremental improvement relative to the cost of past improvements. In this manner, multidimensional growth models provide the necessary information to set reasonable program goals for the further evolution of a particular technological approach or to establish the need for revolutionary approaches in light of the constraining limits of conventional approaches.

CHAPTER I

MOTIVATION

Sometimes the pointless and the ridiculous are obvious; sometimes they are not. Consider the perpetual motion machine. For centuries, scientists, engineers, and entrepreneurs dreamed of perpetual motion machines and sought to conjure them into existence [2]. It seemed that if one could only set a wheel to spinning exactly so, it might spin forever. If one could lay a watercourse just right, the water would continually push itself along and even drive a power wheel as illustrated in Figure 1.

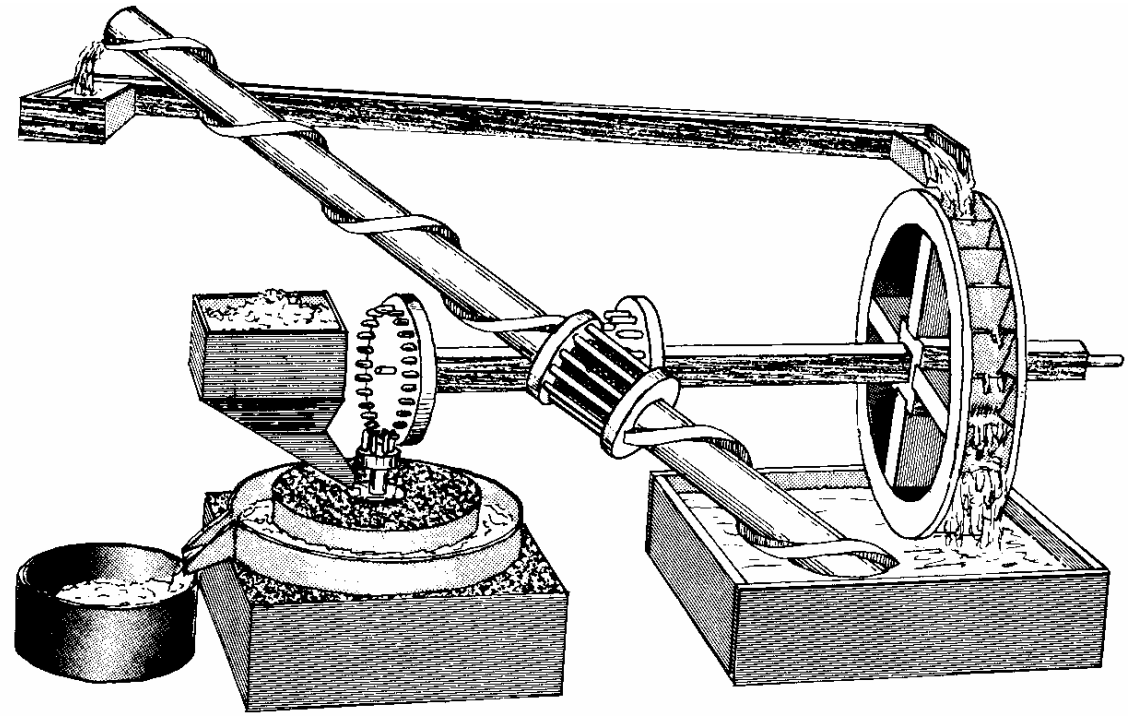

Figure 1: A Proposed Perpetual Motion Machine [2]

These were to be machines that, once placed in operation, would continue to operate indefinitely and, in many cases, even produce useful work with no additional infusion

of energy. Such a development would be a profound contribution to both science and humanity. No wonder even great minds turned their energies to the pursuit of this technical grail. Unfortunately, all attempts have failed completely because of two developmental barriers: the natural conditions expressed in the first and second laws of thermodynamics. No matter how hard one tries, it is not possible to create energy from nothing. No matter how hard one tries, it is not possible to stem the generation of entropy. These are precisely what perpetual motion machines strive to do. While there was a time some centuries ago when it made a certain sense to test these particular physical limits, to accumulate the experiential wisdom that produced the laws of thermodynamics, this is no longer the case. The laws of thermodynamics are time-honored and universally accepted. Perpetual motion machines, though momentarily curious, have become laughable for their blatant disregard for the inevitability of these laws. The perpetual motion machine is pointless and ridiculous.

As universal laws of physics, the first and second laws of thermodynamics establish limits that bound the *design envelope* or design space for *all* plausible systems, even though their applicability in a particular situation may be temporarily obscured. Additionally, there are many other physical laws that, like the first and second law, also establish boundaries limiting the realization of all conceivable systems. Not all such physical laws are as obvious and universal as the first and second laws; however, the boundaries they establish for a particular system are no less insurmountable. Designers may–and probably sometimes do–conceive of schemes that violate one or another of a myriad of natural laws, and while such schemes may be brilliant with promise, they are no more likely to succeed than a perpetual motion machine.

1.1 Perpetual Motion Implausibility

There are two primary characteristics of the perpetual motion design problem that make the nonexistence of a solution obvious. The first is its simplicity as a design

problem. There is a single objective—perpetual motion—that is easily quantified by one engineering parameter. This single objective can be expressed as the constancy or increase of the aggregate kinetic and potential energies over all time for the system undergoing perpetual motion. Having only one objective greatly simplifies the evaluation of proposed designs.

The second characteristic that makes it easy to evaluate the potential for a solution is the clearly defined upper bounds relative to the single objective. Again, these are the laws of thermodynamics. In the case of increasing the aggregate energies of the system, the objective exceeds the theoretical limits of the design envelope; that is, it violates the first law of thermodynamics by intending to create energy from nothing. In the case of maintaining the aggregate energies of the system, there are, again, clear theoretical and practical limits. Only in the case of a purely reversible system is literal, perpetual motion even theoretically possible. Given that all real systems are subject to irreversibility—the ravages of entropy, of time, friction, and the like,—this theoretical limit cannot be achieved or exceeded, only approached. This clearly defined upper limit for the only system objective of all perpetual motion machines definitively establishes the implausibility of all such systems.

For more complex multi-objective systems with few, if any, *clearly* defined upper limits it is much more difficult to identify the boundaries of the design envelope for all realizable systems. Such systems may be repeatedly refined and redesigned in hopes of achieving higher and higher levels of performance with little consideration for whether or not the design envelope allows for further improvement. In a world of amateurs dedicating spare hours to hobbies such a gamble might not matter, but in a world with limited resources to invest, much hinges upon whether or not a technology can be significantly improved.

1.2 Design Limits

The *Thomas W. Lawson*, a sailing ship, was designed to compete with the speed and capacity of steamships. Her seven masts, required to achieve such speeds, greatly reduced her stability, and she capsized on December 13, 1907, while at anchor [3]. The features that made her fast had compromised her ability to stay afloat; her fate eloquently illustrates the limits of a technology, of mast and sail as a means of achieving speed over water.

There are design envelopes that limit the potential of any future system within a general technology base or system architecture. Analogous to operating beyond the operational envelope of a system is attempting to design beyond the theoretical and engineering limits of a particular technology base. The resulting system may not always be condemned to catastrophic failure as was the *Thomas W. Lawson*; however, all are destined to operate below their targeted capability. The investment required to research and develop the system intended to achieve these targets is lost.

The possibility, for example, that turbine engine technology has reached its engineering limit has been a point of discussion for decades. Earnest Simpson, the former Turbine Engine Division Chief for the United States Air Force (serving from 1956 to 1980), has been quoted as saying, "I have been told three times in my career . . . there was no more research to be done on the gas turbine engine" [4]. Clearly, there were premature opinions that the technology had filled the design envelope, when in fact it had not. His successor, Jeffrey Striker, has been met with similar doubt concerning the future development of turbine engines at the onset of the Integrated High Performance Turbine Engine Technology program and the Versatile, Affordable, Advanced Turbine Engine program—two aggressive programs for the further development of the gas turbine engine [5]. These programs have raised the question of just how much research remains to be done on the gas turbine engine. The pertinent question, however, is not just how much research remains to be done; more research can

always be done. The pertinent question is what improvement can be expected from that research. In effect, what availability for further improvement remains? Are the proposed performance targets and time lines for these programs reasonable? Are they even possible? Has turbine engine technology reached a limit beyond which it cannot improve? These are the types of questions this research is devoted to answering, not solely for the turbofan but by formulating the necessary tools, for any technology architecture. At risk on the one hand is excessive investment in the technology, that is, too much time and engineering effort given to pursuing a solution that lies without the bounds of physical possibility. There is the risk of pursuing a solution that simply does not exist. At risk on the other hand is failing to finish technological improvement that is nearly completed and into which much has already been invested. There is the risk of abandoning a technological promised land.

The objective of this research is to formulate an approach to evaluate the current state of the art of a technology architecture having multiple attributes relative to impending limits. This will enable decision-makers to include consideration of the availability for further improvement within a given technology architecture when choosing between technology alternatives.

CHAPTER II

INTRODUCTION TO TECHNOLOGY GROWTH MODELS

This chapter reviews concepts regarding technology development and some of the highly disparate language used to describe that development. The discussion necessarily focuses on the concepts and terms that this study uses in its development of a multidimensional growth model for assessment and forecasting technology attributes. The first part of this chapter speaks generally to the terminology of technology development, and the second half focuses the discussion on an introduction of the current best quantitative and graphic model for measuring technology development, namely the S-curve.

2.1 Technology

2.1.1 Definition

Technology is a term that is used by many different disciplines and that brings to mind a host of gadgetry and technique, machinery and process. It derives from a Greek word meaning 'the systematic treatment of an art [or skill],' yet its use, throughout a wide variety of literature, implies much more [6]. Here follows a sample of the definitions found in the literature:

> *[Technology is] the totality of means employed to provide objects necessary for human sustenance and comfort [7].*
>
> *[It is] the application of scientific knowledge for the satisfaction of human needs [8].*

[It is] the stock of knowledge that pertains primarily to the production of goods and services [9].

[Technology is] a knowledge of techniques, methods and designs which work even if, at times, the reason why they work cannot always be explained [10].

[It is] the structured application of scientific principles and practical knowledge to physical entities and systems [11].

[Technology comprises] the tools, techniques, and procedures used to accomplish some desired human purpose [12].

Collectively these definitions address three distinct aspects of technology: its source, that is, knowledge; its substance, such as techniques or equipment; and its purpose, namely, serving humanity.

Knowledge is the source for technology. This may mean scientific principles, or it may refer to practical knowledge, to craft or skill [11]. The distinct difference between *scientific principles* and *practical knowledge* is addressed by Rosenberg [10]. According to Rosenberg technology derived from scientific principles, through the rigors of mathematics and the strict application of scientific laws, is based on an understanding of those fundamental laws that govern a system. In contrast, technology derived from practical knowledge is based on astute empirical observation without particular understanding of, or concern for, the underlying principles. This distinction is made to clarify that technology is not only the result of scientific pursuits but can also result from practical experience. Moreover, the distinction is important to this study. Identifying the scientific laws that apply to a technology and, more specifically, the physical limitations that are expressed by those laws has long been considered a critical component of assessing technology development, because the physical limitations expressed in the scientific laws directly affect the potential for technological development [13, 8, 14].

The substance of technology constitutes both the tangible and the intangible. It consists of the totality of means—the stock of knowledge, techniques, procedures, and methods—as well as the resulting objects—the tools, goods, physical entities, systems, and even services—that are developed for the purpose of fulfilling human needs and desires. As used within this research, *technology* will more precisely refer to physical devices used to fulfill a specified set of objectives.

In regard to purpose, recall the old adage that necessity is the mother of invention. Of course, the inventor's vision often outstrips need, requiring the suggestion that technology is the fulfillment of human needs *and* desires. Whose needs and desires? They are those of investors, consumers, marketers, technicians, engineers, manufacturers, and more, each with a separate notion of what a technology should provide.

2.1.2 Descriptors and Classifications

Of greater difficulty than marshaling a definition of technology is clearly organizing the myriad descriptors and the overlapping technology classifications that abound in the literature. It seems that there are as many descriptors and classifications as there are humans to need or desire technology. At least, this nearly holds true for those who write the literature on the analysis of technology development. Historians, designers, and forecasters—to name some varied people groups with an interest in technology development—all have different perspectives and different ways of discussing technology. Perhaps this is why the literature of technology development is not unified in its terminology. In the interest of brevity, the following discussion will introduce and explain those terms and classifications that are pertinent to this study and its perspective.

This research is interested in developing tools to assess and forecast the development of technology attributes. For the purposes of exploring the relevant terminology,

there are five questions that organize the numerous considerations into classification systems.

- First, what should the technology do or accomplish?
- Second, what are the physical possibilities for achieving a technology's goals?
- Third, how developed is the technology in terms of accomplishing its goals?
- Fourth, how much research and development has been required or will be required for a technology to accomplish its goals?
- Fifth, how can an analyst organize and understand the information addressed by the preceding four questions?

Again, this section intends only to introduce the terminology related to each of these questions. Mathematical and graphical expressions, interactions, and manipulations of the concepts and realities represented by the terminology are the matter of the subsequent sections and chapters.

What should the technology do or accomplish? *Attributes*, *metrics*, *dimensions*, and *capability* are terms that practitioners use relative to this question. *Attributes* addresses the question most directly, for it is used to suggest what characteristics a technology should have. Speed, reliability, and efficiency are examples of attributes that a technology might be expected to have. *Metrics* implies that the attributes have been identified or expressed in a way that they may be evaluated or measured. Sometimes, the term *figures of merit* is used synonymously with *metrics*. *Dimensions* is typically employed to reference succinctly the number of attributes that are of concern. If a single attribute is in question, the term *unidimensional* describes the technology. For multiple attributes, the term *multidimensional* applies. The term *capability* implies that at least in some way or at some level the technology of interest does possess the attribute in question.

What are the physical possibilities for achieving a technology's goals, for acquiring the desired attributes? This set of concerns finds expression in words such as *limits* and *design space*. *Limits* refers to the fact that physical realities prevent the realization of some schemes that designers might envision. For example, the first and second laws of thermodynamics prohibit perpetual motion machines. Generally, analysts write and speak of *upper limits*, which describe the best that a technology can hope to accomplish. Sometimes limits are distinguished as *scientific* or *theoretical* as opposed to *engineering* or *practical*. The theoretical area bounded by limits is referred to as the *design envelope*, which describes the possibilities for design. Throughout most of the literature that deals with quantitative evaluation of technology, limits and design space refer to the possibility for acquiring a single attribute. This study's interest extends to the limits, that is the possibilities of development, for a technology with multiple attributes.

Technology potential is defined here as the possibility for further development or more precisely the availability for further improvement of a technology attribute relative to impending limits. It is the remaining distance between the current state of the art of a technology attribute and its upper limit. *Technology potential* quantifies the future potential of a technology architecture for a specified dimension of capability. This potential, however, will only be realized if both the willingness and resources exist to further advance the dimension of capability within technology architecture. Consequently, *technology potential* is not a forecast of what will actually be achieved but rather the additional improvement that is possible given the willingness and necessary resources.

Because the third question requires extended treatment, the discussion will first address the fourth and fifth questions. How much research and development has been required and will be required for a technology to accomplish its goals? This set of issues is sometimes described in terms of the *effort* devoted to the development

of the technology. Because, however, it can be difficult to distinguish the quality and intensity of the effort expended, sometimes analysts refer instead to the passage of *time* once development begins. How can an analyst organize and understand the information addressed by the technology development? Analysts refer to *tools*, *approaches*, *models*, and *methods* that allow them to *assess*, to *predict*, and to *forecast* trends in technology development. Two common tools are S-curves and technology frontiers, which later sections will explore.

How developed is a technology in terms of accomplishing its goals? This question, perhaps, references the set of concepts and issues most important to this study. These issues also seem to be the most complex and confused. The literature usually describes development by comparing available technologies in terms of their newness, where newer technologies are equated with being more advanced. A literature review by Garcia has revealed twenty-five distinctly different classification schemes based on the relative newness of a technology [15, 16]. These schemes vary in a number of aspects. For example, there is disagreement on the number of categories necessary to adequately classify technologies based on relative newness. Some classification constructs have as many as eight different classes into which technologies are categorized [17], while others have as few as two [18, 19, 20]. There is also little commonality in taxonomy of classification categories. Within the twenty-five qualitative classification constructs identified, fifty-two different category descriptors have been found. Some of the more common categorical descriptors include *incremental, discontinuous, evolutionary, revolutionary, radical, sustaining,* and *disruptive.* (See Appendix A for a full list.) Even in cases where researchers have agreed on the number and taxonomy of classification categories, the same technology has been categorized differently based on the utilization of dissimilar factors to delineate relative newness. Fifty-one different factors have been identified in literature that have been employed as criteria for classifying technologies [15].

These inconsistencies in classification constructs have inhibited the advancement of the new product development (NPD) processes regarding different types of innovations. Garcia alludes to the confusion and its limitations:

> *Researchers often believe that their work is 'new' and 'important' when instead it just relabels/redefines/reiterates findings from previous studies with different labeling of innovations. Findings from other fields . . . are often overlooked because they emphasize a 'different' type of innovation* [15].

Acceptance of new product research by practitioners has also been hindered by the incongruity within the field.

The objective of this research is not to resolve the many classification inconsistencies and establish a common foundation for NPD taxonomy. The purpose here is to define clearly the terminology that will be used throughout this research and establish its relationship to existing vocabulary.

Despite the many differences between classification constructs, there is one similarity. They are all based on the degree of discontinuity of a new technology or product relative to those that already exist. The disparity in classification results from inconsistent answers to the following questions: Exactly what constitutes discontinuity? For which factors is discontinuity of interest? And, from whose perspective does the discontinuity exist?

Any new product line or technology, no matter how similar to a previous technology, is discreetly different. Thus, the transition from the previous technology to the new could be seen as discontinuous. Oftentimes, however, the differences between subsequent products, although discrete, are minor and the transition between them is viewed as continuous. At what point are product (i.e. technology) differences sufficiently large to warrant the classification of their transition as discontinuous? This

question has been one of several points of divergence for many NPD researchers. The question of discontinuity, however, is not answered based on product similarity or dissimilarity but on the divergence of the underlying knowledge base on which subsequent innovations are developed. Discontinuity results when the knowledge base used to develop an existing product must be abandoned and a new knowledge base explored for the development of a subsequent product, regardless of product similarity—in appearance or performance. The first automobiles, for example, looked very much like horse-drawn carriages and in many cases performed no better. They were, however, based on a radically different knowledge base than their predecessors and represented a technical discontinuity.

According to Utterback, discontinuity characterizes a "change that sweeps away much of a firm's existing investment in technical skills and knowledge, designs, production technique, plant and equipment" [20]. Utterback's definition is focused on a firm's abandonment of existing practices. The displacement of existing practices, however, may occur at several levels—consumer, firm, industry, market, or world. A discontinuity may occur with respect to any one or more of these entities.

Discontinuity also seems to be a matter of perspective, and classification constructs have reflected this. The different perspectives have been grouped into two levels, macrolevels and microlevels. The macrolevel is concerned with the perceived degree of discontinuity from the perspective of an industry, the market, or the world. The microlevel is concerned with the degree of discontinuity perceived by a firm or customer. For example, imagine the leap Pratt & Whitney, long-time manufacturer of aircraft engines, would have to make to enter the business of making airframes for those engines. The effort would constitute a microlevel discontinuity. The endeavor would require a drastically different knowledge base than the firm currently possesses, although it would not be new to the industry, market, or world.

For the purpose of classifying an innovation or establishing its relative newness,

the factors of interest must span both the technical and the marketing aspects of the innovation's development. Innovation embodies *both* the invention and technical development of a product *as well as* the production and market introduction of that product [15]. Thus, when assessing the degree of discontinuity of an innovation from existing products, the factors considered must include both technical and marketing aspects throughout micro and macrolevels of consideration.

Garcia has proposed a classification construct for labeling innovations based on these two foundational dimensions—macro/microlevel and technical/marketing [15]. The construct is based on identifying the presence of a discontinuity in technical and/or marketing factors at the micro and/or macrolevels. In this construct, *radical* innovations are defined as those having micro and macrolevel discontinuities in *both* technical *and* marketing factors. *Really new* innovations are those having *either* a macrolevel technological *or* marketing discontinuity but *not* both. *Incremental* innovations are defined as those having a technological *and/or* marketing discontinuity at the micro level with *no* macrolevel discontinuities.

The subject of this research is concerned only with technical factors of innovation from the macrolevel perspective. There are, therefore, only two innovation categories of interest—those innovations having a macrolevel technological discontinuity and those that do not. Those innovations having a macrolevel technological discontinuity independent of market considerations will be referred to herein as *revolutionary* innovations or technologies. Under Garcia's classification construct, revolutionary innovations, as defined here, may be categorized as either *radical* or *really new* based on the presence of a macrolevel marketing discontinuity [15]. Also under Garcia's construct, innovations having no macrolevel technological discontinuity may be classified as either incremental or really new depending on the presence of a macrolevel marketing discontinuity. This type of innovation will be referred to herein as *evolutionary*—those innovations having no macrolevel technological discontinuities regardless

of marketing considerations.

The objective of this research is to formulate the necessary tools to identify developing technologies that, because of their physical limits, designers cannot evolve appreciably beyond their current capability. It is envisioned that these tools will aid decision-makers to identify when to stop investing in the evolution of a technology and begin or increase investing in a revolutionary technology.

2.2 Technology S-curve

The technology S-curve is a graphical representation of the maturing phases of a particular technology. A notional technology S-curve is displayed in Figure 2. On the ordinate axis is technical capability, which is representative of any measure of merit that characterizes the technology of interest. On the abscissa is the engineering effort—the aggregate effort devoted to implementing physics in hardware in order to improve the specific technical capability. Time is also frequently used on the abscissa with slightly different implications.

The level of technical capability achieved by a technology base or system architecture as represented by the vertical scale of a technology S-curve is solely dependent on the *physics* of the particular design problem. The capability at any point in time results from implementing the *known* physics in hardware. Consequently, higher levels of technical capability at any point in time are prevented due to limited understanding of the governing physics or a limited understanding of how to implement the known physics in hardware.

The time required for advancements in technical capability is solely dependent on the *programmatics* of the technology development as represented by the horizontal scale of the technology S-curve. The progression of a technology towards its upper limit is not solely dependent on the potential for additional improvement, the technology potential, but also the availability of resources and the willingness to devote those

resources to its further development. As a result, a technology may 'stall' indefinitely at a particular capability level due to low or no investment. In order to normalize this variability resulting from programmatics, engineering effort can be used as the horizontal scale for technology S-curves. However, time is most frequently used due to the difficulty of tracking cumulative engineering effort over the lifetime of a system architecture. The differences between time and engineering effort as the horizontal scale for technology S-curves will be addressed in greater detail in later sections.

The limits portrayed in the figure represent the bounds established by the theoretical physics and the engineering limitations of realizing that physics in hardware. These are "hard" limits for the subject technology; they do not change regardless of engineering effort. The Carnot efficiency for thermodynamic cycles is an example. The curve itself is the technology S-curve and represents the level of maturity or capability for the subject technology with respect to the engineering effort invested.

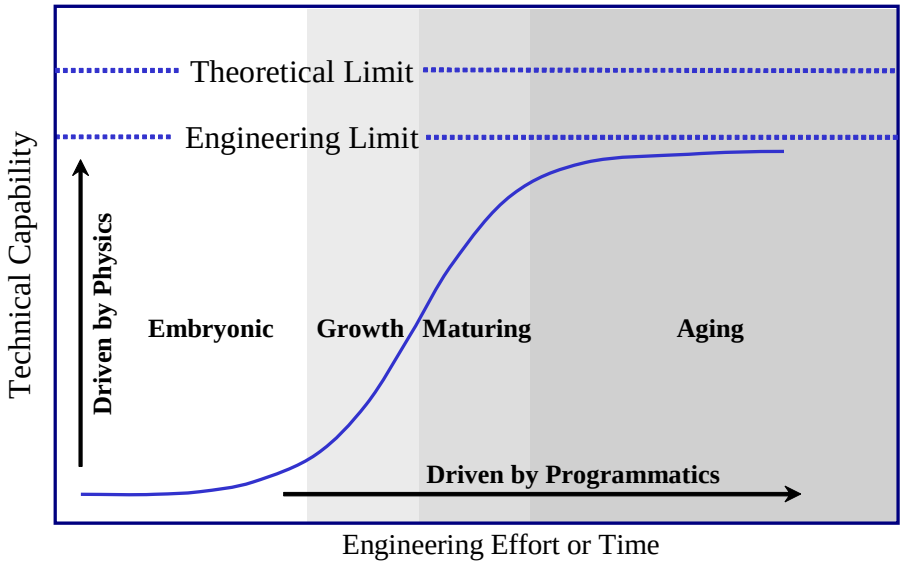

Figure 2: Technology S-curve

Technology S-curves are used to model technological "growth" based on an analogy to biological growth patterns. There are four key stages of technology development that are made evident by the S-curve [21]. The first stage is often referred to as

the *embryonic* phase of development. Beginning at the lower left end of the curve the technology is very young. Many hours of effort are required to achieve even the slightest degree of improvement. As more and more effort is invested, breakthroughs are gradually made. With each improvement, additional improvement becomes easier and easier. The technology transitions into the growth stage, a phase of rapid development in which subsequent improvements are achieved with significantly less effort. Analytically, this transition occurs at the point of maximum curvature on the lower half of the S-curve. At the inflection point of the S-curve the technology transitions from the growth phase to the maturing phase of development. This stage of development is characterized by continued growth, although subsequent improvements become progressively more difficult to achieve. As the technology approaches its engineering limit, it transitions into the *aging* stage in which each additional unit of improvement requires exponentially more engineering effort and finally flattens to asymptotically approach the engineering limit. The transition into the aging stage of development occurs at the point of maximum curvature on the top half of the S-curve and is often referred to as the "point of diminishing returns."

2.2.1 Research and Development Productivity

The slope of the technology S-curve is representative of research and development (R&D) productivity—the technical improvement per unit of engineering effort. A plot of R&D productivity is shown in Figure 3. The maximum of the R&D productivity curve corresponds to the inflection point of the S-curve. The 'tails' of the productivity curve represent the early embryonic stage of technology exploration and the final aging stage as the technology approaches its upper limits. The inflection points of the productivity curve are most critical to the strategic planning of technology development. The left inflection point of the productivity curve—the transition between the embryonic and growth stages of development—indicates the transition

into a phase of rapid development during which, if a firm is prepared, it can exploit that explosion in productivity. The right inflection point—the transition between the maturing and aging stages of development coined the point of diminishing returns—signals the transition into the phase of rapidly diminishing developmental productivity. This signals the need to search for a more advanced technology if further progress in technical capability is to be achieved.

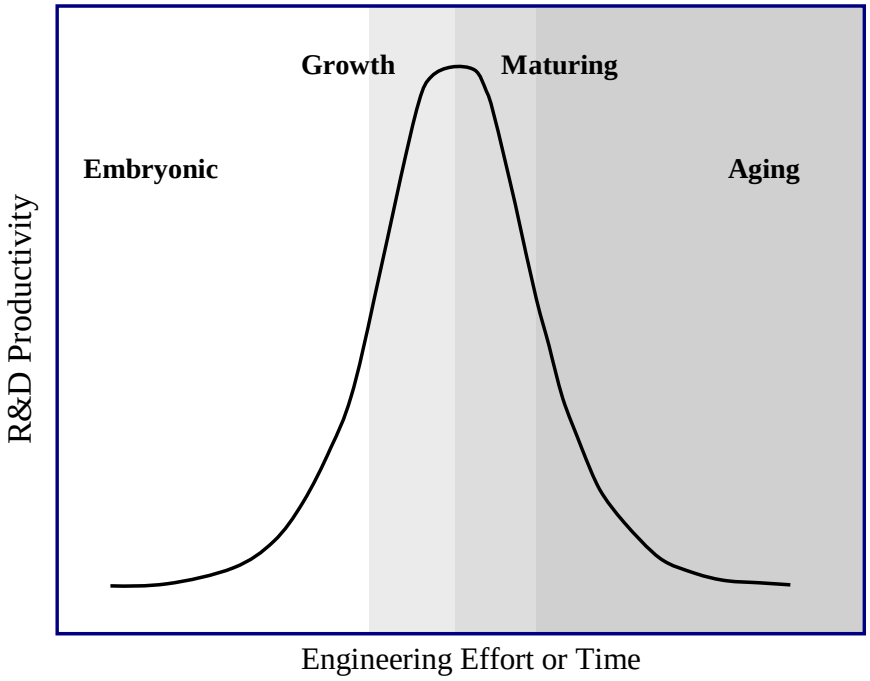

Figure 3: R&D Productivity

2.2.2 Technology Cycles

The phrase *technology cycles* refers to the reoccurring pattern of the embryonic, growth, maturing, and aging stages of subsequently more advanced revolutionary technologies designed to fulfill a similar function. As one technology approaches its upper limits and R&D efforts provide little improvement, effort is diverted to a new technology that may initially have lower performance capability than the incumbent

technology but possesses greater potential for improvement and higher returns on engineering effort. A series of notional technology cycles is provided in Figure 4. Each technological cycle is represented by a separate S-curve and unique upper limit.

Notice that each subsequent technology S-curve overlaps the preceding S-curve. This indicates that research and development for a revolutionary technology begins while further advancements are still being made to the incumbent technology, and consequently, that engineering effort is applied to the emerging technology before the incumbent has exhausted availability for further improvement, i.e. its technology potential.

In some cases the 'tail' of a new S-curve may intersect the S-curve of the incumbent technology before it has reached its aging stage of development, indicating comparable levels of performance for that specific technical capability. However, due to the faster R&D productivity of the incumbent technology and the consideration of other performance criteria, its pursuit was maintained despite the ultimate potential for higher levels of performance with the emergent, or revolutionary, technology.

2.2.3 Market S-curves

Growth curves, similar to technology S-curves, have also been used to illustrate the emergence of new technologies into a market. On the ordinate axis is the market share of a new technology in a particular market, not the market share of an emerging firm. Upon introduction of the technology it has a very low market share, and initially grows very slowly. As more is learned about the market and the technology is adapted to market demand, the new technology's market share begins to grow with increasing momentum. As the inflection point of the S-curve is reached, the upper limit to market share (100%) begins to inhibit the continued rate of growth and the S-curve begins flattening to asymptotically approach this limit. Unlike technology S-curves, market S-curves fall after reaching a maximum as they begin to be replaced by more

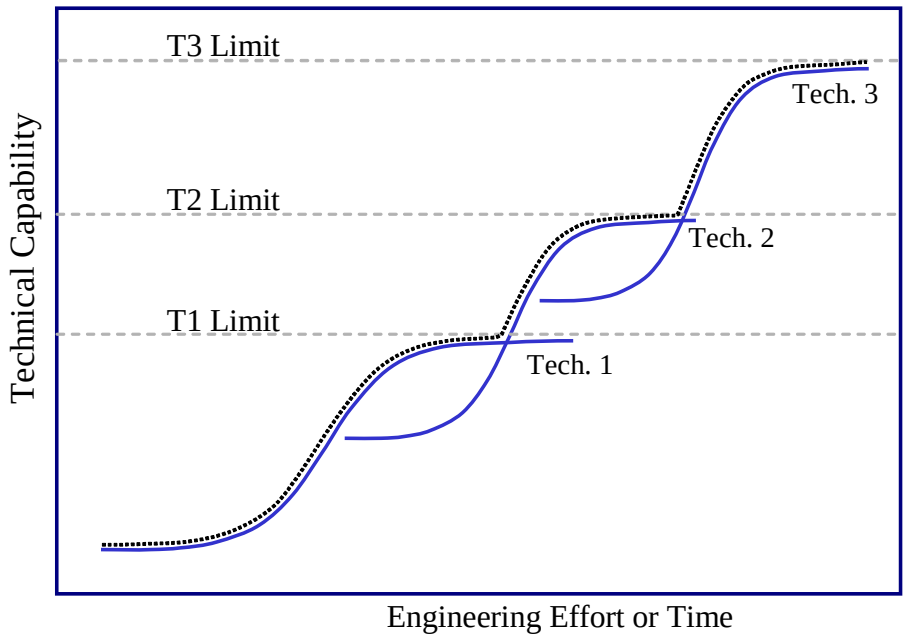

Figure 4: Technology Cycles: Reoccurring Developmental Patterns of Subsequently More Advanced Revolutionary Technologies

advanced technologies. There are many detailed aspects of market S-curves that have not been extensively discussed herein. They have been introduced only to make the distinction from technology S-curves and prevent possible confusion. For more information on market S-curves consult Garcia and Martino [12, 15].

2.3 Technology Capability

Until this point, the technology S-curve has been addressed from a notional perspective only. However, in order for its application to be meaningful for real technologies, there are several aspects that require further consideration. This and the remaining sections of this chapter will address some practical considerations of actually using the growth curves to assess real technologies.

2.3.1 Technology S-curve Resolution

The first practical issue to consider when assessing a real technology by means of a technology S-curve is the resolution at which the technology is to be assessed. Resolution refers to the degree of precision used to define the technology under consideration. A highly resolved technology would be one that is very precisely defined by a specific and detailed hardware implementation. A lesser resolved technology would have a higher degree of flexibility in the technical implementation of its functional objectives.

As an example, consider the sole functional objective of transportation with the single technical capability of speed. Most generally, and hence least resolved, the theoretical upper limit is the speed of light and there are numerous mechanisms—horse drawn carriage, automobile, piston prop aircraft, turbine engine aircraft, ion rocket space craft—that can fulfill the objective of transportation with varying speed capabilities. A handful are shown on a common S-curve in Figure 5.

A more resolved S-curve may only assess a single class of vehicles from the list above, aircraft, for example. An even higher resolution S-curve may only assess turbine engine aircraft, and at higher resolution only turbojets, and so on. The more highly resolved the S-curve assessment the more restricted the assessment is to a narrow technology class.

Of most interest to this research is an intermediate level of resolution. A high level of technology resolution results in an assessment that is too narrow to be of practical value as it applies only to a very precisely defined technology. This level of assessment tends to be more the analysis of a single system than a class of systems. Conversely an assessment that is conducted at an extremely low level of technology resolution results in an assessment that is too broad to be of practical value. An assessment at this level of resolution is not hardware specific enough to draw conclusions concerning the technology potential within a technology class. The only resulting information from such an assessment is the distance of a technology class from the ultimate upper

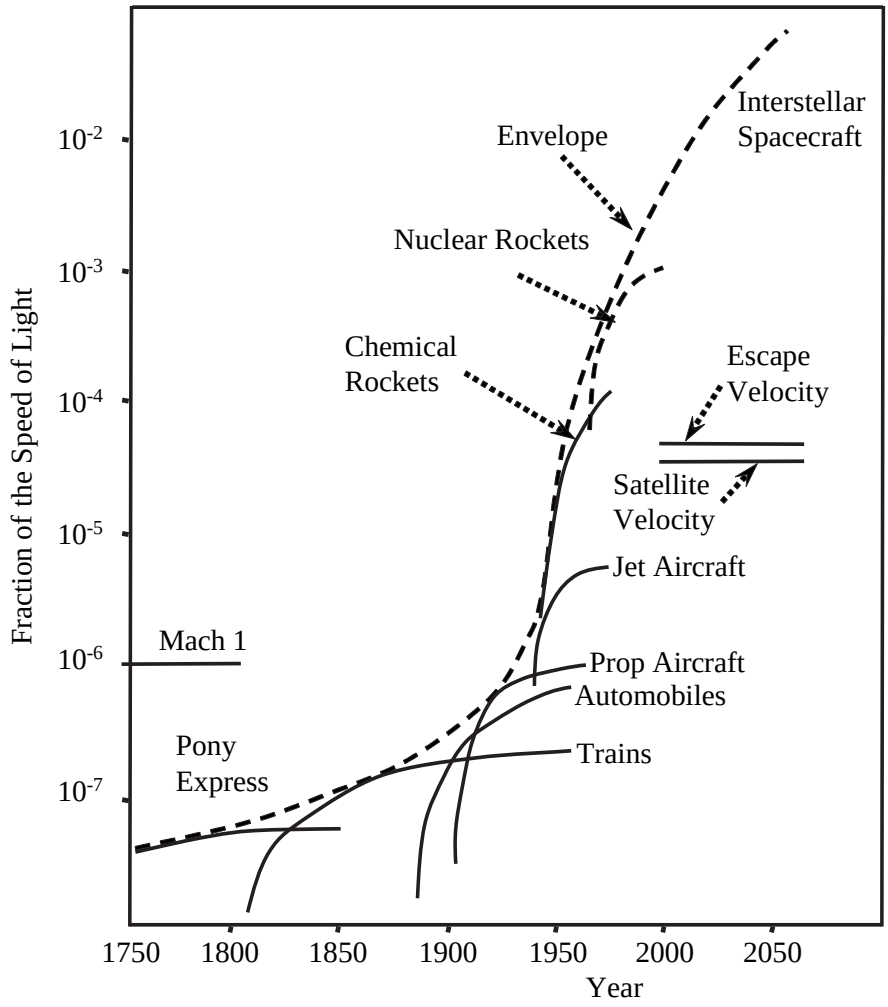

Figure 5: Speed Envelope, modified from Lanford and Makridakis [22, 23]

limit bounding all technologies fulfilling a particular functional objective. Proper selection of the technology resolution will have significant impact on the usefulness of the resulting assessment. The resolution will also have an impact on both the metric selection and the upper limit identification.

At lower levels of technology resolution, metric selection must be more general in order to be applicable to a broader set of possible alternative technologies. Likewise, upper limit determination must be independent of both the hardware and processes employed by any one technology alternative; it is dependent only on more general

physical laws such as the speed of light in the case of speed. For higher levels of technology resolution, technology capability metrics that are more specific to a particular technology class can be selected, and upper limits can be determined based on the specific processes employed by the technology class.

Of most interest to this research is a level of resolution commensurate with system architectures—a class of systems that are based on common fundamental processes, although the exact manner in which these processes have been realized in hardware may differ. Examples of differing system architectures within the field of propulsion are steam engines, internal combustion engines, turbine engines, rockets, etc. Additionally each of these would also be classified as revolutionary or radical as compared to its predecessor.

Also note that for complex technologies such as propulsion systems the evolution of components comprising the system may individually be described by a technology S-curve. For instance, the advancement of a turbine engine compressor, combustor, or turbine may be described according to a technology S-curve. As each component S-curve approaches its corresponding limits the system as a whole also approaches its limits. It is by means of component improvement that the system as a whole improves.

2.3.2 Metric Selection

The usefulness of the technology S-curve is in its ability to establish a technology's current capability relative to its upper limits, thereby identifying the technology potential. The next practical consideration that must be addressed is the choice of technical capability. What measures of technical capability should be selected in order to adequately assess the future viability of a further evolved technology? Recognizing the vital importance of identifying technology limits before they inhibited a technology's further improvement and subsequently a firms future viability, Foster

[3] asked a similar question, *limits of what*? Phrased either way, these two questions are the same; what technology metrics are most significant to the future viability of a technology and its developing firm? The answer Owens Corning gave to this question was the *technical factors of our product that were most important to the customer* [3]. This can be further generalized to include all factors that influence product design.

The more dedicated a technology is to a single function or objective, the easier it is to identify an appropriate technical capability to monitor. As an example, consider a clock which most generally has a single fundamental objective—to accurately measure time as quantified by error per day, the ultimate limit to which is clearly zero. Independent of cost and specific hardware implementation, an S-curve representation of time measurement accuracy is shown in Figure 6. Note the reformulation of the technical capability as to yield a growth curve.

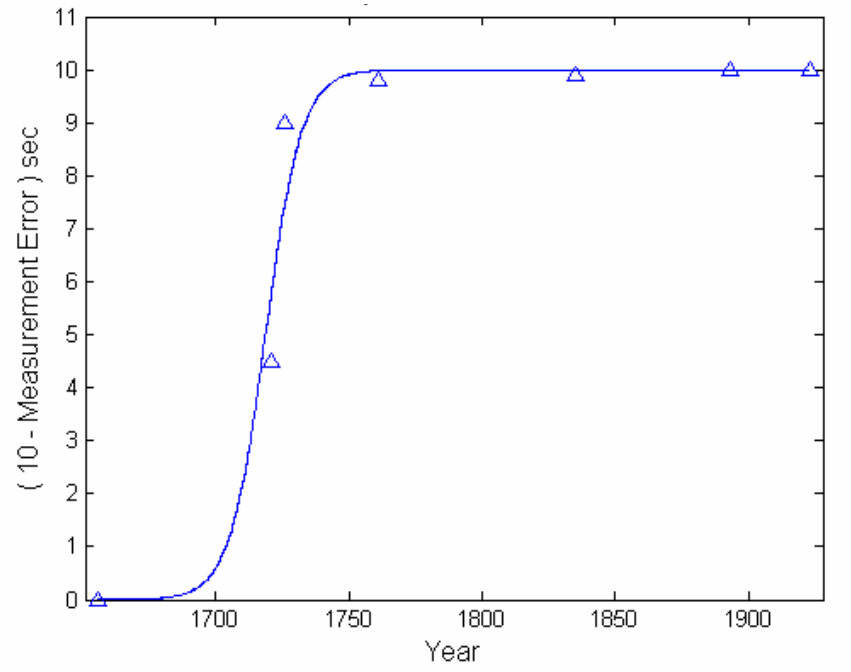

Figure 6: Accuracy of time measurement, as quantified by error per day

For more complex technologies that have multiple performance and economic objectives, identifying and monitoring appropriate metrics that comprehensively assess

the technology is much more difficult. As an example, consider high bypass turbofan engines. The number of system level metrics necessary to completely evaluate the maturity of such a technology are numerous: thrust, weight, fuel consumption, emissions, noise, reliability, etc. Furthermore, as multiple technology attributes are necessary to fully describe a system, interactions between these attributes must be considered in order to accurately capture the overall system maturity level relative to its upper limits.

2.3.3 Multi-Objective Metric Correlation

The present application of technology S-curves has been limited to a single technical capability for any subject technology. For technologies having only one objective, this approach is quite meaningful and relatively simple to establish an accurate S-curve model. There are, however, few technologies that truly possess only a single technical capability. Even for a technology required to fulfill only one functional objective there are often several metrics that are used to describe its overall performance. Inherent in all technology designs beyond objective fulfillment are measures of durability, "easy of use", maintainability, etc.—all of which can be used to assess the maturity of a given technology. Technologies having a single objective are modeled using technology S-curves by eliminating the variability due to all other figures of merit. For very simple technologies this approach can result in a meaningful assessment. However, for more complex multi-objective technologies, far too much information is lost in order to reduce the merit of the technology to a single technical capability providing marginal insight at best.

As an example, consider a high-temperature alloy for which the technical capability of interest is the maximum temperature it can withstand. For meaningful results, a precise definition must be given to "withstand." This could be defined as the alloy's melting point, or, more meaningful, a set threshold of strength, hardness,

or fatigue performance. The temperature at which any of these properties for the subject alloy drop below the threshold will be considered its maximum temperature. The result is an S-curve of alloy maximum temperature as defined by fixed property characteristics—variability due to other technical capabilities has been removed from the assessment.

Often in the case of simple systems this type of assessment may be adequate, however, as the complexity of the subject technology increases so do the number of system metrics that must be fixed in order to provide a meaningful assessment. In many cases, this may be both undesirable and impractical. Consider again the alloy example. How would the resulting maximum temperature S-curve change if either the tensile strength or hardness thresholds were decreased or increased? While fixing these thresholds does provide a single meaningful S-curve there is a whole family of maximum temperature S-curves that could be generated corresponding to different settings of other attributes.

There are two primary disadvantages to removing the variability of a technical capability due to all other capability metrics when assessing real technologies. The first is a practical issue of data collection—seldom is there adequate historical and even current data to establish a single S-curve independent of variability due to other technology characteristics. Particularly for complex technologies, available data is far too sparse to reduce it to a single decoupled S-curve. A second disadvantage to fully decoupling a single metric from all others is the limited usefulness of the resulting S-curve. This technology S-curve is only applicable for a single setting of all other technology attributes. Should interest shift to a different setting for any of the remaining metrics a completely new assessment would have to be conducted. Furthermore, the maturity of a technology is rarely defined by a single capability attribute. Consequently, an S-curve would have to be generated for each metric of interest in order to conduct a comprehensive assessment. However, to decouple each

metric from all others during the creation of individual S-curves would not provide an accurate picture of the underlying physics as it completely neglects the interactions that exist between the metrics. A more comprehensive approach is required whereby these interactions can be accurately captured in order to provide an overall picture of technology maturity.

2.4 Time, Investment, & Engineering Effort

In the notional concept of the technology S-curve, engineering effort is the independent parameter of the abscissa. Fundamentally, the curve itself represents the level of technological capability relative to the cumulative effort invested in developing the technology. However, due to the difficulty in tracking the cumulative effort over an entire technology cycle, which may last several years or even decades, engineering effort is rarely used as the independent parameter during the practical application of technology S-curves. There are two alternative parameters that are often used in place of engineering effort: research and development investment or time. R&D investment is the most representative of engineering effort; although, it too can be very difficult to monitor over an entire technology cycle. As a result, time is most often used. The date a technology reaches a particular level of technical capability is much more readily available than either the cumulative engineering effort or R&D investment devoted to achieving that level of capability. The disadvantage to using time is that it is not always proportional to engineering effort and as a result technology S-curves based on time must be interpreted slightly differently.

Time would be an ideal replacement for engineering effort as the independent parameter of the technology S-curve only if engineering effort were constant with time. This is illustrated in Figure 7a wherein engineering effort is constant with time and as a result the S-curves based on engineering effort and time are identical. However, variability of engineering effort over time which may result from any number of

socio-economic factors prevents time from being a direct replacement for engineering effort as illustrated in Figure 7b. Note that any increase or decrease in the rate of advancement of a technology observed on an S-curve based on time may be the result of increased or decreased engineering effort over that time rather than the natural cycle of technology development. Despite this disadvantage, time has proven to be an effective replacement for engineering effort in the practical application of technology S-curves. However, some flexibility must be used in the interpretation of these curves to allow for any variation of engineering effort over time.

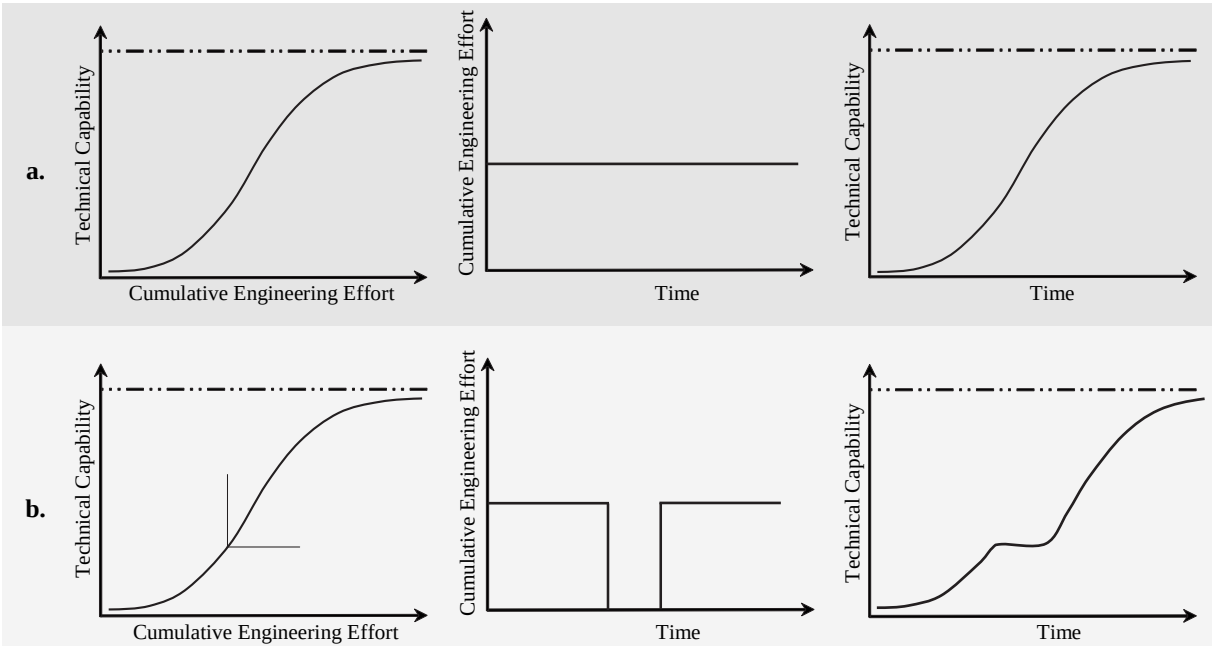

Figure 7: Engineering Effort Versus Time as the S-curve Independent Parameter

This research will be conducted using time as the independent parameter for the S-curve because of the extreme difficulty in quantifying and compiling engineering effort data. However, if such data is available the process of conducting the necessary transformation from time to engineering effort is trivial.

2.5 The Process of Technology Advancement

A technology advances along an S-curve by means of progressively more advanced hardware implementations. Despite the continuous lines used to depict S-curves, they are actually comprised of discrete points which collectively form the s-shaped curve. Each point signifies the technical capability of a specific hardware implementation or individual system within the system architecture of which the S-curve is representative as illustrated in Figure 8.

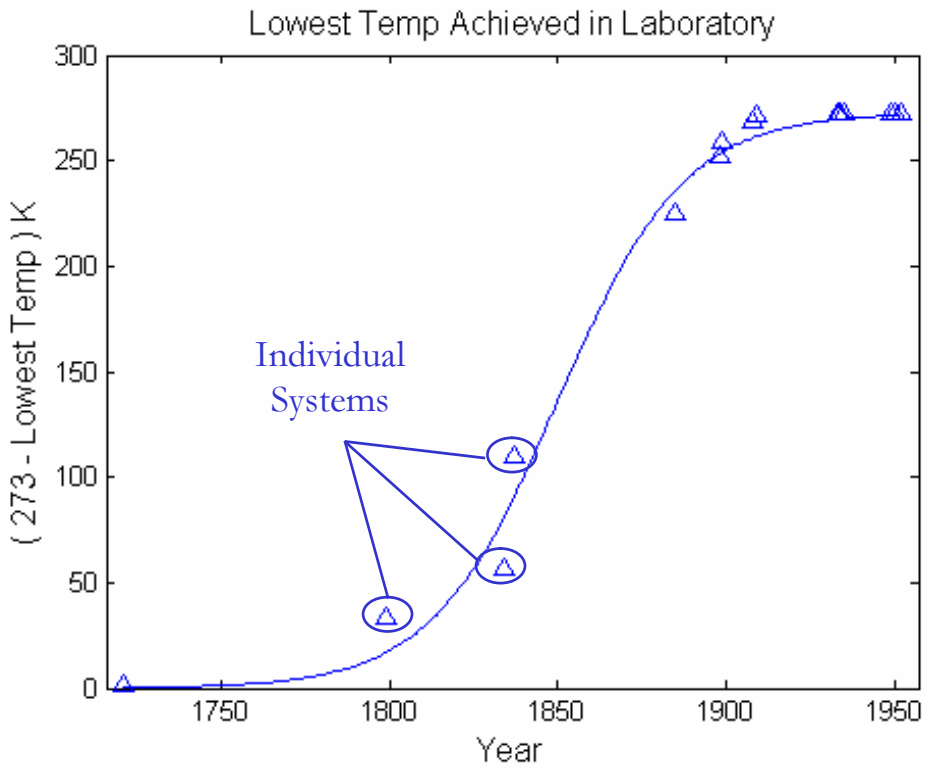

Figure 8: Individual Systems Comprising S-curve

Each individual system portrayed on an S-curve is the result of a complete design process that generally includes multiple stages of development. Consequently, all capability levels used to generate a single technology S-curve must be indicative of similar stages of development for each system incorporated into the S-curve. Incorporating capability levels representing systems at different stages of their individual

development would introduce variability within the S-curve due to the disparate stages of development for the individual systems rather than the development of the system architecture as a whole. The developmental stages of an individual system or hardware implementation can be described by Technology and Manufacturing Readiness Levels (TRLs & MRLs) [24, 25] as defined in Tables 1 & 2, respectively.

Table 1: NASA Technology Readiness Levels, reproduced from the National Research Council, [24], "Maintaining U.S. Leadership in Aeronautics: Break-through Technologies to Meet Future Air and Space Transportation Needs and Goals"

Level	Technology Readiness Description
1	Basic principles observed and reported, paper studies
2	Technology concept and/or application formulated (candidate selected)
3	Analytical and experimental critical function or characteristic proof of concept or completed design
4	Component and/or application formulated
5	Component (or breadboard) verification in a relevant environment
6	System/subsystem (configuration) model or prototype demonstrated or validated in relevant environment
7	System prototype demonstrated in flight
8	Actual system completed and flight qualified through test and demonstration
9	Actual system flight proven on operational vehicle

Evident from Table 1 is that TRLs quantify the maturity of a technology relative to its degree of operability [26]. A technology reaches the top of the scale, a TRL of nine, once the technology has been proven in an operational vehicle. TRLs have also been used as a basis for quantifying uncertainty in the expected capability of an *individual* system prior to achieving operability [27]. This is accomplished by attributing a distribution to each technology readiness level as illustrated in Figure 9. A TRL of 1 has the broadest distribution in expected capability and each subsequent distribution is narrower as the technology approaches operational maturity ($TRL =$

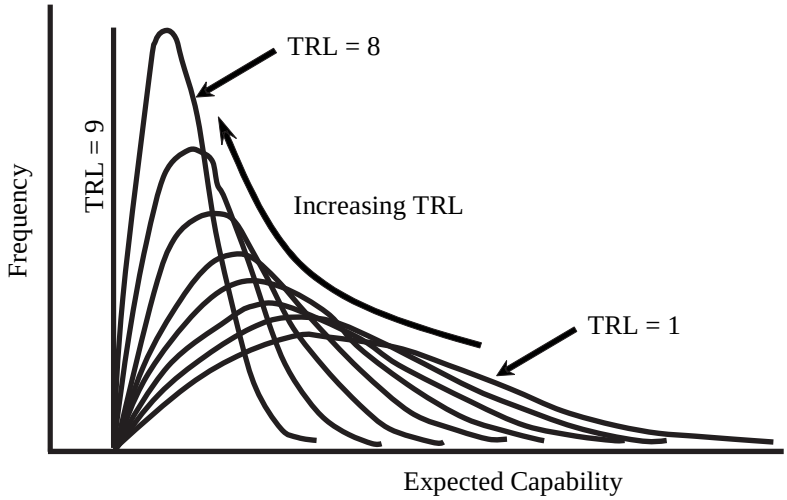

Figure 9: Relative Uncertainty of at Various Technology Readiness Levels

9) at which stage the distribution has reduced to a single level of *known* capability with no uncertainty.

The technology readiness scale which quantifies the level of operability of an *individual* system should not be confused with the technology S-curve which describes the evolution of subsequent systems in a *system architecture* relative to the architecture's upper limit. Consequently, each system comprising a technology S-curve should have achieved the same level of technology readiness. Specifically, they must have a TRL of nine as it is only then that the technical capability of a system can be known for certain.

The development of an individual system or technology along the TRL scale, from 1-9, is very different from the development of a system architecture along its S-curve. The distinction is most obvious by recognizing that all points along an S-curve depict actual operational systems. Yet, TRLs 1-5 do not describe operational systems. Furthermore, a TRL of 9, though indicating an operational system, does in no way suggest its current capability level has attained the upper limit bounding the system architecture. A technology having achieved a TRL of nine represents a

single point on a technology S-curve. Subsequent points on an S-curve result from progressively more advanced systems achieving a technology readiness level of 9 as illustrated in Figure 10. Technology readiness levels do not quantify the evolutionary advancements of operational technologies [28].

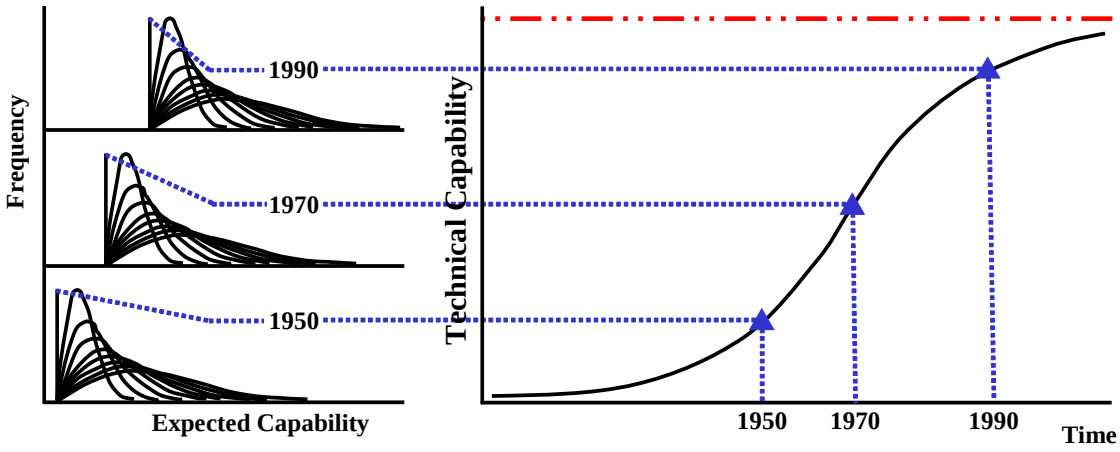

Figure 10: Relative Significance of Technology Readiness Levels and Technology S-curve

Manufacturing Readiness Levels quantify the maturity of a particular manufacturing process for a technology under develop. They emphasize the need and quantify the degree to which concurrent product and process design is implemented. The manufacturing readiness level scale has been developed to parallel the technology readiness scale. Thus an MRL of nine corresponds to a product in low rate production much like a TRL of nine corresponds to a product or technology proven in an operational flight. An additional MRL level of ten has been included to distinguish between initial low rate production and full rate production. If concurrent engineering is not employed a technology may achieve a TRL of nine while still having a relatively low MRL stalling its market introduction until manufacturing processes can be developed. Because manufacturing processes cannot be finalized until the product or technology is proven the MRL of a technology will always be equal to or lower than the technology's TRL. Technology S-curves should be formulated with systems that

have the same MRLs (9 or 10) to eliminate any variability due to different levels of producibility between subject systems.

Table 2: Manufacturing Readiness Levels defined by the National Center for Advanced Technologies [25]

Level	Manufacturing Readiness Description
1-3	Manufacturing concepts identified
4	System, component or item validation in laboratory environment
5	System, component or item validation in initial relevant environment
6	System, component or item in prototype demonstration beyond bread board, brass board development
7	System, component or item in advanced development.
8	System, component or item in advanced development. Ready for low rate production
9	System, component or item previously produced or in low rate production
10	System, component or item previously produced or in full rate production

Technology and manufacturing readiness levels are not only significant to the generation of a technology S-curve but also to the interpretation of forecasts resulting from a technology S-curve. Because all systems used to generate a technology S-curve have TRLs equal to nine and MRLs greater than eight the resulting forecasts also correspond to operational systems in low or full rate production.

CHAPTER III

BACKGROUND

The basis for this research has its foundation in three general areas of knowledge: technology forecasting, multi-attribute technology assessment, and limit identification, some of which have already been mentioned. This chapter will discuss pertinent elements of each of these fields.

3.1 Technology Forecasting

The elements of technology forecasting of interest to this research are those devoted to the prediction of a system architecture's growth as measured by the improvement in technical capability. Chapter 2 introduced the growth curve or S-curve as a potential means of forecasting such improvement. Whereas that discussion addressed the qualitative significance of the S-curve relative to the general elements of technology development, this chapter will examine the mathematical aspects of generating and forecasting technology-specific S-curves.

There are many mathematical equations that, at least in part, bear some resemblance to an S-shaped curve that can be used to describe the technology growth patterns discussed in Chapter 2. These equations can be categorized into two main groups, absolute and relative models. Absolute models quantify the technical capability, y_t, as a function of the independent parameter time, t. Conversely, relative models quantify the rate of change in technical capability, dy_t, as a function of the most recently achieved level of technical capability, y_{t-1}. These growth models have found utility for modeling biological growth patterns, sales and marketing patterns, and technology development patterns. The Logistic and Gompertz equations are most

commonly used to depict technology development. Table 3 lists several absolute and relative growth models equations.

Table 3: Commonly Used Growth Model Equations

Model Name	**Equation**
Absolute Models	
Logistic [29]	$y_t = \frac{L}{1+ae^{-bt}}$
Gompertz [23]	$y_t = Le^{-ae^{-bt}}$
Mansfield-Blackman [30, 31, 32]	$\ln\left(\frac{y_t}{L-y_t}\right) = \beta_0 + \beta_1 t$
Linear Gompertz [33]	$\ln\left(-\ln\left(\frac{y_t}{L}\right)\right) = \beta_0 + \beta_1 t$
Weibull [34]	$\ln\left(\ln\left\lvert\frac{y_t}{L-y_t}\right\rvert\right) = \beta_0 + \beta_1 \ln t$
Von Bertalanffy's [23]	$y_t = (1 - ae^{-bt})^3$
n/a [23]	$y_t = e^{a-(b/t)}$
Relative Models	
Bass [35, 36, 37]	$dy_t = \beta_0 + \beta_1 y_{t-1} + \beta_2 (t_{t-1})^2$
Nonsymmetric Responding Logistic [38, 39]	$\ln dy_t = \beta_0 + \beta_1 \ln y_{t-1} + \beta_2 \ln(L - y_{t-1})$
Harvey [40]	$\ln dy_t = \beta_0 + \beta_1 t + \beta_2 \ln(y_{t-1})$
Extended Riccati [41]	$\frac{dy_t}{y_{t-1}} = \beta_0 + \beta_1 y_{t-1} + \beta_2 (\frac{1}{y_{t-1}}) + \beta_3 \ln(y_{t-1})$

In order to make technological forecasts based on any of the above growth models, forecasters must regress the technological performance data of a technology architecture and must extrapolate the curves into the future beyond the range of available data. In this way, future technical capability is predicted. Multiple forecasters have described similar approaches to this process [8, 14, 40], which Twiss succinctly outlines in the following six steps [8]:

1. Identify the appropriate market attribute for the product of the system in which it is embedded.

2. Determine the technology parameter(s) by which the attribute can be measured.

3. Collect data for the past progress of this parameter over time.

4. Establish the natural/physical limit for the parameter using the technology being forecasted.

5. Fit an S-curve to the data which becomes asymptotic at the limiting level.

6. Consider events or other trends which may affect the future development of the technology and thereby influence the shape of the curve, i.e. the emergence of a new technology or other factor which might affect the funding necessary to drive the advance.

The accuracy of the resulting forecast, Martino notes, is dependent on the following three assumptions: the upper limit is accurately determined, the correct growth curve with which to regress historical data is selected, and historical data accurately estimates the coefficients of the growth curve [13]. Each of these requirements has a pivotal role in ensuring the accuracy of a technology forecast and will be considered in turn.

3.1.1 Upper Limit Estimations

It is imperative to estimate the upper limit of a growth curve accurately, for this can have the greatest impact on the accuracy of the forecasts resulting from extrapolating the curve. There are two approaches often employed for establishing upper limits to technology growth curves: regression and physics-based calculation. Regression is the easiest of these approaches. It involves estimating the upper limit simultaneously with the other growth curve parameters, which result from regressing against

historical data. Some researchers employ and advocate this approach [1, 42], while Martino warns against this practice, arguing that the productivity of early technology development is only minimally influenced by the upper limit [13]. Thus, historical data from the early stages of development contain little information as to the location of the upper limit. As a result, limits estimated in this manner are prone to error, and this can have a significant impact on the resulting forecast. As an illustration of this, Martino varied the upper limit to steam engine efficiency from 45 to 55 percent. Using the Logistic curve to regress available data, Martino found that the midpoint of the resultant development curve, that is, the projected shift in the technology from growth to maturity, varied across time significantly. With an upper limit of 45 percent, the midpoint of the curve projected the shift to occur in 1900. With an upper limit of 55 percent, the forecast put the shift in 1925. [43]. Martino concluded that, "even a small error in the upper limit can result in a fairly significant error in the forecast" [13].

Martino proposes that the only proper approach to upper limit estimation is to employ physics-based calculations. Forecasters perform these through the evaluation of the limits imposed by nature on a technical approach. Because the specific technical approach of a developing technology system directly affects the extent to which an estimated upper limit is meaningful, a forecaster should consult specialists in the particular field of interest [13]. For certain cases, when the need for accuracy with high confidence justifies the expense of a team of specialists, forecasters certainly should follow Martino's recommendations. For more common analyses, however, regression may be a credible option. DeBecker and Modis have further investigated the accuracy of regressing for upper limits and have attempted to quantify any error that might result from this practice [1]. Because of the conflicting opinions and the importance of upper limit estimations Chapter 6 will be devoted to these considerations.

3.1.2 Selecting a Growth Model

Selecting an appropriate growth curve to model the improvement of a technical approach as it advances towards its upper limit also has a significant impact on the accuracy of the resulting forecast. Similar to estimating upper limits, a growth curve should not be selected based on goodness of fit but on matching the behavior of the selected growth curve to the underlying dynamics of technology growth [44, 45]. Young provides a detailed comparison of growth models as applied to technology development in "Technical Growth Curves, a competition of forecasting models," [42]. Results from Young's research suggest that in general, relative models are more accurate than absolute models, and in particular the Bass and Harvey growth models perform well under most circumstances. It is expected that relative models will perform better than absolute models, because each new point in a relative model is anchored to the previous data point. One disadvantage to relative models is that they generally require a higher number of fitting parameters for which to solve than do absolute models. Of the absolute models included in Young's research, the Logistic and Gompertz models were found to provide the most accurate forecasts. Both Martino and Franses have investigated the relative appropriateness of these curves [13, 46].

The primary means by which Martino differentiates between the behavior of growth curves is by evaluating their slopes. Compare the slope of the Logistic curve in Equation 1 with the slope approximation for $y \geq L/2$ of the Gompertz curve in Equation 2, where y is the technical capability, t is time, L is the upper limit, and a and b are curve parameters.

$$\frac{dy}{dt} = \frac{by(L-y)}{L} \tag{1}$$

$$\frac{dy}{dt} = ab(L - y) \tag{2}$$

Based on these slopes, the distinction between the Logistic and Gompertz curve is clear. Change in the Logistic curve is proportional to both the progress to date, y, and the distance to the upper limit, $(L - y)$; whereas, change in the Gompertz curve is only proportional to the distance from the upper limit. This distinction between the behavior of the Logistic versus Gompertz curves can be mapped to differences in the nature of the underlying dynamics for technology development. That the slope of a growth curve is proportional to the technical capability (progress to date), y, indicates that ease of further improvement is dependent on the level of technical capability already achieved; past progress would seem to make future progress easier. Martino suggests that this momentum may result from the synergetic interaction between advancing past progress to its full potential and incorporating additional improvement [13]. This underlying assumption that future advancement is facilitated by previous progress may not always be true. In these cases, a growth curve such as the Gompertz curve may be more representative where further progress is only dependent upon the relative closeness to the upper limit $(L - y)$.

Franses provides a quantitative approach for selecting between the Logistic and Gompertz models based on the difference equations provided as Equations 3 and 4 for each the Logistic and Gompertz models, respectively, where c_1 & c_2 are constants [46]. Note that the Logistic difference equation is non-linear while the Gompertz logistic equation is linear. By conducting an auxiliary regression according to Equation 5, the appropriate model can be selected based on the significance of the parameter τ. If τ is found to be statistically significant, the Logistic curve should be selected, because the auxiliary function is non-linear; conversely, if the τ parameter is not found to be significant, then the Gompertz curve should be selected.

Additional consideration will be given to the selection of a growth model following

the formulation of the multidimensional growth models.

$$log(log(y_t) - log(y_{t-1})) \approx c_1 - k_1 t + (log(log(y_t) - log(L)) \tag{3}$$

$$log(log(y_t) - log(y_{t-1})) = c_2 - k_2 t \tag{4}$$

$$log(log(y_t) - log(y_{t-1})) = \delta + \gamma t + \tau t^2 \tag{5}$$

3.1.3 Calculating Parameter Estimates

The last assumption Martino declared is required for accurate forecasting based on growth curve extrapolation—that the parameters of the growth curve can be estimated correctly from historical data—is trivial and will not be considered at length. Both linear and non-linear regression techniques have been shown to accurately determine parameter estimates [13, 47].

Similar approaches to forecasting technological advancement by means of growth curves are presented by numerous researchers [8, 13, 14]. Twiss is the only of these to consider the interaction between multiple attributes of the same technology, each following its own individual growth curve. His consideration, however, is only notional and qualitative. He does not provide a quantitative approach for *simultaneously* generating growth curve forecasts for each technical capability of a multi-attribute technology. In fact, in order to quantitatively assess multi-attribute technologies, Twiss abandons growth curves and turns to scoring models to quantify the overall state of the art (SoA) for multi-attribute technologies [8].

3.2 Multi-Attribute Technology Assessment

The key capability that is lacking in current modeling by technology growth curves is the simultaneous consideration of multiple attributes. Although Twiss does briefly

address the need to consider the S-curves for each individual technology attribute when making development decisions for the technology, as a whole, no approach is presented for generating the S-curve for each attribute. The topic is only addressed qualitatively. There is, however, a body of literature that quantifies the merit of multi-attribute systems through scoring models and technology frontiers. The next sections review these methods.

3.2.1 Scoring Models

Scoring models are used to combine multiple technology attributes into a single technology measure, often where no physical basis exists to do so [12]. These models are often technology specific and non-unique. Two researchers may produce two distinctly different scoring models for the same set of technology attributes, both of which may adequately capture the overall technology capability. Regardless of the precise form of a scoring model as a comprehensive measure of technology capability, all have a single unifying characteristic. They convert or collapse multiple distinct technology attributes into a single, aggregate technology measure by means of a transformation. As a result, scoring models do not provide a reliable means of investigating the *interdependence* between system attributes. Rather than exploring the interdependence between attributes, scoring models ignore such interactions.

By collapsing the technology measure to a single quantity, the scoring model counters the need to accommodate attribute interactions by establishing an overall measure of merit. While this does provide the ability to assess the technology as a whole, scoring models are not equipped to capture the necessary information to simultaneously evaluate each system attribute relative to the remaining attributes. In short, this approach to technology measurement does not allow for the tradeoffs between system attributes in the development of a complex technology system. Because such comparative evaluation is one of the primary focuses of this research, scoring

models will not be investigated further here. For more information, consult Martino, who presents a systematic procedure for developing scoring models [13].

3.2.2 Technology Frontiers

Scoring models collapse a multidimensional technology into a single dimension, and as a result, they eliminate the potential to evaluate the relationship between these dimensions. Technology frontiers, on the other hand, preserve the multidimensionality of complex technologies for the purpose of exploring the relationship between a system's attributes. The single composite measure of the scoring model is represented as a surface within the framework of technology frontiers. Multiple combinations of system capabilities that have the same composite measure fall on this surface. Each surface within the context of technology frontiers represents a single level of the state of the art and each point on the surface is a unique combination of attribute values. These surfaces are often called trade-off surfaces [48], technology frontiers [13], or Pareto frontiers [49].

Frontiers are used to depict a technology in an n-dimensional space in which each dimension corresponds to a different technology attribute. A notional, two-dimensional technology frontier is shown in Figure 11. Each axis represents a different system attribute or technology capability, where each combination of technical capability represents a unique system. The curve depicts the technology frontier and represents the current state of the art—combinations of the two attributes that are presently achievable with available technology. The region of the space above the frontier represents the combinations of the two attributes that are unattainable with the current state of the art. Conversely, the region below the frontier represents the combinations of the two attributes that do not fully utilize available technology. As a result, the corresponding systems perform below the state of the art. While this notional example has been bound to only two dimensions, the same principles apply

to systems having numerous measures of technical capability and can be depicted by an n-dimensional technology frontier.

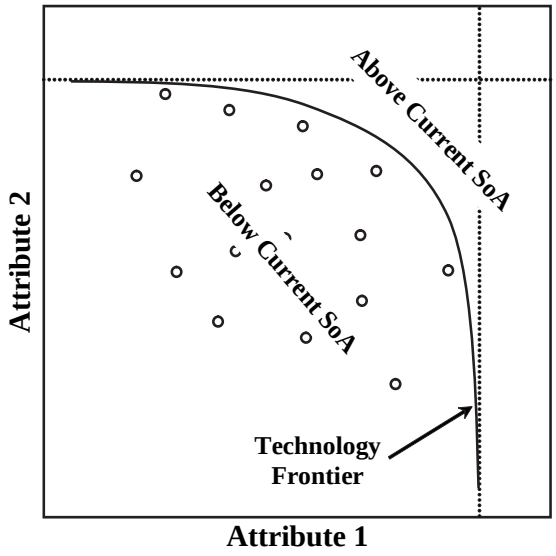

Figure 11: Notional Technology Frontier

There are two key questions of interest to researchers concerning technology frontiers—how best to define the frontier at any stage of technical development and how to forecast its growth over time.

Consider first the definition of technology frontiers. Numerous approaches have been employed to define the shape of technology frontiers, ranging from planar frontiers, where the relationship between any two attributes is to be assumed linear, to concave frontiers, as depicted in Figure 11, and convex frontiers. Alexander and Nelson developed an approach to planar technology frontiers given by Equation 6, whereby each level of the state of the art is defined by a hyperplane in an n-dimensional space as described by [50].

$$M = \beta_1 y_1 + \beta_2 y_2 + ... + \beta_n y_n \tag{6}$$

The state of the art, M, is defined as a linear combination of the system attributes, y_i; the coefficients β_i establish the relationship between each system metric and the state of the art. The coefficients of this planar frontier model, as described by Alexander and Nelson, are determined by the regression of historical data. Rather than attempting to define a numerical measure of the state of the art as in scoring models, the date of introduction for a system is used to quantify the state of the art. The coefficients are then determined by regressing the model of Equation 6 against the introduction date of a system and its corresponding technical capabilities, y_i. An advantage of this approach to defining technology frontiers is the ease of forecasting the growth for the future frontiers. One need only input a future date to investigate potential combinations of technical capability, or one could define desired levels of technical capability in order to predict the expected date for achieving those levels of capability.

There are, however, several disadvantages. The first of these is the potentially poor accuracy of projecting future levels of the state of the art. No consideration of upper limits is incorporated into the model. As a result, there is no limit to the technical capability that may be predicted for a future year. Another disadvantage is that the planar technology frontier assumes that the relationship between time and the development of each system attribute is linear. This suggests that the growth of planar technology frontiers may be accurate *only* for periods of technology development spanning the linear section of the technology S-curve. Planar technology frontiers also assume that the trade-off rate between system attribute pairs will be constant without consideration of where the system falls on the frontier. Often this does not accurately describe the underlying nature of trade-offs between system attributes. Generally, increasingly more of one attribute must be surrendered to improve each additional unit. This characteristic of technology trade-offs suggests the need for concave technology frontiers.

Dodson proposed an approach for defining concave technology frontiers by means of fitting n-dimensional ellipsoids to historical data using a model of the form shown in Equation 7 [51, 52].

$$1 = \sum_{i=1}^{n} \left(\frac{x_{i,j}}{c_i}\right)^2 \tag{7}$$

Here n is the number of system attributes included in the model; x is the i_{th} value of the j_{th} system; c_i is the ellipsoid intercept of the i_{th} axis [13]. The result of Dodson's approach for two system attributes is a technology frontier defined by the first quadrant of an ellipse as shown in Figure 12. Note the increasing quantity of y_2 relinquished for each additional unit of y_1 while moving left on the curve and vice versa when moving to the right. Martino later modified Dodson's work by allowing any even exponent in Equation 7 [53]. The result of raising this exponent increases the "squareness" of the frontier, as shown by the remaining curves of Figure 12.

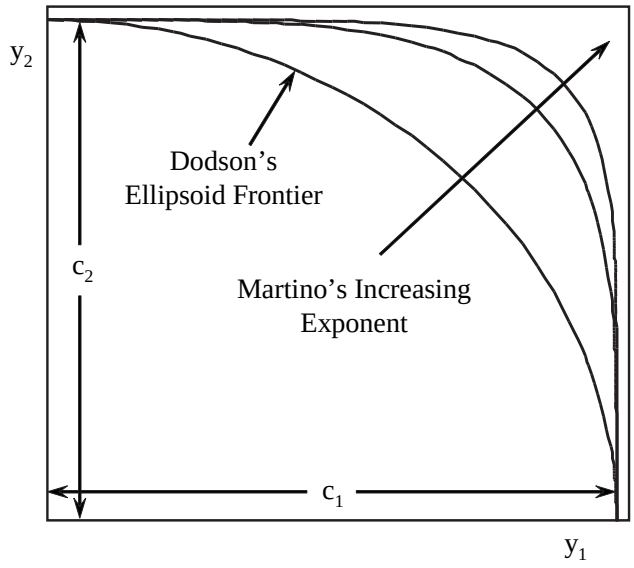

Figure 12: Notional Ellipsoid Frontier

Both Dodson's and Martino's approaches are implemented in a similar manner. Analysts compile a database of existing attributes, each at the same level of the state of the art. An ellipsoid frontier is then fit to the data using the model of Equation 7. The resultant expression describes the technology frontier for that particular level of the state of the art.

Another approach to evaluating technology frontiers is Data Envelopment Analysis (DEA). Rather than attempting to fit a predefined function through data of a common technological level, DEA establishes an envelope which is anchored to the most advanced systems within a historical database [54, 55]. A notional envelope is illustrated in Figure 13.

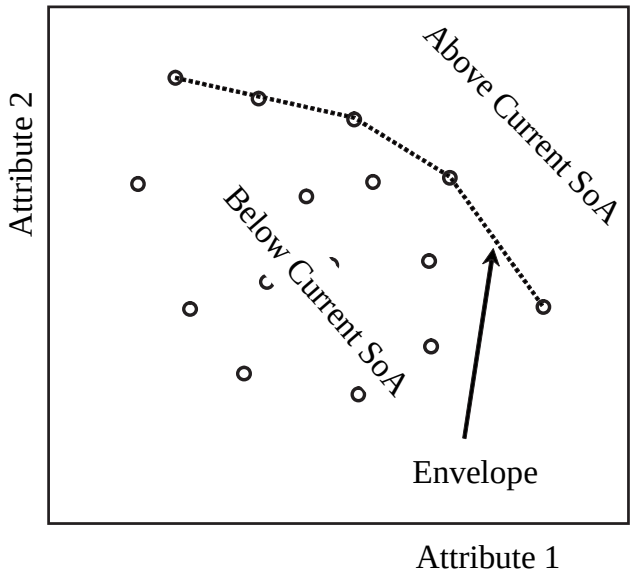

Figure 13: Data Envelopment Analysis

The discussion has considered several mathematical models used to represent technology frontiers. Now it will turn to forecasting their growth into the future. Few detailed approaches have been identified to address this issue. As already discussed, one such approach is inherent in the definition of planar technology frontiers by Alexander and Nelson [50]. The frontiers are defined by a specified year capability (or state of the

art), and in this model forecasting is simply a matter of extrapolating the regressed model into the future. These extrapolations are suspect because they assume a linear relationship between technology development and time. Also, with this approach, a researcher is bound to the contrived linear relationship between system attributes, which describes only limited situations that may or may not be of interest.

Another approach to forecasting technology frontier growth is proposed by Martino and only generally described here [13]. This approach requires that a researcher collect several successive sets of data. Each of these sets must contain systems of varying attribute capabilities, yet each also represents a common level of the SoA. Each set of data is then regressed using an appropriate frontier model. The separation between successive frontiers is evaluated, and an appropriate forecast for future frontiers is extrapolated accordingly. However, no formalized approach for making this forecast is proposed. A disadvantage to this approach is the amount of historical data required. Such an extensive data requirement can be an inhibiting factor in attempting to forecast most technologies in this manner.

3.3 Technology Impact Forecasting

Discussion has thus far been directed to the assessment of technology development based solely on the past improvements that have been realized in system-level attributes. An approach to forecasting has been presented whereby future levels of technical capability are predicted by extrapolating appropriately defined growth models from the pattern of past development. No consideration has yet been given to the specific technical changes required by a system in order to realize forecasted levels of technical capability.

Technology Impact Forecasting (TIF) is a systematic method for identifying the specific changes required to a baseline system to provide the greatest potential for overall system improvement according to customer preferences [56]. By means of

modeling and simulation, TIF quantifies the system level departure from a specified baseline resulting from the infusion of a new or alternative technologies as quantified by technology metrics. TIF possesses the necessary capability to identify the specific technological changes required to advance a system along its metric-specific, technology growth curve. The remainder of this section will be devoted to a description of the TIF methodology.

The first step to Technology Impact Forecasting is devoted to framing a design problem in terms of customer requirements, available budget, and specified time frame. The objective is to translate customer wants and needs, "the voice of the customer," into quantifiable economic and engineering terminology, the "voice of the engineer." These quantifiable figures of merit, or metrics, form the basis of comparison to judge the relative goodness of design alternatives [57].

Defining the concept space encompasses identifying both the alternative concept space and the design space. These form the basis from which potential systems can be selected to satisfy customer requirements. The alternative concept space is defined by all possible system configurations. The purpose of the alterative concept space is to help prevent the exclusion of possible design alternatives from consideration. One alternative concept, usually indicative of current capability, is selected as the baseline concept to investigate system feasibility [57].

The design space is defined by identifying the physical design parameters or control variables over which the designer has control [58]. These control variables form an n-dimensional coordinate system, a subspace of which is the design space. The bounds of the design space are defined according to specified deviations of the control variables from the baseline system.

Modeling and Simulation (M&S) is used throughout the TIF approach to facilitate rapid assessment of alternative concepts with minimal expenditure of time and money. Despite its heavy dependence on a M&S tool, TIF is not model or system specific.

It has been developed generally to be used with any system for which a M&S tool possessing several basic features can be found. These required M&S characteristics are outlined in References [57, 59]. The purpose of the M&S tool is to track the dependence of quantifiable system metrics on the design space parameters, or control variables.

M&S is used to track variation in the system metrics that result from changes in the control variables spanning the entire design space. In effect, the design space, as defined by the control variables and corresponding ranges, is mapped to the system metrics by means of the M&S tool. As a result, the system metrics can be determined for any combination of control variables. In order to evaluate numerous possible combinations, the M&S is commonly replaced with a metamodel which is then linked with a Monte Carlo simulation [60, 61, 62, 63, 64]. This linkage allows for the entire design space to be explored as defined by combinations of control variable settings [57].

The design space is then investigated for system feasibility—systems that meet or exceed the targets or constraints specified by the customer. The fraction (if any) of the design space that lies within the customer's constraints is identified. This subspace is called the feasible space. If adequate feasible space is not found, TIF simulates the infusion of new or alternative technologies to the baseline system as quantified by technology metrics. Kirby defines a technology metric as "a standard of measurement used to define the impact of a generic technology area ... on the system and includes benefits and degradations," [56].

A new design space is generated based on these technology metrics, or disciplinary metrics, and subsequently searched for feasible space. In this way, TIF identifies both the disciplinary metrics which require technological development and the magnitude of that improvement that will allow system level targets and constraints to be achieved. TIF provides the necessary framework within which specific technical improvements

can be identified that enable a technology to evolve along its technology growth curve [56, 57].

CHAPTER IV

RESEARCH FOCUS AND SCOPE

Perpetual motion machines always fail. There are numerous cases that make this plain. The failure, however, does not explain why perpetual motion machines will not, cannot work. Some people keep hoping and keep trying to cheat the laws of thermodynamics. Perhaps, they must reason to themselves, it is a matter of the particular design and not the impossibility for design. Because they do not or cannot recognize that the pertinent physical limits disallow any design space for their simple—yet impossible—problem, they are doomed to fail. Even for design problems in which the physical limits allow for successful design of one or more attributes considered individually, that same success may not be possible when all the attributes are required of a single system. Remember, the *Thomas W. Lawson* failed because her designers did not adequately consider the interaction between vital system attributes, specifically speed and stability. It was possible to achieve the target speeds through an extensive set of masts and sails, yet the system as a whole failed. The vessel also had to be stable, and the weighty assembly of masts was fatefully lacking in terms of that attribute.

In the case of the *Thomas W. Lawson*, a carefully constructed technology growth model would have revealed the challenges preventing the success of the target systems. In the case of the *Thomas W. Lawson* a multidimensional growth model could organize the requirements (e.g. for speed, stability, etc.) and their limits in such a way that it would be apparent how the treatment of one attribute would likely affect—maybe compromise or enhance—the other attributes. Although the components of such a model are evident in the literature on technology development and

evaluation, a multidimensional growth model suitable for quantitative assessment and forecasting does not exist.

The objective of this research is to formulate an approach to assess and forecast the maturity of technologies that have multiple objectives relative to their upper limits in order to determine the availability for further improvement within their respective technology architectures.

4.1 Requirements for the Assessment and Forecasting Method

Technology growth models will serve as the foundation for the proposed formulation. Research will focus on extending the practical application of the technology growth curve from modeling only single-objective systems to comprehensively modeling complex systems that have multiple objectives. The intent is to transform the growth model from a notional concept of technology maturation to a practical tool for strategic decision-making. This research will accomplish this goal by developing a form of gap analysis that will focus on technology growth models and will provide answers to the following research questions:

RQ1 What is the current state of the art as defined by achievable combinations of attribute capabilities?

RQ2 What is the technology potential of any one attribute relative to specified levels of the remaining attributes?

RQ3 Has the point of diminishing returns been reached for any of the system attributes?

RQ4 What is the forecasted improvement for each attribute relative to the remaining attributes?

Answers to these questions would provide decision makers with the necessary information to gauge the potential of a technology architecture and establish reasonable program goals for its further development or retirement.

4.2 Improvements to the State of the Art

The previous two chapters offered a general introduction to and evaluation of existing models of assessment and forecasting for technology development. In several ways, S-curves offer the best current practice for understanding a technology's development. Current S-curve models, however, are not sufficient to meet the requirements of a functional assessment and forecasting model. There are several general aspects of technology S-curve modeling that will require further development in order for these questions to be answered. These include upper limit determination, technology growth forecasting, and quantifying uncertainty. Even for simple systems having a single functional objective, these aspects of technology S-curve modeling require further development to ensure meaningful results. Moreover, for technology S-curves to become a practical tool for the assessment of complex systems, it is necessary to develop an approach that incorporates *multiple* technology attributes into technology S-curve modeling. To do so requires extensive development beyond the current use of growth curves for technology modeling.

The nature of multi-objective systems will not allow all of the system objectives to be maximized in a single design; recall the *Thomas W. Lawson*. Therefore, any one historical system may be designed to favor a particular system objective with the result that the remaining system objectives perform seemingly below the state of the art. The actual systems that designers create do not, cannot accurately reflect the full range of possibilities for all attributes, that is, all of the potential design space. Actual systems are always subject to compromise, and it is more helpful to track the range of options available at a given time than to track the history of

compromises. Consequently, it is necessary to develop an approach for historical data reduction that is able to capture these interactions between system attributes and modeling their individual historical trends on coupled technology S-curves. Finally, the approach formulated to forecast the S-curves into the future must also capture those interactions providing accurate projections of attribute maturity levels based on their interdependence.

This research will focus on the formulation of a multidimensional approach to technology growth modeling and forecasting in order to capture the overall level of technology maturity relative to upper limits.

4.3 Hypotheses

As stated, the objective of this research is to formulate an approach to assess and forecast the maturity of multi-objective technologies relative to their upper limits in order to determine the technology potential within their respective architectures. In order to formulate such an approach, a revolutionary forecasting model must be developed, for which attribute upper limits must be established to within an acceptable degree of certainty. The hypotheses of this research formulated to achieve these objectives are as follows:

Hypothesis A *The proven success of technology growth models for the forecast of a single attribute can be extended to also accurately model multiple system attributes by precisely defining their mathematical significance to technology frontiers.*

Hypothesis B *Knowledge of attribute upper limits for multi-attribute technologies can be identified by both physics-based approaches and by regressing limit-dependent growth models against available historical data.*

Hypothesis C *Analysis methods founded on exergy and work potential provide a suitable framework for the identification of upper limits to select attributes of energy-based systems.*

CHAPTER V

MULTIDIMENSIONAL GROWTH MODEL FORMULATION

The technology growth model introduced in Chapter 2, the S-curve, provides a clear means for the assessment of a technology's current capability and expected growth relative to an impending upper limit. Because the current formulation of growth models is restricted to the consideration of only one attribute the utility of the technology S-curve for the assessment of complex systems is limited. Conversely, the scoring models and technology frontiers presented in Chapter 3 provide for the evaluation of multiple technology attributes but provide little capability for the assessment of these relationships relative to attribute upper limits or time. This chapter devotes itself to the formulation of multidimensional growth models that combine the desirable characteristics from technology frontiers and S-curves resulting in a single model for the simultaneous assessment and forecast of multiple attributes relative to their respective upper limits.

5.1 Multidimensional Growth Model Formulation

The formulation of multidimensional growth models is based on understanding the relationship between technology frontiers and technology growth models. Consider the illustration provided in Figure 14. Each axis of the technology frontier corresponds to one of two measures of technical capability describing a subject technology. Each curve within the technology frontier plot represents the feasible combinations of technical capabilities that can be achieved at any single point in time. A growth model or S-curve is also a frontier which forms a boundary of achievable levels of

technical capability for a single metric at progressive points in time given constant settings for all other system metrics [8]. This is the underlying principle that enables the formulation of multidimensional growth models, and it can be restated as:

Assertion 1 *The feasible levels of capability that can be achieved by any one attribute of a complex technology advance over time according to a technology S-curve provided all other attributes remain constant.*

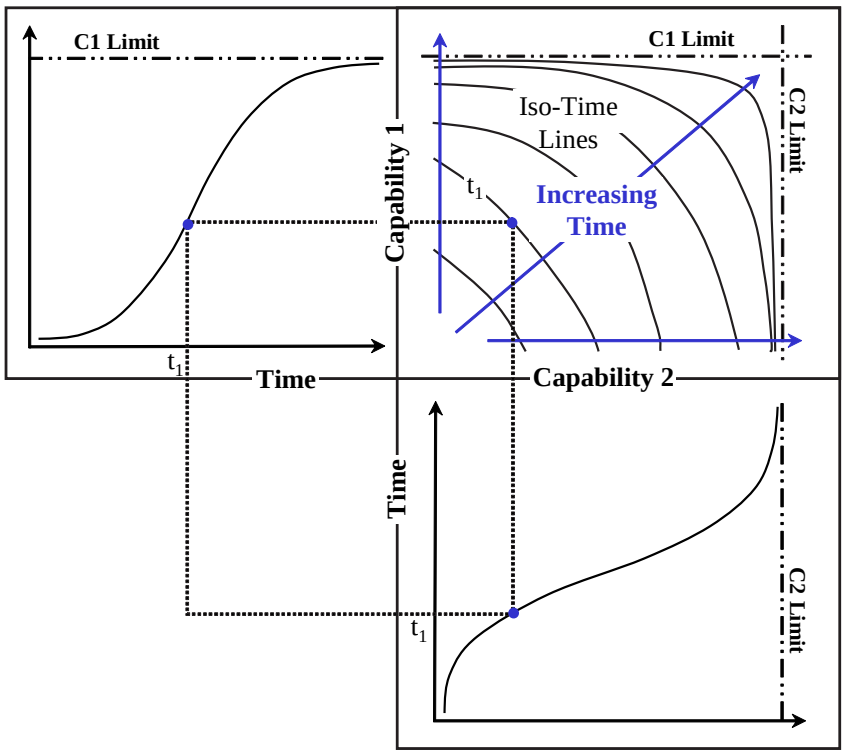

Figure 14: Technology Frontier and S-curve Relationship

Consider this statement with respect to a technology that has two measures which completely describe the technology's performance as illustrated by the technology frontier of Figure 15. If the metric of the abscissa axis, Capability 2, is held constant indicated by the vertical line, then the rate of advancement of Capability 1 along that line can be described by a technology S-curve such as illustrated in the right side of the figure. This relationship is based on the assumption that engineering effort

remains constant over time implying that both the willingness and resources exist to further advance Capability 1. Note from Figure 14 that time advances along the vertical line which denotes a fixed setting for Capability 2.

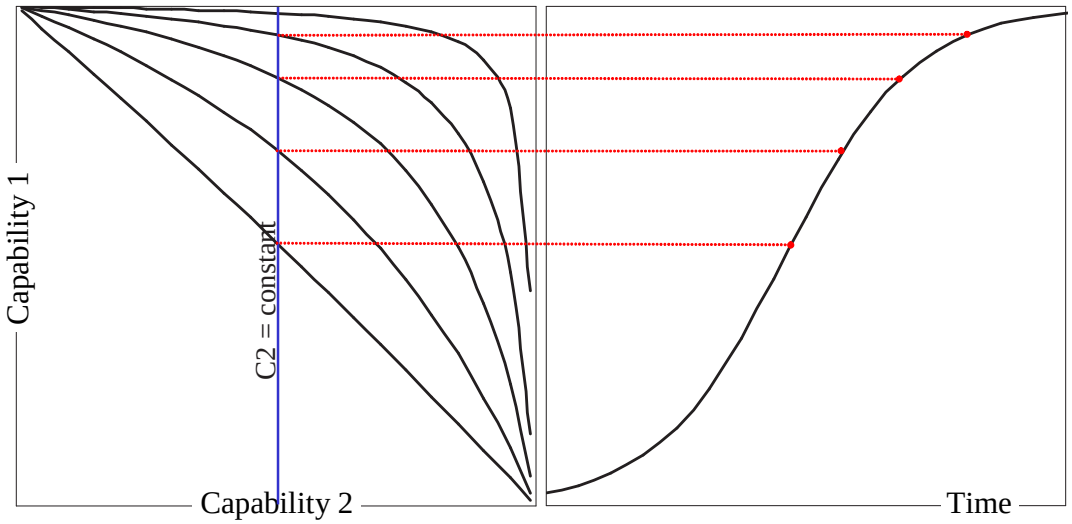

Figure 15: Technology Frontier and S-curve Relationship

Now observe the impact of increasing Capability 2 on the Capability 1 S-curve as shown in Figure 16. With Capability 2, y_2, fixed at level A the corresponding growth curve results as designated A in the right side of Figure 16. With an increase in Capability 2 to $y_2 = B$ each point of the S-curve designated A is shifted downward forming the new S-curve designated B. Note, however, the magnitude of that downward shift varies along the length of the S-curve approaching zero at each extreme. If the assumption is made that the limit of each attribute can be simultaneously achieved as time approaches infinity, then this down shift, in fact, approaches zero as time goes to infinity. An equivalent statement of this assumption is that the limit of Capability 1 is unchanged as a result of changes in Capability 2. Consequently, this downward shift can also be modeled as a rightward shift. This suggests that the influence of a second metric on a single dimension S-curve can be quantified as a shift in time.

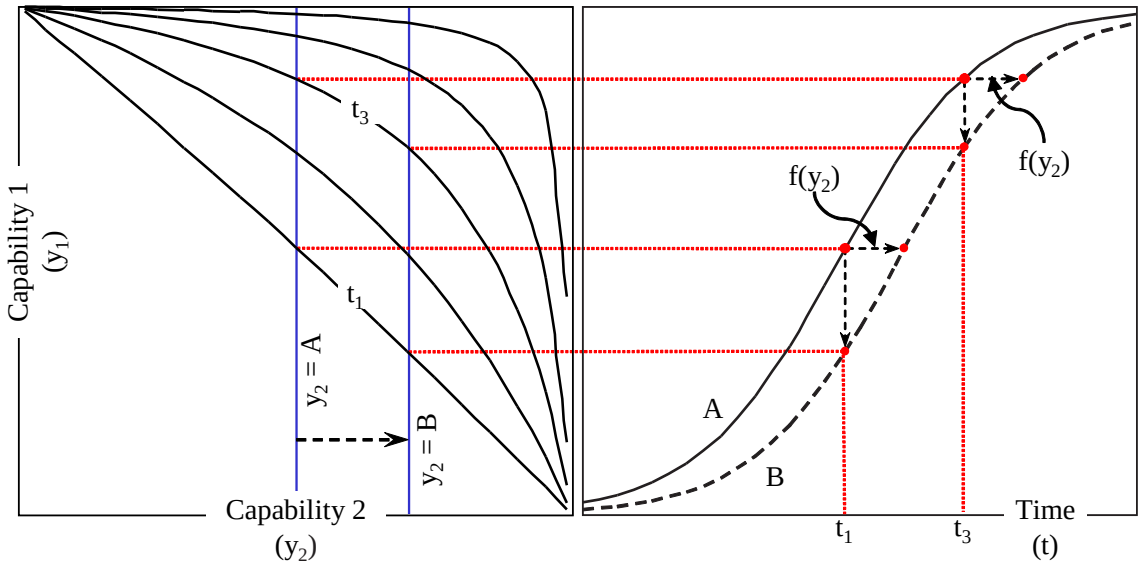

Figure 16: Impact of an Additional Attribute on an Attribute Specific S-curve

Very important to note at this point is that neither S-curve *A* nor *B* is intended to model the actual path of improvement for Capability 1, but two possible pathes given a specified setting of Capability 2. For as many settings of Capability 2 that are possible at a single point in time, so number the S-curves that describe possible pathes for the development of Capability 1. The objective of this formulation is to capture the variability of a metric-specific S-curve as a function of changes to additional metrics. In this way, this formulation of multidimensional growth models is able to capture the growth pattern of a single dimension, which otherwise would not appear smooth due to the variability of other dimensions of capability. Given the assumption that the limit of each attribute is not influenced by the level of capability of the remaining attributes, the variability of a metric-specific S-curve can be modeled as a left- or rightward shift. The magnitude of that shift is some function of the remaining metrics. As illustrated in Figure 16 the rightward shift of the Capability 1 S-curve is a function of magnitude of Capability 2. A basis for determining what this function should be can be established by considering the functional form of the Logistic equation provided here as Equation 8. The graphical observation of the relationship between

time and Capability 1 and Capability 2 can be generically described by Equation 9, where y_1 quantifies the magnitude Capability 1 and y_2 quantifies the magnitude Capability 2. Likewise, Equation 10 generically describes the Capability 2 S-curve provided Capability 1 is permitted to change. Given that both Equations 9 and 10 independently describe the relationships between y_1 and y_2 and time they can be solved to yield $f(y_1)$ and $f(y_2)$.

$$y = \frac{L}{1 + ae^{-bt}} \tag{8}$$

$$y_1 = \frac{L_1}{1 + a_1 e^{-b_1(t - f(y_2))}} \tag{9}$$

$$y_2 = \frac{L_2}{1 + a_2 e^{-b_2(t - f(y_1))}} \tag{10}$$

Solving Equations 9 and 10 for time and equating yields Equation 11 from which the solutions for $f(y_1)$ and $f(y_2)$ can be concluded as provided by Equations 12 and 13, respectively.

$$f(y_2) - \frac{1}{b_1} ln\Big(\frac{L_1 - y_1}{a_1 y_1}\Big) = f(y_1) - \frac{1}{b_2} ln\Big(\frac{L_2 - y_2}{a_2 y_2}\Big) \tag{11}$$

$$f(y_1) = -\frac{1}{b_1} ln\Big(\frac{L_1 - y_1}{a_1 y_1}\Big) \tag{12}$$

$$f(y_2) = -\frac{1}{b_2} ln\Big(\frac{L_2 - y_2}{a_2 y_2}\Big) \tag{13}$$

Inserting these solutions back into Equations 9 and 10 result in the two-dimensional growth models of Equation 14 and 15 which consequently are the exact same model—one solved for y_1 and the other for y_2. The model of Equation 14 captures the S-curve

describing the y_1 metric relative to the level of capability specified for y_2. Similarly, solving Equation 14 for y_2 results in Equations 15 the S-curve describing y_2 at a specified capability of y_1. This same model that describes the y_1 and y_2 S-curves relative to one another can also be used to define the technology frontier by solving for y_1 at a specified date over a range of y_2 capability levels.

$$y_1 = \frac{L_1}{1 + a_1 e^{-b_1\left(t + \frac{1}{b_2} ln\left(\frac{L_2 - y_2}{a_2 y_2}\right)\right)}} \tag{14}$$

$$y_2 = \frac{L_2}{1 + a_2 e^{-b_2\left(t + \frac{1}{b_1} ln\left(\frac{L_1 - y_1}{a_1 y_1}\right)\right)}} \tag{15}$$

The two dimensional growth model proposed in Equations 14 and 15 seems to capture the relationships between time and each system metric relative to their respective upper limits, holding promise for providing insight into many of the research questions posed throughout this document. Two considerations should be taken into account before proposing a finalized multidimensional growth model. The first of these can be addressed with respect to the Logistic growth model on which Equations 14 and 15 are based shown here as equation 16. This growth model assumes that the initial level of capability of the system metric y is zero from which it advances towards its upper limit L. Many system metrics, however, may have non-zero starting points, which will be introduced into the model as an offset, y_o, as shown in Equation 17. Note that the limit is decremented by the offset to prevent y_1 from ranging between the lower bound y_o and the upper bound $L + y_o$ as opposed its actual upper limit L.

$$y = \frac{L}{1 + ae^{-bt}} \tag{16}$$

$$y = \frac{L - y_o}{1 + ae^{-bt}} + y_o \tag{17}$$

The second consideration involves the redundancy of parameters a_1 and a_2 in Equations 14 and 15. This redundancy can be made apparent by first rearranging the Logistic growth model of Equation 16. Equation 18 provides an equivalent form of this Logistic equation in which the parameter a has been moved to the exponential, and in Equation 19 the constant $ln(a)/b$ has been replaced with the constant c.

$$y = \frac{L}{1 + e^{-b(t-ln(a)/b)}} \tag{18}$$

$$y = \frac{L}{1 + e^{-b(t-c)}} \tag{19}$$

When this form of the Logistic equation is used to generate a two dimensional growth model using the same approach employed to generate Equations 14 and 15, Equation 20 results. Note that the constants c_1 and c_2 can be replaced by a single constant a as shown in Equation 21, and finally combing this result with the y_o offset results in the two-dimensional growth model of Equation 22. A three-dimensional surface plot of this equation is shown in Figure 17, wherein each limit has been set to one, each y_o has been set to zero, each b has been set to 0.1, and a has been set to 200. Note each metric-specific S-curve and the technology frontier formed by passing appropriate planes through this surface.

$$y_1 = \frac{L_1}{1 + e^{-b_1\left(t-c_1-c_2+\frac{1}{b_2}ln\left(\frac{L_2-y_2}{y_2}\right)\right)}} \tag{20}$$

$$y_1 = \frac{L_1}{1 + e^{-b_1\left(t-a+\frac{1}{b_2}ln\left(\frac{L_2-y_2}{y_2}\right)\right)}} \tag{21}$$

$$y_1 = \frac{L_1 - y_{o,1}}{1 + e^{-b_1\left(t-a+\frac{1}{b_2}ln\left(\frac{L_2-y_2}{y_2-y_{o,2}}\right)\right)}} + y_{o,1} \tag{22}$$

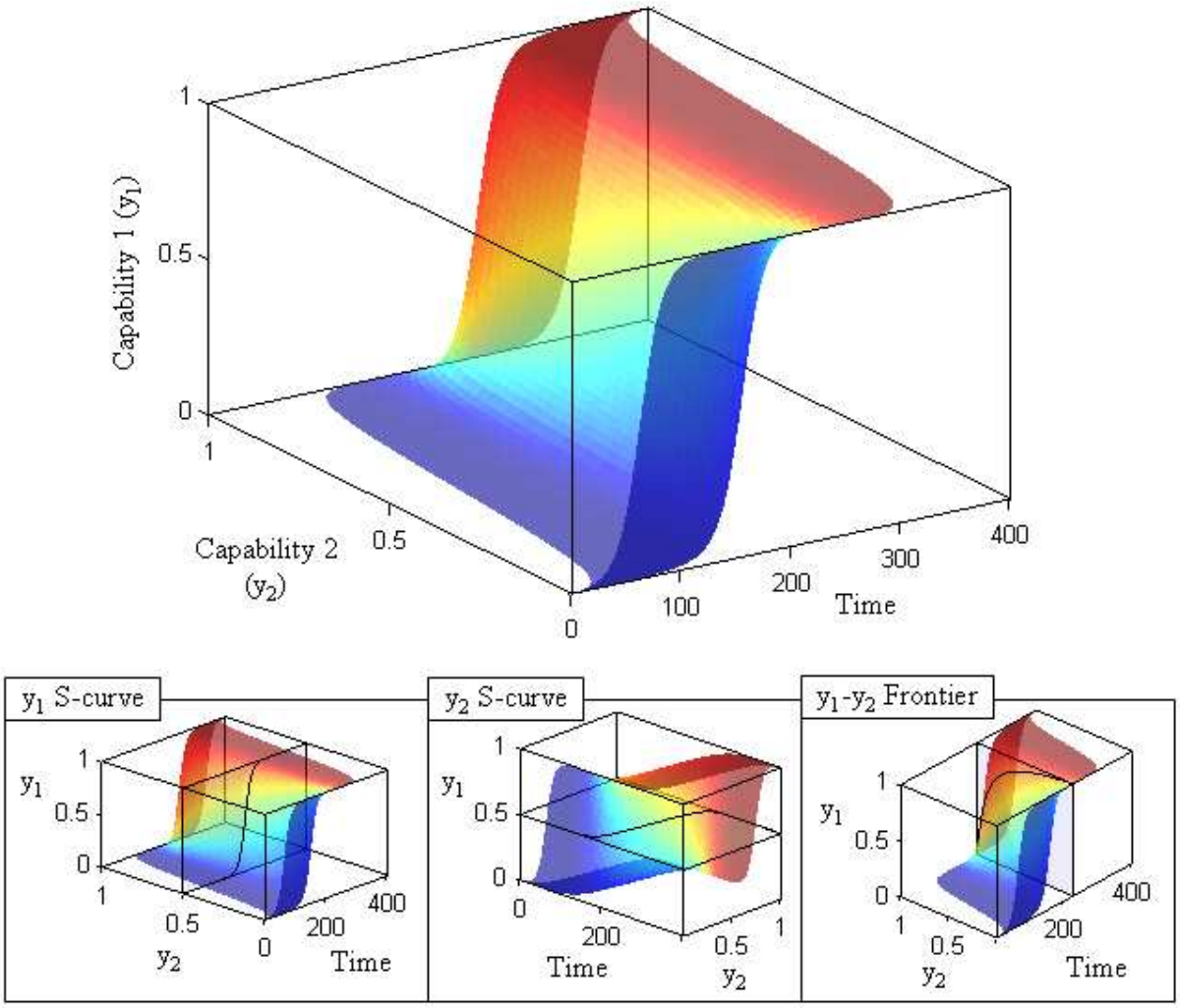

Figure 17: Three-Dimensional View of a Multidimensional Growth Model

The final step to establishing a multidimensional growth model is to extend this formulation to n-dimensions. This is easiest to visualize when Equation 22 is solved for time, as shown in Equation 23. In this form it is clear that each dimension or metric is mathematically represented by each of the logarithmic terms and can be extend to n-dimensions according to Equation 24. Equation 25 provides this same n-dimensional growth model solved for a single attribute, y_j.

$$t = a - \frac{1}{b_1} ln\Big(\frac{L_1 - y_1}{y_1 - y_{o,1}}\Big) - \frac{1}{b_2} ln\Big(\frac{L_2 - y_2}{y_2 - y_{o,2}}\Big) \tag{23}$$

$$t = a - \sum_{i=1}^{n} \frac{1}{b_i} ln\Big(\frac{L_i - y_i}{y_i - y_{o,i}}\Big) \tag{24}$$

$$y_j = \frac{L_j - y_{o,j}}{1 + e^{-b_j\left(t - a + \sum_{i=1}^{n} \frac{1}{b_i} ln\left(\frac{L_i - y_i}{y_i - y_{o,i}}\right)\right)}} + y_{o,j} \tag{25}$$

Recall that several assumptions were required to result in this multidimensional growth model. First was the assertion that the feasible levels of capability achieved by any one attribute of a complex technology advance over time according to a technology S-curve provided all other attributes remain constant. Second, the resulting metric-specific S-curves are based on the assumption that engineering effort remains constant over time, in effect, both willingness and resources exist to further advance that metric. And third, the limit of each metric is assumed constant regardless of settings for the remaining metrics. In addition to this assertion and these two assumption one additional limitation must be specified for the resulting multidimensional growth model (MDGM). Because the model parameters a and each b_i will be estimated based on regression with historical data, the dimensions of capability, or metrics, included in the model must be independent—any correlation between two metrics will result in a misrepresentation of the significance of those metrics within the model.

There is one notable model characteristic resulting from these assumptions that warrants additional discussion. That characteristic is the manner in which the model is able to capture both the growth of each attribute over time and the interaction, or tradeoff, between those dimensions of capability. The accuracy with which the multidimensional growth model is able to capture each of these behaviors reduces to a question of sufficient degrees of freedom within the model. The Logistic MDGM of Equations 24 and 25 has n degrees of freedom—one for each dimension of capability

as modeled by each b_i. Note that each b_i defines the "steepness" of the growth curve modelling its corresponding dimension. This "steepness" as quantified by b_i also defines the rate of exchange, or tradeoff, between the other dimensions of capability. This dual significance of b_i is a direct result of the underlying assertion and subsequent assumptions put forward during the formulation of the MDGM.

Recall that the increase in one dimension of capability, y_2, impacts the S-curve of another dimension, y_1, by shifting it to the right. This results in a lower capability level for y_1 which suggests a reduction in the aggregate engineering effort, or time, invested to advance y_1. The magnitude of this reduction in engineering effort or time devoted to y_1 is exactly equal to the the increase in engineering effort or time needed to accommodate the higher capability level of y_2. This increase in engineering effort or time required to achieve a higher capability level of y_2 is inversely proportional to the "steepness" of its corresponding growth curve as quantified by b_2. Furthermore, the decrease in the y_1 capability level resulting from diverting engineering effort or time to y_2 is also inversely proportional to the "steepness" of its corresponding growth curve as quantified by b_1. In this way, the interaction, or tradeoff, between dimensions of capability is modeled by the same degree(s) of freedom that define the rate of growth in a single dimension.

5.2 Composite Growth Model

The proposed multidimensional growth model (MDGM) of Equation 24 provides the ability to assess the level of capability for each metric relative to its respective upper limit. This model even provides the rate of advancement for each individual metric at any point in time, although in this form it provides limited insight into the rate of growth for the system architecture as a whole. A composite measure is desired that quantifies the rate of growth of the technology as a whole relative to a generalized

upper limit. Consider that if each metric characterizing the capability of a system advances in time according to an S-curve, then the composite measure of the technology should also advance over time according to a similar growth model. This composite measure can be visualized in Figure 18, wherein if each dimension of capability evolves according to a Logistic curve, then the composite growth of the technology should also evolve according to a Logistic curve. Starting with the Logistic equation used to derive the above MDGM shown here as Equation 26, a suitable composite measure will now be derived.

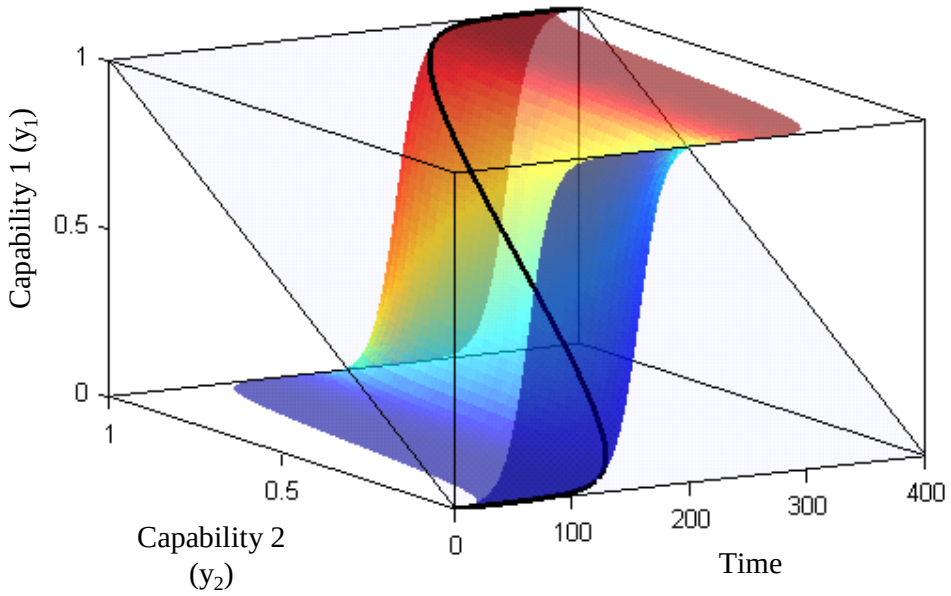

Figure 18: Three-Dimensional View of the Composite Technology Growth

$$y = \frac{L - y_o}{1 + e^{-b(t-a)}} + y_o \tag{26}$$

Before the discussion investigates settings for each model parameter, consider the desired behavior of the composite model. The objective of the composite model is to capture the overall state of a technology in a single measure wherein the state

of the technology is quantified by the technical capability of each metric relative to its respective upper limit. Consequently, if all technical capabilities are at the same fraction of their respective upper limit, the composite model should also be at that same fraction of its upper limit. In effect, the composite growth model describes the growth of the technology over time, given that each metric advances towards its upper limit at the same rate. Even if all metrics describing a technology do not advance at the same rate, which is more commonly the case, the composite model should still capture the collective growth of the metrics and as a result the growth of the technology as a whole.

With this as the basis of the composite model, consider the specific parameters of the Logistic curve in Equation 26. Because the composite growth model does not directly describe a physical quantity but the fractional improvement of a collection of metrics, the bounds, y_o and L, cannot be determined by physics-based analysis but can be defined according to any scale describing the relative growth of the technology. Zero and one are obvious choices to bound the composite model resulting in Equation 27 where the growth curve parameters b_c and a_c must be defined according to the regression parameters of the MDGM. This can be accomplished by solving both the composite growth model and the MDGM for time and equating. This results in Equation 28 from which it is clear that $a_c = a$. Thus, Equation 28 reduces to Equation 29. Recall that the composite model is defined at any point in time as the level of capability that can be simultaneously achieved by all metrics relative to their total range of capability—i.e. all $y_i/(L_i - y_{o,i})$ are equal. Thus all $(L_i - y_i)/(y_i - y_{o,i})$ are also the same and equal to $(1 - y_c)/y_c$ revealing that $b_c = (\sum 1/b_i)^{-1}$. This completely defines the composite growth model of Equation 27, quantifying the growth of the technology as a whole. Note that given settings for each system metric y_i, the composite measure, y_c can be found according to Equation 30.

$$y_c = \frac{1}{1 + e^{-b_c(t-a_c)}} \tag{27}$$

$$a_c - \frac{1}{b_c} ln\Big(\frac{1-y_c}{y_c}\Big) = a - \sum_{i=1}^{n} \frac{1}{b_i} ln\Big(\frac{L_i - y_i}{y_i - y_{o,i}}\Big) \tag{28}$$

$$\frac{1}{b_c} ln\Big(\frac{1-y_c}{y_c}\Big) = \sum_{i=1}^{n} \frac{1}{b_i} ln\Big(\frac{L_i - y_i}{y_i - y_{o,i}}\Big) \tag{29}$$

$$y_c = \Big(1 + \prod_{i=1}^{n} \Big(\frac{L_i - y_i}{y_i - y_{o,i}}\Big)^{b_c/b_i}\Big)^{-1} \tag{30}$$

5.3 Alternative Growth Models

The multidimensional growth model presented in Equation 24 is only one of a family of potential models that can be used to assess technology architectures. It assumes that the development of each technology attribute can be described by a Logistic equation. Similar MDGMs can be development by assuming other growth curve relationships between each technology attribute and time. Because of the gross functional difference between absolute and relative growth models, the discussion will consider each in turn.

5.3.1 Absolute Growth Models

Three additional MDGMs were formulated in a similar manner to Equation 24 and are listed in Table 4. Each is based on different absolute growth curves. Appendix B outlines in detail the specific steps taken to create the remaining three models. Each of the four technology assessment models presented in Table 4 have slightly different characteristics and these can be evaluated by considering the differences between the S-curves on which each model is based. Some of the key characteristics for each S-curve equation are listed in Table 5 for comparison. To facilitate discussion, each curve has been designated as A, B, C, or D corresponding to its respective column in Table 5.

Table 4: Multidimensional Technology Growth Models

S-curve Equation	Multidimensional Technology Growth Model
$y = \frac{L}{1+ae^{-bt}}$	$t = \sum_{i=1}^{n} \frac{-1}{b_i} ln\left(\frac{L_i - y_i}{a(y_i - y_{o,i})}\right)$
$y = Le^{-ae^{-bt}}$	$t = \sum_{i=1}^{n} \frac{-1}{b_i} lnln\left(\left(\frac{L_i - y_{o,i}}{y_i - y_{o,i}}\right)\right)^{\frac{1}{a}}$
$y = (1 - ae^{-bt})^3$	$t = \sum_{i=1}^{n} \frac{-1}{b_i} ln\left(\frac{1}{a}\left(1 - \left(\frac{y_i - y_{o,i}}{L_i - y_{o,i}}\right)^{\frac{1}{3}}\right)\right)$
$y = e^{a-(b/t)}$	$t = a + \sum_{i=1}^{n} b_i \left(ln\left(\frac{L_i - y_{o,i}}{y_i - y_{o,i}}\right)\right)^{-1}$

The first characteristics to consider when comparing these curves are the limits as t approaches ∞, 0, and $-\infty$. These boundaries greatly influence the practical usage of each curve. Consider the limit as time approaches infinity, curves A and B approach the specified upper limit, L. Whereas, curve C approaches 1 and curve D approaches e^a. As a result, using curves C or D requires normalizing the data to these limits or modifying curves C and D to also have an upper limit as $t \to \infty$ of L. This latter option was used for the creation of the corresponding technology growth models presented in Table 4. Appendix B also details these modifications to curves C and D.

Consider now the limit of each curve as time approaches zero. The limits of curves A, B, and C as $t \to 0$ are each functions of the parameter a while the limit of curve D is zero. This limit of zero is desirable, indicating that at the introductory date of a system architecture its technology capability is very low on the S-curve. Because the limits as $t \to 0$ of A, B, and C are all functions of the parameter a, it is mathematically possible for these curves to have limits as $t \to 0$ near their respective upper bounds. Typical regressed values of a, however, result in each of these functions approaching zero as desired. As discussed previously, in many cases, entry level technical capability of a technology architecture may be other than zero.

Table 5: Absolute Growth Model Comparison

	A	B	C	D
Characteristic	$y = \frac{L}{1+ae^{-bt}}$	$y = Le^{-ae^{-bt}}$	$y = (1 - ae^{-bt})^3$	$y = e^{a-(b/t)}$
Curve Name	Pearl's Equation	Gompertz's Equation	Von Bertalanffy's Equation	n/a
$\lim_{t\to\infty}$	L	L	1	e^a
$\lim_{t\to 0}$	$\frac{L}{1+a}$	$\frac{L}{e^a}$	$(1-a)^3$	0
$\lim_{t\to-\infty}$	0	0	$-\infty$	e^a
t-location of inflection	$ln(a)/b$	$ln(a)/b$	$ln(3a)/b$	$b/2$
y-location of inflection	0.5L	$Le^{-1} \sim 0.363L$	$(2/3)^3 \sim 0.296$	$e^{-2a} \sim 0.135e^a$

Because the limits of all four curves as $t \to 0$ are near zero, they can easily be shifted up by the entry level capability, y_o. This modification has been made in the creation of each of the models in Table 4.

The limit as $t \to -\infty$ is only of minimal importance. Attempting to model the maturation of a technology prior to its introduction is of no practical significance. It is, however, instructive to note that the limit as $t \to -\infty$ of curves A and B is zero or y_o, if appropriately adjusted, while the limits for curves C and D are $-\infty$ and e^a, respectively. These limits suggest that the domain of the s-shaped curves A and B includes all values of t, $-\infty$ to ∞, while the domain of the s-shaped curves C and D has a lower bound. Beyond this lower bound curves C and D no longer maintain an s-shape. Although they are defined for all values of t, the s-shaped portion of these equations is confined to the domain $t \geq 0$.

The next characteristic to consider for each of the s-shaped curves is the location of each inflection point along the curves. Note that the y-location of the inflection point for each curve is independent of the parameters a and b. The inflection point always occurs at the same fraction of the upper limit. This is the most distinguishing characteristic of the proposed models in Table 4. Recall that the inflection point of an

S-curve results from the growth-retarding influence of the upper limit on the curve. As a result, the y-location of the inflection point also indicates the rate of convergence of the curve to its limit. The smaller fraction of the upper limit at which an inflection point occurs, the more retarding influence the upper limit has on the growth of the curve, and consequently, the slower the curve approaches its upper limit. Curve A is least influenced by its upper limit in the early stages of growth and more rapidly approaches its upper limit. Curves B, C, and D are progressively more influenced by their upper limits such that the productivity of curve D begins to decline after only achieving 13.5% of its upper limit.

As a result of this characteristic, curves A and B are most commonly used to model technology development. The low inflection points of curves C and D indicate very early influence of the upper limit to technology development. More commonly poor understanding and lack of experience in implementing new physical principles in hardware limit the early stages of technology development. Curves A and B, particularly A, better quantify this principle and as a result are more commonly used to model technology growth. This does not, however, discount curves C and D as potential models. Cases may arise where the early influence of the upper limit on technology growth is more appropriate than the later influences modeled by curves A and B.

5.3.2 Relative Growth Models

Formulating a multidimensional growth model based on a relative growth model is significantly more difficult than on an absolute model because of the dramatic differences in their functional forms. To explore the significance of these differences on the formulation of a MDGM consider the Logistic MDGM derived earlier and shown here as Equation 31. Recall that each term in the summation is the inverse function of each attribute-specific S-curve as illustrated in Figure 19, where t_{y_i} is defined by

Equation 32.

$$t = a - \sum_{i=1}^{n} \frac{1}{b_i} ln\Big(\frac{L_i - y_i}{y_i - y_{o,i}}\Big) \tag{31}$$

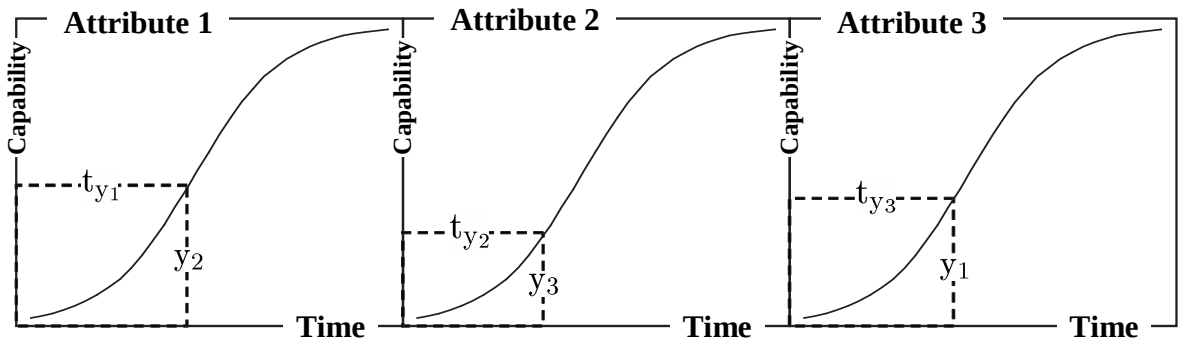

Figure 19: Multi-Attribute Growth Curve Inverse

$$t_{y_i} = \frac{-1}{b_i} ln\Big(\frac{L_i - y_i}{y_i - y_{o,i}}\Big) \tag{32}$$

Also recall that the time required to advance multiple metric attributes towards their upper limits is not concurrent but additive. Consequently, the time required to advance each attribute to a specified level of capability (y_1, y_2, & y_3) from their entry levels of capability is given by Equation 33; thus, the date at which a system is expected to be operational with these specified levels of capability is given by Equation 34.

$$\Delta t = t_{y_1} + t_{y_2} + t_{y_3} \tag{33}$$

$$year = a + \Delta t = a + \sum_{i=1}^{n} t_{y_i} \tag{34}$$

This same very general principle illustrated in Figure 19 and quantified by Equations 33 and 34 apply to both absolute and relative growth models alike. The complexity in formulating a relative MDGM arises because no closed form solution for the inverse to the relative (i.e. incremental) growth model equations can be found. As a result, no single equation can completely capture a MDGM formulated on a relative model. At least it can do this no more explicitly than Equation 35, where $y_i^{-1}(t)$ is the inverse of the integrated relative growth model, which can only be evaluated numerically.

$$year = a + \sum_{i=1}^{n} y_i^{-1}(t) \tag{35}$$

The following five steps outline an approach to evaluating Equation 35.

1. The initial condition for each of the i^{th} attributes should be set to zero, $y_i(0) = 0$

2. Each attribute-specific S-curve should be numerically integrated according to the desired relative growth model and timeframe of interest. Equations 36 and 37 employ the Bass relative growth model to demonstrate this process.

$$dy_i(t) = \beta_{0,i} + \beta_{0,i} y_i(t-1) + \beta_{0,i} y_i^2(t-1) \tag{36}$$

$$y_i(t) = dy_i(t) + y_i(t-1) \tag{37}$$

3. Add the appropriate attribute offsets, $y_{o,i}$, to all y_i.

$$y_i(t) = y_i(t) + y_{o,i} \tag{38}$$

4. Given a setting for each technical capability y_i, perform an inverse on Equation 38 to find the corresponding t_{y_i}, or equivalently $y_i^{-1}(t)$.

5. Evaluate Equation 35.

The above steps provide a means to evaluate the expected date of introduction of a system with technical capability settings y_i given parameter estimates for each $\beta_{k,i}$ and a, where $\beta_{k,i}$ is the k^{th} curve parameter of the i^{th} technology attribute. These parameter estimates can be calculated by regressing Equation 35 against historical data using an appropriate objective function, mean square error (MSE), χ^2 distribution, etc. However, both MSE and χ^2 were found to be highly multi-modal objective functions for the regression of relative MDGMs. As a result of these ill-behaved objective functions finding the necessary parameter estimates for relative MDGMs is extremely computationally intensive. Also note that for the Bass, Nonsymmetrical Responding Logistic, and Harvey relative MDGMs there are $3n + 1$ unknowns, and for the Extended Riccati relative MDGM there are $4n + 1$ unknowns requiring significantly more data than most absolute MDGMs, which can have as few as $n + 1$ unknowns.

5.3.3 Non-S-shaped Growth Patterns

Cases may exist where a dimension of capability advances over time according to a growth pattern other than that of an S-shaped growth model. An example of such a growth pattern is Moore's Law which successfully describes the technological growth of integrated circuits [65]. Moore's Law states that the complexity of integrated circuits as quantified by the transistor density doubles every two years [65]. This growth pattern is generally modeled by Equation 39.

$$y = y_o(2^{t/2}) \tag{39}$$

The very general form of the multidimensional growth model provided by Equation 40 allows for the seamless inclusion of dimensions of capability that advance over time according to Moore's Law. Furthermore, any growth model which is based on

the independent parameter of time and for which an inverse can be found can also be formulated into a multidimensional growth model according to Equation 40.

$$year = a + \sum_{i=1}^{n} y_i^{-1}(t) \tag{40}$$

CHAPTER VI

IDENTIFYING UPPER LIMITS

Accurately identifying upper limits for each metric included in a technology assessment is key to formulating an accurate multidimensional growth model. This chapter will investigate two general approaches for identifying upper limits: statistical and physics-based approaches. Martino has argued that the only appropriate approach to identifying attribute upper limits is through physics-based analysis [13]. More recently he restated this premise as a result of the comparative study conducted by Young between nine different growth models [42, 66]. Young compared the predictive capability of each model on its ability to predict the final three data points for each of thirty-two data sets. In cases where the upper limits were not known, the Logistic model, Gompertz model, and their variants performed poorly, which suggests that it is poor practice to solve for the upper limit of an attribute on the basis of available historical data. DeBecker and Modis, however, explored this possibility further and attempted to quantify the level of uncertainty associated with a limit that is calculated from available historical data [1]. Their study suggests that it is indeed possible to determine attribute upper limits statistically with a known confidence interval. The discussion in this chapter will first consider the physics-based approaches, and then it will explore a statistical approach to determining upper limits.

6.1 Physics-Based Approach to Limit Identification

Because upper limit identification is highly specific and requires detailed knowledge of the precise technical approach employed by a developing technology, this study

will not propose a general, physics-based approach for identifying upper limits. The numerous and diverse physical laws governing the vast pool of potential technologies prevent the development of a universal approach to upper limit identification. However, because technical approaches can be described within a single field of science, the number of governing principles can, in some cases, be reduced to a manageable number. As a result, it is possible to formulate systematic approaches to identifying upper limits within a particular field of science. This is the case for energy-related technologies.

6.1.1 Fundamentals of Energy-Based Systems

There are only a few very basic principles that govern the general conditions for energy transfer. These principles dictate a remarkably systematic approach to the consideration of upper limit identification for select metrics of energy intensive systems.

Newton's first law specifies that the dynamic characteristics of a system can only be altered with the application of an unbalanced force [67]. Furthermore, all force imbalances and consequently work can only result from preexisting imbalances between interacting energy reservoirs. In other words, energy gradients must exist between interacting systems for the potential for work to exist.

Consider most generally the concept of energy. Energy is often understood as a measure of the ability to do work. Although this definition is often functionally adequate, it is technically inaccurate. Energy can exist with no ability to do work. For example, the atmosphere is rich with thermal energy, although, in isolation, this energy has no ability to do work. No amount of energy in complete isolation can do work. Consequently, energy cannot be a measure of the ability to do work. Furthermore, energy is conserved; whereas, the ability to do work is not. Therefore, the two cannot be equated. The common misconception that energy is a measure

of the ability to do work disregards the second law of thermodynamics. The Kelvin-Plank statement of the second law is as follows: *It is impossible for any system to operate in a thermodynamic cycle and deliver a net amount of work to its surroundings while receiving energy by heat transfer from a single thermal reservoir* [68]. It is not merely the existence of energy that provides the capacity for work but rather the non-equilibrium that exists between interacting energy reservoirs. Non-equilibrium in conjunction with energy supplies the universe with the potential for work, not solely energy. If energy is not a measure of the ability to do work, what is it? Poincaré said this of energy in *Science and Hypothesis*:

> *In every particular case we clearly see what energy is, and we can give it at least a provisory definition: but it is impossible to find a general definition of it. If we wish to enunciate the principle in all its generality and apply it to the universe, we see it vanish, so to speak, and nothing is left but this—there is something which remains constant.* [69]

This principle has informed the creation of many energy-based design and analysis methods [70, 71, 72]. The conservation principle of energy provides a convenient bookkeeping framework for the design and analysis of many diverse technologies. The concept of energy alone, however, is not adequate for establishing the upper limit to technical capability of energy intensive technologies. Such determinations also need to consider the concept of exergy. Exergy is a measure of the ability to do work. More precisely, it is "a thermodynamic state property quantifying the maximum theoretical work that can be obtained from a system in taking it from a given chemical composition, temperature, and pressure to a state of chemical, thermal, and mechanical equilibrium with the environment," [73].

As previously stated, all force imbalances, and thus work, can only result from preexisting imbalances between interacting energy reservoirs. Exergy is a quantification of the maximum work that can be produced as a result of the energy imbalances

that exist between these reservoirs. Unlike energy, exergy is not conserved. It can be and is destroyed as entropy increases, just as the ability to do work is diminished as the imbalances between energy reservoirs vanish and come to equilibrium. Conversely, like energy, exergy cannot be created, although it can be converted from one form to another. Exergy has the same units as energy and can itself be described as non-equalized energy.

The concept of exergy simultaneously employs the first and second laws of thermodynamics to quantify the available work contained within a specified quantity of energy. The following derivation of an expression of exergy roughly follows that presented by Bejan [74].

Consider the first and second laws of thermodynamics for an open system in thermal contact with only the environment and having one inlet and outlet shown here as Equations 41 and 42, respectively. In these equations h°, methalpy, is shorthand for the quantity $(h + \frac{V^2}{2} + gz)$.

$$\frac{dE}{dt} = \dot{Q}_{\circ} - \dot{W} + \dot{m}h^{\circ}_{in} - \dot{m}h^{\circ}_{out} \tag{41}$$

$$\dot{S}_{gen} = \frac{dS}{dt} - \frac{\dot{Q}_{\circ}}{T_{\circ}} - \dot{m}s_{in} + \dot{m}s_{out} \geq 0 \tag{42}$$

where E is the total internal energy of the system;

t is time;

$\dot{Q}_{\circ}$ is the rate of heat transfer with the environment;

$\dot{W}$ is the rate of work production;

$\dot{m}$ is the rate of mass flow through the system;

$\dot{S}_{gen}$ is the rate of entropy generation;

S is the total entropy internal to the system;

$s_{in/out}$ is the mass specific entropy flowing into and out of the system;

$T_\circ$ is the temperature of the environment.

$$\dot{W} = \dot{m}(h^\circ_{in} - h^\circ_{out}) - \dot{m}T_\circ(s_{in} - s_{out}) - T_\circ \dot{S}_{gen} \tag{43}$$

$$\frac{\dot{W}}{\dot{m}} = (h^\circ_{in} - h^\circ_{out}) - T_\circ(s_{in} - s_{out}) \tag{44}$$

If these two laws are combined by eliminating $Q_\circ$, and steady state is assumed for simplicity, Equation 43 results, and this provides the work production and accounts for irreversibilities. The maximum achievable work, or exergy, results when entropy generation is zero, as depicted by Equations 44. This simplistic derivation of exergy establishes the basic mathematical relationship between the first and second laws and the definition of exergy.

This analytical definition of exergy can be used to calculate limits for a single process. Furthermore, complex energy systems can be decomposed into basic processes, the limits of each can be evaluated, and the system recomposed to identify the upper limits for the systems as a whole. Ahern in *The Exergy Method of Energy Systems Analysis* proposed a systematic approach to evaluating the transfer of exergy through a system, the block method of exergy analysis [75]. In this method Ahern decomposes a system into blocks, each representing a system process or component. The method calculates the difference between exergy entering and exiting each block. The second law dependence of exergy requires that this difference always be negative; less exergy will always exit a block than did enter. Ahern quantifies the efficiency of exergy transfer through a system block as depicted in Equation 45. For maximum

performance, this efficiency should be unity for all system blocks. This condition allows for the calculation of related metric upper limits.

$$Ex = \frac{Ex_{available} - Ex_{loss}}{Ex_{available}} \tag{45}$$

Ahern's exergy block analysis forms a basis for identifying the upper limit to select metrics of energy systems [75]. However, the resulting upper limit is based on the assumption that the technical approach employed by the energy systems has the capacity to extract all the useable work from mechanical, thermal, *and* chemical equilibration. This is often not the case. For example, a turbojet engine does not employ devices capable of extracting work from the thermal energy contained in the exhaust flow. Using exergy to calculate the upper limit to turbojet performance would result in a gross overestimation, because the thermal energy of the exhaust flow is not available to the engine and would appear as an inefficiency. The use of exergy for calculating upper limits to energy systems is only applicable to those technologies employing technical approaches capable of extracting work from all three energy forms: mechanical, thermal, and chemical. This greatly restricts the applicability of exergy-based methods for the identification of upper limit calculation. Exergy, however, is only one of a family of metrics that falls under a broader classification of *work potential*.

Whereas exergy is a very precisely defined thermodynamic property, the term *work potential* refers to a family of thermodynamic properties that quantify the amount of work that can be accomplished by bringing a system into complete or partial equilibrium with its environment. Partial equilibrium in this case refers to bringing fewer than all existing energy mode imbalances into *complete* equilibrium with the environment. An example of partial equilibrium would be a system brought into thermal equilibrium with its environment but neither chemical nor mechanical equilibrium.

Partial equilibrium *does not* refer to any single energy mode moving only *partially* towards equilibrium. Although these energy modes can be altered independently, they can and frequently do interact in many work potential systems. Three of the most common energy modes appear in the exergy definition above: thermal, chemical, and mechanical.

Gas horsepower, also called available energy [73] or ideal work [76], is an example of a work potential figure of merit. It is defined as the maximum work that can be achieved by isentropic expansion of a fluid at a specified pressure and temperature to atmospheric pressure [77]. Gas horsepower is defined mathematically for ideal air by Equation 46 and only quantifies work available from a pressure differential. This work potential metric is better suited to applications such as turbine engines, wherein technical approaches are not employed to extract work from either the chemical or thermal energy modes of the exhaust flow.

$$ghp = c_p T\Big[1 - \Big(\frac{P_\circ}{P}\Big)^{\frac{\gamma-1}{\gamma}}\Big] \tag{46}$$

Roth provides further discussion on various work potential metrics as pertaining to gas turbines in "A Comparison of Thermodynamic Loss Models Suitable for Gas Turbine Propulsion: Theory and Taxonomy," [78].

The same block-type analysis method employed to analyze exergy flow through a system can also be used for work potential figures of merit. Numerous researchers have formulated similar techniques capable of employing any one or more work potential metrics for the analysis of highly integrated systems [74, 79, 80, 81, 82]. Roth and others have implemented several of these techniques in the Numerical Propulsion System Simulation program to assist users in the conceptual and preliminary design of a wide range of propulsion concepts [76, 83].

Exergy and work potential analysis methods provide a foundation for a general

approach to the calculation of *select* energy and work related limits such as rates of work generation or minimum fuel consumption. These analysis methods, however, are best suited for establishing upper limits to well defined systems such as a turbine engine with specified cycle parameters. They are unable to establish an upper limit on turbine engines as a system architecture without first identifying limitations on pertinent cycle parameters, which are limited by the technology (i.e. hardware) employed at the subsystem level. Each subsystem, like the system architecture, advances along its own growth curve and is also bound by some natural limit. In order to establish an upper limit for a system architecture, the system must be progressively decomposed until the limit for each subsystem is no longer dependent on the limit of an internal component. Once subsystem limits are determined, the system can be recomposed and system-level limitations calculated based on subsystem limits. For the assessment of complex systems, this process will without exception span multiple branches of physics requiring the participation of an interdisciplinary team of experts. A major investment of time and resources is required to accurately estimate the natural limits of a complex system. Because of the substantial investment required to establish credible upper limits through physics-based approaches, these approaches are not often practical, especially to the independent researcher. Fortunately, despite the fact that statistical approaches have been previously dismissed, if appropriate historical data is available for a developing system, statistical approaches can provide meaningful upper limits. The remainder of this chapter evaluates a promising statistical method offered by DeBecker and Modis and adjusts that method to fit the requirements of this research.

6.2 Regression-Based Approach to Limit Identification

The statistical approach to identifying an attribute's upper limit treats the limit as a regression parameter and calculates its value based on historical data. This process of determining an upper limit is very simple in practice. The accuracy of the resulting limit, however, is highly sensitive to any error present in either the historical database or in the segment of the total growth curve spanned by the available data. DeBecker and Modis attempted to quantify this sensitivity and to establish confidence intervals for predicted limits based on an assumed degree of error in the historical data. They expected that data samples that have a low degree of error and that span a significant segment of the entire S-curve can be used to statistically predict the upper limit with a high degree of confidence. The greater the segment of the curve for which there is data, the more accurately the limit can be predicted by regression. The basis of their study is a known Logistic curve of the form shown in Equation 47, where the upper limit, L, is 1, and the curve parameters, b and a are 1 and 0, respectively.

$$y(t) = \frac{L}{1 + e^{-b(t-a)}} \tag{47}$$

DeBecker and Modis began by selecting twenty equal time bins which span a specified segment of the complete S-curve. The left side of Figure 20 illustrates one such range, covering $1 - 50\%$ of the upper limit L. They proceeded to introduce statistical fluctuations on the rate of growth of the S-curve to simulate error within the historical data. These fluctuations were introduced into the data set according to the equation $\tilde{g}_k = q_k + \epsilon q_k$, where q_k is the theoretical growth rate of the k^{th} time bin defined by Equation 48 and where ϵ is the normal distribution, $N(0, \sigma)$, in which σ is the assumed degree of error in the data ranging between 0 and 30%. The right side of

Figure 20 illustrates the result of applying these statistical fluctuations as introduced to the growth rate of the known S-curve.

$$q(t_k) = \frac{L}{(1 + e^{-b(t-a)})(1 + e^{b(t-a)})} \tag{48}$$

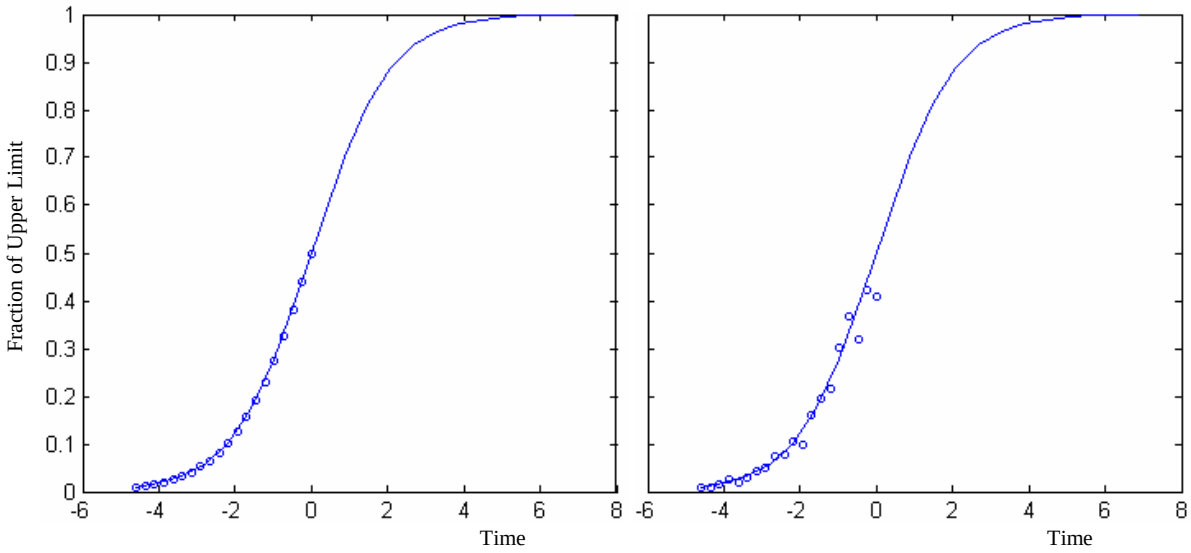

Figure 20: Limit Uncertainty Analysis Data Sample

Once the fluctuations are introduced, the model is regressed for L, b, and a by minimizing the χ^2 of Equation 49. A Monte Carlo Simulation is then conducted around the specified range of data (1 to 50 percent of L=1, in this case), and a distribution of each regressed parameter is obtained, from which confidence intervals can be established for specified levels of σ, as shown in Table 6. Figure 2 illustrates the result of five hundred simulations at the 1 to 50 percent data range and 10 percent error on the data sample.

$$U = \sum_{k=1}^{m} \left(\frac{q_k - E(Q(t_k))}{\sigma(Q(t_k))} \right)^2 \tag{49}$$

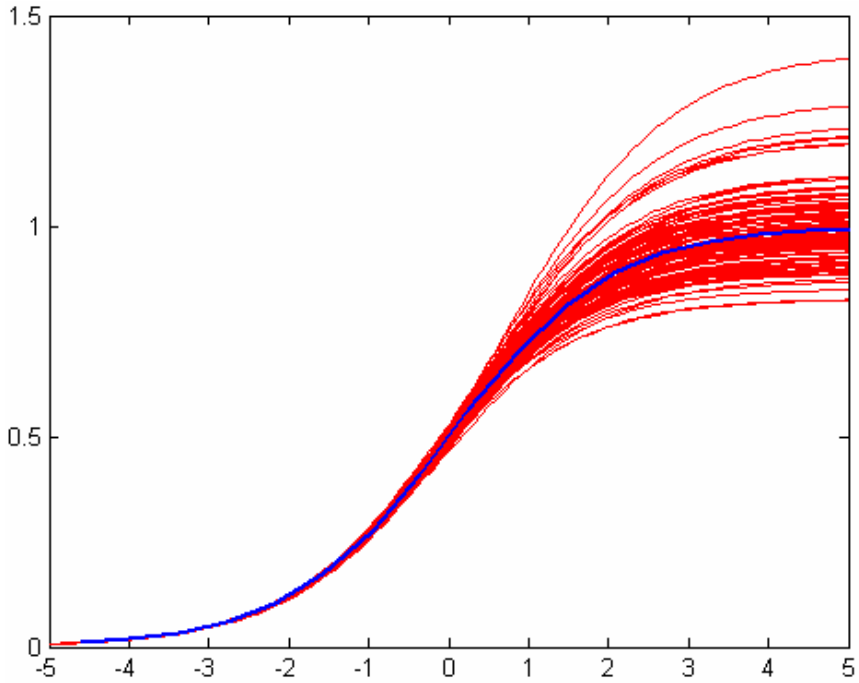

Figure 21: Regression-Based Limit Predictions

DeBecker and Modis [1] provide similar tables for each data range provided in Table 7, and these provide researchers with the ability to establish confidence intervals for statistically predicted limits given an estimated degree of error present in the historical data. This confidence interval is calculated according to Equation 50, where the expected error, EE_{CL}, corresponds to a specific range of the historical data, estimated degree of error on historical data, and the confidence level of interest.

$$L_{real} = L_{pred}(1 \pm EE_{CL}) \tag{50}$$

Table 6: Expected error for the data range 1-50 percent as a function of confidence level and error on historical data, reproduced from [1].

	Percent Error on Historical Data					
Confidence Level	1	5	10	15	20	25
70	1.2	5.1	11	17	23	29
75	1.4	5.5	12	19	26	32
80	1.8	6.4	14	22	29	36
85	2.1	7.3	16	25	36	42
90	2.6	8.8	18	29	42	48
95	3.1	11	21	39	56	66
99	4.6	22	30	55	150	110

Table 7: Data Ranges Provided by DeBecker and Modis [1]

1 to 20 percent of L
1 to 30 percent of L
1 to 40 percent of L
... ...
1 to 90 percent of L
1 to 99 percent of L

Consider the following example provided by DeBecker and Modis:

Example: A fit on yearly historical data of supertanker construction gives $L = 115$. The historical period stops at 80 ships and we estimate an uncertainty on the reported yearly construction of 5 percent. The range thus defined is $80/115 = 70\%$ percent. From Table 8 we obtain the uncertainty on L, namely $L = 115 \pm 4.3\%$ with 90 percent confidence level.

Table 8: Expected uncertainties for the data range 1-70 percent as a function of confidence level and error on historical data, reproduced from DeBecker and Modis [1].

	Percent Error on Historical Data					
Confidence Level	1	5	10	15	20	25
70	0.8	2.5	5.1	9.2	11	14
75	0.9	2.8	5.6	10	12	16
80	1	3.4	6.6	11	13	18
85	1.2	3.8	7.5	13	15	20
90	1.5	4.3	8.5	14	16	22
95	1.9	5.6	9.8	16	20	25
99	2.8	7.5	15	21	28	30

This technique proposed by DeBecker and Modis for establishing confidence intervals around statistically predicted upper limits is a promising approach. Several adjustments to their approach must be made, however, before it can be broadly applied. The most significant of these adjustments pertains to the definition of the data range as used to generate Table 8 relative to the definition of the data range used in the supertanker example. The range of data on which Table 8 is based, covers 1 to 70 percent of the *real* upper limit. However, the range identified in the quoted example by 80/115 covers the range 1 to 70 percent of the *predicted* upper limit. This discrepancy in the definition of the data range can—and does—have a significant impact on the resulting confidence interval. For instance, given a data sample ranging between 0 and 0.7, which is known to have 25 percent random error, the data is regressed against the Logistic model of Equation 47, and the limit is found to be 1. This suggests a data range of 70 percent, and according to Table 8, the 90 percent confidence interval should be 1 ± 0.22. Now consider a new sample of data describing the same process as the first and also ranging between 0 and 0.7 with a 25 percent error. The confidence interval from the first set of data suggests that the predicted limit from this new data set is likely to fall somewhere between 0.78 and 1.22, which corresponds

to data ranges of $0.7/0.78 = 89.7\%$ and $0.7/1.22 = 57.4\%$. Clearly the same absolute data range, 0 to 0.7 in this case, can result in drastically different relative ranges 1 to 70, 90, or 57 percent because of dependence on the predicted upper limit. This suggests that the data from which the confidence intervals are established should also be generated relative to the predicted upper limit rather than fixed to the real upper limit, which in practice will not be known.

A similar discrepancy is in the calculation of the expected uncertainty. This discrepancy is most obvious in the uncertainty intervals for the 1-30 percent data range as provided by DeBecker and Modis and reproduced here as Table 9. Note, for example, the expected uncertainty of 820 percent, given 25 percent error on the historical data and a 95 percent confidence interval. This uncertainty is unduly large. Consider the two possibilities for error when predicting an upper limit: under prediction or over prediction. In the case of an over prediction, the uncertainty should never exceed 100 percent, because $L_{pred} \pm 100\%$ will, with a 100 percent confidence level, include the real limit. Thus any expected uncertainty that exceeds 100 percent can only be the result of an under prediction that assumes the confidence interval definition of Equation 51.

These extraordinary results called for a test to recreate DeBecker and Modis' results for this portion of their work. Consequently, this study included a Monte Carlo simulation that emulated DeBecker and Modis'. In order to test just how low a limit may be predicted, the simulation (by this author) used a data range of 1-30 percent of the real limit ($L = 1$) and an error of 25 percent on the sample data. The lowest under-predicted limit out of one hundred thousand simulations was 0.343. This would therefore correspond to an expected uncertainty of 1/0.343 - 1 = $\pm$191 percent with a confidence level of 99.999 percent. Of this sample, 99 percent of the regressed limits were predicted above 0.489—an expected uncertainty of $\pm$104 percent with a 99 percent confidence level. The expected uncertainty at a 95 percent confidence

level is ±74 percent. How does an expected uncertainty of ±820 percent result? Most likely it results because the expected uncertainty provided by DeBecker and Modis is not generated according to Equation 51, the equation that DeBecker and Modis state they intend for such calculations. Rather, the resultant data fit the faulty Equation 52. That is, it seems that when they calculated the confidence intervals, DeBecker and Modis inadvertently reversed the significance of L_{pred} and L_{real}.

The seemingly minor differences in these equations can have a drastic impact on the resulting confidence intervals. For example, an over predicted limit could result in an otherwise impossible expected uncertainty greater than 100 percent. Out of the same one hundred thousand simulations used to identify the lowest predicted limit of 0.343, five percent of the limits were predicted above 11, which according to Equation 52 would yield an expected uncertainty of $\pm 1,000$ percent with a confidence level of 95 percent. The corresponding expected uncertainty for a confidence level of 90 percent is ±210 percent. This explains how DeBecker and Modis estimated 820 percent with a 95 percent confidence level. It also equates to a 926 percent difference (that is, $1000\% - 74\%$) at the 95 percent confidence level between how the expected uncertainties calculated by DeBecker and Modis were generated and how they were expected to be utilized.

$$L_{real} = L_{pred}(1 \pm EE_{CL}) \tag{51}$$

$$L_{pred} = L_{real}(1 \pm EE_{CL}) \tag{52}$$

This research reformulated the approach employed by DeBecker and Modis to yield confidence intervals for statistically predicting upper limits according to a known degree of error and the relative range of data available as dependent on the *predicted*

Table 9: Limit uncertainties for the data range 1-30 percent as a function of confidence level and error on historical data, reproduced from [1].

	Percent Error on Historical Data					
Confidence Level	1	5	10	15	20	25
70	2.7	13	28	47	69	120
75	3.2	15	32	53	81	190
80	3.9	17	36	62	110	240
85	4.8	19	41	71	130	370
90	5.9	22	48	110	210	470
95	8.5	29	66	140	350	820
99	48	49	180	350	690	

upper limit. In order to allow direct comparison to the results from DeBecker and Modis, error fluctuations were also introduced on the rate of growth and regression was performed by minimizing the χ^2 of Equation 49. Unlike in the DeBecker and Modis study, the upper bound on the data range was allowed to vary flatly between 20 and 99.9 percent of the *real limit*, $M_{real} = 1$, and six levels of error fluctuations were introduced to the data sample in turn, $\sigma = [0.01, 0.05, 0.1, 0.15, 0.2, 0.25]$. After predicting the upper limit, the data range was transformed relative to the resulting *predicted* limit. Distributions were then generated according to the upper bound of their corresponding data range. Distributions corresponding to each of the data range upper bounds listed in Table 10 were created:

Table 10: Upper Bounds to Data Ranges

19.5-20.5 percent of L_{pred}
29.5-30.5 percent of L_{pred}
39.5-40.5 percent of L_{pred}
... ...
89.5-90.5 percent of L_{pred}
98.5-99.5 percent of L_{pred}

From these distributions, the expected uncertainties on predicted limits were established. Table 11 provides these uncertainties for all combinations of the above data ranges and levels of data fluctuations. This table provides the expected uncertainty of a regressed limit given a range defined relative to the *predicted* limit and according to the confidence interval of Equation 51 rather than Equation 52. Confidence intervals are established in the same manner as provided in the supertanker example. Reworking the supertanker example with these formulated uncertainties yields a confidence interval of $115 \pm 4.8\%$—only a minor difference from the 4.3% of DeBecker and Modis. Consequently the discrepancy between how DeBecker and Modis generated their expected uncertainty tables and how they were intended to be used is most significant for small data ranges and high error fluctuations. Table 12 allows for direct comparison between the expected uncertainties for the 1-30 percent data range as estimated by DeBecker and Modis and those estimated by this research. Uncertainties from DeBecker and Modis are shown in italics.

Note that for all levels of error and confidence the expected uncertainties estimated by this research are lower than those estimated by DeBecker and Modis. This is least significant at low error and confidence levels. For instance, given 1 percent error fluctuations on historical data, for a confidence level of 70 percent, DeBecker and Modis estimated the expected error at 2.7 percent; this research estimated 2.1 percent. At high error and confidence levels, however, the differences are most significant. Compare the 820 percent expected error estimated by DeBecker and Modis for the 95 percent confidence level and 25 percent error to the 43 percent estimated by this research. Contrast these differences with those for a larger data range. Table 13 provides the expected uncertainty for the 1-90 percent data range as estimated by both DeBecker and Modis and by this research. Expected uncertainties from DeBecker and Modis are shown in italics.

Table 11: Limit Uncertainties as a Function of the Predicted Limit

	Confidence Level	Data Range								
		1-20%	1-30%	1-40%	1-50%	1-60%	1-70%	1-80%	1-90%	1-99%
1% Data Error	70	2.9	2.1	1.5	1.1	0.8	0.6	0.4	0.3	0.3
	75	3.2	2.4	1.7	1.2	0.9	0.6	0.5	0.3	0.3
	80	3.5	2.7	1.8	1.3	1.0	0.7	0.5	0.4	0.4
	85	4.0	3.0	2.1	1.5	1.1	0.8	0.6	0.4	0.4
	90	4.5	3.5	2.3	1.7	1.3	0.9	0.7	0.5	0.5
	95	5.3	4.2	2.8	2.0	1.5	1.1	0.8	0.6	0.5
	99	7.1	5.7	3.8	2.7	1.9	1.4	1.0	0.7	0.7
5% Data Error	70	14	9.9	6.7	4.6	3.4	2.4	1.8	1.5	1.1
	75	15	11	7.4	5.1	3.8	2.7	2.0	1.6	1.3
	80	16	12	8.3	5.8	4.2	3.0	2.2	1.8	1.5
	85	18	14	9.4	6.5	4.7	3.4	2.5	2.0	1.7
	90	20	17	11	7.6	5.4	4.0	2.9	2.3	2.0
	95	23	21	13	9.2	6.5	4.8	3.5	2.8	2.4
	99	27	32	20	13	9.1	6.6	4.8	3.7	3.2
10% Data Error	70	24	18	13	9.3	6.6	4.8	3.6	2.9	2.4
	75	25	20	15	10	7.3	5.4	4.1	3.2	2.8
	80	27	22	17	12	8.2	6.0	4.5	3.6	3.2
	85	30	25	19	13	9.3	6.8	5.1	4.1	3.7
	90	32	30	24	16	11	7.9	5.9	4.7	4.3
	95	36	37	32	21	14	10	7.4	5.8	5.3
	99	42	47	53	33	21	15	11.1	8.1	7.4
15% Data Error	70	31	23	19	14	10	7.1	5.5	4.4	3.8
	75	33	25	21	15	11	8.0	6.1	4.9	4.3
	80	35	27	24	18	12	8.9	6.8	5.5	5.0
	85	38	30	29	20	14	10	7.8	6.2	5.7
	90	41	33	36	25	17	12	9.2	7.3	6.7
	95	45	39	52	36	24	17	12	8.9	8.3
	99	51	47	84	64	41	28	19	14	12
20% Data Error	70	36	26	23	18	13	10	7	6	5
	75	39	28	26	20	15	11	8	6	6
	80	41	31	30	23	17	12	9.1	7.3	7.0
	85	44	33	37	29	20	14	11	8.3	8.0
	90	47	37	48	38	25	18	13	9.4	9.7
	95	50	41	66	58	37	26	18	13	12
	99	56	48	91	108	68	47	31	22	20
25% Data Error	70	41	29	27	22	16	12	9	7.1	7.0
	75	43	31	30	25	18	13	10	7.9	8.0
	80	46	33	34	29	21	15	11	8.8	9.2
	85	48	36	41	38	27	18	14	10	11
	90	51	39	53	51	36	24	17	13	13
	95	55	43	70	77	53	36	25	19	17
	99	61	49	93	123	110	67	48	34	29

Note that for error fluctuations between 1-15 percent there is little difference between the two estimates at all confidence levels. For 20 percent and 25 percent error

Table 12: Comparison of Limit Uncertainties for the Data Range 1-30 Percent

	Percent Error on Historical Data											
Confidence Level	1		5		10		15		20		25	
70	2.1	*2.7*	9.9	*13*	18	*28*	23	*47*	26	*69*	29	*120*
75	2.4	*3.2*	11	*15*	20	*32*	25	*53*	28	*81*	31	*190*
80	2.7	*3.9*	12	*17*	22	*36*	27	*62*	31	*110*	33	*240*
85	3.0	*4.8*	14	*19*	25	*41*	30	*71*	33	*130*	36	*370*
90	3.5	*5.9*	17	*22*	30	*48*	33	*110*	37	*210*	39	*470*
95	4.2	*8.5*	21	*29*	37	*66*	39	*140*	41	*350*	43	*820*
99	*5.7*	*48*	32	*49*	47	*180*	47	*350*	48	*690*	49	

Table 13: Comparison of Limit Uncertainties for the Data Range 1-90 Percent

	Percent Error on Historical Data											
Confidence Level	1		5		10		15		20		25	
70	0.3	*0.3*	1.5	*1.4*	2.9	*2.9*	4.4	*4.2*	5.9	*6.0*	7.1	*7.1*
75	0.3	*0.4*	1.6	*1.5*	3.2	*3.2*	4.9	*4.6*	6.5	*7.1*	7.9	*7.8*
80	0.4	*0.5*	1.8	*1.9*	3.6	*3.5*	5.5	*5.2*	7.3	*8.1*	8.8	*8.5*
85	0.4	*0.5*	2.0	*2.2*	4.1	*4.0*	6.2	*6.1*	8.3	*8.7*	10.0	*9.9*
90	0.5	*0.6*	2.3	*2.5*	4.7	*4.7*	7.3	*7.0*	9.4	*10.0*	13.0	*11.0*
95	0.6	*0.9*	2.8	*3.2*	5.8	*5.8*	8.9	*8.6*	12.5	*12.0*	18.8	*14.0*
99	0.7	*1.5*	3.7	*4.6*	8.1	*8.6*	13.8	*12.0*	22.2	*16.0*	33.9	20.0

fluctuations, the differences are minimal for low confidence levels but become more significant with increased confidence. At the 99 percent confidence level with 25 percent error on historical data, this research estimates an expected uncertainty of 34 percent as compared to the 20 percent estimate of DeBecker and Modis—a 14 percent difference. This difference drops to only 5 percent at the 95 percent confidence level and 2 percent at the 90 percent confidence level. The reason for greater uncertainty at higher confidence levels than DeBecker and Modis predicted is that a vast under prediction in the limit will result in a higher data range as compared to DeBecker and Modis' original formulation.

One peculiarity of the data provided in Table 11 is that the maximum expected uncertainty for high confidence level and high data error occurs near the 40 and 50 percent data range rather than the 20 percent data range. It was expected that a smaller data range would always result in a higher expected uncertainty than a larger data range. Clearly these results indicate otherwise. Observe the trend in the expected uncertainty for 25 percent data error and 99 percent confidence level. The maximum expected uncertainty occurs at a 50 percent data range, two and half times the expected uncertainty for the 30 percent data range. Also note that the expected uncertainty for the 30 percent data range is lower than both the 20 and 40 percent data ranges. There are two phenomena causing this unexpected trend. Both are related to the manner in which the data ranges are defined relative to the *predicted* limit. The first is related to gross over predictions and the second to gross under predictions.

In the case of a gross over prediction, a small data range will result which increases the uncertainty at very low data ranges. For instance, consider a data range that spans 0.01 to 0.5 with data error of 25 percent which is used to regress an upper limit known to be one. If the regressed limit is a gross over prediction, 2.5, for example, the resulting data range would be $2.5/0.5 = 20$ percent, and the corresponding expected uncertainty would be 60 percent. Consequently, gross over predictions result in high expected uncertainties for the low data ranges. The more drastic an over prediction is, the higher the expected uncertainty will be and the lower the data range will appear. The 20 percent data range, therefore, is most impacted by this phenomena, significantly more so than even the 30 percent data range.

Recall that a gross under prediction will result in a greater expected uncertainty than a gross over prediction. An over predicted limit will never result in an expected uncertainty greater than 100 percent, where as an under prediction could result in an expected uncertainty of 191 percent or more as shown previously. Consequently,

the impact of this second phenomena is more significant than the first. In cases of a gross under prediction, the resulting data range appears larger and the expected uncertainty is also much higher. For instance, consider a data range that spans 0.01 to 0.2 with data error of 25 percent. If the regressed limit is found to be 0.4 this would indicate a data range of 50 percent and an expected uncertainty of 150 percent. The middle data ranges (40, 50, and 60 percent) are most impacted by this phenomena. Higher data ranges are only minimally influenced because rarely is a limit so grossly under predicted that it results in a data range on the order of 70 or 80 percent or higher. Consider the 1-30 percent data range analyzed previously. The lowest predicted limit out of one hundred thousand trials was 0.343, which results in an data range of $0.3/0.343 = 87$ percent and corresponds to the 99.999 percent confidence level. At the 99 percent confidence level the corresponding limit prediction is 0.489 which results in a $0.3/0.489 = 61$ percent data range. Consequently, only at much higher confidence levels are larger data ranges significantly influenced by this phenomena.

This research has shown that upper limits can be predicted by means of regression and that it can be done even more accurately for most data ranges and confidence levels than DeBecker and Modis proposed. These expected uncertainties can be used to establish the degree of certainty, or uncertainty, associated with a statistically predicted upper limit given a known degree of error present in the available historical data if is comprised of precisely twenty data points. There is one other consideration, however, that should be taken into account before applying the above uncertainties to just any statistically predicted limit. All the above data as well as that provided by DeBecker and Modis is based on a sample size of twenty points regardless of whether the sample spans 20 percent or 99 percent of the complete S-curve. It is more likely that the sample size increases with the data range, since larger segments of the S-curve tend to represent more effort and more technology development. This variation

in sample size can have a significant impact on the resulting confidence interval. Note in Table 14 the difference between the expected error for each 10, 20, and 30 data points all with error fluctuations of 10 percent. Note that the increase in sample size from 10 to 30 data points generally decreases the expected uncertainty by roughly half for the higher data ranges, although only minor reductions occur at the lower data ranges.

Table 14: Influence of Sample Size on Limit Uncertainty

Confidence Level		Data Range								
		1-20%	1-30%	1-40%	1-50%	1-60%	1-70%	1-80%	1-90%	1-99%
Sample Size of 10	70	26	21	17	12	8.8	6.5	5.0	4.3	3.8
	75	29	23	19	14	10	7.3	5.6	4.8	4.3
	80	31	25	22	16	11	8.3	6.3	5.4	4.9
	85	34	28	27	19	13	10	7.2	6.1	5.7
	90	37	33	35	23	16	11	8.5	7.1	6.6
	95	41	40	48	32	21	15	11	8.6	8.2
	99	47	47	77	52	33	24	17	13	11
Sample Size of 20	70	24	18	13	9.3	6.6	4.8	3.6	2.9	2.4
	75	25	20	15	10	7.3	5.4	4.1	3.2	2.8
	80	27	22	17	12	8.2	6.0	4.5	3.6	3.2
	85	30	25	19	13	9.3	6.8	5.1	4.1	3.7
	90	32	30	24	16	11	7.9	5.9	4.7	4.3
	95	36	37	32	21	14	10	7.4	5.8	5.3
	99	42	47	53	33	21	15	11	8.1	7.4
Sample Size of 30	70	21	16	11	7.7	5.5	4.0	3.0	2.4	1.9
	75	23	18	13	8.6	6.2	4.5	3.3	2.6	2.1
	80	25	20	14	10	7.0	5.0	3.7	2.9	2.4
	85	27	22	16	11	7.9	5.6	4.2	3.3	2.8
	90	29	26	19	13	9.1	6.5	4.8	3.8	3.3
	95	33	34	25	16	11	8.1	5.9	4.6	4.1
	99	39	45	40	25	17	12	8.4	6.4	5.5

This approach to estimating expected uncertainties for regressed limits, initially proposed by DeBecker and Modis and then reformulated here, establishes regression as a reasonable approach to identifying upper limits for single-dimension S-curves. Careful consideration, however, should be given to the sample size and to correctly identifying the magnitude of error fluctuations within a sample during application.

6.2.1 Statistically Predicted Upper Limits in Multiple Dimensions

The last section discussed a statistical approach that makes it possible to predict upper limits with some confidence for a single attribute. This section explores the reformulation of this technique for multiple dimensions. The first step is to define the initial growth model into which error fluctuations will be introduced. This initial MDGM is defined by Equation 53, where all b_i are one, all L_i are also one, and a is zero.

$$t = a - \sum_{i=1}^{n} \frac{1}{b_i} \ln\left(\frac{L_i - y_i}{y_i}\right) \tag{53}$$

Not surprisingly, the change of data over which a data sample spans is not as clearly defined in multiple dimensions as for a single dimension. For a single dimension the range of data is defined by the highest level of capability within the data sample, normalized by the upper limit. For multiple dimensions the highest level of capability is characterized by several attributes, namely all y_i. Consequently, the range of data must be defined according to the composite form of the MDGM shown here as Equation 54, where $b_i = (\sum 1/b_i)^{-1}$ and $a = 0$. Recall that y_c can be directly calculated from all y_i's according to Equation 55. Thus, the data range is defined by normalizing the highest level of y_i achieved by each predicted limit, L_i.

$$y_c = \frac{1}{1 + e^{-b_c(t-a)}} \tag{54}$$

$$y_c = \left(1 + \prod_{i=1}^{n} \left(\frac{L_i - y_i}{y_i}\right)^{b_c/b_i}\right)^{-1} \tag{55}$$

It is also more involved to define the initial data sample in multiple dimensions than in a single dimension. For a single dimension, 20 sample data points were assumed

to be evenly distributed throughout the time of the defined data range. This same procedure can be applied to the composite form of a MDGM. Each resulting point of the composite measure, however, corresponds to a family of y_i combinations. By definition, the composite model progresses in time as if all attributes y_i were always at the same frontier of their respective upper limits. In actuality, they will more often than not be at different fractions of their respective upper limits. In order to model this behavior in a simulated data sample, all but one of the attributes was set at a random fraction of its limits, while the remaining attribute was calculated based on the random setting according to Equation 56.

$$y_j = \frac{L_j}{1 + e^{-b_j\left(t-a+\sum_{i\neq j}^{n}\frac{1}{b_i}\ln\left(\frac{L_i-y_i}{y_i}\right)\right)}} \tag{56}$$

Recall that a single attribute's error fluctuations were introduced to the growth rate of the Logistic S-curve, according to Equation 57 and 58, where $\tilde{g}_k$ is the rate of change corresponding to the k^{th} data point of the sample and ϵ the normal distribution, $N(0, \sigma)$.

$$\tilde{g}_k = q_k + \epsilon q_k \tag{57}$$

$$q(t_k) = \frac{L}{(1 + e^{-b(t-a)})(1 + e^{b(t-a)})} \tag{58}$$

DeBecker and Modis introduced error in this manner, suggesting that historical data is most often available in terms of growth rate. They cite examples of reproduction rates, productivities, units sold per trimester, and the like. Data for growth curves modeling technology advancement is most often available in terms of absolute capability levels not rates of change in capability. Consequently, error fluctuations should be applied

directly to the growth curve and not to its derivative. Thus, for multidimensional analysis, error will be applied according to Equation 59, where $y_{i,k}$ is the k^{th} setting of the i^{th} attribute within the sample.

$$\tilde{g}_{i,k} = y_{i,k} + \epsilon y_{i,k} \tag{59}$$

Once error fluctuations are introduced, the model is then regressed by minimizing the sum of χ^2 distributions for each dimension as defined by Equation 60. Following the regression procedure, the data range is redefined according to the predicted limits and composite model. As before, a Monte Carlo simulation is conducted, after each simulation of which predicted limits are grouped into distributions according to the data ranges listed in Table 15. Expected uncertainties are then estimated for confidence intervals of interest.

$$U = \sum_{i=1}^{n} \sum_{k=1}^{m} \left(\frac{q_{i,k} - E(Q_i(t_k))}{\sigma(Q_i(t_k))} \right)^2 \tag{60}$$

Table 15: Upper Bounds to Data Ranges

1 to 19.5-20.5 percent of L_{pred}
1 to 29.5-30.5 percent of L_{pred}
1 to 39.5-40.5 percent of L_{pred}
... ...
1 to 89.5-90.5 percent of L_{pred}
1 to 98.5-99.5 percent of L_{pred}

Table 16 provides the expected uncertainties for each of the above data ranges for one, two, and three dimensions, assuming 5 percent error fluctuations on historical data. These uncertainties apply to each of the predicted limits in the MDGM. For instance, if the limits of a three-dimensional growth model are regressed and the data range has been estimated to be 1-70 percent and error fluctuations of 5 percent, the 90 percent

confidence intervals would be $L_1 \pm 28\%$, $L_2 \pm 28\%$, and $L_3 \pm 28\%$. The first point to note is the difference between the single dimensional growth model uncertainties and those estimated previously and displayed in Table 11. These estimates are shown side by side in Table 17 for easy comparison, wherein the previous estimates are shown in italics. The only effective difference between these estimates is the manner in which error fluctuations are introduced. The difference in introducing error directly to the growth model as opposed to its rate of change results in uncertainties three to four times larger. Consequently, this is an indirect quantification of why relative models generally perform better than absolute models. Error introduced to the curve's derivative has less of an impact on the resulting prediction than error on the curve itself.

Table 16: Expected uncertainty for limits predicted in multiple dimensions with 5% error fluctuations

Confidence Level		Data Range								
		1-20%	1-30%	1-40%	1-50%	1-60%	1-70%	1-80%	1-90%	1-99%
1-D Growth Model	70	37	26	22	17	13	10	7.6	5.6	3.5
	75	40	28	24	18	14	11	8.4	6.1	4.1
	80	42	30	27	20	16	12	9.2	6.8	4.8
	85	45	33	30	23	17	14	10	7.5	5.8
	90	47	36	35	26	20	16	12	8.4	7.0
	95	51	40	51	36	27	20	14	10	9.1
	99	56	46	81	70	47	34	23	16	14
2-D Growth Model	70	45	39	30	23	17	12	9.0	7.3	7.3
	75	54	44	34	25	19	14	10	8.2	8.0
	80	61	50	38	29	21	16	12	8.9	8.8
	85	69	57	44	34	24	18	13	10	10
	90	78	66	51	39	29	21	16	12	11
	95	92	78	62	48	37	27	21	15	14
	99	137	129	95	68	52	43	33	22	21
3-D Growth Model	70	48	38	29	22	17	13	10	9.0	8.9
	75	56	44	34	25	20	16	12	10	10
	80	64	51	39	29	23	18	14	12	11
	85	74	60	46	35	27	22	16	14	13
	90	85	72	54	42	34	28	21	17	17
	95	98	88	69	55	46	39	28	24	24
	99	103	130	91	85	77	64	53	41	41

Table 17: Comparison of error introduction at the 5% error level

Data Range		Confidence Level													
		70		75		80		85		90		95		99	
1-D Growth Model	1-20%	37	*14*	40	*15*	42	*16*	45	*18*	47	*20*	51	*23*	56	*27*
	1-30%	26	*10*	28	*11*	30	*12*	33	*14*	36	*17*	40	*21*	46	*32*
	1-40%	22	*6.7*	24	*7.4*	27	*8.3*	30	*9.4*	35	*11*	51	*13*	81	*20*
	1-50%	17	*4.6*	18	*5.1*	20	*5.8*	23	*6.5*	26	*7.6*	36	*9*	70	*13*
	1-60%	13	*3.4*	14	*3.8*	16	*4.2*	17	*4.7*	20	*5.4*	27	*7*	47	*9*
	1-70%	10	*2.4*	11	*2.7*	12	*3.0*	14	*3.4*	16	*4.0*	20	*5*	34	*7*
	1-80%	7.6	*1.8*	8.4	*2.0*	9.2	*2.2*	10	*2.5*	12	*2.9*	14	*4*	23	*5*
	1-90%	5.6	*1.5*	6.1	*1.6*	6.8	*1.8*	7.5	*2.0*	8.4	*2.3*	9.8	*2.8*	16	*3.7*
	1-99%	3.5	*1.1*	4.1	*1.3*	4.8	*1.5*	5.8	*1.7*	7.0	*2.0*	9.1	*2.4*	14	*3.2*

Also note the increase in the expected uncertainty for each additional dimension. Consider the 1-90 percent data range and a confidence level of 95 percent. For a single dimension the expected uncertainty is 10 percent. For two dimensions the expected uncertainty increases to 15 percent, and for three dimensions the expected uncertainty rises to 24 percent. At 25 percent uncertainty a regressed limit provides limited practical benefit for technology assessment. Furthermore, achieving an uncertainty as *low* as 25% requires a data range of 1-90 percent with only 5 percent error fluctuation. This 25 percent expected uncertainty is also based on randomly distributing the data points throughout the range of each dimension. In reality, this distribution is not guaranteed and as a result uncertainties will likely be higher.

Through the research initiated by DeBecker and Modis and its continuation here, it is possible to evaluate the reasonableness of predicting an upper limit by means of regression through estimating the corresponding expected uncertainty. In many instances, this expected uncertainty is likely to fall within a region of acceptability making limit predictions based on regression a very practical and sound method. The level of practicality is very dependent on the specific characteristics of a particular

assessment, however, and its applicability should be tested on a case by case basis. In general, for high dimensional growth models the expected uncertainty will likely exceed useful levels.

6.3 Multidimensional Limit Identification

The large investment in time and resources required to implement a physics-based approach for limit identification has been the motivation for exploring regressive techniques. These have proven to be much faster but require a larger historical database with a lower degree of error in order to achieve accurate results. Both physics-based and regressive approaches have merit. Which proves to be the best option will greatly depend on the available resources pertaining to any particular technology assessment. This research aims to quantify the impact that limit uncertainty will have on the MDGM, regardless of the approach employed to establish the required limits. If the impact is found to be excessive, additional time and resources can be devoted to reducing limit uncertainty as objectives of the technology assessment dictate. Details of the proposed method are provided in the following chapter on methodology procedure.

CHAPTER VII

TECHNOLOGY ASSESSMENT PROCEDURE

Chapter 5 provides the formulation of multidimensional growth models (MDGMs) that are the basis for the assessment of multi-attribute technologies relative to their upper limits. This chapter presents the actual process for conducting that assessment. The discussion will address the way in which the assessment marshalls the information of the MDGM in order to determine the overall availability for future improvement in the subject technology. Also covered is how the MDGM is used to set reasonable program goals for the future evolution of the technology.

The technology assessment procedure has been formulated into five primary steps:

1. *Problem Definition.* The problem definition includes identifying the technology of interest and the resolution at which the technology is to be assessed, and it also includes identifying the system level metrics that adequately describe the pertinent system attributes.

2. *Compilation of Historical Data.* Collect historical data regarding development for each identified system level metric.

3. *Upper Limits Estimation.* By means of either a regression or physics-based approach, estimate the limits bounding technology growth.

4. *Generation of the Multidimensional Growth Model.* Using historical data and the identified upper limits, formulate and fit an appropriate multidimensional growth model.

5. *Technology Assessment.* Evaluate information provided by the technology growth

model to draw conclusions on the technology's current maturity level and expected growth.

Detailed discussion of each step follows. A notional example is conducted throughout the chapter to illustrate each step of the procedure.

7.1 Step 1: Problem Definition

7.1.1 Technology Identification

Identifying the technology includes both identifying the technology of interest and precisely defining the level of abstraction—the technology resolution—at which the technology is to be assessed. The technology or system for which the assessment is desired must be identified. The degree to which the assessment will be dependent on specific processes, hardware, or applications must also be determined.

The level of technology resolution at which to conduct the maturity assessment entirely dictates the type of information desired from the assessment. The forecaster should select a technology resolution that provides both adequate breadth to encompass all technology variations of interest and adequate precision to provide meaningful conclusions regarding the maturity of the specific technical approaches employed.

Consider the technology envelope provided in Figure 22. A technology assessment can be conducted at three different levels of abstraction (1) the envelope, (2) widget A, B, or C or (3) sublevels of widget A or B—each more resolved than the previous.

Conducting an assessment on the envelope may provide some insight into the level of capability that may be achieved by some future technology architecture, but it would provide no information concerning the development of any particular hardware implementation. Conversely, conducting an assessment on a sublevel of technology A or B will provide detailed insight into a specific hardware implementation, but the results may be too narrow in scope to be of practical significance. An assessment representative of technology A, B, and C is of most interest because it provides insight

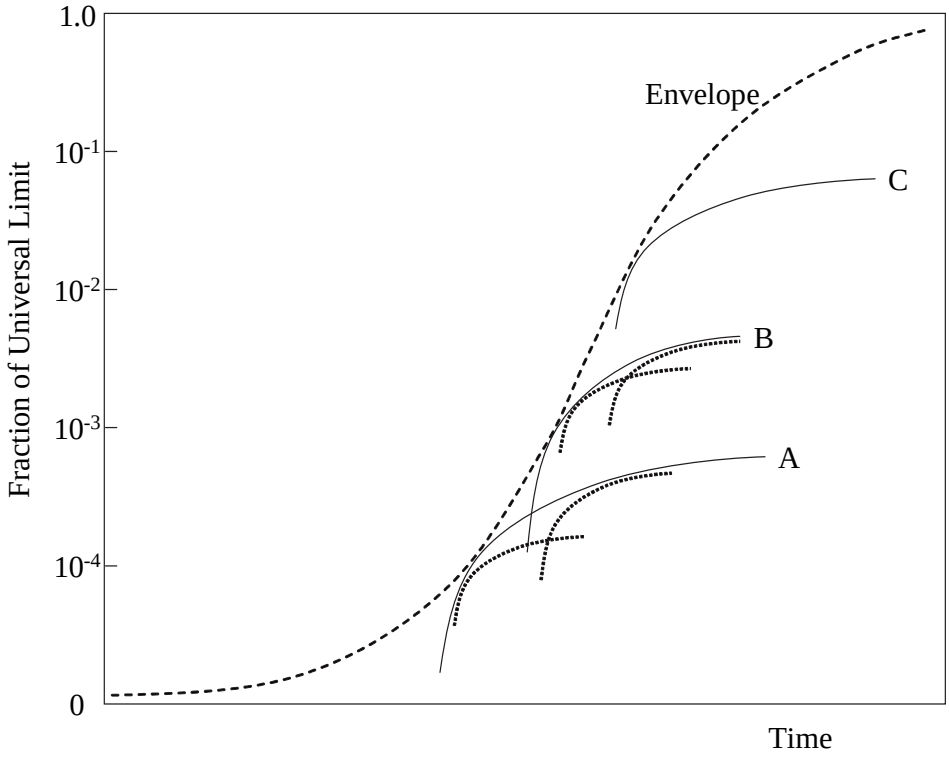

Figure 22: Example Technology Envelope

into the availability of future improvement of a broad class of systems possibly representing a handful of hardware implementations based on a common set of physical processes.

7.1.2 Metrics Identification

Once the technology and the resolution of interest have been identified, the forecaster can select an appropriate set of metrics. The metrics should be in accordance with the technology resolution specified. For high levels of resolution, the chosen metrics should be more hardware specific in order to provide an assessment of adequate precision as indicated by the high level of resolution. For lower levels of technology resolution, metrics should be more general since they must apply to a broader class of technologies rather than only a few specific hardware configurations. While the technology resolution of interest is determined when the technology is identified, it is

realized in the modeling process as a result of metric selection.

After identifying the level of abstraction chosen for each metric, the forecaster must select an appropriate set of metrics that comprehensively captures the system attributes of interest. To date, S-curve modeling has been based on a single metric whereby data has been collected and subsequently reduced to remove variation due to other attributes. The result is a historic trend of a single metric independent of all others. While this approach does yield an accurate assessment of the state of the art for the particular metric being considered, it does not give an accurate assessment of the technology as a whole. For more complex multi-attribute systems, this approach provides little meaningful insight for decision-makers. The strategy proposed in this research attempts to attribute the variation within any one metric to the other significant system level metrics. As a result it is imperative to identify significant design drivers.

Furthermore, all metrics included in the assessment must be independent. Because of the regression that will subsequently be used to fit the MDGM, correlation between any two metrics can misrepresent the importance of the those metrics. Following the collection of historical data, a test will be conducted to establish the correlation between identified metrics.

Example

Four hypothetical metrics of interest have been identified that comprehensively quantify the state of the art for the hypothetical technology identified. They will be denoted as y_1, y_2, y_3, and y_4.

7.2 Step 2: Compilation of Historical Data

The purpose of this step is to collect the historical data necessary to develop an accurate growth model of the subject technology. The forecaster should compile a database of past and present systems within the technology architecture and it should

contain the entry date of each system along with the system's capability levels for each metric identified in Step 1. Each system included in the database must represent the state of the art at the time it was introduced. Including 'sub-par' systems will negatively impact the validity of the assessment. Additionally, indiscriminately compiling experimental systems concurrently with operational systems will also distort the growth model. All systems included in the database should have had a technology readiness level of 9 and manufacturing readiness level of 9 for their corresponding introductory dates.

Each system included in the database represents a point on the technology frontier for the date it was introduced; thus, it must employ the most advanced technology available at the time of its development. Systems not employing the most advanced technology for their date of introduction do not represent the state of the art and do not fall on the technology frontier. Such systems should not be included in the growth model because they do not accurately represent what was actually possible at that time in the technology architecture's development. Each system included in the database must have been designed to push the envelope of technical capability in one or more system level metrics.

Example

Data points were generated for each of the first three metrics by randomly selecting settings between defined upper and lower bounds. Data for the fourth was generated as a linear combination of the previous three to simulate a correlated metric. Using predefined Logistic curve parameters for these metrics, the date corresponding to each vector of metric settings was calculated within which a small degree of random error was introduced to simulate real data. Table 18 provides the resulting data.

The correlation coefficient was then calculated for each pair of metrics in order to establish the independence of each metric. Figure 23 provides a bivariate plot for each pair of metrics, illustrating their correlation while Table 19 provides quantification of

Table 18: Notional Historical Data

	Date	y_1	y_2	y_3	y_4
1	1953	0.75	1.01	1.95	1.44
2	1953	0.03	1.90	1.99	1.63
3	1954	0.00	1.41	0.25	0.59
4	1957	0.03	1.54	1.81	1.43
5	1959	0.03	1.29	1.10	0.99
6	1965	0.82	1.55	2.00	1.65
7	1965	0.04	1.79	1.50	1.35
8	1973	0.23	1.48	1.29	1.18
9	1973	0.21	1.39	0.84	0.92
10	1975	0.17	1.65	1.01	1.09
11	1976	0.32	1.25	0.37	0.65
12	1977	0.29	1.56	0.81	0.97
13	1979	0.36	1.15	0.15	0.52
14	1981	0.48	1.74	1.43	1.38
15	1983	0.51	1.14	0.12	0.52
16	1984	0.68	1.42	1.77	1.47
17	1988	0.35	1.52	0.11	0.62
18	1988	0.69	1.73	1.14	1.26
19	1990	0.44	1.83	1.47	1.42
20	1990	0.84	1.74	1.27	1.35
21	1991	0.36	1.40	0.32	0.69
22	1994	0.94	1.15	0.25	0.66
23	1997	0.85	1.77	1.79	1.63
24	1999	0.79	1.71	0.17	0.79
25	2003	0.87	1.65	0.72	1.06

this correlation for each metric pair. As can be observed in Figure 23, metric y_4 is highly correlated with each of the remaining metrics most of all metric y_3, indicated by the linear trend in the respective bivariate plot. Note the especially high correlation coefficient between y_3 and y_4 in the correlation matrix of Table 19. As a result of this correlation, y_4 will be removed from the model and no longer included in the assessment. One of any highly correlated pair of metrics should be removed from the model to ensure independence between all metrics remaining in the assessment.

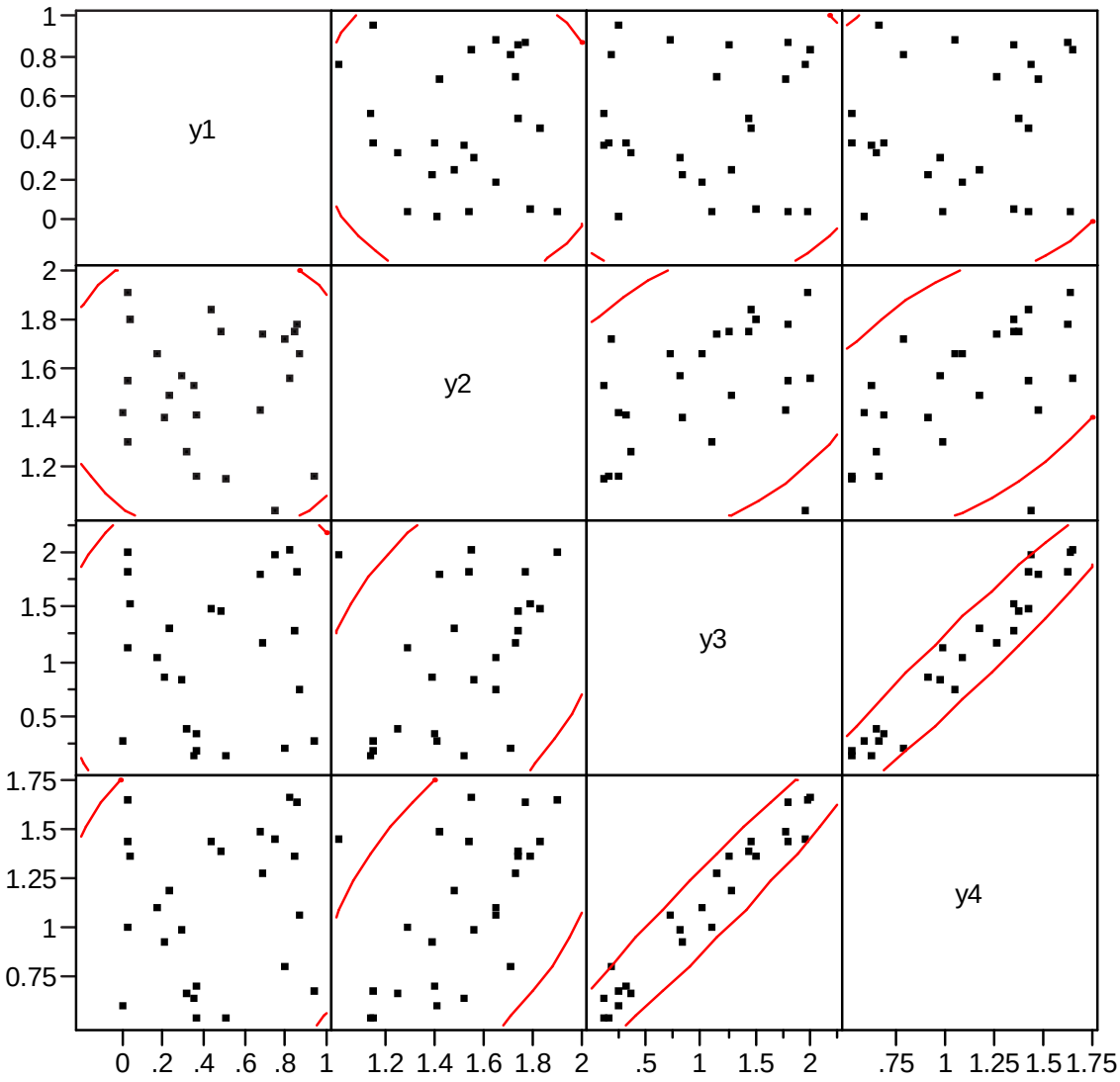

Figure 23: Bivariate Correlation Plots

Table 19: Metric Correlation Matrix

	y1	y2	y3	y4
y1	1.0000	-0.0369	0.0249	0.1491
y2	-0.0369	1.0000	0.4005	0.5644
y3	0.0249	0.4005	1.0000	0.9723
y4	0.1491	0.5644	0.9723	1.0000

7.3 Step 3: Upper Limits Estimation

Two primary approaches for identifying upper limits were extensively presented in Chapter 6. That discussion concluded that regression is a reasonable approach if expected uncertainties can be estimated for the resulting limit predictions. In order for these expected uncertainties to fall within an acceptable range, however, historical databases must be large, have very small error, and span a large segment of the overall growth curve. Physics-based limits, on the other hand, are not at all dependent on historical data. This frees them from the troubles of scant erroneous or skewed lists of data. Physics-based approaches, however, may require significant investment in time and resources to assemble the disciplinary experts necessary to accurately estimate upper limits for each metric.

Whether a regression or physics-based approach is employed, the resulting limit will not be known precisely but only known with some degree of certainty. Thus, the approach employed by this research is to quantify the impact of limit uncertainty on the technology rather than simply endorse one method or the other. This is accomplished by defining probability distributions to the upper limit of each metric considered in the assessment. These distributions can result from statistical techniques similar to those presented in the previous chapter or physics-based approaches or even expert best guesses. Furthermore, these distributions can take the form of a very narrow normal distribution, that indicates a high degree of certainty or a very broad uniform distribution which suggests the limit is only known to be bound between two extremes. Certainly a more precisely defined limit is desired, but either can provide valuable information even if the information only indicates that additional investment should be devoted to more precisely defining the limit.

Consequently, the farther a technology is from its upper limit, the less the upper limit influences additional growth, while the closer the technology is to its upper limit the more likely it will be that both limit identification approaches are able to provide

more precise predictions. If, therefore, a technology assessment is updated periodically, the level of uncertainty can be reduced as the technology proceeds along the S-curve and strategic goals can be simultaneously updated as knowledge of availability for improvement becomes more certain.

Example

A distribution that describes the expected uncertainty for each specific limit should be selected. The same distribution does not necessarily have to be used for all three metrics. In cases were very little is known about the limit, a uniform distribution should be used which would indicate only that the limit is bound between two extremes. The following Weibull distributions are used to quantify the expected limit uncertainty for each metric in this example. Weibull distributions are used here to simulate a high degree of certainty in one limit extreme as illustrated by the left bound of the Weibull distribution and a lower degree of certainty for the right limit extreme.

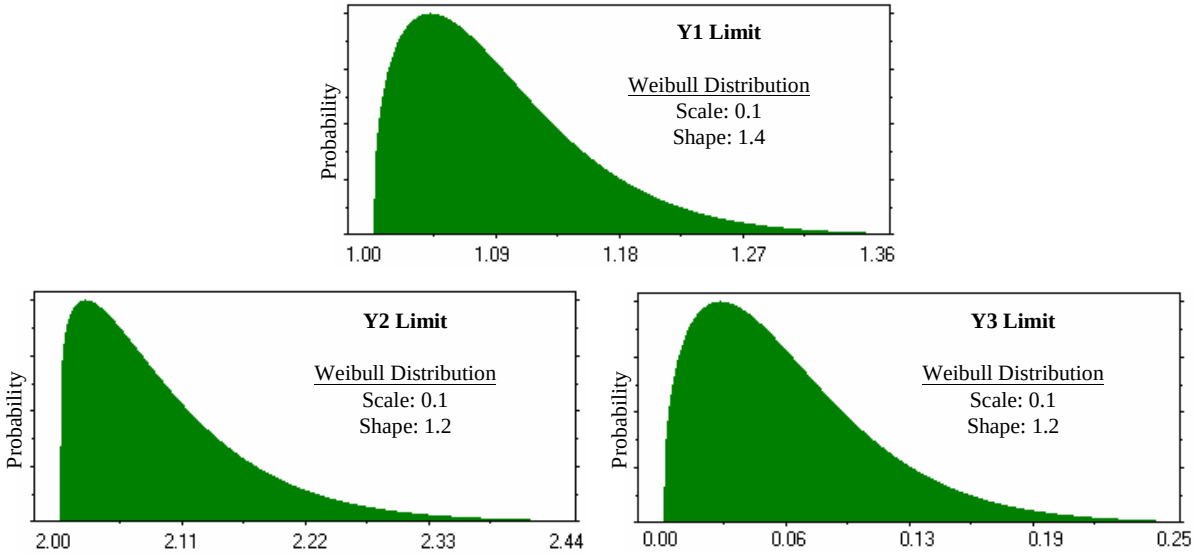

Figure 24: Metric Limit Distributions

7.4 Step 4: Generation of the Multidimensional Growth Model

Step 4 is the core of the assessment procedure. In this step the forecaster integrates the information gathered in the previous steps into a multidimensional growth model. This step includes formulating and fitting an appropriate growth model, evaluating its goodness of fit relative to the historical data, and establishing confidence intervals around the resulting MDGM.

7.4.1 Formulation of the Multidimensional Growth Model

Formulating the MDGM involves choosing an appropriate growth model to describe the evolution of the technology towards its upper limits and expanding the selected model to accommodate each metric identified in Step 1.

Several techniques and considerations for choosing an appropriate growth model were discussed both in Chapters 3 and 5 and will only briefly be discussed here. The most significant choice to be made is whether a relative or absolute model will be employed. Recall that relative models generally have a higher number of unknowns ($3n + 1$ or $4n + 1$), are much more computationally intensive to solve, though in some cases they do not require knowledge of the upper limit, and often provide more accurate predictions than absolute models. Conversely, absolute models can have as few as $n + 1$ unknowns and can often be linearized such that regression is computationally trivial. Once an appropriate growth model is selected, the model should be extended into n-dimensions as outlined in Chapter 5.

Example

The Logistic growth model will be utilized for this example because of its popularity for simulating technology growth and because of its simplified linear form. Equation 61 provides the expected MDGM used for this example.

$$t = a - \frac{1}{b_1} ln\Big(\frac{L_1 - y_1}{y_1 - y_{o,1}}\Big) - \frac{1}{b_2} ln\Big(\frac{L_2 - y_2}{y_2 - y_{o,2}}\Big) - \frac{1}{b_3} ln\Big(\frac{L_3 - y_3}{y_3 - y_{o,3}}\Big) \tag{61}$$

7.4.2 Fitting the Model

The specific procedure used to fit the MDGM will depend on which growth model is utilized. Regardless of the selected MDGM, however, there are numerous regression techniques that can be employed to fit each model. Many of the absolute growth models can be linearized and least squares fit can be employed, while each of the relative models requires a more sophisticated regression technique. The exact regression technique employed is not significant to the overall assessment procedure and because of the wealth of knowledge available on both linear and non-linear regression techniques they will not be discussed in further detail here [47, 84, 85, 86, 87]. Once the model has been regressed, the goodness of fit should be evaluated. This research will focus its attention on three primary considerations, the coefficient of multiple determination (R^2), residual plots, and parameter significance.

R^2. The coefficient of multiple determination, R^2, should be near unity in which case the predicted dates resulting from the MDGM would perfectly match the actual dates of introduction for each historical data point. R^2 values should preferably be no lower than 0.90 and preferably greater than 0.95. A low R^2 may indicate a number of potential problems. There may be systems included in the historical data that did not represent the state of the art for their introduction date. As a result, the regression process attempts to fit points to the model that do not lie on the technology frontier that the model is intended to simulate. This can be remedied by removing those points that have the highest positive residuals. A low R^2 may also suggest that one or more metrics significant to the state of the art were omitted from consideration—a reevaluation of the metrics used to quantify the technology should be conducted. Poor selection of a growth model may also be cause for a low R^2.

Residual Plot. The residuals should be randomly distributed about zero with no discernable patterns observed on a residual plot. Any patterns present in the residual plot would suggest that either the selected growth model did not adequately describe the technology behavior or a metric significant to the state of the art was neglected from consideration.

If there are no discernable patterns in the residual plot but the points are not equally distributed about zero, the systems represented in the historical database may not all represent the state of the art for their date of introduction. If there are significantly fewer positive residuals, this suggests that one or more of the systems contained in the historical database were not state of the art for their introduction date. Significantly few negative residuals would indicate that one or more systems in the historical data were unusually advanced for their date of introduction. This might result from including systems in the historical database that were not yet at a technology readiness level of 9 for their corresponding date of introduction, or it might result from a significant increase in engineering effort that was devoted to those systems relative to other systems in the database.

Parameter Significance. The significance of each metric should be evaluated to assess its importance to the model. The manner in which this is accomplished will be dependent on the particular model employed. For models that can be linearized this is most easily assessed by evaluating the t-statistic or P-value for each coefficient in the model. Metrics having coefficients with a t-statistic greater than 2 or less than -2 and a P-value less than 0.05 will be considered significant and should remain in the model. This ensures with 97.5 percent confidence that coefficients meeting these criteria should be nonzero and as such are significant to the model. Metrics having coefficients that do not meet these criteria may not be significant to the model, or it may suggest that the systems contained within the historical database do not provide enough variation in those particular metrics to adequately capture their significance.

These metrics should either be removed from the model, or if possible, additional systems should be included in the historical database that provide a larger range of variation in these metrics.

Example

The first step to fitting the multidimensional growth model provided in Equation 61 is estimating the S-curve starting point, y_o, for each metric. By observation of the historical data provided in Table 18, starting points, $y_{o,i}$, for each y_1, y_2, and y_3 are estimated at 0, 1, and 2, respectively. These values are in agreement with those initially specified to generate the hypothetical data.

By comparing these starting points to the limit distributions specified previously, it is clear that metric y_3 is a "minimum is best" attribute, where as the other two are "maximum is best" attributes. That is, the direction of improvement for metric y_3 is towards a lower limit rather than towards an upper limit. The fundamental pattern of technological development, however, is the same as that of an attribute approaching its upper limit, only the direction of improvement is different. Consequently, the same growth curves can be employed to model this advancement towards a lower limit as those used to model advancement towards an upper limit. Only minor changes are required. In fact, for many growth curves such as the Logistic and Gompertz no adjustments are required. The limit, L, in these models can just as easily correspond to a lower limit as an upper limit. Likewise, the starting point, y_o, can also be a level of capability from which the system evolves downward rather than upward. This is illustrated in Figure 25. Some growth models, however, may require transforming the data to invert the curve prior to fitting the model. This can be accomplished in many ways. Figure 26 illustrates one approach whereby the data is reflected about y_o.

Once the direction of improvement for each attribute is addressed the MDGM is linearized by applying the transformation provided in Equation 62. This results in the regression model of Equation 63, where $\beta_0 = a$ and $\beta_i = -1/b_i$. The only additional

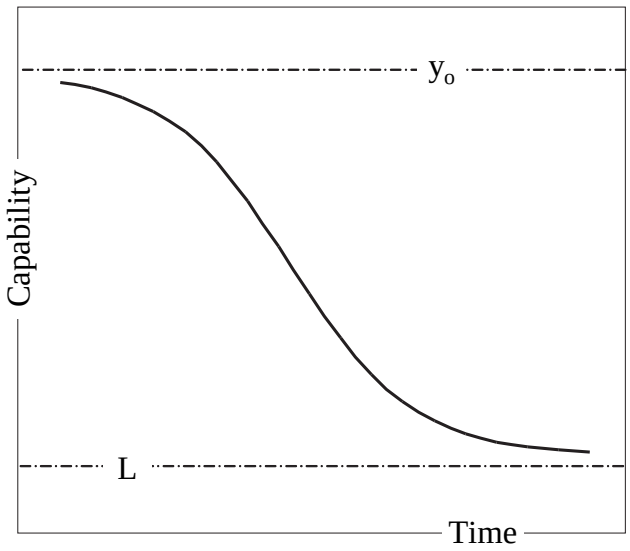

Figure 25: Inverted S-curve

information required to conduct the regression procedure is the specification of the upper limits. This initial regression is conducted to evaluate the goodness of fit for the model, which is not significantly dependent on the specific limits utilized provided that the distribution for each limit is not excessive. A limit should be selected for each metric near its most probable value. For this demonstration limits of 1, 2, and 0 were selected for each L_1, L_2, and L_3, respectively. Applying the transformation of Equation 62 to the historical data according to each $y_{o,i}$ and L_i specified above results in the design matrix shown in Table 27.

$$X_i = ln\left[\frac{L_i - y_i}{y_i - y_{o,i}}\right] \tag{62}$$

$$t = \beta_0 + \beta_1 X_1 + \beta_2 X_2 + \beta_3 X_3 \tag{63}$$

Numerous approaches can be employed to regress the linear model of Equation 63 against the transformed data provided in Table 27. The statistical package JMP was used for this demonstration resulting in the fit summarized by Figure 27. Note

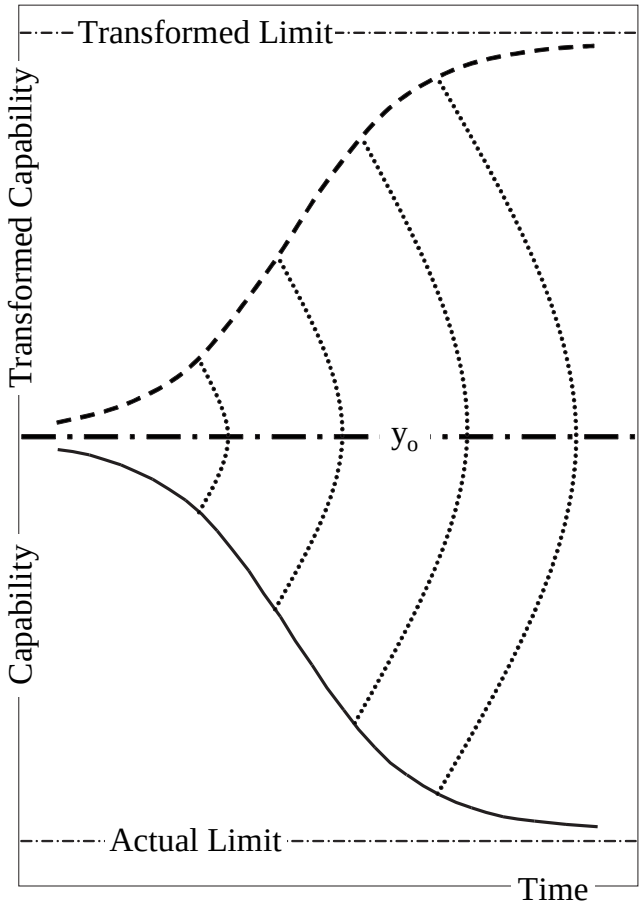

Figure 26: Reflected S-curve Data

each of the three measures describing the goodness of fit. The R^2 value of 0.95 is at an acceptable level which indicates a good fit; however, the residual is noticeably unbalanced with the majority of points falling below zero. This suggests that one or more points within the historical database was significantly below the state of the art for its introduction date, which produced large positive residuals. Note the five red points distinctly offset from the remainder of the data set. The significantly higher residuals for these points indicate that they were considerably below the state of the art as quantified by the dimensions of capability included in the model. Points that appear below the SoA for their introduction dates may indicate design preference for a dimension of capability not included in the model. These outliers can be investigated

Table 20: Transformed Regression Data

	Date	X_1	X_2	X_3
1	1953	-1.10	4.93	3.72
2	1953	3.51	-2.15	5.56
3	1954	6.24	0.38	-1.95
4	1957	3.40	-0.16	2.28
5	1959	3.54	0.89	0.21
6	1965	-1.51	-0.20	6.98
7	1965	3.24	-1.31	1.11
8	1973	1.22	0.06	0.59
9	1973	1.31	0.46	-0.32
10	1975	1.55	-0.63	0.02
11	1976	0.74	1.11	-1.49
12	1977	0.89	-0.23	-0.38
13	1981	0.09	-1.04	0.93
14	1983	-0.04	1.79	-2.77
15	1984	-0.75	0.30	2.03
16	1979	0.59	1.70	-2.48
17	1988	0.62	-0.07	-2.84
18	1988	-0.81	-1.00	0.28
19	1990	0.24	-1.61	1.02
20	1990	-1.62	-1.03	0.55
21	1991	0.58	0.39	-1.66
22	1994	-2.67	1.77	-1.97
23	1997	-1.75	-1.21	2.13
24	1999	-1.34	-0.91	-2.41
25	2003	-1.92	-0.61	-0.57

to identify any additional system metrics that should be included in the model. If no additional metrics are identified which included in the model do not serve to lower the residuals for these systems, they should be removed from consideration. That is the coarse of action used for this simple demonstration. Before proceeding with the omission of these points, also note the *t-ratio* and $Prob >| \ t \ |$ shown in Figure 27 which exactly correspond to the the t-statistic and P-value, respectively. Each metric more than satisfies the criteria set forth above for significance, which confirms that all three metrics should be included in the model.

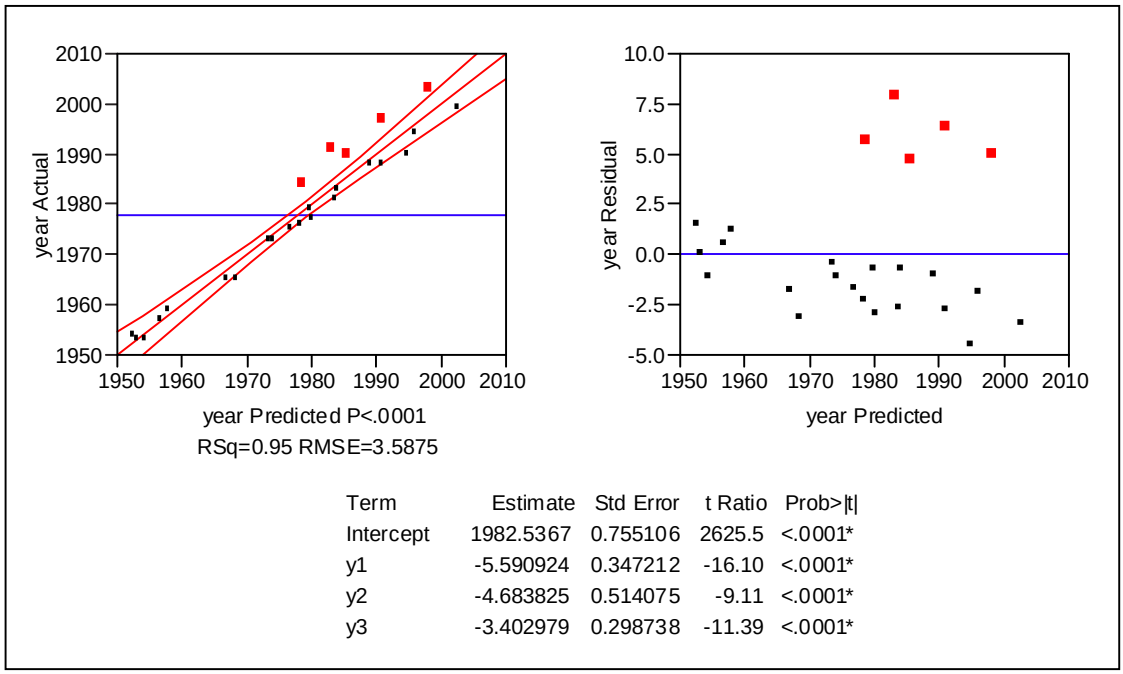

Term	Estimate	Std Error	t Ratio	Prob>|t|
Intercept	1982.5367	0.755106	2625.5	<.0001*
y1	-5.590924	0.347212	-16.10	<.0001*
y2	-4.683825	0.514075	-9.11	<.0001*
y3	-3.402979	0.298738	-11.39	<.0001*

Figure 27: Goodness of Fit Prior to Data Reduction

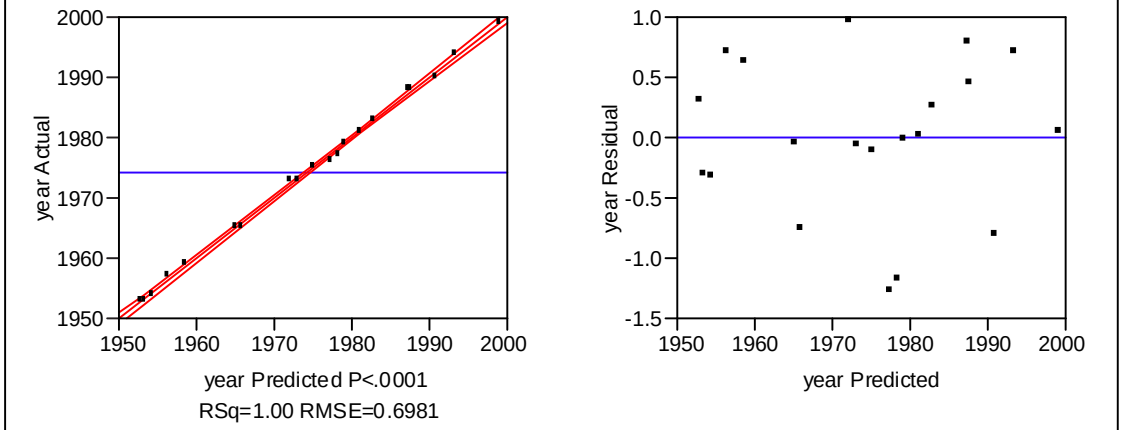

Term	Estimate	Std Error	t Ratio	Prob>|t|
Intercept	1980.3959	0.174687	11337	<.0001*
y1	-4.998085	0.074474	-67.11	<.0001*
y2	-4.046848	0.107623	-37.60	<.0001*
y3	-3.397709	0.060225	-56.42	<.0001*

Figure 28: Goodness of Fit After Data Reduction

Omitting each of the five outlying data points and refitting the model results in the fit summarized by Figure 28. Again note that R^2 is now very nearly one, which indicates an excellent fit. Notice the change in the residual plot. It does not appear to have any discernable pattern and now seems to be randomly distributed around zero, also indicating a good fit. Finally, consider the *t-ratio* and $Prob >| \ t \ |$, each of which indicate even stronger significance than previously noted. With each criterion for the goodness of fit satisfied, a forecaster can be fairly confident in the resulting MDGM. The next step quantifies that confidence by establishing confidence intervals around forecasts resulting from the MDGM.

7.4.3 Establishing Confidence Intervals

Once the general form of the MDGM model has been formulated and tested for goodness of fit, uncertainty in the model must be quantified by establishing confidence intervals around the resulting forecasts. There are two primary sources of uncertainty, and their effect must be quantified: upper limit estimations and random error present in the historical database. These sources of uncertainty must be quantified collectively into a single confidence interval.

Consider how each source of uncertainty contributes to the overall uncertainty of the MDGM. Uncertainty in the upper limits results from the inability to precisely calculate the upper limits that a metric approaches. In order to accommodate for this imprecision, distributions describing its probable location have been defined for each limit. This uncertainty is introduced into the MDGM during the transformation of the historical database in order to acquire the design matrix. This uncertainty is then introduced into the parameter estimates as a result of the regression process.

Random error within the historical database can result from several sources. One major source of error results from the inevitability that not all systems in the database will fall precisely on the technology frontier for their respective dates of introduction.

Another source of error is fluctuations in engineering effort overtime that are not quantified by a time-based formulation of growth models. Other sources may be as untraceable as reporting errors or the discretization of reported data. Regardless of the exact source, this error is accumulated within the historical database. As a result, it is present even before the MDGM is formulated, and it is propagated through to the parameter estimates during regression.

Because of the substantially different characteristics between each source of uncertainty, separate steps must be employed to quantify each. The uncertainty resulting from upper limit estimations will first be quantified, to which the contribution of uncertainty resulting from the error present in the historical database will be added.

Limit Uncertainty. Because the limit distributions are predefined, a reasonable approach to quantify their aggregate influence on the resulting MDGM is to employ a Monte Carlo (MC) simulation. During each iteration, settings for each metric limit are selected according to the predefined distributions, and the MDGM is refitted accordingly. The parameter estimates from each iteration are accumulated, which results in a distribution for each parameter estimate. A convenient form in which to visualize the accumulated effects of the limit uncertainties is in the composite S-curve shown in Figure 29. A unique composite S-curve results from each Monte Carlo simulation, providing a distribution of dates within which a specific level of capability is achieved. Shown in Figure 29 are the distributions resulting at 25 and 75 percent of the upper limit.

Once the Monte Carlo simulation has been conducted, it is possible to determine the mean composite S-curve and the $1-\alpha$ confidence region. A forecaster can establish the confidence intervals by identifying the two S-curves within the Monte Carlo simulation between which the $1-\alpha$ fraction of the remaining curves reside. These two S-curves are identified by analyzing the distributions occurring at two different fractions of the normalized upper limit—shown in Figure 29 at 25 and 75 percent of

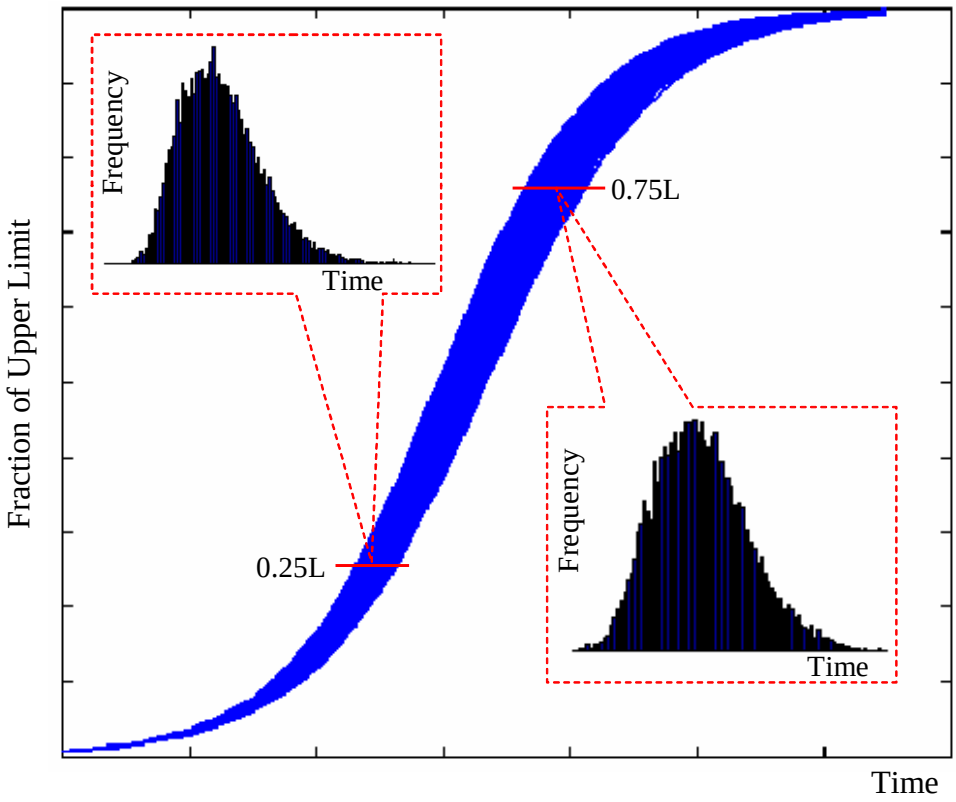

Figure 29: Uncertainty in a Technologies Composite Measure

the upper limit. For these distributions, the dates corresponding to the mean and each of the $\alpha/2$ and $1-\alpha/2$ quantiles are identified. These quantiles are shown graphically in Figure 30. The mean date at each fraction of the upper limit can be represented by a single S-curve that intersects the mean date at both the 25 and 75 percent capability levels as depicted by the dashed curve in Figure 30. In this same manner the $\alpha/2$ and $1-\alpha/2$ confidence bands can also be determined.

Because these confidence intervals are based on the distribution at only two levels of capability, they are inherently based on the assumption that the S-curves resulting from the MC simulations do not intersect. If a high percentage of the S-curves intersect, then the distributions of curves at the 25 and 75 percent performance level will not necessarily be representative of the distributions at other levels of capability. Conversely, if no two curves intersect between the 0 and 100 percent capability levels

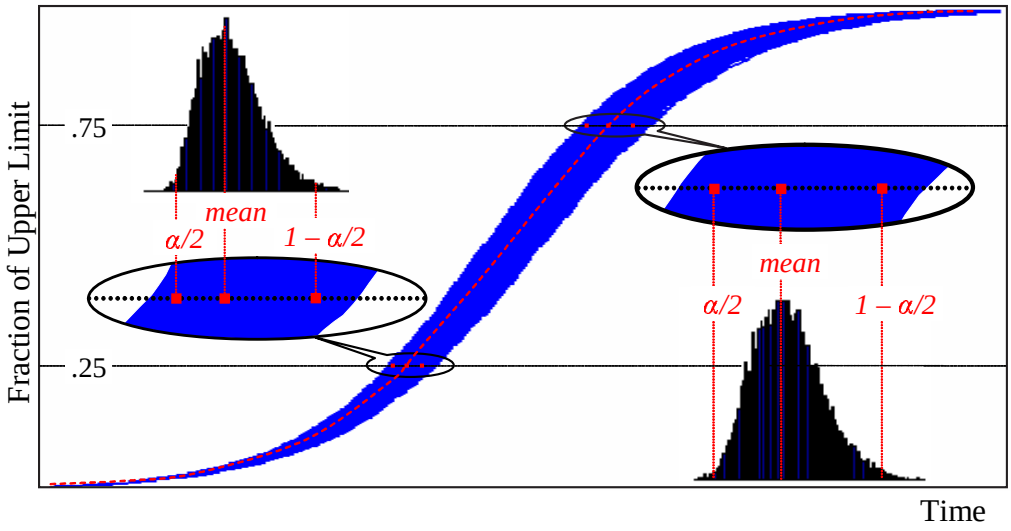

Figure 30: Establishing Limit-Based Confidence Intervals

then the S-curve representing a specified probability of occurrence for a particular level of a capability will represent that same probability of occurrence at all other levels of capability.

The assumption that the curves contained within the composite S-curve distribution do not intersect can be tested by conducting a MC simulation on the S-curves. Two curves are selected at random from the composite S-curve distribution and tested to determine at what fraction of the normalized upper limit they intersect. All S-curves from the above distributions intersect at both 0 and 100 percent capability levels. As a result small differences between parameter estimates can also cause S-curves to intersect in regions near 0 and 100 percent. For the example problem being conducted throughout this chapter 10.2 percent of the S-curves were found to intersect between the 10 and 90 percent capability levels, indicating that it is reasonable to assume that a single S-curve represents the same probability of occurrence at all capability levels. This assumption is expected to hold for all MDGM formulations having a high goodness of fit, but can be easily validated for any specific formulation.

Explicit details of the above procedures for quantifying the impacts of uncertainty

in upper limit estimations will be provided in the example at the conclusion of this section. The impacts of random error within the historical database will first be considered.

Once the combined confidence interval width is satisfactory, the confidence intervals can be utilized in one of two ways, Figure 31 provides the resulting confidence intervals, including uncertainty resulting from both the upper limit estimations and the historical database. One usage establishes the time interval over which a specified capability level will be achieved with $1 - \alpha$ confidence. This can be employed to bound the forecast of the expected introduction date of a system having specified capability levels for each metric. Another usage of the confidence intervals establishes the capability interval that will (with a confidence of $1 - \alpha$) include the capability achieved on a specified introduction date. This can be used to bound the relative distance a system is from its upper limit at any point in time.

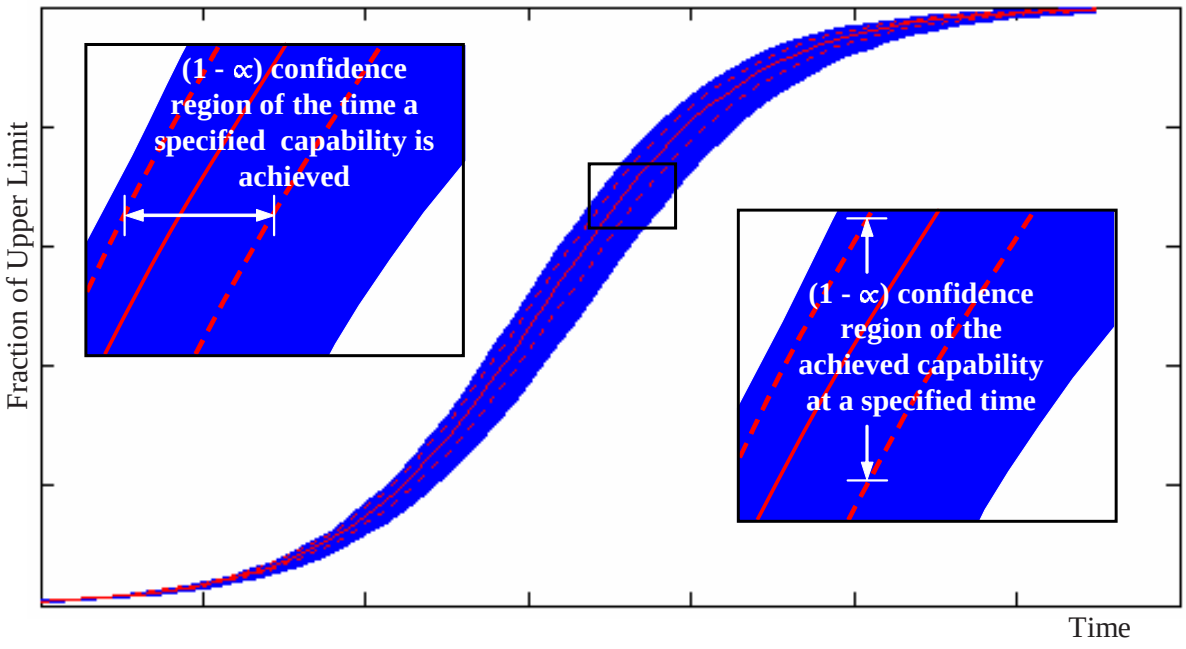

Figure 31: Confidence Intervals Resulting from Limit Uncertainty

Data Uncertainty. Forecasters can quantify the uncertainty in the MDGM resulting from random error within the historical database by using standard statistical techniques for calculating confidence intervals on regression parameters and responses. Anytime the MDGM is regressed against the historical data, confidence intervals can be determined for both the parameter estimates and responses that account for random error within the historical database. In order that the resulting confidence interval can be accumulated with the intervals established for upper limit uncertainty, the regression confidence interval should be determined with respect to time. By establishing the $1-\alpha$ confidence region resulting from the regression process for the mean and each the $\alpha/2$ and $1-\alpha/2$ S-curves identified previously, the total confidence interval accounting for both random error in the historical database and limit uncertainty can be established. Figure 32 illustrates how this is accomplished. The combined $1-\alpha$ confidence interval can be estimated by applying a one-sided $1-\alpha$ regression confidence interval to each of the S-curves bounding the $1-\alpha$ limit confidence interval. The distance between these one-sided regression confidence intervals comprises the combined $1-\alpha$ confidence interval accounting for both random error present in the historical database and limit uncertainty.

Figure 32 also provides for the comparison of the relative contributions of uncertainty resulting from random error in the historical database and upper limit estimations. Generally, the contribution from error in the historical data will be small compared to the limit contribution as large data error would have failed to meet the goodness of fit criteria. If the combined confidence interval width is found to be excessive, additional research should be applied to more precisely identify metric limits. The resulting reduction in distribution width for each metric's limit will subsequently diminish the confidence interval for the MDGM.

The following example will demonstrate in detail the formation of these confidence intervals.

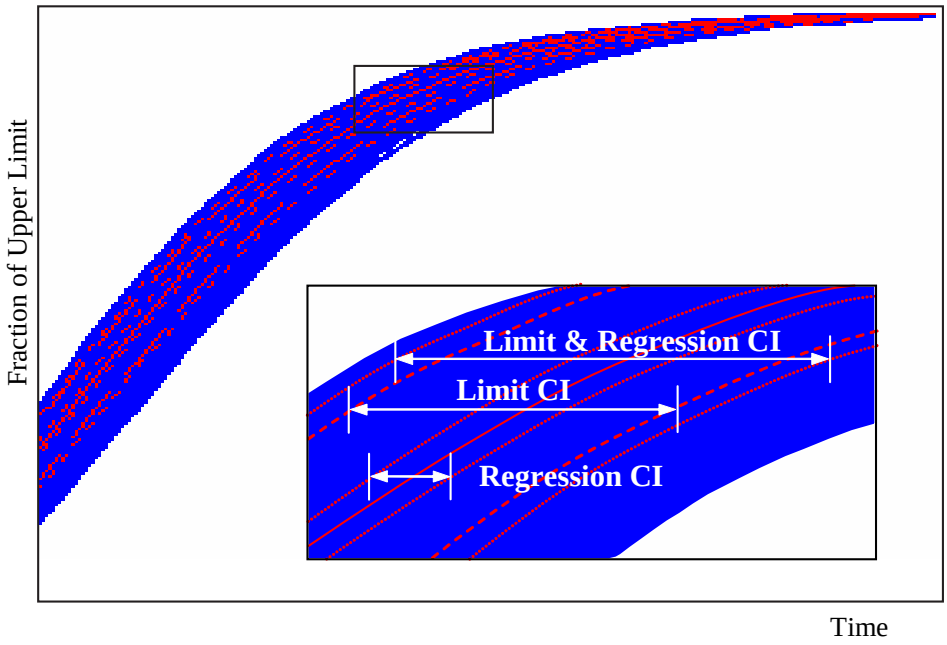

Figure 32: Combined Limit and Data Error Confidence Intervals

Example

The first step to estimating the combined confidence intervals is to conduct a Monte Carlo simulation on the MDGM provided as Equation 61. The software package Crystal Ball [88] was used to generate 20,000 combinations of limit settings according to the probability density functions provided in Figure 24. Matlab was then employed to regress the MDGM for each of the 20,000 simulations. Each simulation included the following steps:

1. Transform the historical data according to

$$X_i = ln\left[\frac{L_i - y_i}{y_i - y_{o,i}}\right] \tag{64}$$

2. Regress the following model by least squares fit

$$t = \beta_0 + \beta_1 X_1 + \beta_2 X_2 + \beta_3 X_3 \tag{65}$$

3. Calculate and record the dates at which the composite model achieved 25 and 75 percent of the upper limit, where

$$t_{.25} = \beta_0 + \frac{-1}{(\sum_1^3 \beta_i)^{-1}} ln(3) \tag{66}$$

and

$$t_{.75} = \beta_0 + \frac{-1}{(\sum_1^3 \beta_i)^{-1}} ln\left(\frac{1}{3}\right) \tag{67}$$

In order to establish the contribution to the overall confidence interval of limit uncertainty, the $\alpha/2$ and $1-\alpha/2$ quantiles must be identified at each 25 and 75 percent of the upper limit. This is accomplished by generating histograms of the dates calculated for achieving each of these levels of capability. Figure 33 shows the resulting distributions wherein the mean and 5 and 95 percent quantiles are specified corresponding to a 90 percent confidence interval.

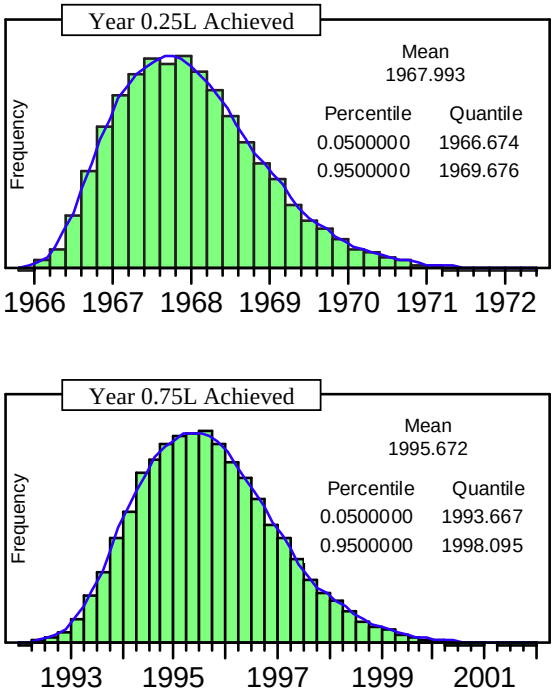

Figure 33: Distributions Resulting from Monte Carlo Simulation

The mean at all levels of capability is represented by identifying the S-curve—from among the MC simulations—that most nearly intersects the mean at each the 25 and 75 percent capability levels. This MC simulation is identified by minimizing the Euclidean distance between the dates calculated for the 25 and 75 percent capability levels and for those identified as the means for each corresponding distribution. This distance was calculated according to Equation 68. The MC simulation having the lowest distance corresponds to that S-curve which most nearly intersects the mean at both the 25 and 75 percent capability levels and approximates the mean at all other levels of capability.

$$s_{mean} = \sqrt{(t_{.25,i} - \bar{t}_{.25})^2 + (t_{.75,i} - \bar{t}_{.75})^2} \tag{68}$$

This same approach is used to identify the two S-curves that form the boundaries of the 90 percent confidence interval each corresponding to the 5 and 95 percent quantiles. The distance used as the criterion for each of these cases is calculated using Equations 69 and 70. The limits and parameter estimates provided in Figure 34 characterize the S-curves identified for each the mean and confidence interval boundaries.

$$s_{\alpha/2} = \sqrt{(t_{.25,i} - t_{.25,\alpha/2})^2 + (t_{.75,i} - t_{.75,\alpha/2})^2} \tag{69}$$

$$s_{1-\alpha/2} = \sqrt{(t_{.25,i} - t_{.25,1-\alpha/2})^2 + (t_{.75,i} - t_{.75,1-\alpha/2})^2} \tag{70}$$

Recall that the accuracy with which these S-curves estimate the same quantiles at other levels of capability is contingent on the assumption that only a small fraction of the S-curves resulting from the MC simulation intersect at levels of capability within

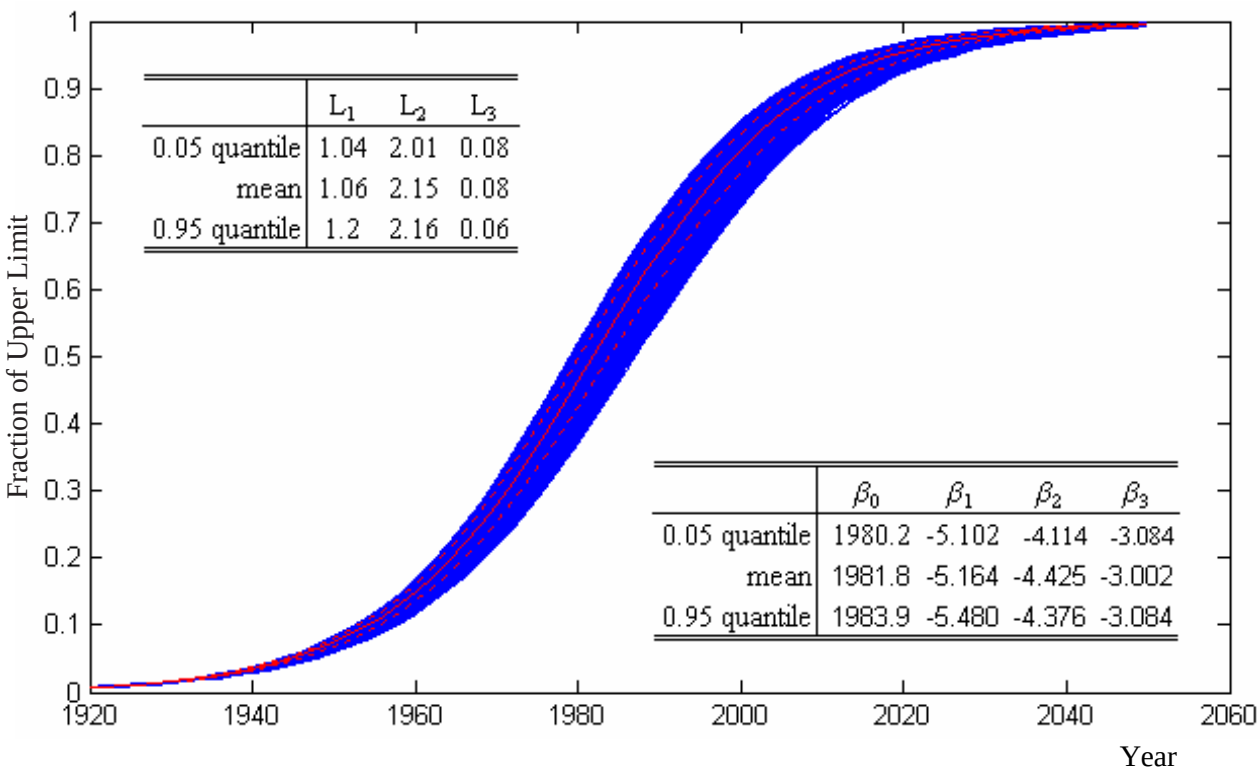

Figure 34: Parameter Estimates for Limit Confidence Intervals

the range of interest. To test this assumption, 100,000 pairs of S-curves resulting from the Monte Carlo simulation were selected at random and tested for an intersection. Figure 35 provides the resulting distribution of intersection locations relative to the level of capability. Of the 100,000 pairs that were tested, 36,924 pairs were found to intersect between the 1 and 99 percent levels of capability. The number of intersections drops by almost a factor of four by accounting for only those intersections occurring between 10 and 90 percent capability level. These results confirm that it is reasonable to assume that the mean and confidence interval boundaries calculated based on the 25 and 75 percent capability levels are valid for other levels of capability, especially those greater than 25 percent capability.

The S-curves provided in Figure 34 describe the mean and the 90 percent confidence interval at all levels of capability that quantify the impact of uncertainty in the

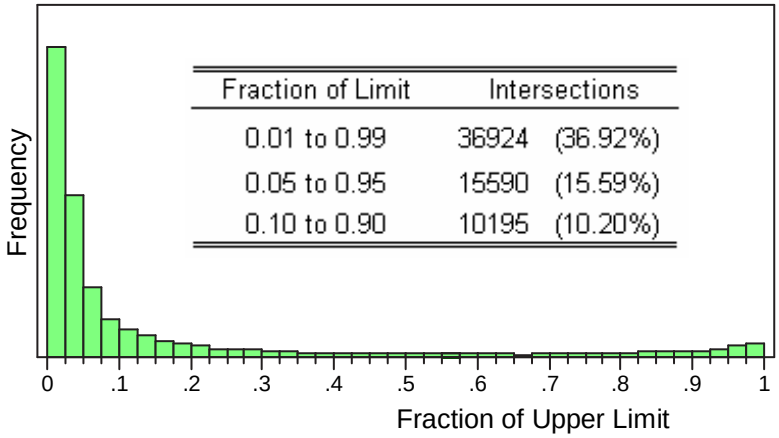

Figure 35: Distribution of S-curve Intersections

estimation of upper limits. Quantifying the impact of random error within the historical database will now be demonstrated. This will be accomplished by estimating the standard $1 - \alpha$ confidence interval on time for the S-curves bounding the confidence region quantifying limit uncertainty.

Recall that a MDGM is regressed against historical data by treating time as the dependent variable or response while each metric's capability is treated as an independent variable. This can be observed in the general form of the multidimensional growth model provided in Equation 71, wherein b_i and a are the regression parameters. Consequently, the desired confidence interval is actually a prediction interval on new observations of time, given settings of the predictor variables y_i. The composite form of the MDGM given in Equation 72 will be used in order that the resulting confidence intervals can be directly applied to the composite S-curves used to describe the mean and interval boundaries above.

$$t = a + \sum_{i=1}^{n} \frac{-1}{b_i} ln\left(\frac{L_i - y_i}{y_i - y_{o,i}}\right) \tag{71}$$

Also recall that the composite form of the MDGM is given by

$$t = a - \frac{1}{b_c} ln\left(\frac{1 - y_c}{y_c}\right) \tag{72}$$

where

$$b_c = \left(\sum_{i=1}^{n} \frac{1}{b_i}\right)^{-1} \tag{73}$$

and

$$y_c = \left(\prod_{i=1}^{n} \left(\frac{L_i - y_i}{y_i - y_{o,i}}\right)^{b_c/b_i} + 1\right)^{-1} \tag{74}$$

The composite S-curve of Equation 72 is transformed according to the transformation of Equation 75 in order to facilitate estimating the prediction intervals. The result is the linear model of Equation 76, where t_c depicts time, $\beta_0 = a$ and $\beta_1 = -1/b_c$.

$$X_c = ln\left(\frac{1 - y_c}{y_c}\right) \tag{75}$$

$$t_c = \beta_0 + \beta_1 X_c \tag{76}$$

With this formulation forecasters can evaluate prediction limits with standard statistical calculations. Equation 77 provides the two-sided prediction interval for the predicted date of introduction, t_h, given a specified composite level of capability, X_h. When applied to the mean S-curve identified above, the relative contribution of uncertainty from upper limit estimations and data error can be directly compared as illustrated by Figure 32.

$$\hat{t}_h = E\{t_h\} \pm t(1 - \alpha/2; n - 2)s\{pred\} \tag{77}$$

where

$$s^2\{pred\} = MSE\left[1 + \frac{1}{n} + \frac{(X_h - \bar{X})^2}{\sum(X_i - \bar{X})^2}\right] \tag{78}$$

In order to evaluate the combined confidence interval, one-sided prediction limits are applied to each S-curve forming the boundaries of the 'limit-only' confidence interval. The one-sided prediction interval of Equation 79 is applied to the $\alpha/2$ (0.05) S-curve, and the one-sided prediction interval of Equation 80 is applied to the $1 - \alpha/2$ (0.95) S-curve. Figure 36 illustrates these results that form the boundaries of the cumulative $1 - \alpha$ (90%) confidence interval accounting for both uncertainty resulting from upper limit estimations and random error within the historical database.

$$\hat{t}_{CI^-,h} = E\{y_{CI^-,h}\} - t(1 - \alpha; n - 2)s\{pred\} \tag{79}$$

$$\hat{t}_{CI^+,h} = E\{y_{CI^+,h}\} + t(1 - \alpha; n - 2)s\{pred\} \tag{80}$$

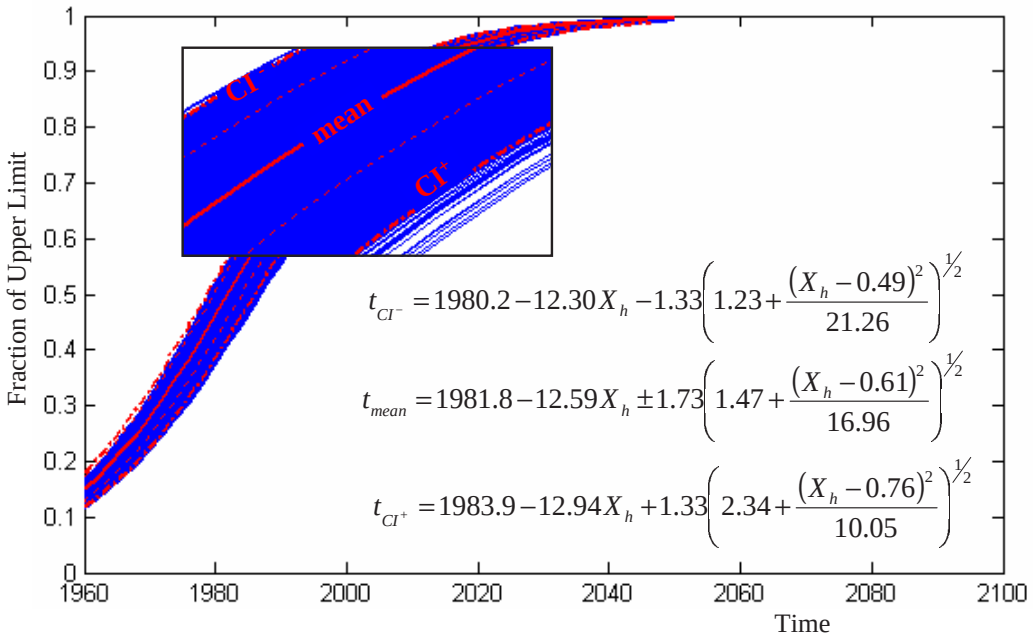

Figure 36: Composite Growth Model with Cumulative Confidence Interval

7.5 Step 5: Technology Assessment

The previous step yields a multidimensional growth model providing interdependent technology capability levels for system metrics at any point in time. Effective technology assessment relies on effectively analyzing and interpreting this comprehensive technology model, which can take the form of a single composite S-curve, interdependent technology S-curves, or advancing technology frontiers. Each form provides a convenient environment to evaluate the current SoA relative to metric upper limits or to forecast future technology capability levels. This section will discuss the pertinent information that can be ascertained from each of these forms.

7.5.1 Composite Assessment

The composite S-curve for the ongoing example is provided in Figure 36 and describes the overall growth of the technology architecture independent of the specific setting of individual metrics. Recall that the composite S-curve is formulated on the basis

that all system metrics are at the same fraction of their respective limits for all time. Consequently, the composite S-curve can be used to estimate the technology's level of performance relative to a normalized upper limit and to other significant stages of development.

The first point of interest is the current state of the art relative to identified upper limits. Figure 37 provides the expected capability levels for the year 2006. With a 90 percent confidence level each metric of this technology has achieved between 82.3 and 90.3 percent of their respective limits. This suggests an additional 9.7 to 17.7 percent is available for further improvement. The availability for improvement relative to the upper limit, however, is not most important because the limit cannot itself be achieved, and the investment required to advance the last several percent is infinite. More important is the availability of improvement relative to the point of diminishing returns.

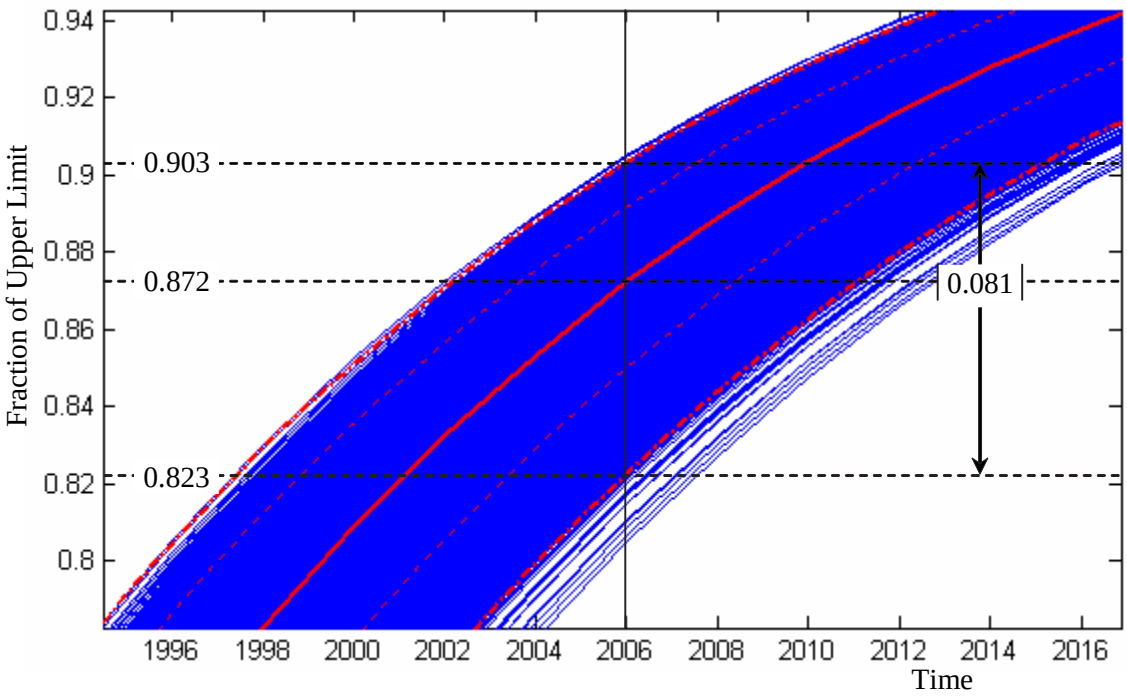

Figure 37: Composite Growth Model Specifying the Current State of the Art

The Point of Diminishing Returns (PDR) by definition occurs at the highest rate of productivity decline, which corresponds to the right inflection point of the productivity, curve shown here in Figure 38b. The left inflection point of the productivity curve corresponds to the maximum rate of productivity growth. Also shown in Figure 38 is the behavior of the second and third derivatives of the Logistic growth model, illustrating that the zeros of the third derivative correspond to each of the maximum rates of productivity change. Equations 81 through 84 correspond to Figures 38a - 38d respectively, and Equation 85 provides the time as a function of curve parameters a and b, at which each maximum rate of productivity change occurs. The latter of these corresponds to the point of diminishing returns.

$$y = \frac{L}{1 + e^{-b(t-a)}} \tag{81}$$

$$\frac{dy}{dt} = \frac{Lbe^{b(-t+a)}}{\left(1 + e^{b(-t+a)}\right)^2} \tag{82}$$

$$\frac{d^2y}{dt^2} = \frac{Lb^2e^{b(-t+a)}\left(e^{b(-t+a)} - 1\right)}{\left(1 + e^{b(-t+a)}\right)^3} \tag{83}$$

$$\frac{d^3y}{dt^3} = \frac{Lb^3e^{b(-t+a)}\left(e^{2\,b(-t+a)} - 4\,e^{b(-t+a)} + 1\right)}{\left(1 + e^{b(-t+a)}\right)^4} \tag{84}$$

$$t_{\text{max curvature}} = \begin{bmatrix} \frac{ba - \ln\left(2+\sqrt{3}\right)}{b} \\ \frac{ba - \ln\left(2-\sqrt{3}\right)}{b} \end{bmatrix} \tag{85}$$

$$y_{pdr} = -\frac{L}{-3 + \sqrt{3}} \tag{86}$$

By substituting the result of Equation 85 into the Logistic model of Equation 81, the limit fraction at which the point of diminishing returns is found and is shown as Equation 86. Note that for the Logistic curve, the point of diminishing returns occurs

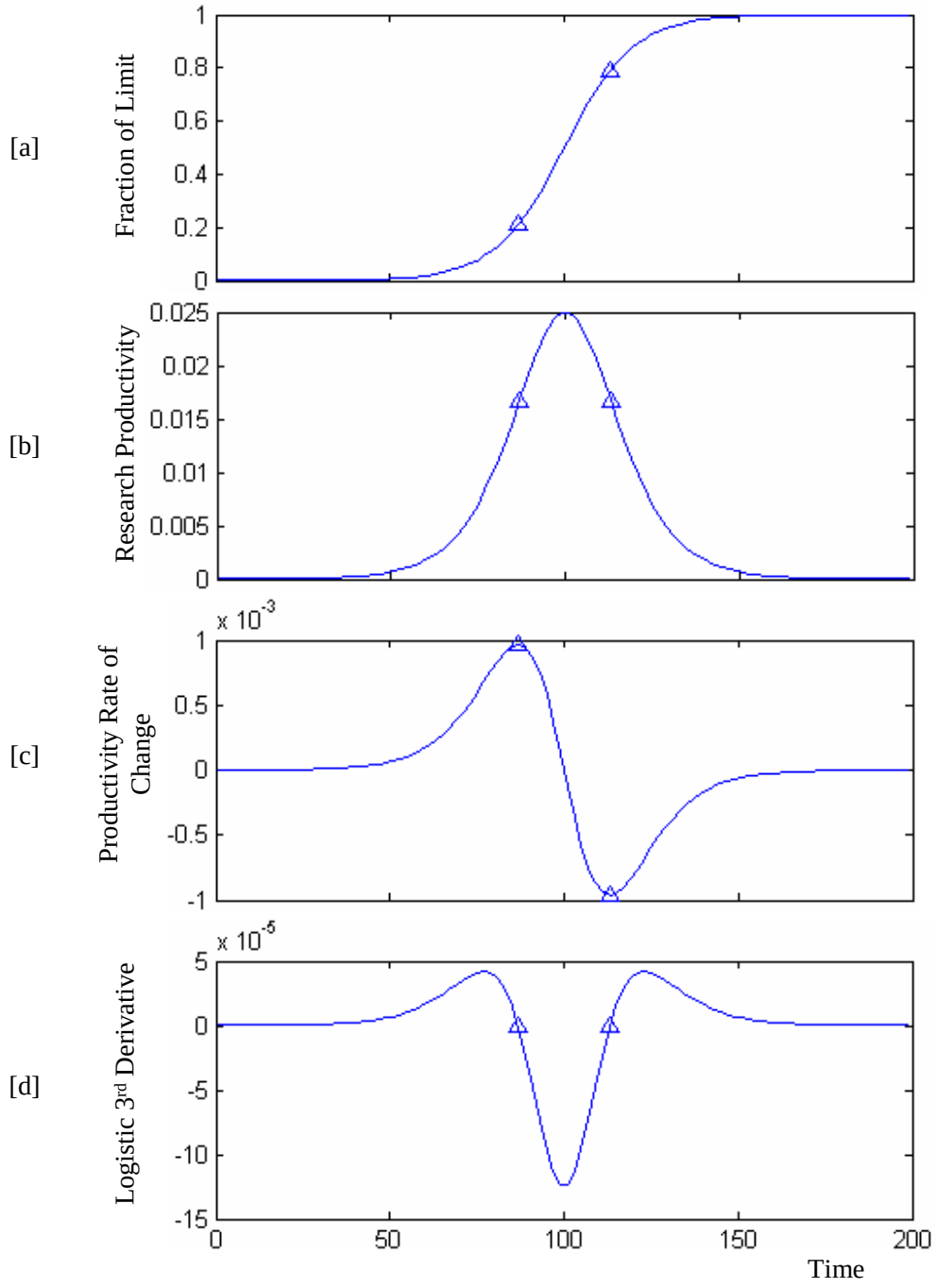

Figure 38: Logistic Growth Model Derivatives

at the same fraction of the upper limit regardless of curve parameters, $y_{pdr} = 0.7887L$. Compare this fraction with the expected limit fraction achieved for the year 2006, which is illustrated in Figure 37. The current state of the art for the year 2006 is bound between 82.3 and 90.3 with a 90 percent confidence. This suggests that with greater than 95 percent confidence the point of diminishing returns has already been surpassed. Figure 39 illustrates the intersection of the y_{pdr} with the S-curves for each the mean and the boundaries of the 90 percent confidence region. The points of intersection are the mean and 90 percent confidence bounds for the date at which the point of diminishing returns is expected to be reached. Note that the upper bound of the confidence interval is the year 2003 again indicating that with greater than 95 percent confidence level the point of diminishing returns has already occurred for this hypothetical technology.

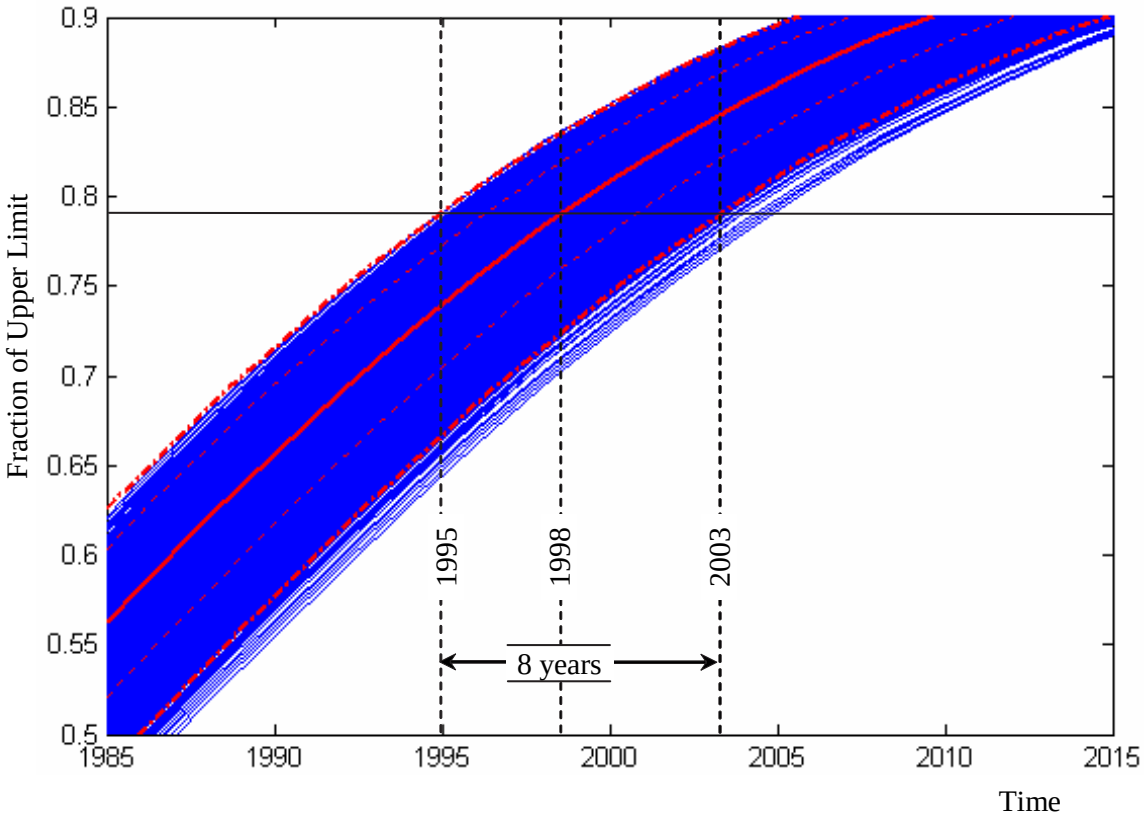

Figure 39: Composite Growth Model Specifying the Point of Diminishing Returns

At this stage in the technology assessment, the impact of limit uncertainty is fully quantified in both the current SoA and the date at which the point of diminishing returns is expected to be the achieved. The width of the resulting confidence intervals can be assessed to establish their acceptability and to determine if additional research should be invested to reduce limit uncertainty and subsequently increase the certainty of the current SoA relative to both the upper limit and the point of diminishing returns.

7.5.2 Setting Program Goals

The composite S-curve quantifies the overall level of performance of a technology relative to a normalized upper limit as it develops over time. Its very nature prevents the assessment of individual metrics relative to one another. This is the objective of interdependent metric S-curves and technology frontiers. Both are derived from slightly different interpretations of the MDGM provided by Equation 87.

$$year = a - \frac{1}{b_1} ln\Big(\frac{L_1 - y_1}{y_1 - y_{o,1}}\Big) - \frac{1}{b_2} ln\Big(\frac{L_2 - y_2}{y_2 - y_{o,2}}\Big) - \frac{1}{b_3} ln\Big(\frac{L_3 - y_3}{y_3 - y_{o,3}}\Big) \tag{87}$$

An interdependent metric S-curve is defined by specifying settings for all $y_{j \neq i}$ and by evaluating y_i over all time—the result is the metric-specific S-curve for y_i, which is dependent on settings for all other metrics. For instance, if y_1 and y_3 are each specified, y_2 can be evaluated for any date according to Equation 88. Each metric-specific S-curve can be determined in this manner.

$$y_2 = \frac{L_2 - y_{o,2}}{1 + e^{-b_2\left(t - a + \frac{1}{b_1} ln\left(\frac{L_1 - y_1}{y_1 - y_{o,1}}\right) + \frac{1}{b_3} ln\left(\frac{L_3 - y_3}{y_3 - y_{o,3}}\right)\right)}} + y_{o,2} \tag{88}$$

An interdependent frontier is defined by specifying settings for the date and all $y_{j \neq i \neq k}$ and evaluating y_i over a range of y_k. The result is a frontier of achievable combinations of y_i and y_k at a specified date given constant settings for all other metrics. This would

correspond to specifying a date and setting for y_3 while evaluating y_2 over a range of y_1 settings. These two forms of the MDGM are shown in Figure 40.

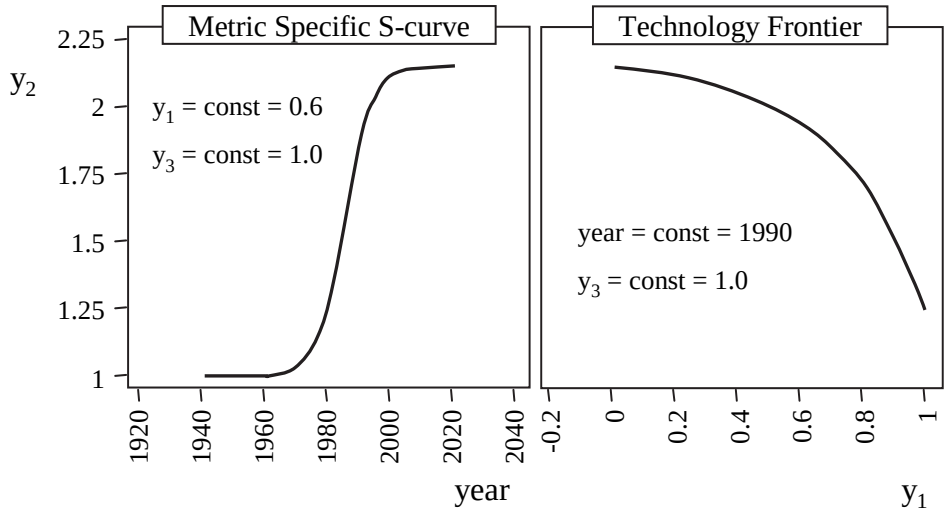

Figure 40: Individual S-curve and Frontier Pair

In the case of the metric specific S-curve, if the settings for either y_1 or y_3 are changed, a completely different y_2 S-curve would result. Likewise, if either the year or y_3 were changed in the case of the frontier, a new and different frontier would result. The static nature of these two-dimensional snapshots of the MDGM significantly limits the degree to which the technology can be assessed.

In order to adequately capture the behavior of the MDGM, a dynamic environment is needed in which all $n+1$ dimensions (n attributes plus time) can be visualized simultaneously. The prediction profiler within the JMP statistical software package provides such an environment [89]. Figure 41 provides a snapshot of this dynamic environment, in which the first column of subplots represent the interdependent S-curves, and all other subplots correspond to the y_i-y_j technology frontier. The advantages of this environment are twofold; interdependent S-curves and frontiers can be viewed simultaneously, but most importantly the S-curves and frontiers respond in real time to changes in year or metric settings.

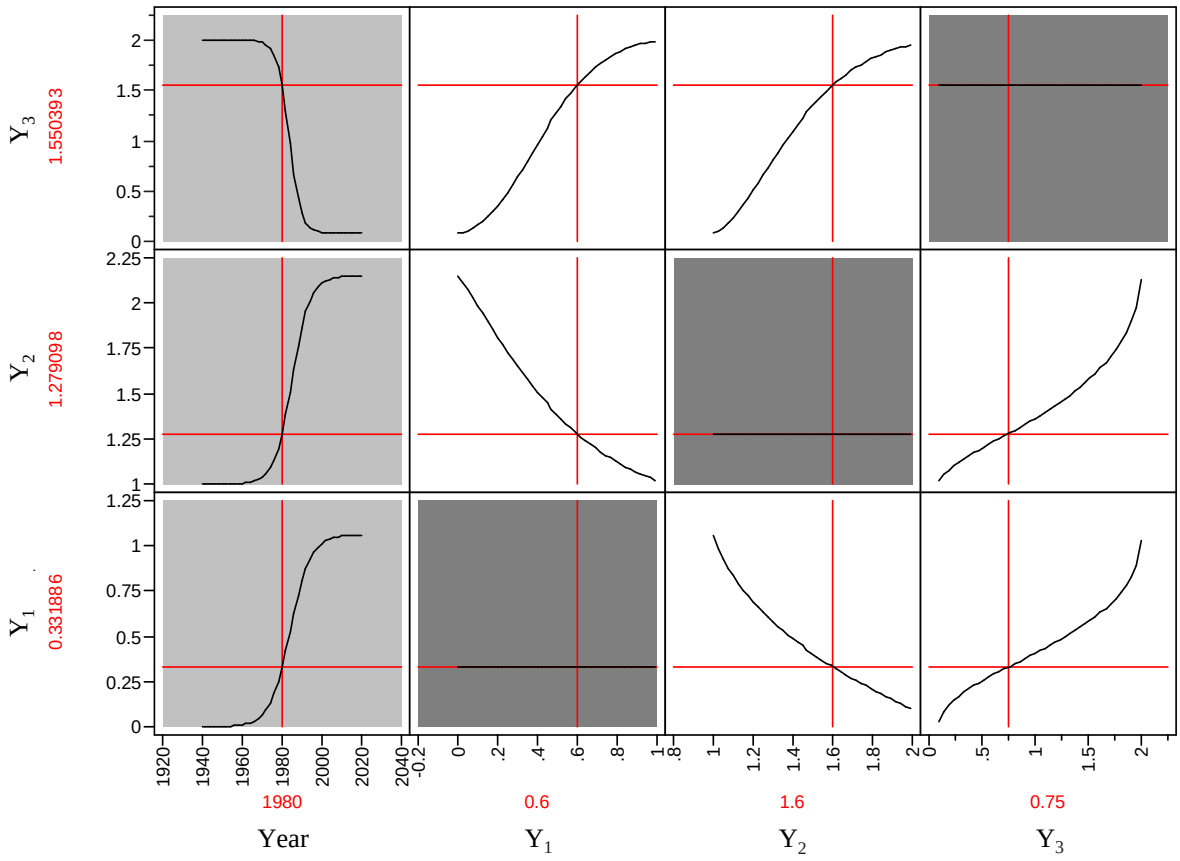

Figure 41: Prediction Profiler Visualization Environment

In the first column of each row is the y_i S-curve. The remaining entries of each row form the y_i-y_j technology frontier. Each row takes the graphical form of Equation 88—that is $y_i = f(t, y_{j \neq i})$. Consequently each row by itself completely describes the MDGM. Additional rows are provided in order that all the y_i S-curves and frontier pairs are graphically represented. At the left of each row is the expected value of y_i that can be achieved for the date specified given settings for each $y_{j \neq i}$ displayed at the bottom of each column. These settings can be adjusted by moving the red hairline in each column.

Note that because each row independently describes the MDGM it is possible for each row to represent a different state of the same MDGM. For instance, in Figure 41 the bottom row yields $y_1 = 0.349$ given $year = 1980$, $y_2 = 1.6$, and $y_3 = 0.75$; the

middle row yields $y_2 = 1.298$ given $year = 1980$, $y_1 = 0.6$ and $y_3 = 0.75$. Each row corresponds to an equally valid but different state of the MDGM characterized by different settings for y_1 and y_2. Making all rows correspond to the same state can be useful for making tradeoffs between metrics and can be achieved by setting any one y_i hairline to its corresponding predicted value. In the case of Figure 41, the y_1 hairline is adjusted to 0.349 resulting in Figure 42, in which all rows represent the same state of the MDGM. Only when all rows represent the same state can the S-curves in the first column be compared with one another. The relative distance to their respective upper limits can only be evaluated if each S-curve (i.e. row) corresponds to the same state.

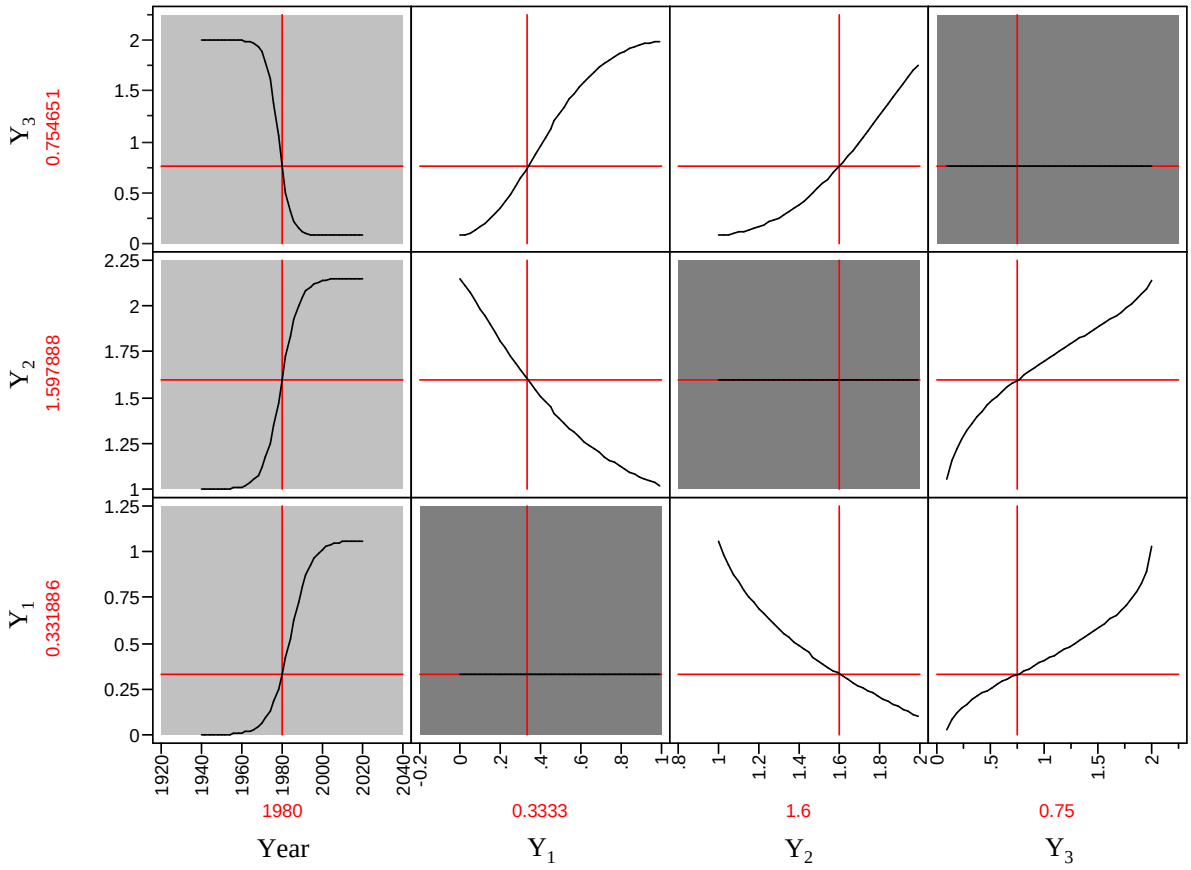

Figure 42: Prediction Profiler Visualization Environment

This dynamic visualization of the MDGM provided by the prediction profiler can be used to observe many of the relationships that characterize the MDGM. Apparent from a snapshot of the environment are the metric S-curves as a function of time and each frontier pair. Not apparent from a snapshot is the relationship between time, each attribute, and each frontier pair. Because each row can independently describe the MDGM, only a single row is necessary to illustrate these relationships. Figure 43 illustrates the relationship between time and each frontier pair. As time progresses, more aggressive settings for both metrics of the frontier pairs are able to be achieved, which is characterized by the rightward movement and increased "squareness" of each frontier.

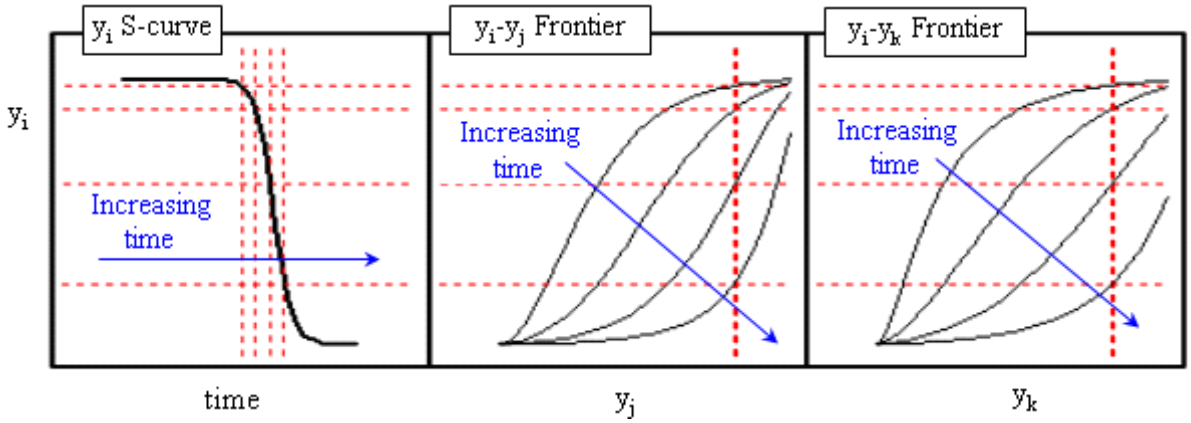

Figure 43: Time Dependence of Attribute Frontiers

Figure 44 illustrates the relationship between y_k and the y_i-y_j frontier pair. Note that changes to y_k have the exact opposite impact as time to the frontier pair. As y_k decreases more aggressive settings for each metric can be achieved. The relationship between y_k and the y_i S-curve is also illustrated in Figure 44. Observe that for decreases in y_k, the y_i S-curve shifts to the left, which indicates that more aggressive capability levels of y_i can be achieved at a given date if lower values of y_k are permitted.

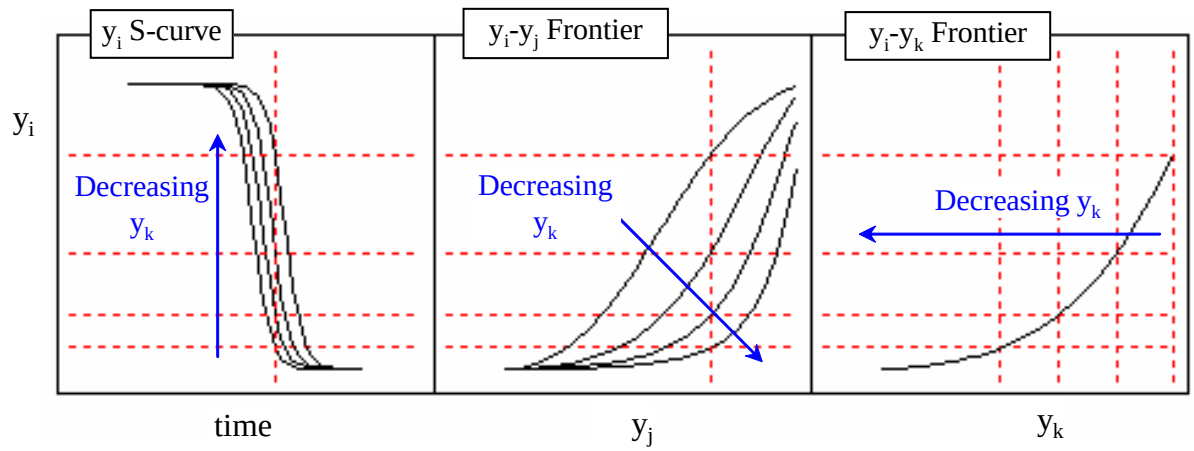

Figure 44: Time Dependence of Attribute Frontiers

Discussion so far has explained the functionality of this environment; now consider its utility. By setting the date hairline to any year of interest, the expected rate of growth for each metric can be estimated, and the tradeoff frontier between any pair of metrics can be examined. This provides the necessary information to comprehensively define the current SoA relative to metric upper limits and as such establishes the technology potential for each metric. Similarly, forecasters can estimate expected levels of performance for any future date, which enables reasonable goals to be set for systems under development. Conversely, given desired levels of performance for one or more metrics the expected date for achieving such levels relative to the capability for the remaining metrics can be estimated.

7.5.3 Time Horizons of Technology Alternatives

The multidimensional growth model formulated in the previous sections forecasts future technical capability based on the fundamental nature of technology growth patterns relative to physical limits and historical data. No consideration, however, is given to the actual evolutionary changes required in order for the subject technology to achieve predicted levels of performance. This is the explicit purpose of the Technology Impact Forecasting (TIF) method; disciplinary changes required to achieve specific

system level targets are determined. Consequently, TIF is a natural successor to the goal setting enabled by MDGMs.

A MDGM is used to forecast the evolved performance levels of specific system over time, after which TIF can be employed to identify the evolutionary changes required to achieve those forecasted levels of performance. This is a natural progression for the two methods, starting with the specification of program goals and proceeding through technology identification for fulfilling those goals.

TIF, which was summarized in Section 3.3, is a well-established methodology which has been demonstrated on numerous design problems [56, 57, 58, 90, 91, 92, 93]. Another demonstration here would add little to the existing research on the topic. What is instructive to note is that the MDGM can provide additional information following the TIF approach by estimating expected introduction dates for combinations of technology metrics. The capability levels achieved by a technology metrics resulting from TIF can be entered into the corresponding MDGM to yield a top-down estimate of introduction date given that past levels of engineering effort are maintained. Recall that the TIF method maps changes in technology metrics, or disciplinary metrics, to the improvements and degradations of system level metrics. Consider that one function of a MDGM maps changes in system level metrics to changes in the state of the art as quantified by introduction date. Consequently, a MDGM can be employed following a TIF implementation to map the necessary disciplinary changes directly to expected date of introduction, as illustrated by Figure 45. In this way, forecasters can simultaneously assess the expected date of introduction with predicted system performance as a result of changes to disciplinary metrics. Note, however, that this expected date of introduction *assumes* previous levels of engineering effort are maintained. If TIF is being implemented at the onset of an aggressive development phase, actual introduction dates of developed systems may occur before those forecasted by the MDGM.

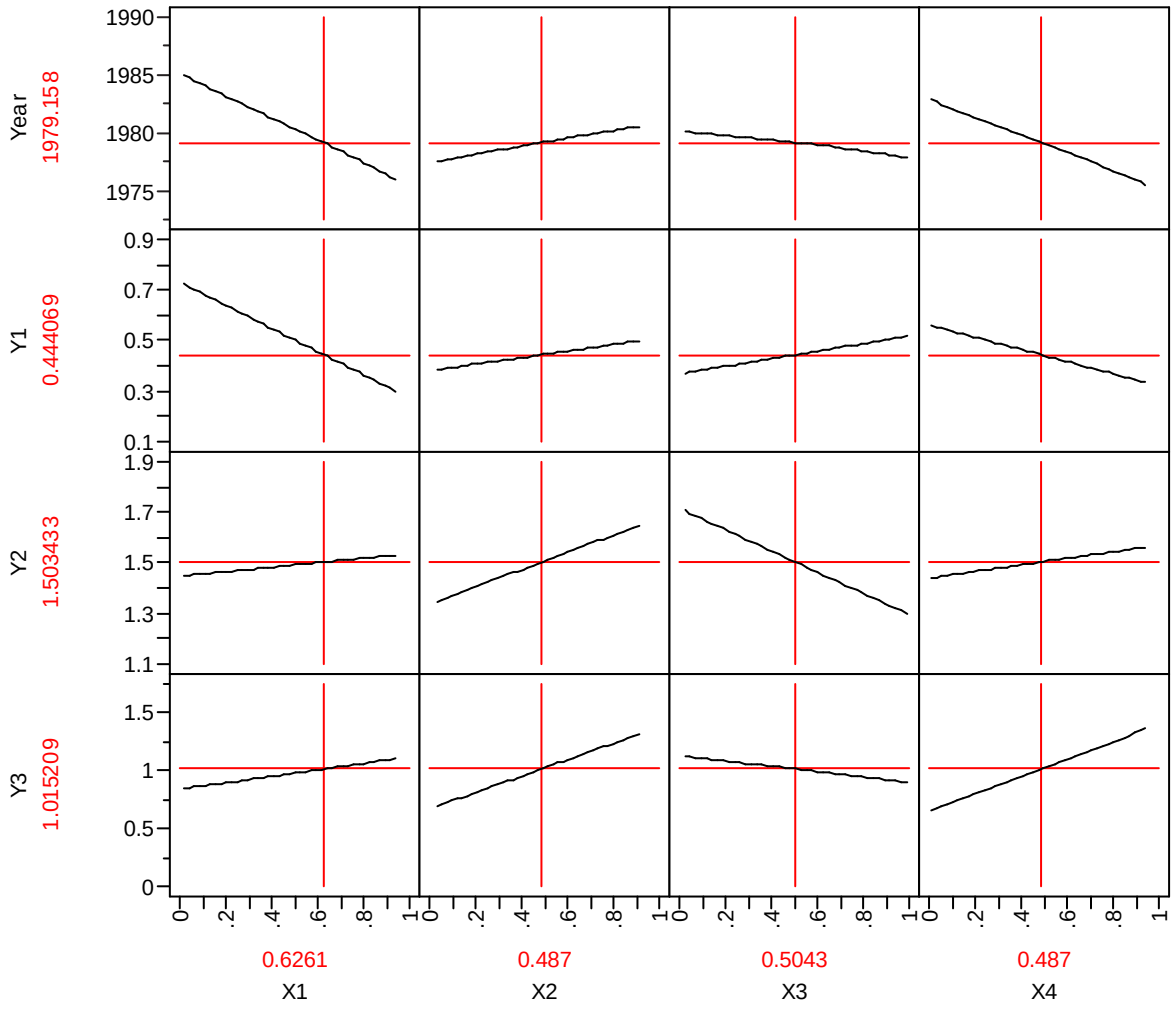

Figure 45: Disciplinary Metric Mapping

7.6 Summary

This chapter set forth a systematic procedure for the assessment and forecast of technology attributes. Central to the procedure is the formulation of a multidimensional growth model that describes the development pattern of each individual system attribute and the growth of the technology as a whole. Attention is given to carefully formulate and test the model's integrity to ensure its accuracy.

The procedure includes an uncertainty analysis to capture imprecision in limit

estimates and error fluctuations on historical data in order to provide confidence intervals on resulting forecasts. The varied interpretations of the MDGM were explored and discussed, including explanation on how to identify the current state of the art relative to both the upper limit and point of diminishing returns. The procedure concludes by providing a visualization environment to facilitate technology assessment and the setting of program goals.

While Chapters 5 & 6 provide the necessary elements for technology modeling, this chapter integrates those elements into a formalized approach to assess a technology's current state of the art relative to both the upper limit and point of diminishing returns, clearly establishing what availability for further improvement exists. The following chapter applies this methodology to assess and forecast turbofan technology.

CHAPTER VIII

PROOF OF CONCEPT

Chapter 8 provides a realistic application of the technology assessment procedure proposed in the previous chapter, specifically the evolution of high-thrust (i.e. high-bypass) turbofan engines relative to the upper limits of several key metrics. Several factors contributed to the selection of turbofan engines as a subject technology for this demonstration. The first factor that makes turbofan technology an appropriate test subject is that engine designers must consider multiple attributes. A high-thrust turbofan must provide significant levels of thrust with minimal fuel consumption, noise, and emissions. This must be accomplished while minimizing its weight and maximizing its reliability. The second factor making the turbofan of interest is the exceptionally high investment necessary to develop a new engine. With nearly five billion dollars at risk, knowledge of the existing availability for further improvement is a significant contribution to decision makers [94]. Furthermore, with over four decades of aggressive turbofan development to date, the question of just how much availability for improvement remains is being asked more frequently. One drawback to turbofan technology as an assessment application is the limited data available in the public domain. In some respects, this is an advantage in that it tests the robustness of the assessment procedure in light of limited data, but it also greatly limits the number of attributes that can be assessed.

The ensuing demonstration will follow step by step the procedure outlined in the previous chapter.

8.1 Problem Definition

As stated, the technology architecture of interest to this assessment is the high-thrust turbofan engine. The level of abstraction of interest is not concerned with the number of spools, gearing, or specific cycles but only with the requirement that the engine has thrust greater than 25,000 lb_f. The attributes of interest to this study, as alluded to in the introduction, include fuel consumption, thrust, weight, noise, emissions, and reliability.

Each attribute will be considered in turn to identify an appropriate corresponding metric.

Fuel consumption is quantified by the thrust specific fuel consumption (SFC) at the cruise condition in terms of the units pounds mass per pounds force hour, lb_m/lb_f-hr.

Thrust is quantified by the maximum sea level static thrust (Fg) in pounds force, lb_f.

Weight is included in the assessment as a compound metric with thrust in the form of the thrust to weight ratio (T/W) of the engine.

Noise is quantified by the total takeoff noise in decibels, dB.

Emissions is quantified by the ratio of total oxides of nitrogen (NOx) emitted during the landing-takeoff cycle per kilogram of fuel burned. This ratio will be denoted as EINOx and will be given in terms of grams of NOx per kg of fuel, g/kg.

Reliability data could not be found consistently in the public domain in any form and, because of this, reliability was removed from consideration.

8.2 Compilation of Historical Data

The historical data for this assessment was collected from a myriad of sources,

most notably noise data was acquired from the Federal Aviation Administration and emissions data from International Civil Aviation Organization [94, 95, 96, 97, 98]. Table 21 provides the initial list of compiled data.

Note that each metric as listed in Table 21 applies to a single engine, except for the takeoff noise, which quantifies both the noise of the aircraft and all engines. In order to normalize this data to a single engine, this study made the assumption that during takeoff, aircraft noise is negligible as compared to engine noise [99]. Thus, the data for noise provided in the table was assumed to only come from the engines. In order to attribute the fraction of this combined engine noise resulting from a single engine, the above noise data was transformed from decibels to the underlying pressure ratio, which was subsequently divided by the number of engines and transformed back into decibels [100, 101]. This normalization procedure is quantified by Equation 89 and was applied to each system entry in the historical database resulting in the noise levels per engine listed in Table 22.

$$dB_{\text{per engine}} = 20 \log \left(\frac{10^{\frac{dB_{tot}}{20}}}{\text{no. of engines}} \right) \tag{89}$$

Also provided in Table 22 is the mass flow (m_dot), bypass ratio (BPR), overall pressure ratio (OPR), length, and diameter for each system in order to provide comparison based on disciplinary metrics. Note that engine mass flow varies between 1140 and 3100 lb_m/s; BPR varies between 4.1 and 8.5; OPR varies between 21.1 and 39; length varies between 118 and 204 inches, and diameter varies between 73.2 and 134 inches. While each engine in the database qualifies as a high bypass or high thrust engine, variability in these disciplinary metrics indicate that as defined this is a rather broad technology architecture.

The correlation coefficient for each system level metric pair is calculated according to the data provided in Table 22. The results are shown here in Table 23 and

Table 21: Initial historical database of turbofan engines with dates of introduction and performance data

	Engine Model	Airframe	No. of Eng	Date	SFC	T/W	Thrust	Noise	EINOx
1	CF6-6D	DC-10-10	3	1970	0.646	5.07	40000	98.94	17.93
2	JT9D-7J	B-747-200	4	1970	0.665	5.65	50000	103.55	18.00
3	CF6-50A	DC-10-30	3	1971	0.656	5.96	49000	94.77	14.07
4	JT9D-7	B-747-100	4	1971	0.665	5.23	46300	103.95	14.98
5	JT9D-7A	B-747-100	4	1972	0.663	5.31	46950	103.83	15.33
6	RB211-22B	L-1011	3	1972	0.628	4.57	42000	102.93	12.80
7	CF6-50C	DC-10-30	3	1973	0.657	5.85	51000	94.53	15.45
8	CF6-50E	B-747-200	4	1973	0.657	6.18	52500	98.79	15.46
9	JT9D-59A	DC-10-40	3	1974	0.646	5.80	53000	104.08	13.76
10	JT9D-70A	B-747-200	4	1974	0.646	5.79	53000	103.62	13.76
11	JT9D-7F	B-747-100	4	1974	0.665	5.42	48000	104.00	17.02
12	RB211-524B	L-1011-200	3	1975	0.643	5.09	50000	102.97	18.43
13	CF6-50C1	DC-10-30	3	1976	0.657	6.02	52500	95.01	15.46
14	CF6-50C2	A300B2-203	2	1976	0.630	6.01	52500	95.63	15.46
15	CF6-50E2	B-747-200	4	1976	0.630	5.99	52500	99.70	16.05
16	CF6-45A2	B-747-SR	4	1978	0.630	5.30	46500	88.81	13.59
17	CF6-50C2-B	DC-10-30	3	1978	0.630	6.18	54000	97.57	16.02
18	JT9D-7Q	B-747-200	4	1979	0.643	5.70	53000	103.38	13.76
19	RB211-524C2	B-747-100	4	1979	0.642	5.22	51500	103.24	16.14
20	JT9D-7R4D	B-767-200	2	1980	0.596	5.39	48000	102.83	16.12
21	CF6-80A	B-767-200	2	1981	0.623	5.65	48000	94.83	15.62
22	CF6-80A2	B-767-200	2	1981	0.623	5.89	50000	94.59	16.24
23	RB211-524D4	B-747-200	4	1981	0.617	5.37	53000	103.20	21.07
24	RB211-535C	B-757-200	2	1981	0.646	5.13	37400	102.71	13.04
25	JT9D-7R4E	B-767-200	2	1982	0.596	5.61	50000	102.83	17.76
26	JT9D-7R4G2	B-747-200	4	1982	0.599	5.99	54750	103.18	16.62
27	PW2037	B-757-200	2	1983	0.582	5.26	38400	103.25	14.32
28	RB211-535E4	B-757-200	2	1983	0.598	5.52	40100	102.70	16.68
29	CF6-80C2A2	A310-304	2	1985	0.578	5.86	53500	95.30	12.67
30	CF6-80C2B1	B-747-300	4	1985	0.576	6.16	57900	96.30	13.14
31	CF6-80C2B1F	B-747-400	4	1986	0.564	6.10	57900	96.41	13.15
32	CF6-80C2B2	B-767-200	2	1986	0.576	5.59	52500	94.30	11.84
33	PW4056	B-747-400	3	1986	0.537	6.04	56750	102.89	15.18
34	CF6-80C2B4	B-767-200	2	1987	0.576	6.16	57900	94.95	13.53
35	CF6-80C2B6	B-767-300	2	1987	0.580	6.47	60800	95.08	14.40
36	PW2040	B-757-200	2	1987	0.582	5.71	41700	102.96	15.93
37	RB211-524G	B-747-400	3	1988	0.570	6.00	58000	102.84	21.99
38	RB211-524H	B-747-400	3	1989	0.570	6.27	60600	102.81	25.08
39	CF6-80C2B6F	B-767-300	2	1992	0.580	6.33	60800	95.06	14.44
40	GE90-85B	B-777-200	2	1995	0.560	5.31	85000	91.44	23.90

illustrated by the bivariate plots of Figure 46. Expectedly, the highest degree of correlation exists between T/W and thrust, each of which are moderately correlated

Table 22: Historical database of turbofan engines with dates of introduction and performance data

	Engine Model	Date	SFC (lb_m/lb_f-hr)	T/W	Thrust (lb_f)	Noise (dB)	EINOx (g/kg)	m_dot (lb_m/s)	BPR	OPR	Length (in)	Diameter (in)
1	CF6-6D	1970	0.646	5.07	40000	89.40	17.93	1303	5.72	24.3	177	86.4
2	JT9D-7J	1970	0.665	5.65	50000	91.51	18.00	1590	5.1	23.5	128.2	92.3
3	CF6-50A	1971	0.656	5.96	49000	85.23	14.07		4.4	30		
4	JT9D-7	1971	0.665	5.23	46300	91.90	14.98	1509	5.2	22.3	128.2	92.3
5	JT9D-7A	1972	0.663	5.31	46950	91.79	15.33	1534	5.1	22.5	128.2	92.3
6	RB211-22B	1972	0.628	4.57	42000	93.39	12.80	1380	4.8	24.5	119.4	84.8
7	CF6-50C	1973	0.657	5.85	51000	84.99	15.45		4.24	29.3	173	86.4
8	CF6-50E	1973	0.657	6.18	52500	86.75	15.46	1470	4.24	30.1	173	86.4
9	JT9D-59A	1974	0.646	5.80	53000	94.54	13.76	1639	4.9	24.5	132.2	93.6
10	JT9D-70A	1974	0.646	5.79	53000	91.58	13.76	1639	4.9	24.5	132.2	93.6
11	JT9D-7F	1974	0.665	5.42	48000	91.95	17.02	1565	5.1	22.8	128.2	92.3
12	RB211-524B	1975	0.643	5.09	50000	93.43	18.43	1513	4.5	28.4	119.4	84.8
13	CF6-50C1	1976	0.657	6.02	52500	85.47	15.46	1470	4.24	30.1	173	86.4
14	CF6-50C2	1976	0.630	6.01	52500	87.68	15.46	1476	4.31	30.4	173	86.4
15	CF6-50E2	1976	0.630	5.99	52500	87.66	16.05	1476	4.31	30.4	173	86.4
16	CF6-45A2	1978	0.630	5.30	46500	76.77	13.59	1393	4.64	26.3	173	86.4
17	CF6-50C2-B	1978	0.630	6.18	54000	88.02	16.02	1504	4.25	31.1	173	86.4
18	JT9D-7Q	1979	0.643	5.70	53000	91.34	13.76	1640	4.9	24.5	132.1	93.6
19	RB211-524C2	1979	0.642	5.22	51500	91.20	16.14	1532	4.5	28.6	119.4	84.8
20	JT9D-7R4D	1980	0.596	5.39	48000	96.81	16.12	1585	5	23.4	132.7	93.4
21	CF6-80A	1981	0.623	5.65	48000	88.81	15.62	1435	4.66	28	157.4	86.4
22	CF6-80A2	1981	0.623	5.89	50000	88.57	16.24	1460	4.59	29	157.4	86.4
23	RB211-524D4	1981	0.617	5.37	53000	91.16	21.07	1548	4.4	29.3	122.3	85.8
24	RB211-535C	1981	0.646	5.13	37400	96.69	13.04	1140	4.4	21.1	118.5	73.2
25	JT9D-7R4E	1982	0.596	5.61	50000	96.81	17.76	1615	5	24.2	132.7	93.4
26	JT9D-7R4G2	1982	0.599	5.99	54750	91.14	16.62	1695	4.8	26.3	132.7	93.4
27	PW2037	1983	0.582	5.26	38400	97.23	14.32	1210	6	27.6	141.4	78.5
28	RB211-535E4	1983	0.598	5.52	40100	96.68	16.68	1151	4.3	25.8	117.9	74.1
29	CF6-80C2A2	1985	0.578	5.86	53500	89.28	12.67	1769	5.05	27.8	160.9	93
30	CF6-80C2B1	1985	0.576	6.16	57900	84.26	13.14	1710	5.19	29.3	160.9	93
31	CF6-80C2B1F	1986	0.564	6.10	57900	84.37	13.15	1764	5.15	29.9	160.9	93
32	CF6-80C2B2	1986	0.576	5.59	52500	88.28	11.84	1650	5.31	27.1	160.9	93
33	PW4056	1986	0.537	6.04	56750	94.37	15.18		4.9	30	132.7	93.6
34	CF6-80C2B4	1987	0.576	6.16	57900	88.93	13.53	1727	5.15	29.9	160.9	93
35	CF6-80C2B6	1987	0.580	6.47	60800	89.06	14.40	1820	5.05	31.1	160.9	93
36	PW2040	1987	0.582	5.71	41700	96.94	15.93	1255	5.9	27.6	141.4	78.5
37	RB211-524G	1988	0.570	6.00	58000	93.30	21.99	1605	4.3	32.9	125	86.3
38	RB211-524H	1989	0.570	6.27	60600	93.27	25.08	1628	4.1	34.5	125	86.3
39	CF6-80C2B6F	1992	0.580	6.33	60800	89.04	14.44	1820	5.05	31.4	160.9	93
40	GE90-85B	1995	0.560	5.31	85000	85.42	23.90	3100	8.5	39	204	134

with the remaining metrics, most of all SFC. If either T/W or thrust is removed from the assessment based solely on correlation, thrust would be the appropriate choice because it is more strongly correlated with the remaining metrics than T/W. The metrics' significance as a design driver, however, should also be considered in this decision.

Table 23: Metric Correlation Matrix

	SFC	T/W	THRUST	NOISE	EINOx
SFC	1.0000	-0.3420	-0.4525	-0.1040	-0.1484
T/W	-0.3420	1.0000	0.4755	-0.2987	-0.0207
THRUST	-0.4525	0.4755	1.0000	-0.3777	0.3990
NOISE	-0.1040	-0.2987	-0.3777	1.0000	0.1633
EINOx	-0.1484	-0.0207	0.3990	0.1633	1.0000

Does thrust or T/W more strongly influence design decisions? Insight into this question can be gained by viewing the independent advancement of each metric as illustrated by Figures 47 and 48 for T/W and thrust, respectively. Each point included in these graphics most nearly corresponds to the highest performance achieved to date for the respective metric. Note in Figure 47 the very flat T/W frontier that reaches a maximum of 6.47 as of 1987, which is less than half a point higher than the 6.18 achieved in 1973 nearly a decade and half earlier. This indicates that either T/W has already reached its limit or it has ceased to be a dimension of primary interest to advance for high-thrust turbofans. Conversely, note the steady increase in thrust over the past three decades. These recent trends suggest that overall thrust more strongly influences design decisions than does engine thrust to weight in high bypass applications. That is for large transport aircraft where engine weight comprises only a very small fraction of the total gross weight of the aircraft absolute thrust is a more significant design driver than the thrust to weight ratio. Consequently, despite slightly higher correlation with the remaining metrics, thrust will remain in the assessment model while thrust to weight will be eliminated. If the assessment were conducted

on low bypass turbofans for military fighter applications this conclusion would most likely be reversed.

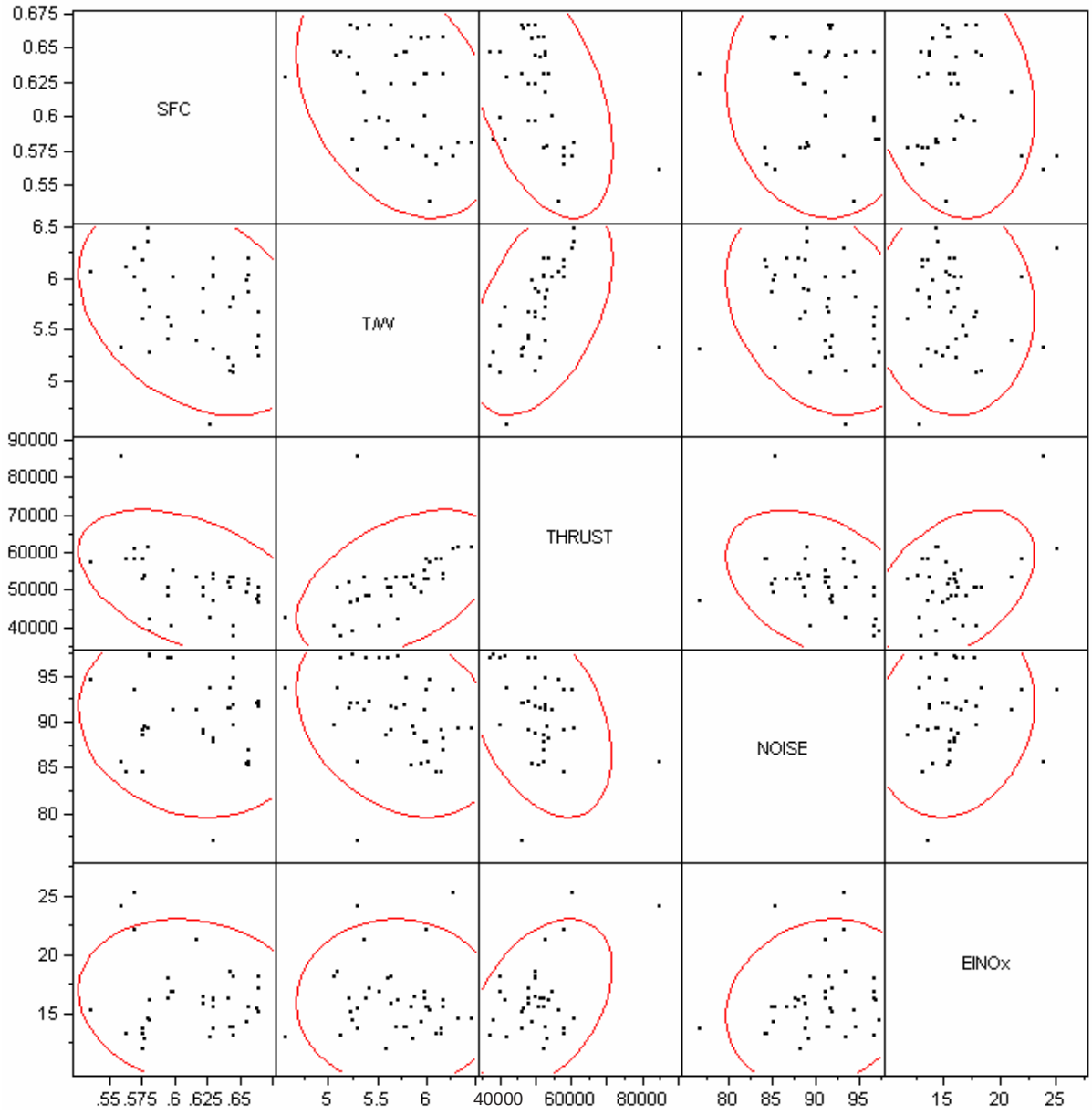

Figure 46: Bivariate Correlation Plots

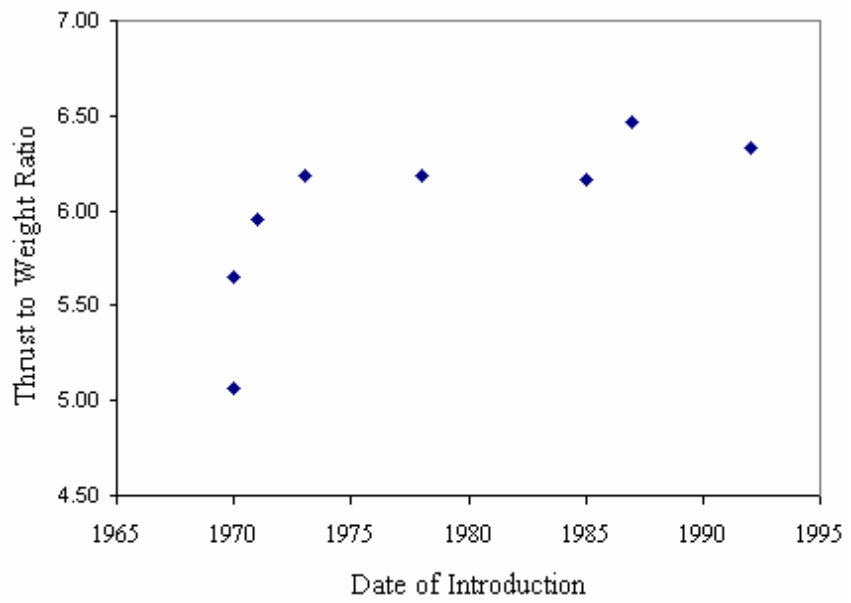

Figure 47: Historical Trend of Turbofan Thrust-to-Weight Ratio

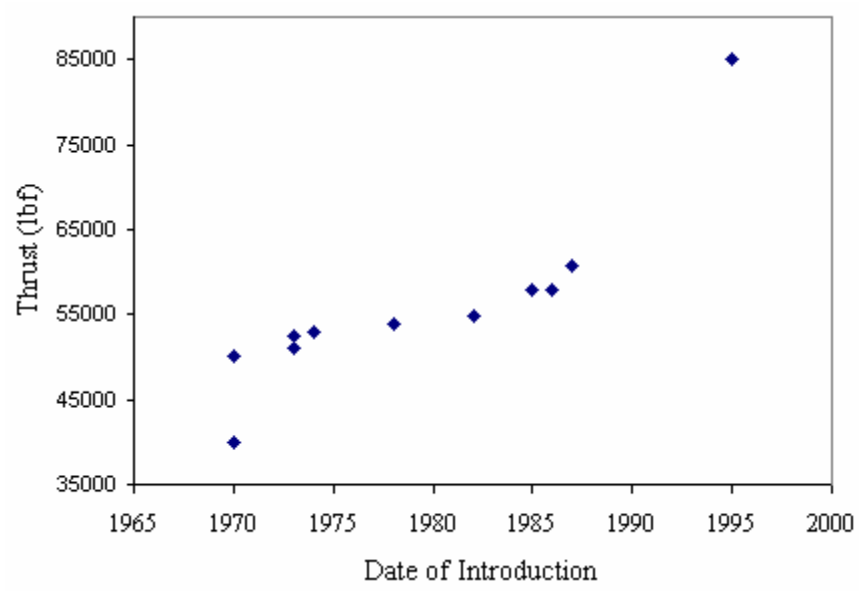

Figure 48: Historical Trend of Turbofan Thrust Levels

8.3 Upper Limits Estimation

As noted in the previous chapter, quantifying the impact of limit uncertainty on the resulting model is of more interest to this research than precisely calculating upper limits. Precisely calculating the upper limit for even a single metric of a highly complex system such as a turbofan may itself be a multi-year endeavor requiring the involvement of many disciplinary experts. Entering into such an endeavor for each of the four remaining metrics within the turbofan model was beyond the scope of this research. Boundaries for the upper limit to each metric were estimated using very basic physics-based analysis. The approach employed for each metric follows.

Specific Fuel Consumption. The turbofan as a technology architecture is a highly coupled system. That is, small changes in the performance of any one component significantly impact the performance of all other system components. Consequently, any improvement to component efficiencies demand changes to other cycle parameters for optimal performance. A first-order turbofan engine model was created in Matlab in order to simulate improvements to component efficiencies after which cycle parameters were optimized for minimal SFC. This model was based on a basic energy balance analysis as outlined by Hill and Peterson and was bench-marked against the GE90-85B cruise condition, thirty-five thousand feet altitude and Mach number of 0.85 [97, 102]. The actual Matlab coding of this model is provided as Appendix C. Pertinent cycle parameters and efficiencies for the GE90-85B at the cruise condition are provided in Table 24. Also provided in Table 24 are cycle parameters corresponding to two limit estimates.

These limit estimates are representative of technological improvements to component efficiencies and compressor pressure ratios. Limit A was estimated by improving each component efficiency by 0.02 and solving for cycle parameter settings in order to minimize specific fuel consumption while maintaining the same thrust, bypass

Table 24: Turbofan Model Parameters for SFC Limit Estimation

	GE90-85B	Limit A	Limit B
Component Efficiencies			
Fan	0.8991	0.9191	0.9391
Low Pressure Compressor	0.8979	0.9179	0.9379
High Pressure Compressor	0.8638	0.8838	0.9038
Burner Pressure Drop	0.045	0.025	0.005
High Pressure Turbine	0.9182	0.9382	0.9582
Low Pressure Turbine	0.9263	0.9463	0.9663
Cycle Parameters			
Fan Pressure Ratio	1.611	1.624	1.630
Low Pressure Compressor Pressure Ratio	1.385	1.379	1.400
High Pressure Compressor Pressure Ratio	20.677	25.686	26.000
Overall Pressure Ratio	46.135	57.534	59.321
Turbine Inlet Temperature (R)	2958.8	2801.8	2586.3
Bypass Ratio	8.34	8.34	8.34
Mass Flow (lb_m/s)	1450.7	1450.7	1450.7
Performance			
SFC ($lb_m/lb_f - hr$)	0.5577	0.4789	0.4107
Thrust (lb_f)	19050.8	19050.8	19050.8

ratio, and mass flow. Bypass ratio and mass flow have been held constant to indicate that the physical size of turbofan engines cannot appreciably increase beyond the GE90-85B without a revolutionary change in system integration. That is, for as long as engines are mounted underwing their maximum diameter will be limited by acceptable ground clearance. The GE90-85B has very nearly reached this limit. Consequently, technological advancements to turbofan engines will be constrained to a physical size comparable to the GE90-85B. Thrust has been held constant to provide for a reasonable comparison between the resulting specific fuel consumptions. Because SFC is normalized against thrust, changes to thrust can result in SFC variability not representative of technological advancement; thrust has, therefore, been held constant to eliminate this variability.

Limit B was estimated in a similar manner to Limit A except component efficiencies were increased by 0.04, an additional 0.02 improvement, and the cycle parameters

were once again optimized in order to minimize SFC. These two estimates, Limit A and B, bound the SFC limit between 0.4789 and 0.4107.

Thrust. The upper limit to turbofan thrust performance was estimated in a very similar manner to that used to estimate SFC limits. The same engine model used for SFC limit estimations was also used for thrust limit estimations. The model was bench-marked against the GE90-85B at the sea level static condition. Pertinent cycle parameters and efficiencies for the GE90-85B at this condition are provided in Table 25. Also provided in Table 25 are cycle parameters corresponding to two limit estimates.

Table 25: Turbofan Model Parameters for Thrust Limit Estimation

	GE90-85B	**Limit A**	**Limit B**
Component Efficiencies			
Fan	0.8914	0.9114	0.9314
Low Pressure Compressor	0.8992	0.9192	0.9392
High Pressure Compressor	0.8650	0.8850	0.9050
Burner Pressure Drop	0.045	0.025	0.005
High Pressure Turbine	0.9200	0.9400	0.9600
Low Pressure Turbine	0.9300	0.9500	0.9700
Cycle Parameters			
Fan Pressure Ratio	1.5	1.65	1.65
Low Pressure Compressor Pressure Ratio	1.3	1.253	1.257
High Pressure Compressor Pressure Ratio	20	15.661	19.876
Overall Pressure Ratio	39	32.381	41.230
Turbine Inlet Temperature (R)	2958.8	4000	4000
Bypass Ratio	8.5	8.5	8.5
Mass Flow (lb_m/s)	3100	3100	3100
Performance			
Thrust (lb_f)	86723	130870	139250

Limit A was calculated by improving component efficiencies by 0.02 and optimizing cycle parameters to maximize thrust while maintaining a constant bypass ratio and mass flow. Note that the turbine inlet temperature was allowed to advance as high

as 4000 degrees Rankine representative of an improvement to materials and/or cooling technology. Limit B was calculated in similar manner with an additional 0.02 improvement to component efficiencies. These two estimates, Limit A and B, bound the thrust limit between 130,870 and 139,250.

Noise. The total takeoff noise of a turbofan engine is the accumulation of noise resulting from numerous engine sources, however, the exhaust jet is the largest contributor [99]. Consequently, total takeoff noise can be roughly quantified as being proportional to jet noise which is itself proportional to the exhaust velocity raised to the eighth power [103]. This relationship is captured by Equation 90, where V_j is the exhaust jet velocity, a_o is the acoustic velocity, and k is a constant of proportionality.

$$dB = 80 \log\left(k \cdot \frac{V_j}{a_o}\right) \tag{90}$$

Estimates for the upper limit to total takeoff noise can be calculated using this equation given expected limitations to the jet velocity and the constant of proportionality k. This constant is estimated by regressing each engine of Table 22 against Equation 90. The exhaust velocity for each engine is estimated as the specific thrust in units of feet per second and the constant of proportionality evaluated according to Equation 91.

$$k = 10^{\frac{dB}{80}}\left(\frac{a}{V_j}\right) \tag{91}$$

The lower bound to these estimates for k was found to be 11.4. Assuming a limit on exhaust velocity of between 750 and 850 ft/s, the limit for total takeoff noise is found to be between 71 and 75 dB.

Emissions. The index for nitrogen oxide emissions is modeled by NASA according to Equation 92, where T_{t4} is the total turbine inlet temperature, and T_{t3} and P_{t3} are the total combustor inlet temperature and pressure, respectively. This indicates that the emissions index is most heavily dependent on overall pressure ratio (OPR) and the turbine inlet temperature, furthermore, that emissions improves with decreasing levels of both. This emissions model only applies to a single combustor type. Similar emissions models exist for other combustor types and are just as heavily dependent on overall pressure ratio and turbine engine temperature. Consequently, emissions can be reduced simply by lowering overall pressure ratio and turbine inlet temperature. The first limit boundary is estimated for EINOx by allowing T_{t4} to be 2800 degrees Rankine and overall pressure ratio to be 28. This yields a limit estimate of EINOx = 10.3. A second limit boundary is established by allowing T_{t4} to drop to as low as 2300 degrees Rankine and OPR to 20. These estimates bound the limit for EINOx between 5 and 10 grams of NOx emissions per kilogram of fuel burned during the landing-takeoff cycle.

$$EINOx = 0.004941 \cdot T_{t4}\left(\frac{P_{t3}}{439}\right)^{0.37} e^{(T_{t3}-1471)/345} \tag{92}$$

For each metric two limits have been estimated between which the actual limit is expected to be. Initially, each metric's upper limit is defined according to a uniform distribution as illustrated in Figure 49, which also provides the mean and bounds for each metric limit. This demonstration selected a uniform distribution because it gives no preference to any one limit value over another within the distribution; it simply places bounds upon the metric's upper limit. Later the demonstration will apply normal distributions to each upper limit to simulate increased knowledge due to investment in further resolving each upper limit's location.

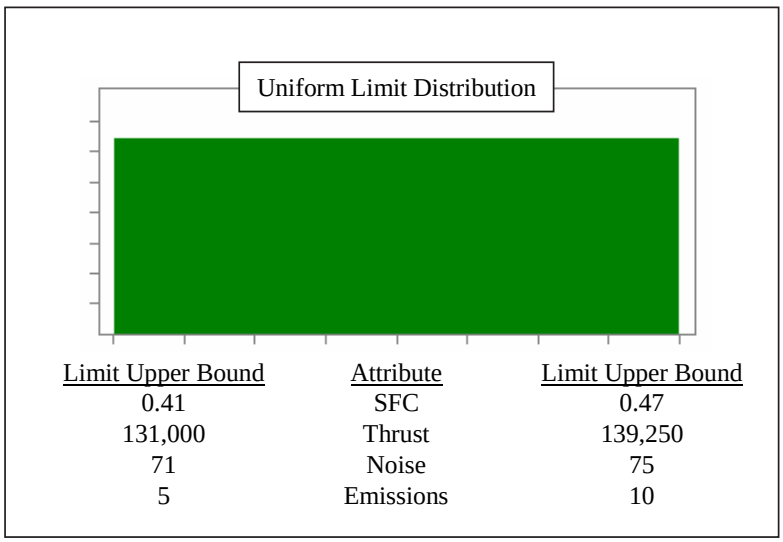

Figure 49: Uniform Limit Distributions

8.4 Generation of the Multidimensional Growth Model

The first step to generating a MDGM is selecting an appropriate growth curve on which to base the model. This demonstration will avoid relative growth curves because of the computational intensity necessary to solve for curve parameters in multiple dimensions. Also, neither Bass nor Harvey relative models require knowledge of the upper limit, thus preventing the proposed uncertainty analysis on limit location. Of the absolute models, Young has shown the Logistic curve to provide more consistently accurate forecasts [42]. Consequently, the Logistic curve will be used for this application, although any growth model, relative or absolute, could be employed to generate MDGMs as demonstrated in Chapter 7.

The general form of the Logistic based MDGM is shown here as Equation 93 and expanded in Equation 94 to accommodate each turbofan metric in which the subscript *sfc* denotes specific fuel consumption, *fg* denotes thrust, *db* denotes total takeoff noise, and *ie* denotes the NOx emissions index. As with the example in the

previous chapter, Equation 94 is linearized which results in Equation 95. Recall that β_i corresponds to $-1/b_i$ and X_i to the historical data y_i that has been transformed according to Equation 96.

$$t = a - \sum_{i=1}^{n} \frac{1}{b_i} ln\Big(\frac{L_i - y_i}{y_i - y_{o,i}}\Big) \tag{93}$$

$$t = a - \frac{1}{b_{sfc}} ln\Big(\frac{L_{sfc} - y_{sfc}}{y_{sfc} - y_{o,sfc}}\Big) - \frac{1}{b_{fg}} ln\Big(\frac{L_{fg} - y_{fg}}{y_{fg} - y_{o,fg}}\Big) - \cdots$$

$$\frac{1}{b_{db}} ln\Big(\frac{L_{db} - y_{db}}{y_{db} - y_{o,db}}\Big) - \frac{1}{b_{ei}} ln\Big(\frac{L_{ei} - y_{ei}}{y_{ei} - y_{o,ei}}\Big) \tag{94}$$

$$t = \beta_0 + \beta_{sfc} X_{sfc} + \beta_{t/w} X_{t/w} + \beta_{db} X_{db} + \beta_{ei} X_{ei} \tag{95}$$

$$X_i = ln\Big[\frac{L_i - y_i}{y_i - y_{o,i}}\Big] \tag{96}$$

In order to test the goodness of fit and significance of each metric that is included in the model, settings for each attribute limit, L_i, and lower bound, $y_{o,i}$, must be identified. In the case of L_i, the mean from the uniform distributions previously defined for each metric was used. For each $y_{o,i}$ a value slightly beyond the worst contained in the historical database was selected. In this way, the worst value within the historical database for each metric represents a starting point for each metric-specific S-curve. Table 26 shows the limit and the lower bound alongside the worst value within the database for each metric. The historical database in Table 22 is transformed using these values according to Equation 96 which results in the regression data provided in Table 27.

Following this transformation, the statistical package JMP was used to regress the linearized form of the Logistic MDGM, Equation 95, which results in the fit

Table 26: Metric Bounds

	Limit	Lower Bound	Worst in Database
SFC	0.44	0.7	0.665
Thrust	135125	25000	37400
Noise	73	98	97.23
Emissions	7	35	25.08

characterized by Figure 50 [89]. Note the correlation coefficient, denoted as RSq below the actual-versus-predicted plot, of 0.84, which is the result of regressing all 40 systems contained within the historical database. Consider the possibility that not all systems within the historical database were representative of the state of the art as quantified by SFC, thrust, noise, and emissions for their respective dates of introduction. Several 'subpar' systems can be identified by inspection of the historical database. Looking back to the historical database in Table 22, note in particular data points 11 and 36, corresponding to the JT9D-7F and PW2040. Each of these engines perform below the levels of capability previously achieved for each and every metric being considered. These data points clearly represent systems that for their respective years of introduction were below the SoA as quantified by the metrics of interest to this study. Systems below the SoA result in predicted dates of introduction much earlier than their actual introduction dates, because based on their levels of capability they could have been introduced sooner and, in many cases, comparable systems were. These low SoA data points appear above the $y = x$ line in the actual versus predicted plot in Figure 50 and as positive residuals in the adjacent residual plot. A total of 10 points appear to represent systems that were below the state of the art for their respective dates of introduction and these systems were removed from the model resulting in the reduced historical database of Table 28. Also note that systems that aggressively advance the state of the art for their respective dates of introduction

Table 27: Design Matrix to Test Model Goodness of Fit

	Engine Model	Date	X_{sfc}	X_{fg}	X_{db}	X_{ei}
1	CF6-6D	1970	1.33889	1.84714	0.64517	-0.4455
2	JT9D-7J	1970	1.86075	1.22524	1.04859	-0.4355
3	CF6-50A	1971	1.59109	1.27775	-0.0431	-1.086
4	JT9D-7	1971	1.86075	1.42796	1.13174	-0.9206
5	JT9D-7A	1972	1.79625	1.39056	1.10755	-0.86
6	RB211-22B	1972	0.95978	1.70073	1.48592	-1.3428
7	CF6-50C	1973	1.6187	1.17421	-0.0815	-0.8388
8	CF6-50E	1973	1.6187	1.10013	0.20118	-0.8369
9	JT9D-59A	1974	1.33889	1.07604	1.82854	-1.1441
10	JT9D-70A	1974	1.33889	1.07604	1.06173	-1.1441
11	JT9D-7F	1974	1.86075	1.33185	1.14263	-0.5845
12	RB211-524B	1975	1.27015	1.22524	1.498	-0.3709
13	CF6-50C1	1976	1.6187	1.10013	-0.0051	-0.8369
14	CF6-50C2	1976	0.99853	1.10013	0.35175	-0.8369
15	CF6-50E2	1976	0.99853	1.10013	0.34961	-0.7383
16	CF6-45A2	1978	0.99853	1.41636	-1.7291	-1.178
17	CF6-50C2-B	1978	0.99853	1.0287	0.40942	-0.744
18	JT9D-7Q	1979	1.27015	1.07604	1.01297	-1.1441
19	RB211-524C2	1979	1.24782	1.1492	0.98391	-0.725
20	JT9D-7R4D	1980	0.40547	1.33185	2.99551	-0.7271
21	CF6-80A	1981	0.86568	1.33185	0.54316	-0.8108
22	CF6-80A2	1981	0.86568	1.22524	0.50168	-0.7079
23	RB211-524D4	1981	0.75731	1.07604	0.97569	0.01054
24	RB211-535C	1981	1.33889	2.06446	2.89686	-1.2901
25	JT9D-7R4E	1982	0.40547	1.22524	2.99384	-0.4715
26	JT9D-7R4G2	1982	0.45378	0.99387	0.97163	-0.6475
27	PW2037	1983	0.18514	1.97662	3.44308	-1.038
28	RB211-535E4	1983	0.43762	1.83945	2.88754	-0.6375
29	CF6-80C2A2	1985	0.12323	1.05223	0.62493	-1.3697
30	CF6-80C2B1	1985	0.09237	0.85325	-0.1993	-1.2699
31	CF6-80C2B1F	1986	-0.0924	0.85325	-0.1812	-1.2685
32	CF6-80C2B2	1986	0.09237	1.10013	0.45305	-1.5664
33	PW4056	1986	-0.519	0.90361	1.77154	-0.8842
34	CF6-80C2B4	1987	0.09237	0.85325	0.56349	-1.1899
35	CF6-80C2B6	1987	0.15415	0.7305	0.58573	-1.0244
36	PW2040	1987	0.18514	1.72175	3.11642	-0.7593
37	RB211-524G	1988	0	0.84892	1.46297	0.14231
38	RB211-524H	1989	0	0.73879	1.45484	0.59956
39	CF6-80C2B6F	1992	0.15415	0.7305	0.58168	-1.0173
40	GE90-85B	1995	-0.1542	-0.1798	-0.0129	0.42033

appear below the $y = x$ line in the actual-versus-predicted plot in Figure 50 and as more strongly negative residuals.

Following this data reduction, the model was once again regressed using JMP, yielding the fit characterized by Figure 51. Note the improved correlation coefficient

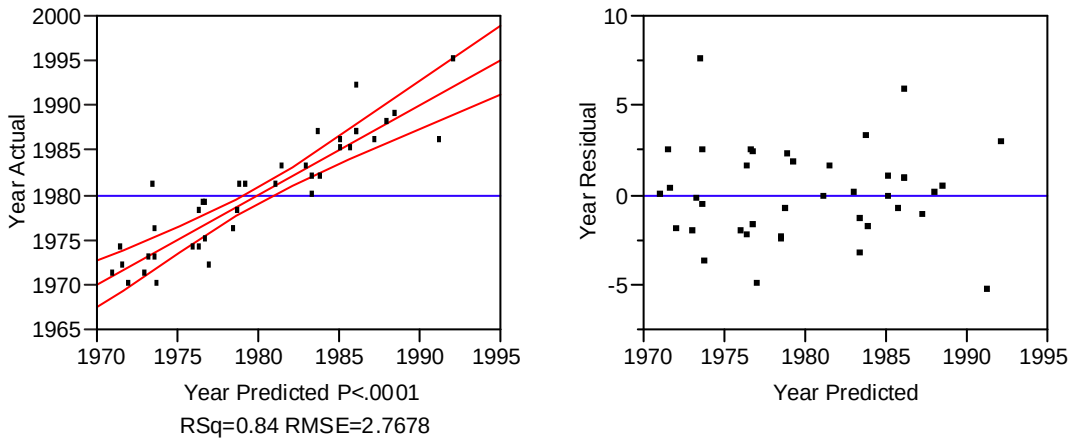

Term	Estimate	Std Error	t Ratio	Prob>|t|
Intercept	1990.0753	1.426377	1395.2	<.0001*
SFC	-7.672327	0.804236	-9.54	<.0001*
Thrust	-3.290909	1.71478	-1.92	0.0631
Noise	0.3961111	0.56266	0.70	0.4861
EINOx	0.5487828	1.097437	0.50	0.6202

Figure 50: Initial Regression Results

of 0.96 and the more evenly distributed residual plot as a result of the data reduction. Now consider the significance of each metric in the model as quantified by the t-statistic and P-value, each denoted in the model as the t-ratio and Prob $> |t|$, respectively. The parameter estimates corresponding to SFC and thrust each have P-values of less than 0.001. This indicates that with a 99.95 percent confidence level these parameters should be nonzero. Conversely, P-values for the parameter estimates that correspond to each noise and emissions are appreciably higher than the threshold of 0.05. This indicates that the certainty that these parameters are nonzero is not significant. Due to their low significance these turbofan attributes, noise and emissions, were removed from the assessment. This does not mean that noise and emissions are not significant design drivers in the ongoing development of turbofan engines. It does, however, suggest that the systems contained within the historical database do not provide enough variability in these metrics relative to the variability

Table 28: Reduced Historical Database

	Engine Model	Date	SFC	Thrust	Noise	EINOx
1	CF6-6D	1970	0.646	40000	89.40	17.93
2	JT9D-7J	1970	0.665	50000	91.51	18.00
3	CF6-50A	1971	0.656	49000	85.23	14.07
4	JT9D-7	1971	0.665	46300	91.90	14.98
5	JT9D-7A	1972	0.663	46950	91.79	15.33
6	RB211-22B	1972	0.628	42000	93.39	12.80
7	CF6-50C	1973	0.657	51000	84.99	15.45
8	CF6-50E	1973	0.657	52500	86.75	15.46
9	JT9D-59A	1974	0.646	53000	94.54	13.76
10	JT9D-70A	1974	0.646	53000	91.58	13.76
11	RB211-524B	1975	0.643	50000	93.43	18.43
12	CF6-50C1	1976	0.657	52500	85.47	15.46
13	CF6-50C2	1976	0.630	52500	87.68	15.46
14	CF6-50E2	1976	0.630	52500	87.66	16.05
15	CF6-45A2	1978	0.630	46500	76.77	13.59
16	CF6-50C2-B	1978	0.630	54000	88.02	16.02
17	JT9D-7R4D	1980	0.596	48000	96.81	16.12
18	RB211-524D4	1981	0.617	53000	91.16	21.07
19	JT9D-7R4E	1982	0.596	50000	96.81	17.76
20	JT9D-7R4G2	1982	0.599	54750	91.14	16.62
21	CF6-80C2A2	1985	0.578	53500	89.28	12.67
22	CF6-80C2B1	1985	0.576	57900	84.26	13.14
23	CF6-80C2B1F	1986	0.564	57900	84.37	13.15
24	CF6-80C2B2	1986	0.576	52500	88.28	11.84
25	PW4056	1986	0.537	56750	94.37	15.18
26	CF6-80C2B4	1987	0.576	57900	88.93	13.53
27	CF6-80C2B6	1987	0.580	60800	89.06	14.40
28	RB211-524G	1988	0.570	58000	93.30	21.99
29	RB211-524H	1989	0.570	60600	93.27	25.08
30	GE90-85B	1995	0.560	85000	85.42	23.90

in SFC or thrust for their contributions to the variability in introduction date to be captured. Consequently, their appearance of insignificance is a result of limited data, although they may in fact have lower significance than do SFC and thrust.

Results from the updated fit including only SFC and thrust are shown in Figure 52. Note the slightly reduced correlation coefficient, 0.96 to 0.95. This is due to the removal of noise and emissions from the model. Using this predictive model, the corresponding composite S-curve was generated as illustrated in Figure 53, wherein the range spanned by the actual data points can be observed. Also shown in Figure 53 is the composite score for each the GE90-90B, GE90-94B, and GE90-115B. These engines were not included in the original historical database because their total

takeoff noise could not be found at the time of this assessment. These engines were not included in the historical data used to regress the composite model of Figure 53, and serve as a sanity check for the near term forecast of the resulting model. Recall, however, that this composite S-curve is based solely on the mean of each limit distribution defined previously. The impacts of this limit uncertainty and any error within the historical database is now explored.

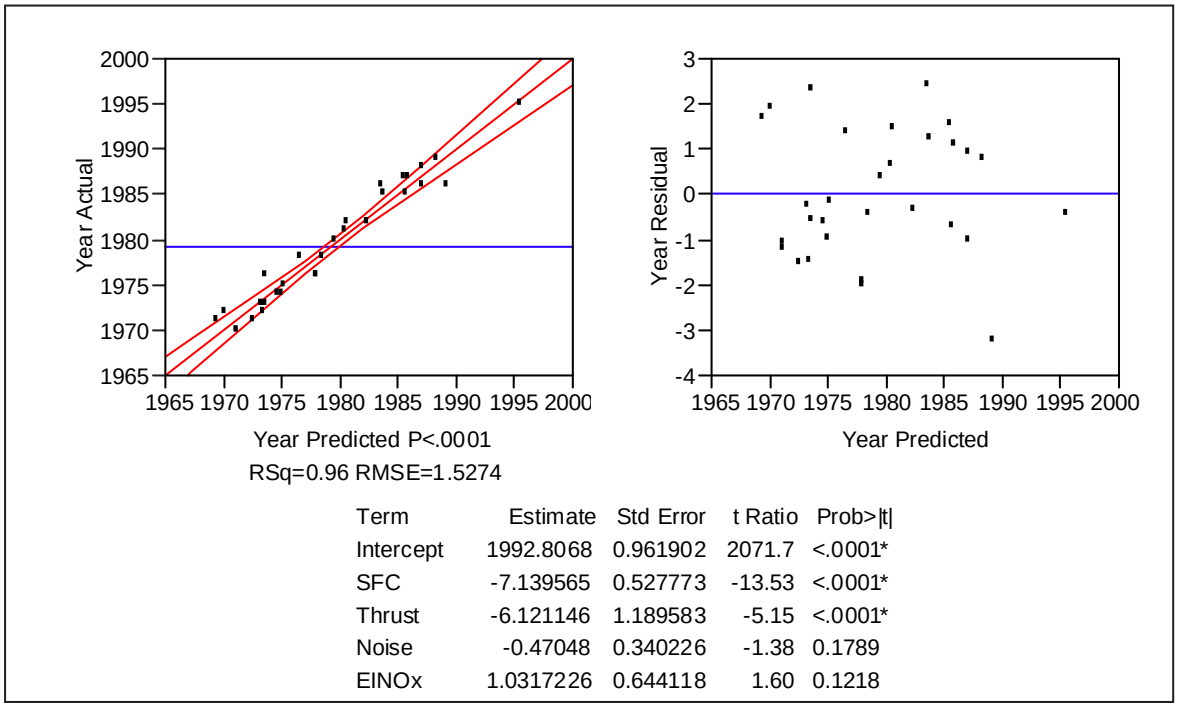

Term	Estimate	Std Error	t Ratio	Prob>|t|
Intercept	1992.8068	0.961902	2071.7	<.0001*
SFC	-7.139565	0.527773	-13.53	<.0001*
Thrust	-6.121146	1.189583	-5.15	<.0001*
Noise	-0.47048	0.340226	-1.38	0.1789
EINOx	1.0317226	0.644118	1.60	0.1218

Figure 51: Regression Results Following Data Reduction

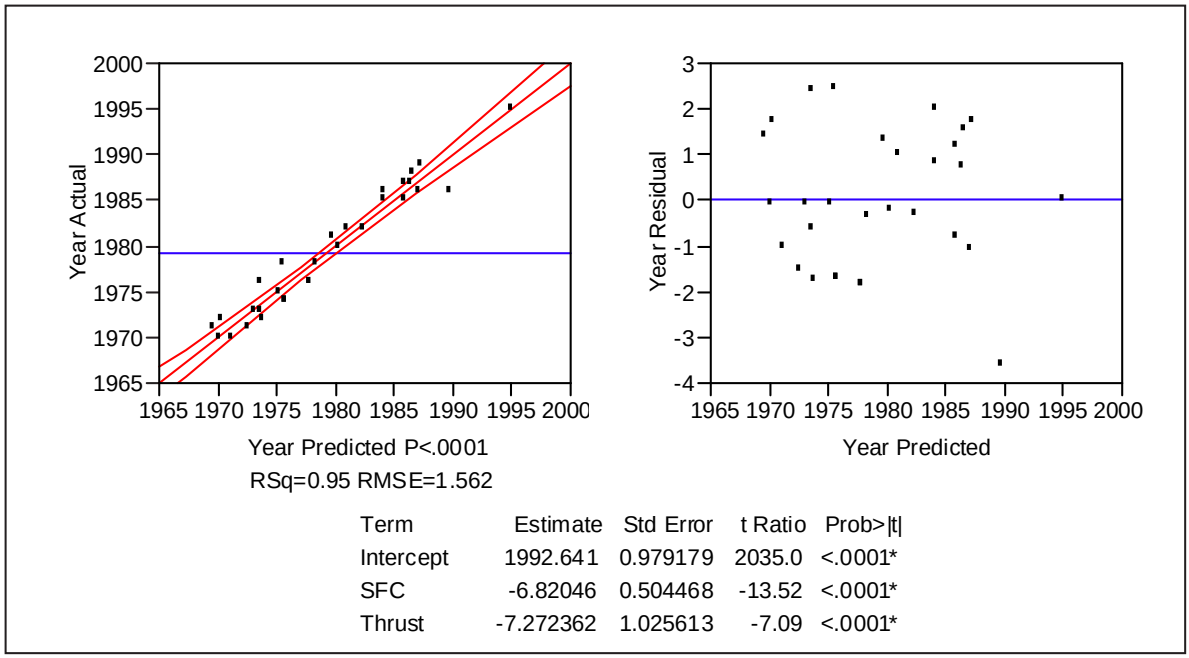

Term	Estimate	Std Error	t Ratio	Prob>|t|
Intercept	1992.641	0.979179	2035.0	<.0001*
SFC	-6.82046	0.504468	-13.52	<.0001*
Thrust	-7.272362	1.025613	-7.09	<.0001*

Figure 52: Regression Results Following Model Reduction

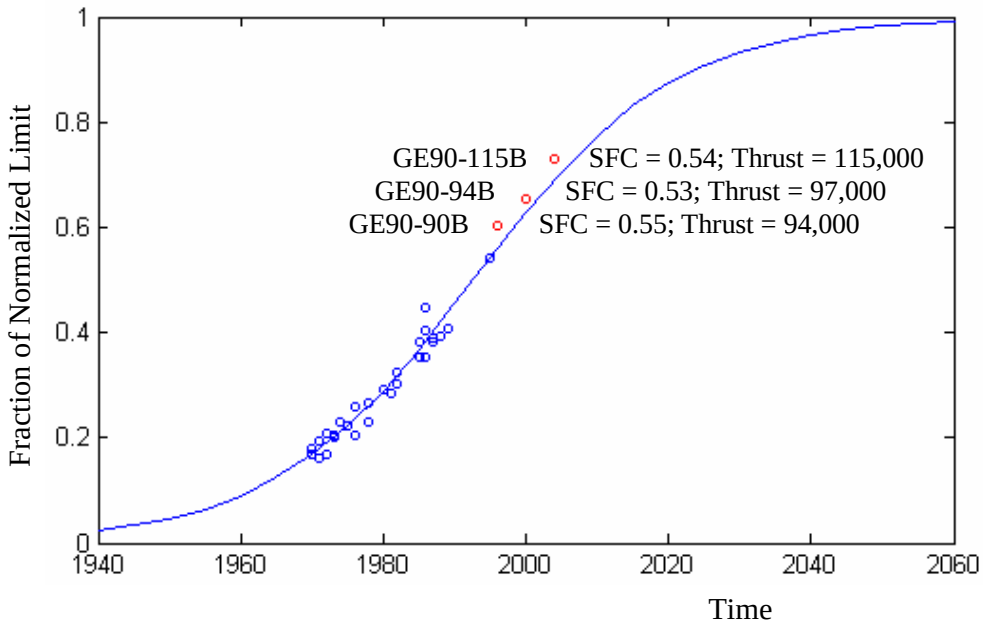

Figure 53: Initial Composite Turbofan Growth Curve

8.4.1 Uncertainty Analysis

Recall that the contributions to model uncertainty from limit estimations and data fluctuations are quantified separately. First the contribution from limit uncertainty is estimated by means of a Monte Carlo simulation. Following this simulation, three composite growth curves are identified from among the thousands generated. One represents the mean technology growth given limit uncertainty, and the remaining two bound the $1-\alpha$ confidence region. Prediction intervals are then calculated for each of the three curves in order to capture the model uncertainty resulting from data fluctuations. This demonstration will establish the 90 percent confidence interval, $\alpha = 0.1$.

A Monte Carlo simulation is conducted to assess the impact of limit uncertainty on the resulting MDGM. During each of 20,000 simulations, an upper limit for each SFC and thrust was selected according to the uniform distributions defined in Figure 49, and linear regression was employed to calculate the parameter estimates of Equation 97. Figure 54 shows the resulting composite growth curve for each simulation as defined by Equation 98. Note the location of the historical data relative to the width of the limit distribution.

$$T = \beta_0 + \beta_{sfc} X_{sfc} + \beta_{fg} X_{fg} \tag{97}$$

$$y_c = \frac{1}{1 + e^{-b_c(t-a)}} \tag{98}$$

where

$$b_c = \left(\frac{1}{b_{sfc}} + \frac{1}{b_{fg}} \right)^{-1} = -(\beta_{sfc} + \beta_{fg})^{-1} \tag{99}$$

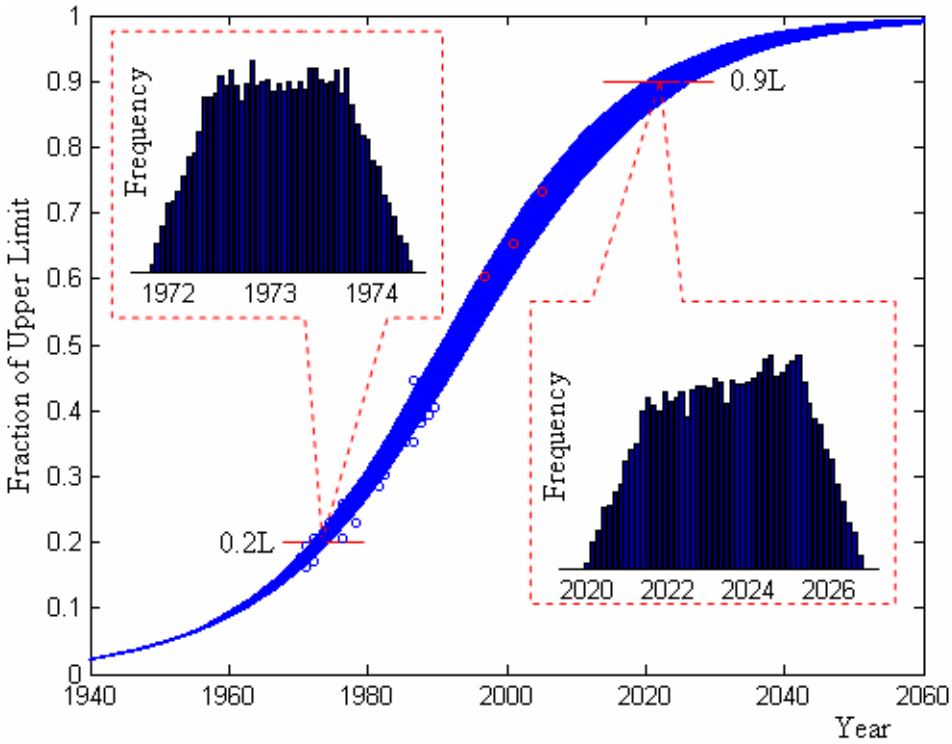

Figure 54: Composite Curves Resulting from Limit Uncertainty Analysis

The distribution of predicted years at which each 20 and 90 percent of the normalized limit was achieved is also shown in Figure 54. These distributions will be used to identify composite curves representative of the mean and of 90 percent confidence interval. The 20 and 90 percent capability levels were selected because of the limited number of intersections that occur between them as illustrated by the distribution shown in Figure 55. This distribution is generated by randomly selecting two composite curves from the 20,000 generated during the Monte Carlo simulation and calculating at what fraction of the normalized limit they intersect. A total of 20,000 pairs of curves were tested to form this distribution. The table within Figure 55 indicates the percentage of composite curve pairs that intersect between the corresponding curve segments. Note that only three percent of all intersections occur above 99 percent of the normalized limit or below 1 percent. Also note that just over one percent intersect between 20 and 90 percent of the normalized limit.

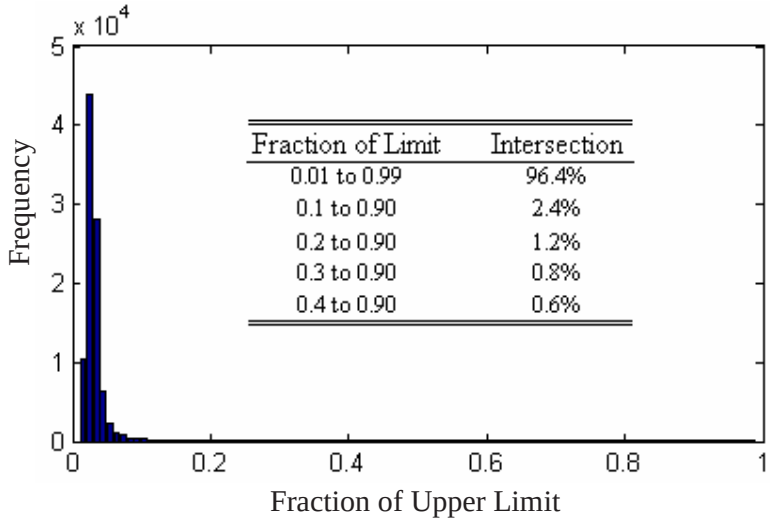

Figure 55: Distribution of Composite Curve Intersections

Composite curves representative of the mean and the 90 percent confidence interval bounds are identified by first establishing the mean as well as the 5 and 95 percentiles of the distributions at both 20 and 90 percent of the normalized limit as provided in Figure 56. The composite curve representative of the mean is identified by finding the Monte Carlo simulation that most nearly intersects the mean established for each distribution. This is accomplished by calculating the Euclidean distance *between* the mean date for each 20 and 90 percent of the normalized limit *and* the dates at which each MC simulation reached the 20 and 90 percent capability levels. Equation 100 defines this distance, where $\bar{t}_{0.2}$ and $\bar{t}_{0.9}$ correspond to the means of each distribution in Figure 56 and each $t_{0.2,i}$ and $t_{0.9,i}$ correspond to the date at which 20 and 90 percent of the normalized limit is achieved by the i_{th} MC simulation. The assessment selects the MC simulation that minimizes this distance to be represent the mean at all levels of capability. Using this same technique, the composite curve representative of each boundary of the 90 percent confidence region is identified whereby the distances to be minimized are calculated according to Equations 101 and 102. The two resulting curves bound 90 percent of the remaining Monte Carlo simulations. All three

composite curves identified as a result of this procedure are illustrated in Figure 57 wherein the limits and parameter estimates for each curve are provided.

$$s_{mean} = \sqrt{(t_{0.2,i} - \bar{t}_{0.2})^2 + (t_{0.9,i} - \bar{t}_{0.9})^2} \tag{100}$$

$$s_{0.05} = \sqrt{(t_{0.2,i} - t_{0.2,0.05})^2 + (t_{0.9,i} - t_{0.9,0.05})^2} \tag{101}$$

$$s_{0.95} = \sqrt{(t_{0.2,i} - t_{0.2,0.95})^2 + (t_{0.9,i} - t_{0.9,0.95})^2} \tag{102}$$

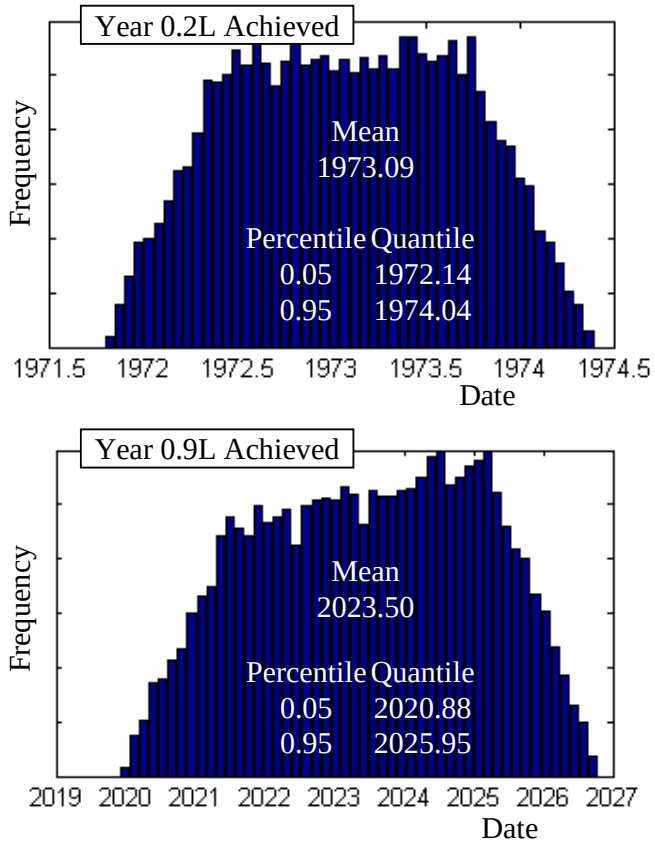

Figure 56: Distribution of Dates for Reaching 0.2L and 0.9L

Once the composite growth curves representative of the mean and boundaries of the 90 percent confidence interval have been identified, the contribution of uncertainty

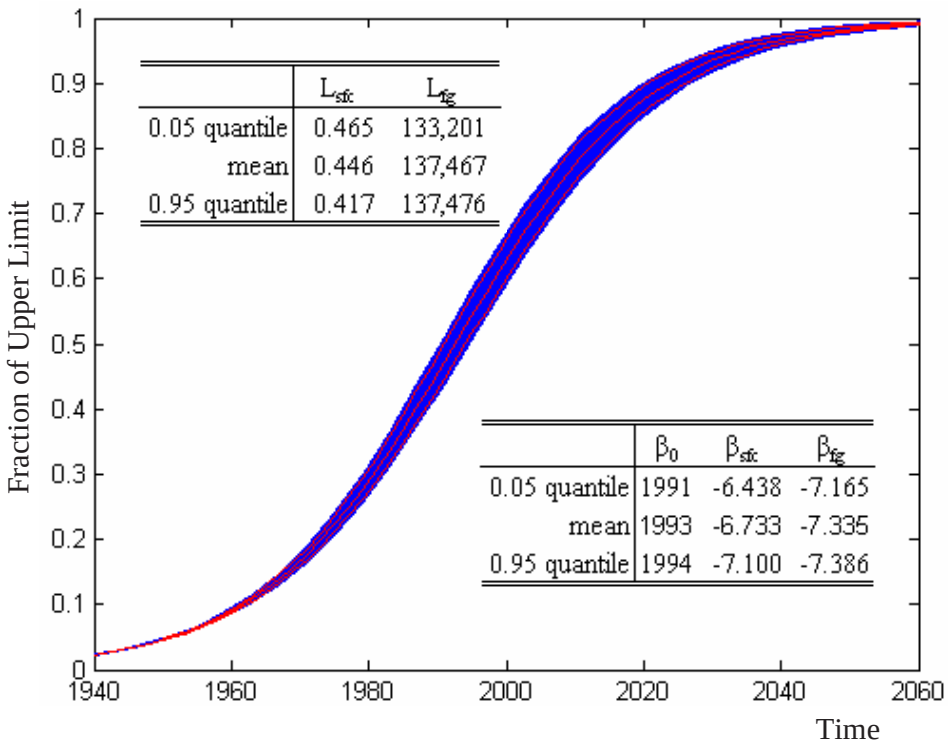

Figure 57: Composite Growth Model with Limit Uncertainty Intervals

from data error can be incorporated. Recall that this is accomplished by calculating the prediction interval on the linearized form of the composite growth model, shown here as Equation 103, where T corresponds to the date of introduction, and X_c corresponds to the transformation of y_c according to Equation 104, wherein y_c can be calculated according to Equation 105.

$$T = \beta_0 + \beta_1 X_c \tag{103}$$

$$X_c = ln\left(\frac{1 - y_c}{y_c}\right) \tag{104}$$

$$y_c = \left(1 + \left(\frac{L_{sfc} - y_{sfc}}{y_{sfc} - y_{o,sfc}}\right)^{\frac{b_c}{b_{sfc}}} \left(\frac{L_{fg} - y_{fg}}{y_{fg} - y_{o,fg}}\right)^{\frac{b_c}{b_{fg}}}\right)^{-1} \tag{105}$$

The linearized model of Equation 103 is regressed against the historical data for each

pair of limits, L_{sfc} and L_{fg}, corresponding to the growth curves representative of the mean and 90 percent confidence region boundaries. The resulting parameter estimates are shown in Table 29 accompanied by the mean, variance, and mean square error, which are also required for the calculation of prediction intervals.

Table 29: Regression Data for Growth Curves Forming the 90% Confidence Region

	L_{sfc}	L_{fg}	β_0	β_1	$\bar{X}$	Sxx	MSE
0.05 quantile	0.465	133,201	1991.0	-13.60	0.86	6.98	2.43
mean	0.446	137,467	1992.6	-14.07	0.95	6.54	2.37
0.95 quantile	0.417	137,476	1994.1	-14.49	1.03	6.17	2.31

Equations 106 and 107 provide the general form of the one-sided prediction intervals and Equation 108 the two-sided. $\hat{T}_h$ is the $1-\alpha$ prediction interval of the expected date corresponding to a new composite level of capability, $X_{c,h}$, where Equation 109 defines the variance.

$$\hat{T}_h = E\{T_h\} + t(1-\alpha; n-2)s\{pred\} \tag{106}$$

$$\hat{T}_h = E\{T_h\} - t(1-\alpha; n-2)s\{pred\} \tag{107}$$

$$\hat{T}_h = E\{T_h\} \pm t(1-\alpha/2; n-2)s\{pred\} \tag{108}$$

$$s^2\{pred\} = MSE\left[1 + \frac{1}{n} + \frac{(X_h - \bar{X})^2}{\sum(X_i - \bar{X})^2}\right] \tag{109}$$

The two-sided prediction interval is applied to the mean composite curve to bound variability in the expected mean due to error fluctuations within the historical database. Equation 110 provides this two-sided confidence interval, which is based on the regression results provided in Table 29, where $t(.95, 28)$ is 1.7011. Equations 111 and

112 are the one-sided prediction intervals applied to the composite growth curves that bound the 90 percent confidence region which result from limit uncertainty as illustrated in Figure 58. These intervals bound the 90 percent confidence region resulting from both limit uncertainty and prediction error due to data fluctuations. The relative contribution of each can be observed in Figure 58 by comparing the width of the two-sided prediction region around the mean to the total confidence interval. In this particular case, the uncertainty contribution to the overall model from each limit uncertainty and prediction error is comparable.

$$\begin{aligned} \hat{T}_{h,mean} &= t_{mean} = \beta_{0,mean} - \beta_{1,mean} X_h \\ &\pm t(0.95, 28)\left[MSE_{mean}\left(1 + \frac{1}{30} + \frac{(X_h - \bar{X}_{mean})^2}{\sum (X_i - \bar{X}_{mean})^2}\right)\right]^{1/2} \end{aligned} \tag{110}$$

$$\begin{aligned} \hat{T}_{h,.05} &= t_{CI^-} = \beta_{0,.05} - \beta_{1,.05} X_h \\ &- t(0.9, 28)\left[MSE_{.05}\left(1 + \frac{1}{30} + \frac{(X_h - \bar{X}_{.05})^2}{\sum (X_i - \bar{X}_{.05})^2}\right)\right]^{1/2} \end{aligned} \tag{111}$$

$$\begin{aligned} \hat{T}_{h,.95} &= t_{CI^+} = \beta_{0,.95} - \beta_{1,.95} X_h \\ &+ t(0.9, 28)\left[MSE_{.95}\left(1 + \frac{1}{30} + \frac{(X_h - \bar{X}_{.95})^2}{\sum (X_i - \bar{X}_{.95})^2}\right)\right]^{1/2} \end{aligned} \tag{112}$$

The following section investigates the impacts of this uncertainty on technology assessment metrics of interest, such as the current level of capability relative to both the upper limit and the point of diminishing returns.

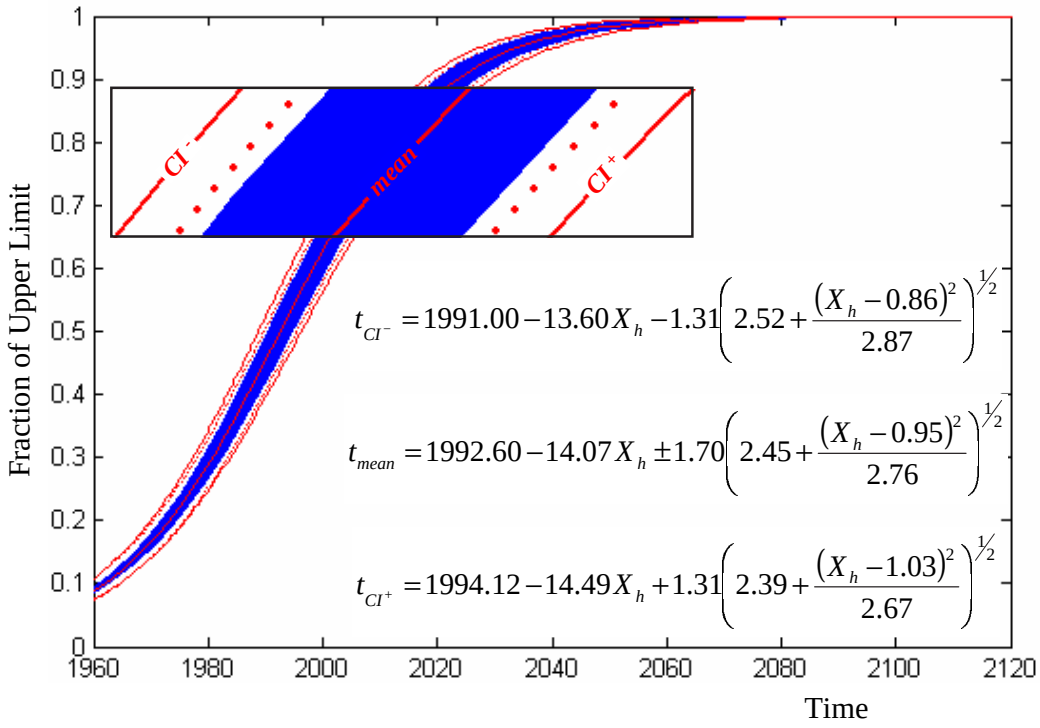

Figure 58: Composite Growth Curve Combined Confidence Interval

8.5 Technology Assessment

Where is the current SoA relative to impending limits as quantified by SFC and thrust? Has the point of diminishing returns been reached? To what degree of certainty can these questions be answered? These questions are the subject of this section, the answers to which are easily ascertained given the MDGM and confidence bounds established in the previous section.

8.5.1 Current State of the Art

The current SoA of turbofan technology as quantified by SFC and thrust can be evaluated by specifying the year, 2006, for the mean and confidence boundary growth curves illustrated in Figure 58. Each equation is solved for the transformed capability X_h that is achieved at the year 2006, which is subsequently converted to y_c according to Equation 113.

$$y_c = (e^{X_i} + 1)^{-1} \tag{113}$$

Figure 59 illustrates the resulting capability levels. The mean expected capability for the year 2006 is 72.2 percent of the normalized upper limit. This corresponds to individual metric settings of $0.722(L_i - y_{o,i}) + y_{o,i}$, which are 0.517 $\mathrm{lb_m/lb_f}$-hr and 106,201 $\mathrm{lb_f}$ for each SFC and thrust, respectively. These settings, however, can be exchanged while maintaining the same overall composite level of capability. The frontier governing this tradeoff for the year 2006 is quantified by Equation 114 or equivalently by Equation 115.

$$y_{sfc} = \frac{L_{sfc} - y_{o,sfc}}{1 + e^{-b_{sfc}\left(2006 - a + \frac{1}{b_{fg}} ln\left(\frac{L_{fg} - y_{fg}}{y_{fg} - y_{o,fg}}\right)\right)}} + y_{o,sfc} \tag{114}$$

$$0.753 = \left(1 + \left(\frac{L_{sfc} - y_{sfc}}{y_{sfc} - y_{o,sfc}}\right)^{\frac{b_c}{b_{sfc}}} \left(\frac{L_{fg} - y_{fg}}{y_{fg} - y_{o,fg}}\right)^{\frac{b_c}{b_{fg}}}\right)^{-1} \tag{115}$$

The 90 percent confidence bands are also shown in Figure 59, which bound the 2006 level of capability between 66 and 79 percent of the normalized upper limit. This indicates that there is anywhere between 21 and 34 percent availability for further improvement. Of more interest than the remaining distance to the upper limit is the location of the point of diminishing returns relative to the current state of the art. This is explored by the following section.

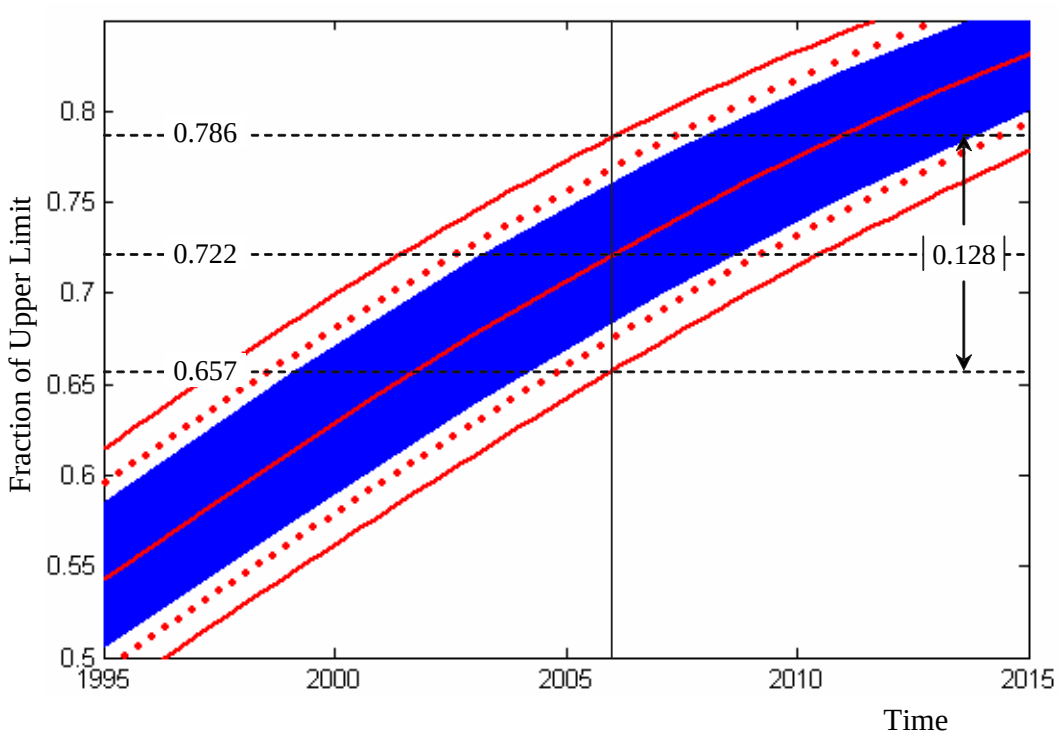

Figure 59: Composite Measure of Current SoA

8.5.2 Point of Diminishing Returns

Recall from the previous chapter that the point of diminishing returns (PDR) always occurs at the same fraction of the upper limit for the Logistic curve, namely $0.789L$. The previous section made clear that it has already been exceeded as quantified by SFC and thrust. The date at which it was reached is calculated by transforming $y_c = 0.789$ according to Equation 116 and substituting X_c into the equations provided in Figure 58. Figure 60 illustrates the results and indicates that the point of diminishing returns will most likely occur in 2011 and with 90 percent confidence will occur between 2006 and 2016.

$$X_c = ln\left(\frac{1 - y_c}{y_c}\right) \tag{116}$$

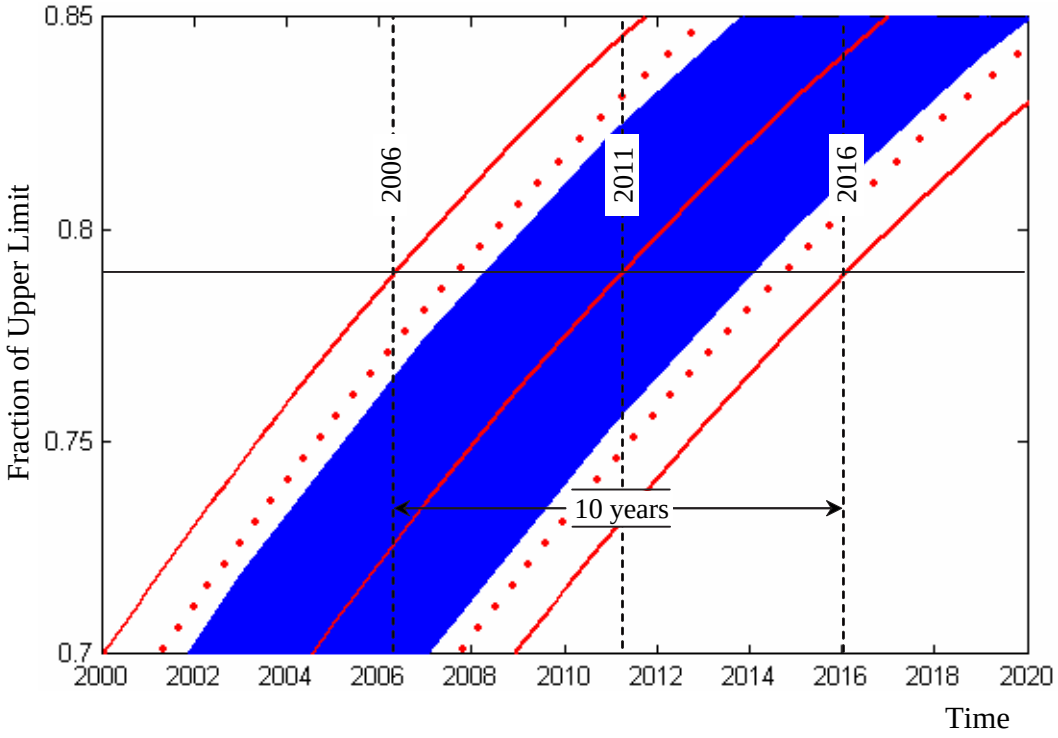

Figure 60: Locating the Point of Diminishing Returns

Once the point of diminishing returns is reached, each incremental improvement in SFC and thrust that is achieved requires increasing development time, that is, investment. Just how much more investment? This can be established by comparing the rate of change in the composite model at the point of diminishing returns to the rate of change at the date of interest. This is accomplished by taking the time derivative of the composite model, which is shown here as Equation 117 and illustrated in Figure 61.

$$\frac{dy_c}{dt} = \frac{b_c e^{b_c(-t+a)}}{\left(1 + e^{b_c(-t+a)}\right)^2} \tag{117}$$

The resulting growth rates for each the expected PDR and the year 2006 are, respectively, $1.2e^{-2}$ and $1.4e^{-2}$ percent of the normalized limit per year. This indicates that

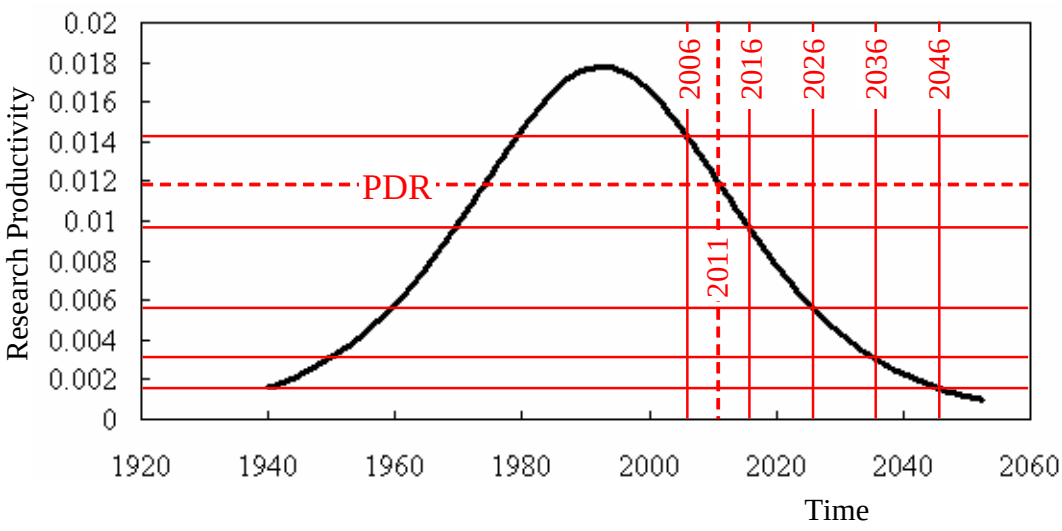

Figure 61: Research and Development Productivity

during the year 2006 both SFC and thrust should advance 0.014 percent of the range between their upper and lower bounds. This also indicates that the time and investment required to advance turbofan technology through SFC or thrust improvements is expected to be slightly higher today than in 2011—the expected date of the point of diminishing returns. The ratio of the current rate of change to the rate of change at the point of diminishing returns provides a factor quantifying current development productivity relative to that at the point of diminishing returns. This factor for the year 2006 is 1.2 which indicate that the current development productivity is 20 percent higher than it will be once the point of diminishing returns is reached. Compare this factor with the 0.8 expected for the year 2016. This indicates that only five years after the point of diminishing returns is reached, one and half times (that is, 1.2/0.8) the engineering effort will be required to achieve the same incremental improvement made in 2006.

The increase in engineering effort required to achieve a specified incremental improvement is a convenient measure to assess the expected investment required to maintain a specified growth rate. This is accomplished by dividing the incremental

improvement achieved in a specified year by the incremental improvement achieved in all other years. For instance, if the incremental improvement achieved in 2011—the expected date of the point of diminishing returns—is divided by the incremental improvement achieved in all other years as quantified by Equation 118, the investment multiple results as illustrated in Figure 62. The investment multiple is here defined as the multiple increase in engineering effort required to maintain the same growth rate achieved at the point of diminishing returns. Note from Figure 62 that the engineering effort required in 2026 is expected to be two times greater than that required in 2011 to make the same incremental improvement. That multiple is expected to jump to four by 2036 and eight by 2046.

$$\text{Investment Multiple} = \left.\frac{dy_c}{dt}\right|_{PDR} \div \frac{dy_c}{dt} \tag{118}$$

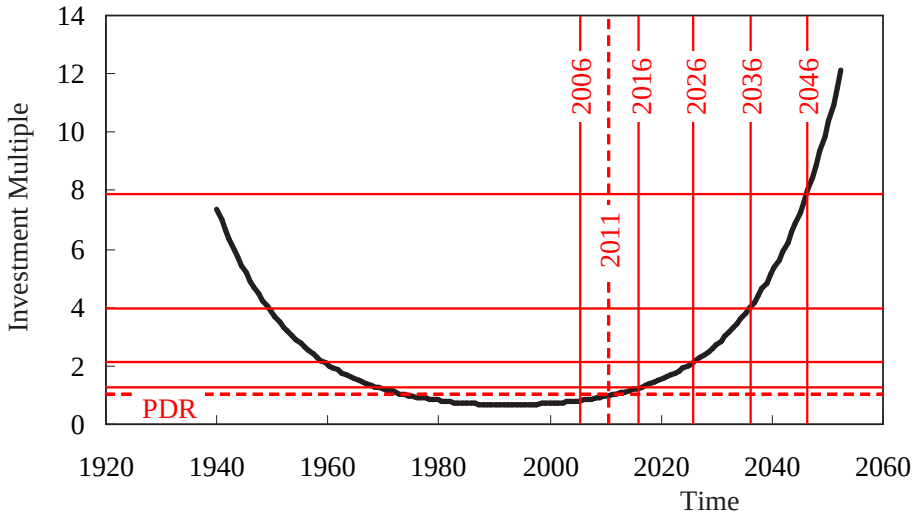

Figure 62: Investment Multiple Required to Maintain PDR Growth Rate

These results, both that 21 to 34 percent availability for improvement exists and that the point of diminishing returns is likely to be achieved within the next decade, apply only to the attributes of SFC and thrust. Nothing can be concluded from

this assessment concerning noise, emissions, reliability, and the like. Furthermore, these results hold only if the actual limit for each SFC and thrust is contained within the distributions specified in Section 8.3, Figure 49. Even these rather broad, uniform distributions provide valuable insight into the current maturity level of turbofan technology as quantified by SFC and thrust. With minimal investment, that is, minimal relative to the development of a new engine, to further resolve these limits, the confidence region can be significantly reduced. The following section will explore the impacts of narrowing limit distributions as a result of such a hypothetical investment.

8.6 Limit Uncertainty Reduction

This section of the demonstration assesses the impact of reduced limit uncertainty on the resulting MDGM. The uniform distributions previously defined for the limits of both SFC and thrust are replaced with the normal distributions shown in Figure 63. The mean for each normal distribution is chosen to correspond to the mean of the uniform distribution used earlier, although the variance was significantly reduced to simulate limit resolution resulting from research investment. As before, a 20,000 case Monte Carlo simulation was conducted, during each simulation of which a limit for each SFC and thrust was selected from the distributions defined in Figure 63, and linear regression was employed to fit the MDGM of Equation 119.

$$T = \beta_0 + \beta_{sfc} X_{sfc} + \beta_{fg} X_{fg} \tag{119}$$

The composite curve resulting from each MC simulation is provided in Figure 64. An additional Monte Carlo simulation was conducted to investigate the location of intersections between composite curve pairs of Figure 64.

The frequency of intersections at each level of capability resulting from the 20,000 curve pairs tested is characterized by the distribution provided in Figure 65. Figure

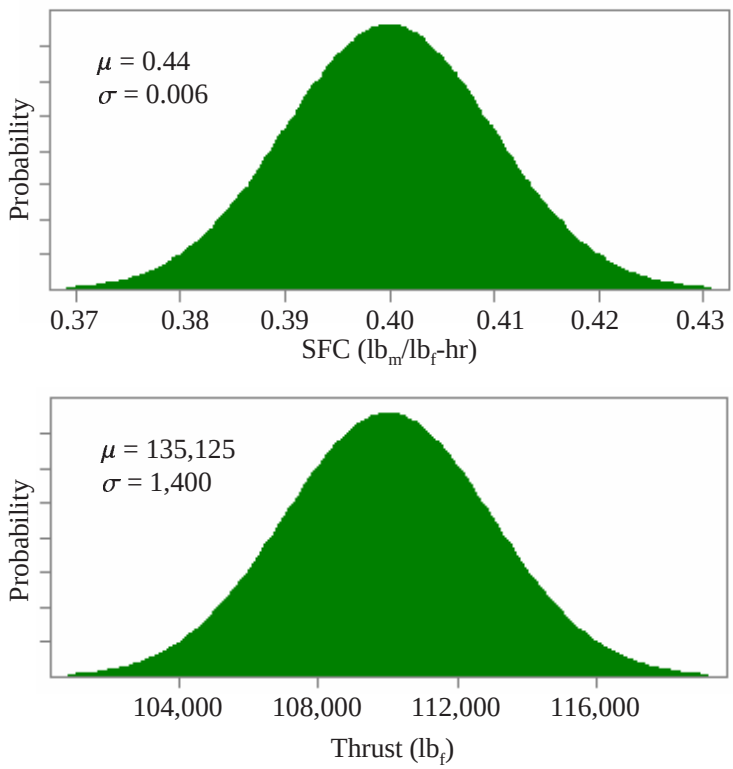

Figure 63: Normal Distributions Applied to Limit Estimations

65 also shows the percentage of intersections that occur between various levels of capability. There is a slight increase over the pervious example in the percentage intersection that occurs between 20 and 90 percent of the normalized limit, 1.2 to 1.6 percent. This increase, however, is minimal, and these capability levels are again used to identify the composite curve that is representative of the mean and of each boundary of the 90 percent confidence interval. The distributions of dates at which each of these capability levels is achieved is shown in Figure 66, wherein the mean and 5th and 95th percentiles are provided.

The Euclidean distance is calculated *between* the dates at which each MC simulation reaches 20 and 90 percent of the normalized limit *and* the mean and 5th and 95th percentiles at each 20 and 90 percent capability levels. The curves minimizing

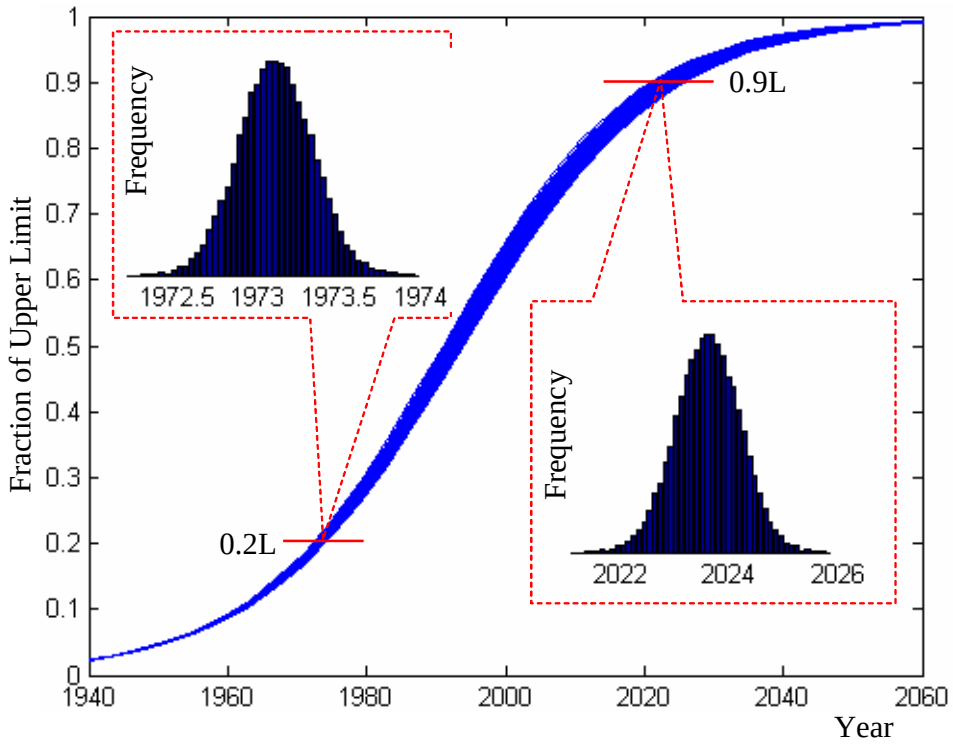

Figure 64: Composite Growth Curves Resulting from Normally Distributed Limits

these distances were identified from among the 20,000 MC simulations as being representative of the mean and boundaries of the 90 percent confidence region. Figure 67 provides the limits and parameter estimates corresponding to each of these curves, and Table 30 provides the mean square error, variance, and parameter estimates resulting from regressing each curve against the linearized composite growth model of Equation 103. With this data, prediction intervals are calculated for each of the three curves in Figure 67 in a similar manner to that previously demonstrated. Figure 68 illustrates these intervals with each accompanied by its corresponding equation.

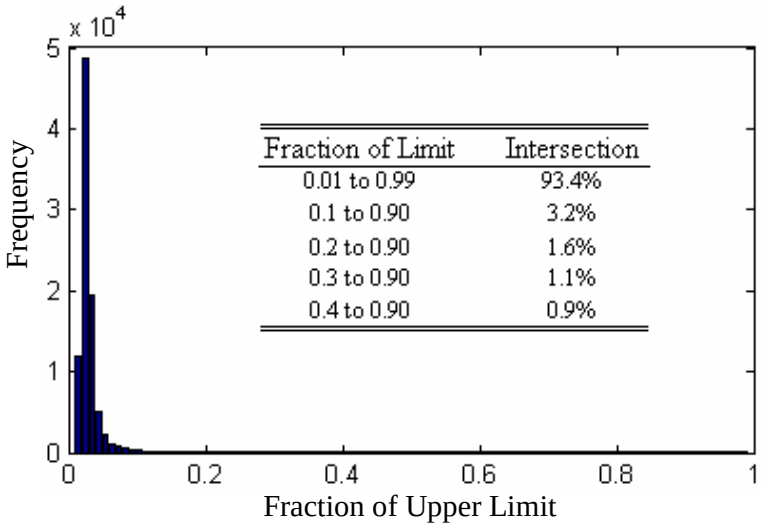

Figure 65: Distribution Composite Curve Intersection Locations

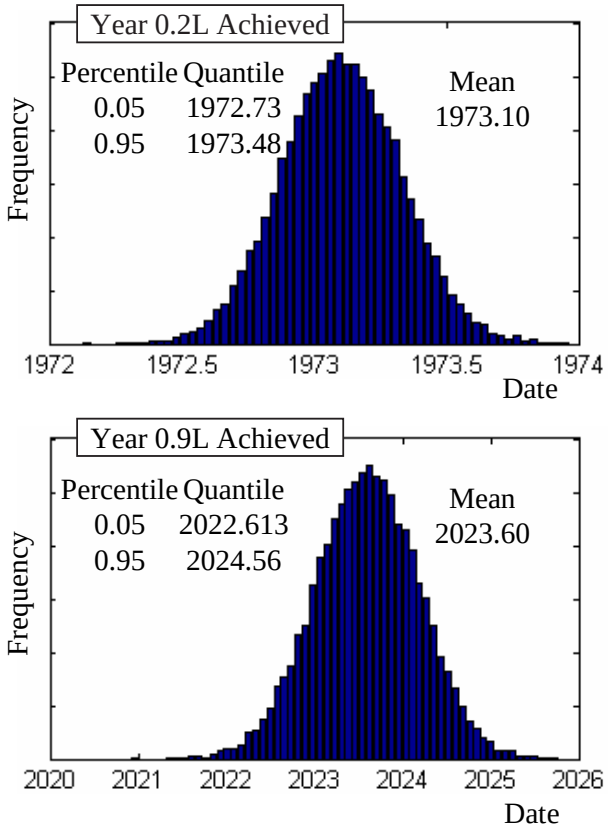

Figure 66: Distribution of Dates for Achieving 20 and 90 Percent of the Normalized Limit

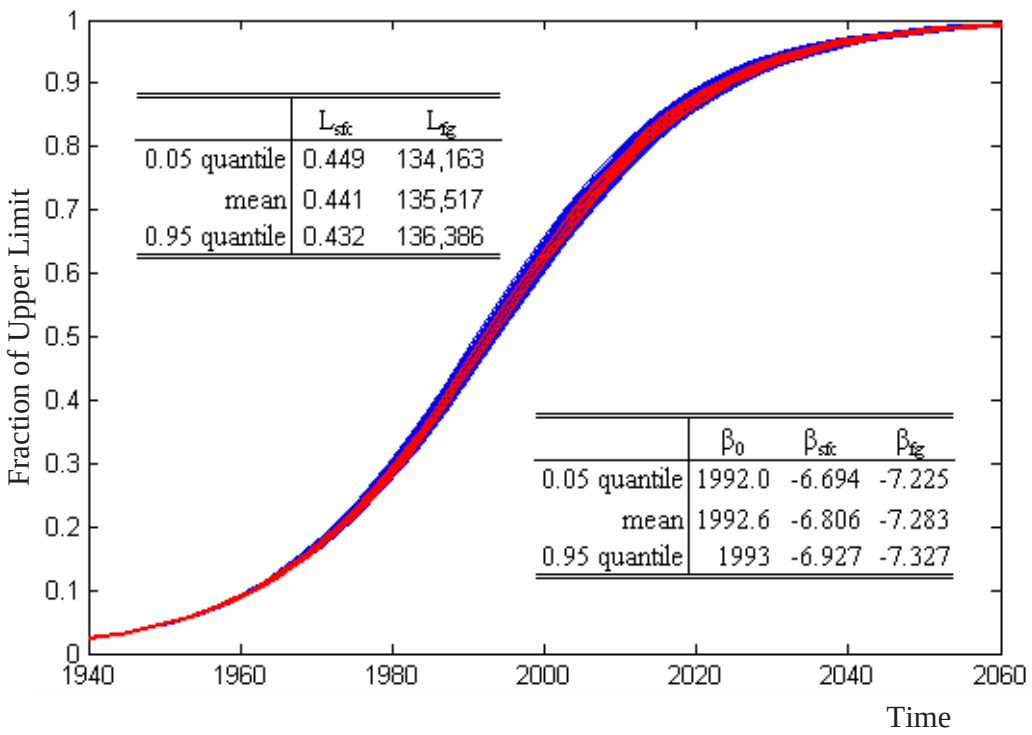

Figure 67: Mean and Confidence Bands Resulting from Limit Uncertainty

Table 30: Regression Data for Composite Growth Curves

	β_0	β_1	$\bar{X}$	Sxx	MSE
0.05 quantile	1992.0	-13.92	0.92	6.68	2.38
mean	1992.6	-14.09	0.95	6.52	2.36
0.95 quantile	1993.2	-14.25	0.98	6.37	2.34

Note that the one-sided prediction intervals for the 0.05 and 0.95 composite curves bound all 20,000 MC simulations. Also note that the two-sided prediction interval around the mean illustrated by the dotted lines extends to each the 0.05 and 0.95 one-sided intervals. This indicates that the uncertainty contributed to the overall model from limit uncertainty is negligible compared to prediction error, and further reduction in limit uncertainty will provide no significant reduction in overall model uncertainty.

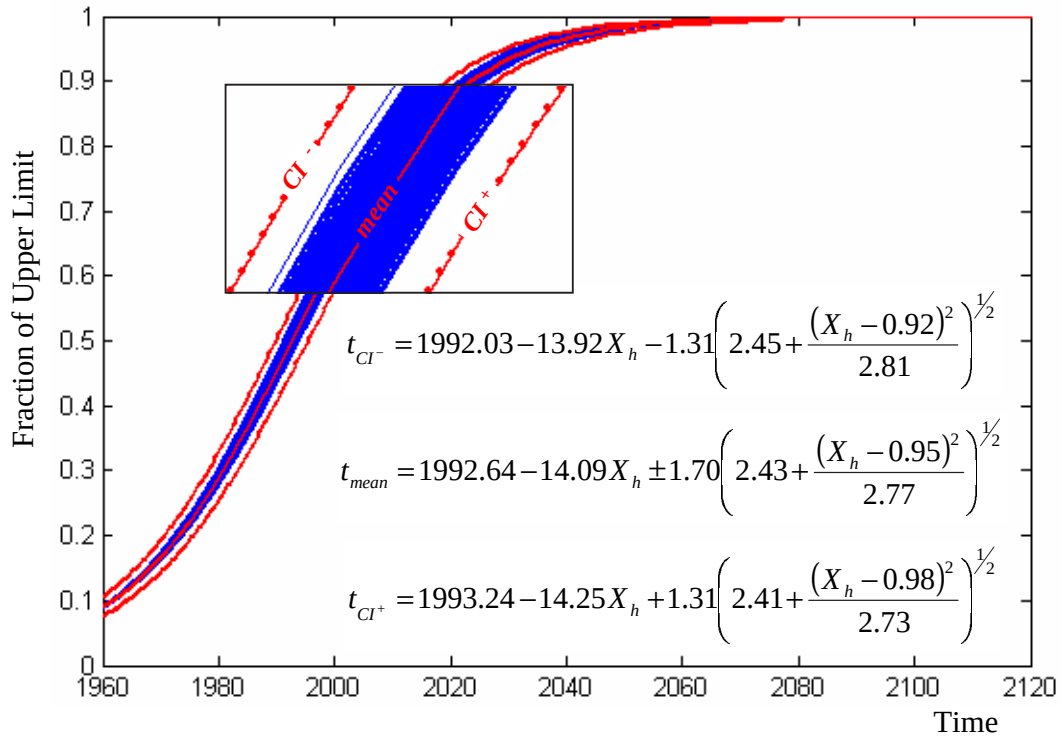

Figure 68: Composite Growth Curve Combined Confidence Interval

This new MDGM is now fully defined, and it allows the current capability level to be compared to both the upper limit and point of diminishing returns. Consider first the expected capability level for the year 2006, which is calculated by setting $\hat{T}_h$ in each equation of Figure 68 to 2006 and solving for X_h and subsequently y_c. Figure 69 shows the results from these calculations and the corresponding estimates based on the uniform limit distributions, which are shown in parentheses. The new expected mean is understandably very close to that calculated previously as the mean of each distribution was unchanged. The 90 percent confidence region, however, has been reduced by 27 percent, which now indicates between 23 and 33 percent availability for further improvement, as opposed to the previous 21 to 34 percent.

Consider now the impact of the reduced limit uncertainty on predicting the date at which the point of diminishing returns is reached. Recall that the date at which the point of diminishing returns is achieved is calculated by transforming $y_c = 0.789$

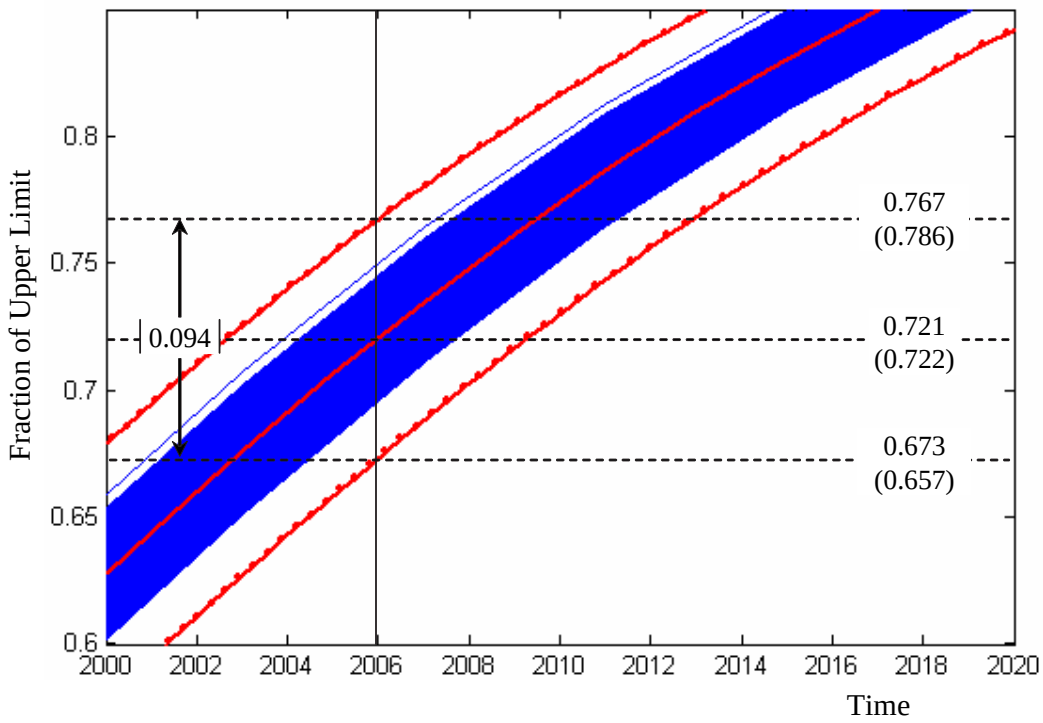

Figure 69: Current Turbofan SoA Based on Normally Distributed Limit Uncertainty

to yield X_c, which is then used in the equations of Figure 68 to calculate $\hat{T}_h$. Figure 70 illustrates the results from these calculations and also provides the previous predictions in parentheses. Again, the mean is very nearly the same as previously calculated, differing by less than a year. The 90 percent confidence region is also reduced by 27 percent, indicating that the PDR is expected to occur between 2008 and 2015.

The turbofan assessment was conducted for different sets of limit assumptions to demonstrate the variability of model uncertainty on the precision of limit knowledge. Also illustrated is that even in cases where little knowledge of the limit exists, demonstrated by the uniform distribution, meaningful conclusions can still result from the proposed assessment procedure. Furthermore, forecasters can establish precision targets on limit estimations that would result in an acceptable level of model certainty.

Disciplinarians charged with limit identification can use these precision targets to determine the level of refinement required for their analysis.

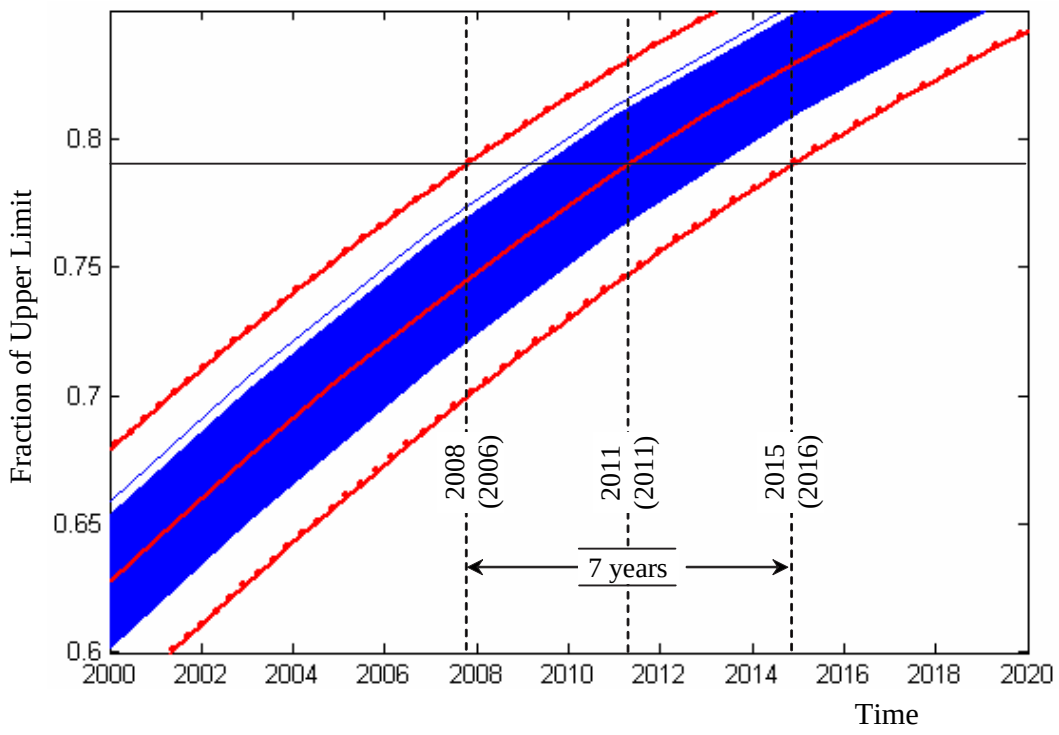

Figure 70: Likely Dates of Achieving the Point of Diminishing Returns

8.7 Setting Program Goals

Assessment of the turbofan architecture has to this point largely been confined to a consideration of the composite model describing the growth of the technology as a whole. The remainder of this demonstration focuses on assessing combinations of specific attribute capability levels and the dates at which they are expected to be introduced. This is accomplished by thoroughly investigating the turbofan MDGM as quantified by SFC and thrust and shown here in general form as Equation 120. In this form the MDGM provides the expected capability level of thrust. This equation can just as easily take the form of Equation 121 or Equation 122. In Equation 121 thrust is dependent on SFC and year, and in Equation 122 date is dependent on SFC

and thrust. The ability to visualize each of these forms simultaneously is best for assessment and goal setting and is illustrated by the prediction profiler of the JMP statistical software package, a snapshot of which is shown here as Figure 71 [89].

$$y_{sfc} = \frac{L_{sfc} - y_{o,sfc}}{1 + e^{-b_{sfc}\left(t - a + \frac{1}{b_{fg}} ln\left(\frac{L_{fg} - y_{fg}}{y_{fg} - y_{o,fg}}\right)\right)}} + y_{o,sfc} \tag{120}$$

$$y_{fg} = \frac{L_{fg} - y_{o,fg}}{1 + e^{-b_{fg}\left(t - a + \frac{1}{b_{sfc}} ln\left(\frac{L_{sfc} - y_{sfc}}{y_{sfc} - y_{o,sfc}}\right)\right)}} + y_{o,fg} \tag{121}$$

$$t = a - \frac{1}{b_{sfc}} ln\left(\frac{L_{sfc} - y_{sfc}}{y_{sfc} - y_{o,sfc}}\right) - \frac{1}{b_{fg}} ln\left(\frac{L_{fg} - y_{fg}}{y_{fg} - y_{o,fg}}\right) \tag{122}$$

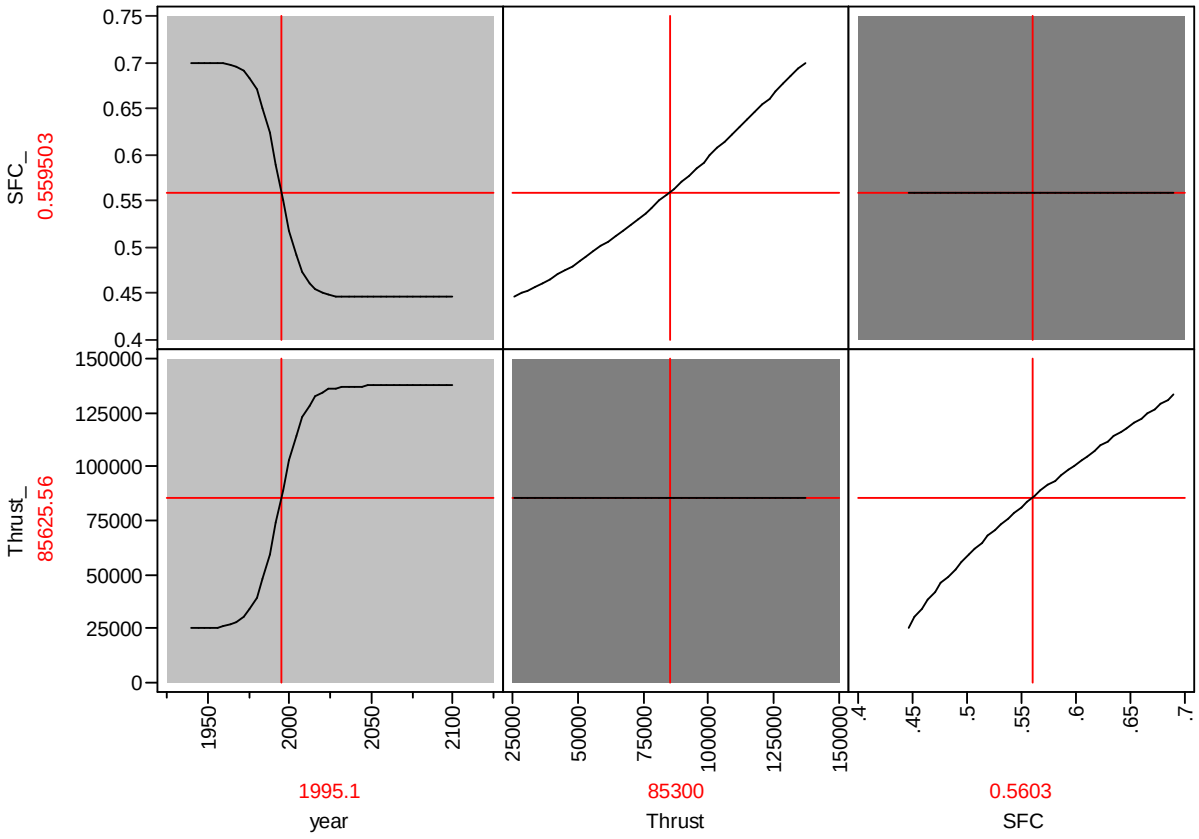

Figure 71: Multidimensional Growth Model Visualization Environment (1995)

The curve parameters used for this rendering are those previously calculated for the mean composite curve resulting from the uniform limit distributions. Recall from

Chapter 7 that each row of the prediction profiler completely describes the MDGM; thus, the top row of plots corresponds to Equation 121 and forecasts SFC (indicated by the horizontal hairline) based on settings of year and thrust (indicated by the vertical hairline), and the bottom row of plots corresponds to Equation 121 and predicts thrust according to settings of year and SFC. Also, recall that the first column of plots in Figure 71 correspond the S-curves for both SFC and thrust and the remaining columns are the technology frontiers between the attribute pairs corresponding to the grid location.

Note that the settings in Figure 71 for year, SFC, and thrust correspond to those of the GE-90-85B, which was introduced in 1995 with a thrust of 85,000 lb_f and SFC of 0.560 lb_m/lb_f-hr. Also note that although each row can independently represent the MDGM, they have been set so as to be in agreement for Figure 71. The S-curves of the first column indicate that those capability levels correspond to roughly 50 percent of the normalized limits for each SFC and thrust. This environment is used to evaluate what could have been achieved for SFC and for thrust had design preferences been different, although the environment is most useful for forecasting the levels of SFC and thrust that are expected in future years.

Figure 72 illustrates the impact of advancing the date by a decade while leaving settings for SFC and thrust unchanged. In this figure, the model represented by the top row indicates that turbofan engines introduced in 2016 with the same thrust as the GE-90-85B (85,000 lb_f) should be capable of achieving an SFC as low as 0.455 lb_m/lb_f-hr, and the model represented by the bottom row indicates that an engine introduced in that same year with an SFC comparable to that of the GE-90-85B should reach a thrust level of nearly 132,000 lb_f. Note that each of these instances results in systems that heavily favor either thrust or SFC as illustrated by each frontier. Figure 73 also shows the expected state of turbofan technology in 2016 but provides combinations of thrust and SFC capability levels representative of a more

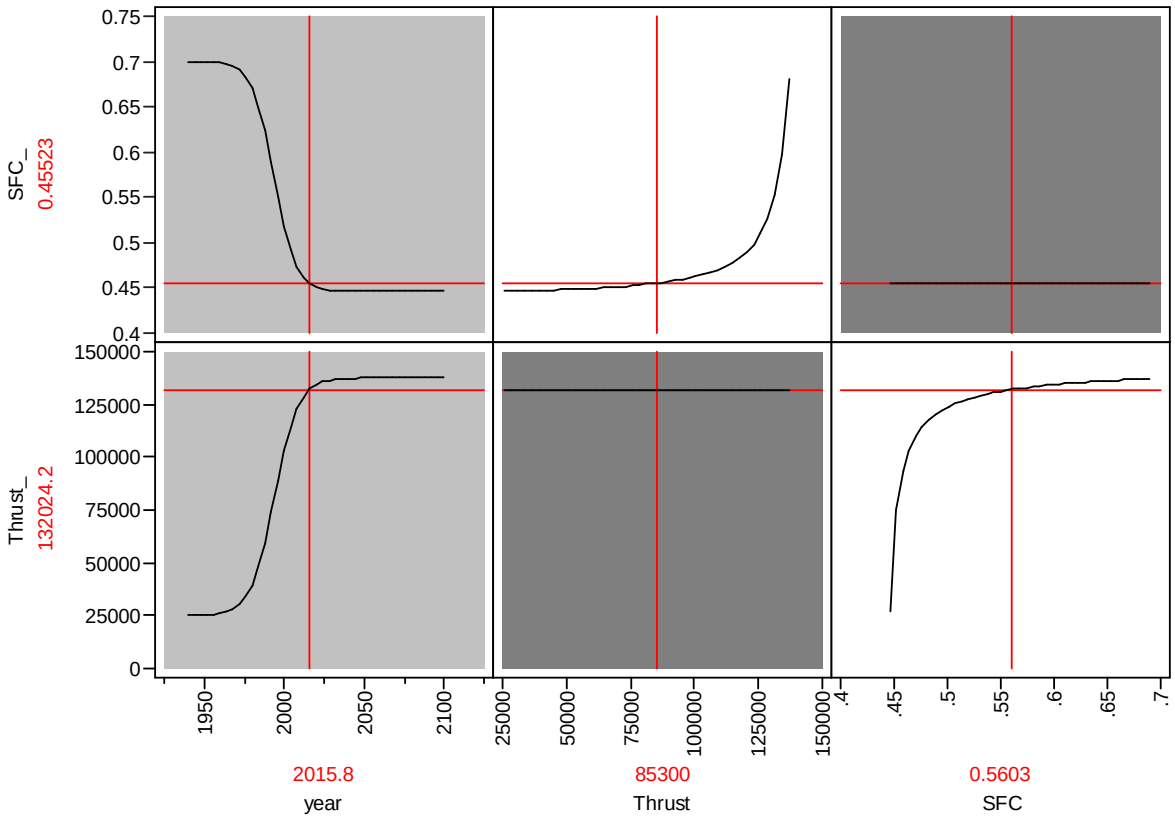

Figure 72: Multidimensional Growth Model Visualization Environment (2016)

balanced system. These forecasts indicate that a turbofan introduced in 2016 should also be capable of achieving thrust levels of approximately 120,000 lb_f with an SFC of 0.49 lb_m/lb_f-hr. Compare this to the performance of the GE-90-85B introduced in 1995, which has an SFC of 0.560 lb_m/lb_f-hr and a thrust of 85,000 lb_f.

Also note that the forecasts presented in Figures 72 and 73 assume that there are no trade-offs between SFC or thrust and any other system attribute. The MDGM only captures trade-offs and expected growth of these attributes included in the model. In other words, the resulting forecasts are based on the assumption that previous levels of investment to advance thrust and SFC will be maintained. If, for instance, resources were diverted from further advancement of SFC and thrust in order to improve noise

or emissions, the forecasted levels of SFC and thrust based on this model would be predicted levels of advancement.

Recall that Figures 71 to 73 are only snapshots of a dynamic environment that instantaneously updates the year, SFC, and thrust and that it can be used to play any number of "what-if" games in realtime. They provide the capability levels expected for further introduction dates; however, no consideration has been given to the physical or hardware changes necessary to achieve these levels of capability. The following section addresses this issue.

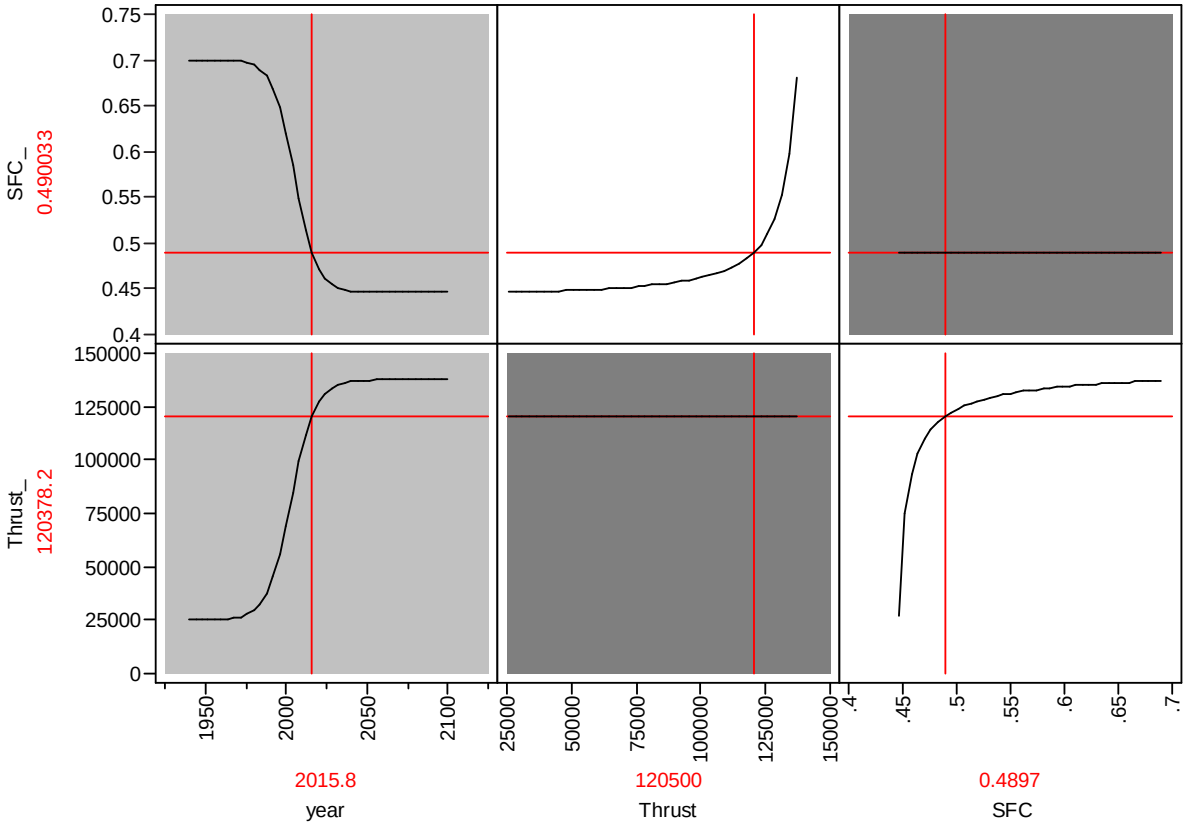

Figure 73: Multidimensional Growth Model Visualization Environment (2016)

8.8 Necessary Hardware Changes

The Technology Impact Forecasting method (TIF) was developed for the explicit purpose of identifying specific disciplinary changes that could be incorporated into a baseline system in order to encourage optimum progress in development and the realization of specified system-level targets [56, 57]. TIF identifies the disciplinary changes that must be made to a baseline system for it to evolve. As noted in Chapter 7, TIF has been employed in numerous studies to identify technological improvements to a broad range of baseline systems [56, 57, 58, 90, 91, 92, 93]. One such study implemented a form of TIF to analyze the the impacts of 29 technologies on a baseline turbofan engine comparable to the GE-90-85B [104]. Resulting from the study were metamodels in the form of response surface equations mapping the impact of sixty technology metrics, or disciplinary parameters, to the variability in numerous system attributes, including SFC and thrust. This research was able to leverage these metamodels. The response surface equations for SFC and thrust—as dependent on fan efficiency (Fan Eff), fan pressure limits (FPR), high-pressure compressor efficiency (HPC Eff), low-pressure turbine efficiency (LPT Eff), and thrust-to-weight ratio (TWR) of the aircraft into which the engine is installed—are illustrated in Figure 74.

FPR and each efficiency parameter directly influence the engine cycle, which results in changes to both SFC and thrust. TWR effectively scales the engine as required by the aircraft and as such, most directly influences engine thrust. In addition to illustrating the mapping *between* each disciplinary metric *and* SFC and thrust, Figure 74 also illustrates the sensitivity of introduction date to the variability of each disciplinary metric. This mapping is created indirectly through the resulting performance levels for each SFC and thrust. The MDGM forecasts the introduction date at which specified levels of SFC and thrust are expected to be achieved, which themselves, are predicted based on the settings of the disciplinary metrics. Each disciplinary metric

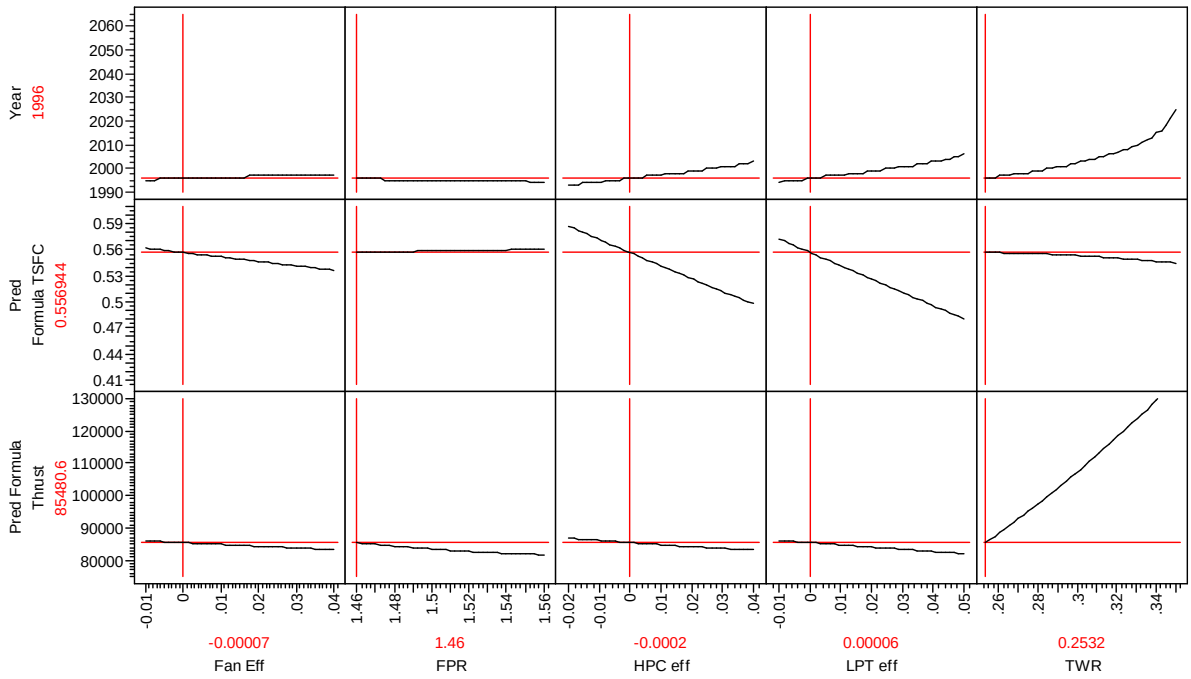

Figure 74: Sensitivity of Introduction Date to Disciplinary Parameters (1996)

in Figure 74 is set to its baseline value, which results in SFC and thrust levels comparable to that of the GE-90-85B. Note that the forecasted introduction date of 1996 is one year after that of the GE-90-85B. Now consider the forecasted levels of SFC and thrust illustrated in Figure 73 for the introduction year of 2016. The expected thrust is approximately 120,000 lb_f, and expected SFC is 0.49 $\text{lb}_\text{m}/\text{lb}_\text{f}$-hr. Figures 75 and 76 illustrate two different settings of disciplinary parameters that result in these levels of performance for the introduction year of 2016.

This suggests that there are multiple combinations of disciplinary changes that can result in the specified performance levels. TIF is formulated specifically to identify the best combinations of technological changes to achieve target levels of performance. The technology assessment procedure is constructed specifically both to assess a technology's rate of growth and to set reasonable performance targets.

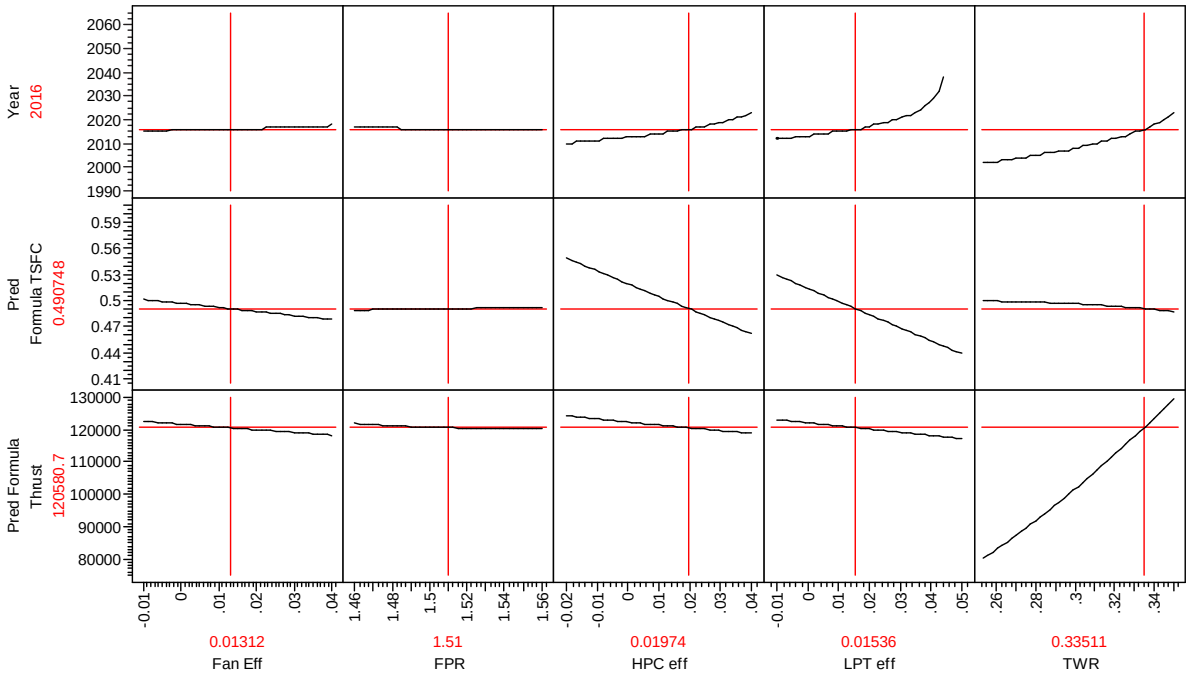

Figure 75: Sensitivity of Introduction Date to Disciplinary Parameters (2016)

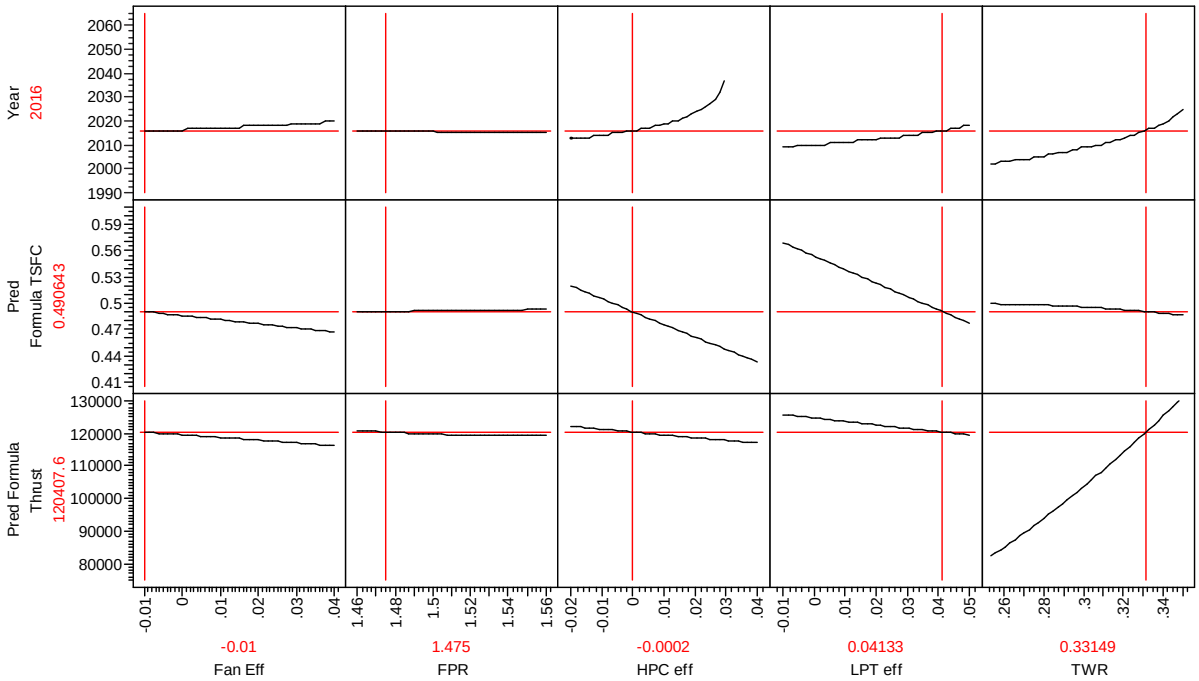

Figure 76: Sensitivity of Introduction Date to Disciplinary Parameters (2016)

8.9 Summary

This chapter applied the assessment procedure formulated in this research to high-thrust turbofan technology as defined by six dimensions of capability: specific fuel consumption, thrust, thrust to weight, noise, emissions, and reliability. Reliability, however, was removed from the assessment due to insufficient data concerning its past trends, and thrust to weight was also removed from the assessment because of its strong correlation with thrust. Finally, noise and emissions were removed from the model due to low significance, leaving SFC and thrust. That noise and emissions appear insignificant is representative of past design preferences which have favored SFC and thrust over environmental considerations. As new engines are introduced that have environmental considerations as a primary design driver, noise and emissions will increase in their significance to the growth model.

Rather than attempting to precisely define upper limits for SFC and thrust, very basic physical analyses were employed to establish broad distributions to demonstrate the impact of limit uncertainty on the resulting model. Even with such a large degree of uncertainty, resulting forecasts provided valuable insight into the current state of the art relative to both upper limits and the point of diminishing returns. More resolved limit distributions were also assessed simulating investment devoted to limit identification. Evidence from this assessment indicates that turbofan technology, as quantified by SFC and thrust, is approaching the point of diminishing returns, and as a result, each additional improvement to thrust and SFC will soon only result from increasingly more investment—all other attributes being constant. This demonstration has illustrated the robust nature of the proposed procedure to formulating a multi-dimensional forecasting model under circumstances of limited data and considerably uncertain limits.

CHAPTER IX

CONCLUSIONS

Developing technology systems requires all manner of investment—engineering talent, prototypes, test facilities, and more. Even for simple design problems the investment can be substantial; for technology systems, the development costs can be staggering. Moreover, investment does not ensure significant technological advance. No wonder decision-makers want to use caution in launching a new technology development program or extending an existing one. On the other hand, to halt attempted development may mean abandoning momentum and the chance to squeeze more improvement from the results of previous investment. Impressions that there is no more work to be done may be accurate, but they may be followed by many years of productive work and successful evolution of a technology architecture which was the case with the development of the turbine engine. For many reasons, a suitable forecasting tool is desirable.

Several forecasting and assessment tools have been available. There are technology growth models, or S-curves, and they can effectively model and forecast the development of a single attribute. But they have not addressed multiple attributes of a single technology. And there have been technology frontiers that can model multiple attributes of a single system, but can not forecast the expected improvements to those attributes. As an alternative one could choose scoring models, but these have been even less helpful because they collapse all measures of merit into a single composite measure eliminating the possibility to assess tradeoffs between attributes.

These modeling tools have use and have provided a starting point for this research, but they leave much more to be desired. In short, there has been no multidimensional

growth model (MDGM), and practitioners have been obliged to choose between forecasting a single attribute or composite measure and assessing multiple attributes at a single point in time.

The contributions to the field of technology assessment and forecasting made by this research will be outlined and discussed in Section 9.1. Limitations to these contributions and considerations for their usage are discussed in Section 9.2. Also provided in Section 9.2 are recommendations for further research.

9.1 Summary of Contributions

During careful examination of the existing assessment and forecasting tools in the search for approaches to transform one or another into a multidimensional forecasting tool, a very useful correlation came to light. The S-curve and technology frontier models relate in a way that allow them to be combined and used to assess and forecast multidimensional technology architectures. More study revealed that the challenge of identifying upper limits can be managed in a way that allows for meaningful assessments and forecasts given bound estimates. Through the manipulation and extension of the relevant equations multidimensional growth models emerged, which can supply prediction and forecast of multiple technology attributes with respect to physical limits. In addition, a systematic procedure was formulated to generate and interpret MDGMs for the assessment and forecast of technology attributes. This section revisits each of the contributions to the field of technology assessment and forecasting made by this research relative to the proposed hypotheses and research questions.

9.1.1 Hypothesis A: Multidimensional Growth Model Formulation

Hypothesis A *The proven success of technology growth models for the forecast of a single attribute can be extended to also accurately model multiple system attributes by precisely defining their mathematical significance to technology frontiers.*

Investigation of the mathematical significance between unidimensional growth models and technology frontiers did in fact lead to the formulation of multidimensional growth models that are able to take the form of interdependent technology S-curves, interdependent technology frontiers, or a composite measure of overall system maturity. These models are founded on **Assertion 1** (Section 5.1), which states that each system attribute evolves towards its respective limit according to an S-curve, given that capability levels for all remaining system attributes are maintained. The proposed formulation of multidimensional growth models allows for their derivation based on any unidimensional growth model, which provides the flexibility to assess a broad range of developmental growth patterns. This 'marriage' between unidimensinal growth models and multidimensional technology frontiers resulting in multidimensional growth models has proven an effective basis for the assessment and forecast of multiple system attributes relative to their respective upper limits. In addition to the above assertion, two assumptions were required for the formulation of multidimensional growth models:

1. Engineering effort must remain constant over time; both willingness and resources must exist to further advance one or more dimensions of capability within the model.

2. The limit of each metric within the multidimensional growth model must be constant regardless of settings for the remaining metrics.

Additionally, this formulation of multidimensional growth models requires that each dimension of capability included in the model be independent. These assumptions and this requirement place some limitations on the range of applicability of multidimensional growth models. Discussion later in this chapter will address potential solutions and alternatives that might avert these limitations.

The capability to simultaneously model the growth and interaction of multiple system attributes over time as they approach their respective limits has until now been unavailable. The formulation of multidimensional growth models which provide this capability is a significant contribution to the field of technology assessment and forecasting.

9.1.2 Hypotheses B and C: Limit Identification Methods

Hypothesis B *Knowledge of attribute upper limits for multi-attribute technologies can be identified by both physics-based approaches and by regressing limit-dependent growth models against available historical data.*

Hypothesis C *Analysis methods founded on exergy and work potential provide a suitable framework for the identification of upper limits to select attributes of energy-based systems.*

While each of these hypotheses was shown to be true given specific circumstances, this research has also shown that in many cases, neither regression-based approaches nor physics-based approaches—founded on exergy or work potential or otherwise—provide the desired rapid and accurate solution to upper limit identification.

The regression-based approach proved to be rapid, although the accuracy is highly dependent on the size of the historical database, the amount of error within that data, the total growth curve spanned by the data, and the number of dimensions included in the model. A method was formulated that enables an analyst to estimate the expected uncertainty on regressed limits based on these dependencies. An analyst can then assess if the expected uncertainty is within an acceptable range.

The accuracy of a physics-based approach is difficult to test. Even if forecasters assume that a physics-based approach can produce accurate upper limits, identifying limits in this manner is neither speedy nor inexpensive because of the highly complex

nature of multi-attribute technologies. Physics-based approaches require the collaboration of a team of interdisciplinary experts whether exergy and work potential analysis methods are employed or not. The time required, however, can be reduced by choosing to bound the limit between two extremes rather than attempting to define it precisely.

Upper limit estimations were incorporated into the multidimensional growth model in the form of distributions which attempt to quantify the uncertainty of limit estimations. This approach to incorporating knowledge of the upper limit into the MDGM has proven very effective. Even given a broad limit distribution (i.e. high limit uncertainty), meaningful insights can result from the technology assessment procedure, both concerning the technology's maturity and the level of certainty required for limit estimations in order to be confident enough in assessment results to base strategic decisions on them.

This research explored two general approaches to upper limit identification, which result in the following contributions to the field of technology assessment and forecasting:

- An existing method for quantifying the expected uncertainty of regression-based limit predictions for unidimensional growth models was refuted and reformulated.
- A method was formulated for estimating the expected uncertainty of regression-based limit predictions for multidimensional growth models.
- A method for quantifying the impact of limit uncertainty on multidimensional growth models was formulated.

9.1.3 Research Questions: Assessment Procedure

The proposed assessment procedure provides a systematic approach for formulating and analyzing a multidimensional growth model that describes the development pattern of a specific technology. This procedure provides answers to each of the following research questions:

RQ1 *What is the current state of the art as defined by achievable combinations of attribute capabilities?*

The answer to this question is addressed in Section 7.5.1. The composite measure formulated in this research is defined relative to the capabilities of each attribute, which is used to assess the state of the art of the technology as a whole relative to a normalized upper limit.

RQ2 *What is the technology potential of any one attribute relative to specified levels of the remaining attributes?*

The visualization environment of the multidimensional growth model presented in Section 7.5.2 enables an analyst to assess the potential for improvement of any one attribute relative to capability levels specified for all others.

RQ3 *Has the point of diminishing returns been reached for any of the system attributes?*

The answer to this question is addressed in Section 7.5.1 wherein the current state of the art as defined by a fraction of the normalized upper limit can be directly compared to the limit fraction at which the point of diminishing returns occurs. This section also provides an approach to forecast the date at which the point of diminishing returns is expected to occur within a specified level of certainty.

RQ4 *What is the forecasted improvement for each attribute relative to the remaining attributes?*

The visualization environment of the multidimensional growth model presented in Section 7.5.2 also enables an analyst to forecast the expected improvement of any one attribute relative to the capability levels specified for all other attributes.

The nature of the multidimensional growth model is that once formulated for a specific technology, the answers to these questions are easily obtained. Answers to questions concerning technology potential relative to physical limits and the point of diminishing returns were once confined to a single dimension of technical capability. This research has contributed the capacity to address these questions in multiple dimensions of technical capability.

There are, however, several limitations inherent to multidimensional growth models that surfaced during the proof of concept demonstration in Chapter 8. These considerations will now be discussed.

9.2 Recommendations and Future Work

Multidimensional growth models and assessment procedure formulated in this research provide decision-makers with quantitative information for the assessment and forecast of multiple technology attributes. The multidimensional growth model is a revolutionary addition to the to field of technology assessment and forecasting, and at the risk of making a qualitative forecast, it seems reasonable to say there is potential for further evolution. The following discussion provides final insights and areas for further research and development.

9.2.1 Usage Considerations

Before the discussion turns to exploring areas for further research, consider both the utility and limitations of the technology assessment and forecasting procedure formulated in this research. Note that conclusions resulting from a technology assessment only apply to that specific set of attributes retained in the multidimensional growth model. Nothing can be said of other system attributes not included in the model. Furthermore, conclusions resulting from the assessment apply only to that technology architecture specified during the problem definition. Consequently, the problem definition, wherein the technology architecture system attributes are identified, is exceptionally important to the interpretation of the resulting assessment.

Consider the turbofan demonstration of the previous chapter. The technology architecture was defined rather broadly, including comprising all turbofan engines with a thrust rating greater than 25,000 lb_f and with a bypass ratio greater than four. This macroscopic assessment of turbofan technology resulted in only two significant dimensions of capability: thrust and specific fuel consumption. The limit for each of these attributes was estimated based on the one contingency that engine size was constrained by its underwing placement. This very broad problem definition and the corresponding limit estimates lead to a macroscopic turbofan assessment providing very general results concerning the productivity of engineering effort devoted to the further improvement of thrust or specific fuel consumption. The formulation of multidimensional growth models proposed in this research seems better suited for microscopic assessments wherein the technology architecture is very precisely defined. The resulting forecasts are contingent on specified limits and are only applicable over a specified time period. This form of contingent forecasting can be used to assess any number of possible technology development scenarios that could unfold in years to come.

Possibly the greatest limitation to the utility of multidimensional growth models for the assessment of technology architectures is the requirement inherent to the model that all dimensions of capability included must be independent. As illustrated in the turbofan demonstration most attributes of a highly complex system are likely to be moderately correlated. As the multidimensional growth model is currently formulated, this correlation can lead to error in technology assessment and forecasting. Consequently, possibly the most important area for further research is eliminating the requirement that technology attributes be independent. One potential solution to this limitation is principal component analysis wherein a set of identified metrics can be transformed or reduced to an independent set of capability dimensions [105].

9.2.2 Multidimensional Growth Model Formulation

The following insights and areas for further research are directly related to the formulation of the multidimensional growth model.

Multidimensional growth models are formulated based on the independent parameter of time. That is, each attribute is assumed to advance through time according to an S-curve. As discussed in this research, engineering effort or research and development investment are more appropriate independent parameters. The transformation required to replace time by either of these independent parameters is quite simple, although acquiring the necessary data for engineering effort or research and development investment is inhibitive. An approach is required to obtain this information directly through consultation with technology development entities or indirectly by analyzing correlated metrics—possibly government expenditures, industry strength, gross domestic product, and the like. Without this element, forecasts based on growth models, whether unidimensional or multidimensional, are relative to past levels of engineering effort. Thus changes to engineering effort void these forecasts unless the model can be updated to account for the relative change in engineering effort.

Further research can also be devoted to MDGMs. As formulated, each attribute of the subject technology must be modeled by the same unidimensional growth model. Is it possible that the development of two attributes of the same technology could be described by different growth models? Maybe one attribute might advance according to a Gompertz curve, while the other according to a Logistic. Can two or more disparate unidimensional growth models be formulated into a single, multidimensional growth model? Because the MDGM is formulated as a summation of the inverse of unidimensional growth models this prospect seems very likely. The difficulty which requires additional research is identifying the appropriate or true unidimensional growth model for each attribute of a complex system. The task of identifying the appropriate unidimensional growth model for even a single-dimensional technology is an area of ongoing research. The added complexity of multiple dimensions further complicates this task increasing the scope of this ongoing research. One potential solution to this issue might be a formulation of multidimensional growth models based on the Lotka-Volterra equations that have been used to date to capture the competition between technology alternatives [14]. It may be possible to form a multidimensional growth model within which the Lotka-Volterra equations are used to model the competition between dimensions of capability within a system architecture.

The formulation of MDGMs on the basis of relative unidimensional growth models invites further development. This study has shown that it is possible to develop a MDGM based on unidimensional relative growth models, but the computational intensity of solving for the high number of curve parameters in a multi-modal space quickly becomes inhibitive as the number of system attributes increases. Alternative regression techniques should be further explored to enable these powerful forecasting models to be employed practically in multiple dimensions.

The last point of further research related to the formulation of the multidimensional growth model concerns the overall measure of performance as defined by the

composite growth model. As currently defined, the composite growth model quantifies the limit fraction that can be simultaneously achieved by all attributes at a specified point in time. Consequently, the starting point of the composite curve corresponds to a system with all attributes also at their starting points. In some cases this system may actually exist. The first system in the technology architecture may very well perform the worst in all dimensions of capability. Other times, however, this condition, that all attributes must be at their lowest values, may correspond to a negative ideal system rather than an actual system. If this latter condition is the case, then the starting point of the composite curve should actually be higher than that defined by all attributes being at their lowest value. The degree to which this assumption is an error will affect both the predicted and forecasted composite measure of growth. In similar manner, the upper limit to the composite model is normalized on the basis that each attribute has achieved its respective limit. This too may represent an ideal situation that cannot be realized.

In the case of the composite curve starting point, this is simply a matter of definition, and research should be devoted to appropriately defining this parameter for any particular technology assessment procedure. In the case of the upper limit, however, this requires knowledge concerning the interaction and interdependence between attribute upper limits. This interdependence would also have to result from the same approach employed for limit identification. Physics-based approaches or possibly, with further research, regression-based approaches could be formulated that would also capture the interdependence between limit estimates. In either case, the ideal result would be a joint probability distribution of attribute limits that can be integrated seamlessly into the assessment procedure proposed by this study.

9.2.3 Limit Identification: Investigation and Extension

The primary area for further research in the area of limit identification is the development of a formal approach to guide the interaction between a broad group of disciplinary experts in order to more rapidly establish upper limit estimations with an acceptable degree of uncertainty. The knowledge base required to identify the limits of a complex system is both too broad and too detailed to focus on the development of a generalized physics-based approach. Research devoted to coordinating the wealth of knowledge available from disciplinarians would be more effective and in the end provide a more valuable contribution to assessment forecasting by means of multidimensional growth models.

Another area for further research, to which the previous section alludes, pertains to the quantification of interdependence between multiple attribute limits of the same system. Potential may exist to extend regression-based techniques to quantify this interdependency, but more likely physics-based approaches will be required to handle this task. This potential for limit interdependence must be formulated into the approach described above for coordinating the efforts of disciplinary experts.

9.2.4 Assessment Procedure Formulation

Three primary areas for further research have been identified relating to the assessment procedure and are discussed below.

Data reduction. A systematic technique is desired to reduce an available historical database to only those systems representing the SoA for their respective dates of introduction. An existing technique that might be modified for this purpose is data envelopment analysis, also known as DEA. Data envelopment analysis establishes a frontier not by fitting a function to the available data but, as the name suggests, by establishing an envelope around the available data [54, 55]. It is capable of analyzing data in multiple dimensions of capability and could possibly be formulated to step

through a historical database removing systems introduced at a later date which fall within the previously established envelope. Each new point in the database should extend the previously defined envelope.

Insignificant attributes. The cause for an attribute being classified as insignificant during the regression should be explored further. What exactly is the interpretation of an attribute removed from the model due to insignificance? If an attribute is in fact insignificant, then the remaining metrics do in actuality quantify the overall state of the art; however, if an eliminated attribute only appears insignificant because there is insufficient data, then the reduced model is incomplete. For instance, although noise and emissions are of significant importance to turbofan engine design today, they have in the past taken a back seat to thrust and SFC and, because of this are not proportionately represented in the historical database. Consequently, metric significance is a function of design preference and may vary over the development of a technology architecture. If preference for a particular metric is not represented in the historical data, it will not appear as significant to the overall model. These considerations should be explored further and the necessary measures taken to appropriately interpret resulting models.

The point of diminishing returns. Achieving or surpassing the point of diminishing returns does not signify that there is no economic value to further advancing a technology towards its upper limit. The decision to continue to advance a technology involves socio-economic considerations not addressed by this research, though results from this research provide a necessary element required to make that decision. This research provides the capability to assess the increase in investment required to achieve each additional unit of technical capability. Only by comparing this increased investment per incremental improvement to the economic benefit resulting from that improvement will it be possible to make the informed decision regarding whether to continue or cease development of a technology. Further research is required to forecast

the economic value of an additional unit of improvement and explore the appropriate stage at which to halt development and invest in a revolutionary technology.

9.3 Closing

The objective of this research has been to formulate an approach to assess and forecast the maturity of technologies that have multiple objectives relative to their upper limits. Resulting from this approach are the models necessary to determine the availability for further improvement within a technology's respective architecture. Achieving this objective has required formulating a revolutionary multidimensional forecasting model, thoroughly investigating and extending existing limit estimation techniques, and formulating a systematic approach to technology maturity assessment. This research is a first step into the field of multidimensional growth models which has proven, even at this stage, to be a valuable tool for technology maturity assessment, although with further refinement, assessment techniques founded on multidimensional growth models can be invaluable decision making tools.

APPENDIX A

Table 31: Innovation Taxonomy: Technology descriptors found throughout literature that are used to classify the relative newness of technological innovations

adaptation	[106]	new parts	[17]
adoption	[107]	new products	[17]
architectural	[108, 109, 110]	new user	[17]
breakthrough	[110, 111]	niche creation	[109]
continuous	[112, 113]	normal	[16]
discontinuous	[112, 113]	original	[114]
evolutionary	[20, 115]	pioneering	[106]
evolutionary market	[115]	radically new	[116]
evolutionary technical	[115]	really new	[117, 118]
disruptive	[18]	reformulated	[17, 114]
fusion	[110]	regular	[108]
high innovativeness	[119]	reinnovations	[120]
imitative	[106]	remerchandising	[17]
innovations	[120]	reorientations	[121]
instrumental	[122]	revolutionary	[20, 108]
low innovativeness	[119]	routine	[123]
major	[124]	sustaining	[18]
market breakthrough	[125]	systematic	[124]
minor	[124]	technical breakthrough	[125]
moderate innovativeness	[119]	transformational	[16]
modular	[108]	transitional	[16]
new customers	[17]	true	[107]
new generation	[116]	ultimate	[122]
new improvements	[17]	unrecorded	[124]
new market	[17]	variations	[121]
radical	[19, 108, 115, 123, 124, 125, 126, 127, 128, 129, 130]		
incremental	[19, 108, 110, 111, 115, 116, 117, 118] [124, 125, 126, 127, 128, 129, 130]		

APPENDIX B

There are five general steps to the creation of a multidimensional growth model starting from a specified S-curve equation, $f(t)$. These five steps are as follows:

1. Identify the domain of the s-shape within $f(t)$; $[t_A, t_B]$.
2. Shift and scale the equation such that the range of the S-shaped segment is bound between y_o and L.
3. Solve for t and expand to accommodate multiple technology driven attributes.
4. Eliminate any redundant variables resulting from the previous step.
5. Insert into the general growth model shown here as Equation 123

$$t = t_o + \sum_{i=1}^{n} (t_{S-curve}) \tag{123}$$

where $t_{S-curve}$ is the expression resulting from *Step 4*.

These steps will be conducted to create three multi-attribute maturation models based on the S-curves defined by Gompertz's equation, Von Bertalanffy's equation, and the expression $e^{a-(b/t)}$.

B.1 Gompertz's Equation

Step 1: The domain of the S-shaped segment of Gopmertz's equation, shown here as Equation 124, is $(-\infty, \infty)$.

$$y = Le^{-ae^{-bt}} \tag{124}$$

Step 2: Adjusting Gompertz equation such that it is bound between y_o and L over the domain of the S-shaped segment results in Equation 125.

$$y = (L - y_o)e^{-ae^{-bt}} + y_o \tag{125}$$

Step 3: Solving Equation 125 for t and expanding to accommodate additional attributes also defined by Gompertz's equation results in Equation 126.

$$t = \sum_{i=1}^{n} \frac{-1}{b_i} lnln\left(\left(\frac{L_i - y_{o,i}}{y_i - y_{o,i}}\right)\right)^{\frac{1}{a_i}} \tag{126}$$

Step 4: Eliminating redundant variables results in replacing attribute specific $a_i's$ with a single a that remains constant for all attributes, as shown in Equation 127.

$$t = \sum_{i=1}^{n} \frac{-1}{b_i} lnln\left(\left(\frac{L_i - y_{o,i}}{y_i - y_{o,i}}\right)\right)^{\frac{1}{a}} \tag{127}$$

Step 5: This time dependence is now inserted into the general SoA model resulting in Equation 128—the multidimensional growth model based on Gompertz's equation.

$$t = t_o + \sum_{i=1}^{n} \frac{-1}{b_i} lnln\left(\left(\frac{L_i - y_{o,i}}{y_i - y_{o,i}}\right)\right)^{\frac{1}{a}} \tag{128}$$

B.2 Von Bertalanffy's Equation

Step 1: The domain the of S-shaped segment of Von Bertalanffy's equation, shown here as Equation 129, is $(0, \infty)$.

$$y = (1 - ae^{-bt})^3 \tag{129}$$

Step 2: Adjusting Von Bertalanffy's equation such that it is bound between y_o and L over the domain of the S-shaped segment results in Equation 130.

$$y = (L - y_o)(1 - ae^{-bt})^3 + y_o \tag{130}$$

Step 3: Solving Equation 130 for t and expanding it to accommodate additional attributes also defined by Von Bertalanffy's equation results in Equation 131.

$$t = \sum_{i=1}^{n} \frac{-1}{b_i} ln\left(\frac{1}{a_i}\left(1 - \left(\frac{y_i - y_{o,i}}{L_i - y_{o,i}}\right)^{\frac{1}{3}}\right)\right) \tag{131}$$

Step 4: Eliminating redundant variables results in replacing attribute specific $a_i's$ with a single a that remains constant for all attributes, as shown in Equation 132.

$$t = \sum_{i=1}^{n} \frac{-1}{b_i} ln\Big(\frac{1}{a}\Big(1 - \Big(\frac{y_i - y_{o,i}}{L_i - y_{o,i}}\Big)^{\frac{1}{3}}\Big)\Big) \tag{132}$$

Step 5: This time dependence is now inserted into the general SoA model resulting in Equation 133—the multidimensional growth model based on Von Bertalanffy's equation.

$$t = t_o + \sum_{i=1}^{n} \frac{-1}{b_i} ln\Big(\frac{1}{a}\Big(1 - \Big(\frac{y_i - y_{o,i}}{L_i - y_{o,i}}\Big)^{\frac{1}{3}}\Big)\Big) \tag{133}$$

B.3 S-curve Expression $e^{a-(b/t)}$

Step 1: The domain of the S-shaped segment of $e^{a-(b/t)}$, shown here as Equation 134, is $(0, \infty)$.

$$y = e^{a-(b/t)} \tag{134}$$

Step 2: Adjusting $e^{a-(b/t)}$ such that it is bound between y_o and L over the domain of the S-shaped segment results in Equation 135.

$$y = (L - y_o)(e^{-b/t}) + y_o \tag{135}$$

Step 3: Solving Equation 135 for t and expanding to accommodate additional attributes also defined by $e^{a-(b/t)}$ results in Equation 136.

$$t = \sum_{i=1}^{n} b_i\Big(ln\Big(\frac{L_i - y_{o,i}}{y_i - y_{o,i}}\Big)\Big)^{-1} + a \tag{136}$$

Step 4: There are no redundant regression variables requiring elimination.

Step 5: This time dependence is now inserted into the general SoA model resulting in Equation 137—the multidimensional growth model based on the S-curve expression $e^{a-(b/t)}$.

$$t = t_o + a + \sum_{i=1}^{n} b_i \Big(ln\big(\frac{L_i - y_{o,i}}{y_i - y_{o,i}}\big)\Big)^{-1} \tag{137}$$

APPENDIX C

```
*************************
***Turbofan Engine Model
*** (GE90-85B)
*** Written by: Travis Danner
*** June 22, 2006
*************************
************************* Constants *************************
gamma1 = 1.39977; %pre-combust ratio specific heats lbf-ft/lbm-R
cp1 = 0.2399379; %pre-combust specific heat BTU/lbm-R
gamma2 = 1.35339; %post-combust ratio specific heats lbf-ft/lbm-R
cp2 = R*gamma2/(gamma2 - 1)/778.17; %post-combust specific heat BTU/lbm-R
************************* Engine Specs *************************
faneff = 0.8991; lpceff = 0.8979;
hpceff = 0.8638; burneff = 0.999;
dpburner = 0.955; hpteff = 0.9182;
lpteff = 0.9263; nozeff = 0.9999;
bypass = 8.3396; T04 = 2958.81; %Rankine
LHV = 18400; %BTU/lbm
************************* Pressure Ratios *************************
FPR = 1.611; LPC = 1.385;
HPC = 20.677; OPR = FPR*LPC*HPC;
************************* Flight Conditions *************************
Alt = 35000; %ft
```

```
speedsound = 973.14; %ft/s
mach = 0.85;
Vinf = mach*speedsound;
pa = 3.45833; %psia
Ta = 394.08; %Rankine
T0a = Ta*(1 + (gamma1 - 1)/2*mach^2);
p0a = pa*(T0a/Ta)^(gamma1/(gamma1-1));
p02 = p0a; T02 = T0a;
************************* Fan ************************
p08 = p02*FPR;
T08 = T02 + T02/(faneff)*(FPR^((gamma1-1)/gamma1) - 1);
************************* LPC and HPC ************************
p03 = p08*LPC*HPC;
T03 = T08 + T08/(lpceff*hpceff)*((LPC*HPC)^((gamma1-1)/gamma1) - 1);
************************* Duct 1 ************************
dp1 = 0.97327; dT1 = 0.90922;
p03 = p03*dp1; T03 = T03*dT1;
************************* Burner ************************
f = ((T04/T03) - 1)/(LHV/cp1*burneff/T03 - (T04/T03));
p04 =p03*dpburner;
************************* HPT and LPT ************************
p05 = p04*(1 - (1/(faneff*lpceff*hpceff)*((FPR*LPC*HPC)^((gamma1-1)/gamma1) ...
- 1) + bypass/faneff*((p08/p0a)^((gamma1-1)/gamma1) - 1))/((1 + f)*...
(T04/T0a)*lpteff*hpteff*(cp2/cp1)))^(gamma2/(gamma2-1));
T05 = T04*(1 - lpteff*hpteff*(1 - (p05/p04)^((gamma2-1)/gamma2)));
************************* Nozzles ************************
exitVprim = (2*gamma2/(gamma2 - 1)*R*32.174*T05*nozeff*(1 - ...
```

(pa/p05)$^{((gamma2-1)/gamma2)}$))$^{0.5}$; % exit velocity primary stream

exitVsec = (2*gamma1/(gamma1 - 1)*R*32.174*T08*nozeff*(1 - ...

(pa/p05)$^{((gamma1-1)/gamma1)}$))$^{0.5}$; % exit velocity secondary stream

acousticVprim = (gamma2*R*T05*32.174)$^{0.5}$;

Mprim = exitVprim/acousticVprim;

Psprim = p05/(1 + (gamma2 - 1)/2*Mprim^2)$^{(gamma2/(gamma2-1))}$;

Tsprim = T05/(1 + (gamma2 - 1)/2*Mprim^2);

acousticVsec = (gamma1*R*T08*32.174)$^{0.5}$;

Msec = exitVsec/acousticVsec;

Pssec = p08/(1 + (gamma1 - 1)/2*Msec^2)$^{(gamma1/(gamma1-1))}$;

Tssec = T08/(1 + (gamma1 - 1)/2*Msec^2);

********** Thrust and SFC **********

massfprim = 155.74; %lbm/s

denprim = Psprim/R/Tsprim/12; %lbm/in3

areaprim = massfprim/exitVprim/denprim/12; %in2

Thrustprim = (1 + f)*exitVprim*massfprim/32.174 + (Psprim - pa)*areaprim;

massfsec = 1288.89; %lbm/s

densec = Pssec/R/Tssec/12; %lbm/in3

areasec = massfsec/exitVsec/densec/12; %in2

Thrustsec = (1 + f)*exitVsec*massfsec/32.174 + (Pssec - pa)*areasec;

Fgross = Thrustprim + Thrustsec;

Fn = Fgross - (massfsec + massfprim)*Vinf/32.174

TSFC = f*massfprim/Fn*3600

REFERENCES

[1] DeBecker, A. and Modis, T. Determination of Uncertainties in S-Curve Logistic Fits. *Technological Forecasting & Social Change*, 46:153–173, 1994.

[2] Ord-Hume. *Perpetual Motion: The History of an Obsession.* St. Martin's Press, New York, 1977.

[3] Foster, R. *Innovation: The Attacker's Advangtage.* Summit Books, New York, 1986.

[4] Stricker, J.M. A Strategic View of Trubine Engine Technolog–Progress and Future Opportunities. Technical report, Turbine Engine Technology Symposium, Dayton, OH, September 2004.

[5] Gahn, S.M. and Morris, R.W. Turbine Engine Technology. *http://www.pr.afrl.af.mil/divisions/prt/ihptet/ihptet_brochure.pdf*, 2004. [Date Accessed: June, 2006].

[6] Merriam-Webster. *Merriam-Webster's Collegiate Dictionary.* Merriam-Webster, Springfield, 2004.

[7] Merriam-Webster. *Webster's Seventh New Colligiate Dictionary.* G. & C. Merriam Co, Springfield, 1965.

[8] Twiss, B.C. *Forecasting for Technologists and Engineers.* Peter Peregrinus Ltd., London, UK, 1992.

[9] Cornwall, J. *Modern Capitalism: Its Growth and Transformation.* Martin Robertson, London, 1977.

[10] Rosenberg, N. *Inside the Black Box.* Cambridge University Press, Cambridge, 1982.

[11] Lowe, P. *The Management of Technology: Perception and Opportunities.* Champman Hall, New York, 1995.

[12] Martino, J.P. *Technological Forecasting for Decision Making.* North-Holland, New York, 1983.

[13] Martino, J.P. *Technological Forecasting for Decision Making.* North-Holland, New York, third edition, 1993.

[14] Porter, A.L., Roper, A.T., Mason, T.W., Rossini, F.A., and Banks, J. *Forecasting and Managment of Technology.* Wiley, New York, 1991.

[15] Garcia, R. and Calantone, R. A Critical Look at Technological Innovation Typology and Innovativeness Terminology: a literature review. *The Journal of Product Innovation Management*, 19:110–132, 2002.

[16] Kash, D.E. and Rycroft, R. Emerging Patterns of Complex Technological Innovation. *Technological Forecasting and Social Change*, 69:581–606, 2002.

[17] Johnson, S.C. and Jones, C. How to Organize for New Products. *Harvard Business Review*, pages 49–67, 1957.

[18] Christensen, C.M. *The Innovator's Dilemma: When New Technologies Cause Great Firms to Fail*. Harvard Business School Press, Boston, 1997.

[19] Kessler, E.H. and Chakrabarti, A.K. Speeding Up the Pace of New Product Development. *Journal of Product Innovation Management*, 16:240–51, 1999.

[20] Utterback, J.M. *Mastering the Dynamics of Innovation: How Companies Can Seize Opportunities in the Face of Technological Change*. Harvard Business School Press, Boston, 1994.

[21] Little, A.D. *The Strategic Management of Technology*. Harvard Business School Press, Cambridge, 1981.

[22] Lanford, H.W. *Technological Forecasting Methodologies*. American Management Association, USA, 1972.

[23] Makridakis, S., Wheelwright, S.C., and McGee, V.E. *Forecasting: Methods and Applications*. John Wiley & Sons, New York, second edition, 1983.

[24] National Research Council. Maintaining U.S. Leadership in Aeronautics: Breakthrough Technologies to Meet Future Air and Space Transportation Needs and Goals. Technical report, National Academy Press, Washington, D.C., 1998.

[25] Hartzell, R. MRL Assist. Technical report, National Center for Advanced Technologies, June 2005.

[26] Moorhouse, D.J. Detailed Definitions and Guidance for Application of Technology Readiness Levels. *Journal of Aircraft*, 39:190–192, 2001.

[27] Kirby, M.R. and Mavris, D.N. Forecasting Technology Uncertainty in Preliminary Aircraft Design. Technical Report 1999-01-5631, SAE, October 1999.

[28] Minning, C.P., Moynihan, P.I., and Stocky, J.F. Technology Readiness Levels for the New Millennium Program. Technical Report 0-7803-7651-X, IEE, 2003.

[29] Chadda, R.L. and Chitgopekar, S.S. A Generalization of the Logistic Curves and Long-Range Forecasts (1966-1991) of Residence Telephones. *The Bell Journal of Economics and Management Science*, 2:542–560, 1971.

[30] Mansfield, E. Technological Change and the Rate of Imitation. *Econometrica*, 26:741–766, 1968.

[31] Blackman, A.W., JR. A Mathematical Model for Trend Forecasts. *Technological Forecasting & Social Change*, 3:441–452, 1972.

[32] Blackman, A.W., JR. The Rate of Innovation in the Commercial Aircraft Jet Engine Market. *Technological Forecasting & Social Change*, 2:269–276, 1971.

[33] Young, P. and Ord, J.K. The Use of Discounted Least Squares Technological Forecasting. *Technological Forecasting & Social Change*, 28:263–274, 1985.

[34] Sharif, M.N. and Islam, M.N. The Weibull Distribution as a General Model for Forecasting Technological Change. *Technological Forecasting & Social Change*, 18:247–256, 1980.

[35] Bass, F.M. A New Product Growth Model for Consumer Durables. *Management Science*, 15:215–227, 1969.

[36] Heeler, R.M and Hustad, T.P. Problems in Predicting New Product Growth for Consumer Durables. *Management Science*, 26:1007–1020, 1980.

[37] Tigert, D. and Farivar, F. The Bass New Product Growth Model: A Sensitivity Analysis for a High Technology Product. *Journal of Marketing*, 45:81–90, 1981.

[38] Easingwood, C., Mahajan, V., and and Mueller, E. A Nonsymmetric Responding Logisitic Model for Forecasting Technological Substitution. *Technological Forecasting & Social Change*, 20:199–213, 1983.

[39] Easingwood, C.J. Product Life Cycle Patterns for New Industrial Products. *R&D Management*, 18:23–32, 1988.

[40] Harvey, A.C. Time Series Forecasting. *Journal of the Operational Research Society*, 35:641–646, 1984.

[41] Levenbach, H. and Reuter, B.E. Forecasting Trending Time Series with Relative Growth Rate Models. *Technometrics*, 18:261–272, 1976.

[42] Young, P. Technological Growth Curves, A Competition of Forecasting Models. *Technological Forecasting & Social Change*, 44:375–389, 1993.

[43] Thirring. *Energy for Man*. Indiana Univeristy Press, Bloomington, IN, 1958.

[44] Makridakis, S., Anderson, A., Carbone, R., Fildes, R., Hibon, M., Lewandowski, R., Newton, J., Parzen, E., and and Winkler, R. *The Forecasting Accuracy of Major Time Series Methods*. Wiley, New York, 1984.

[45] Fildes, R. An Evaluation of Bayesian Forecasting. *Technological Forecasting*, 2:137–150, 1983.

[46] Franses, P.H. A Method to Select Between Gompertz and Logistic Trend Curves. *Technological Forecasting & Social Change*, 46:45–50, 1994.

[47] Neter, Kutner, Nachtsheim, and Wasserman. *Applied Linear Statistical Models*. WCB/McGraw-Hill, New York, fourth edition, 1996.

[48] Jo, H.H and Parsaei, H.R. *Concurrent Engineering: Methodology and Applications*. Elsevier, New York, 1993.

[49] Hazelrigg, G.A. *Systems Engineering: An Approach to Information-Based Design*. Prentice Hall, 1996.

[50] Alexander, A.J. and Nelson, J.R. Measuring Technological Change: Aircraft Turbine Engines. *Technological Forecasting & Social Change*, 5:189–203, 1973.

[51] Dodson, E.N. A General Apporach to Measurement of the State of the Art and Technological Advance. *Technological Forecasting & Social Change*, 1:391–408, 1970.

[52] Dodson, E.N. Measurement of the State of the Art and Technological Advance. *Technological Forecasting & Social Change*, 27:129–146, 1985.

[53] Martino, J.P. Measurement of Technology Using Trade-off Surfaces. *Technological Forecasting & Social Change*, 27:147–160, 1985.

[54] Cooper, W.W., Seiford, L.M., and Tone, K. *Data Envelopment Analysis*. Kluwer Academic Publishers, Norwell, MA, 2000.

[55] Thanassoulis, E. *Introduction to the Theory and Application of Data Envelopment Analysis*. Kluwer Academic Publishers, Norwell, MA, 2001.

[56] Kirby, M.R. and Mavris, D.N. An Approach for the Intelligent Assessment of Future Technology Portfolios. Technical Report AIAA-2002-0515, AIAA, Reno, NV, January 2002.

[57] Kirby, Michelle. *A Methodology for Technology Identification, Evaluation, and Selection in Conceptual and Preliminary Aircraft Design*. PhD thesis, Georgia Institute of Technology, March 2001.

[58] Mavris, D.N., Mantis, G. and Kirby, M.R. Demonstration of a Probabilistic Technique for the Determination of Economic Viability. Technical Report AIAA-97-5585, AIAA, 1997.

[59] Kirby, M.R. and Mavris, D.N. A Technique for Selecting Emerging Technologies for a Fleet of Commercial Aircraft to Maximize R&D Investment. Technical Report 2001-01-3018, SAE, 2001.

[60] Meyers, R.H. and Montgomery, D.C. *Response Surface Methodology: Process and Product Optimization Using Designed Experiments*. Wiley & Sons, New York, 1995.

[61] Box, G.E.P. and Draper, N.R. *Empirical Model-Building and Response Surfaces.* Wiley & Sons, New York, 1987.

[62] Box, G.E.P., Hunter, W.G., and Hunter, J.S. *Statistics for Experimenters: An Introduction to Design, Data Analysis, and Model Building.* Wiley & Sons, New York, 1978.

[63] Mavris, D.N., Bandte, O., and Shrage, D.P. Application of Probabilistic Methods for the Determination of an Economically Robust HSCT Configuration. Technical Report AIAA-96-4090, AIAA, 1996.

[64] Mavris, D.N. and Kirby, M.R. Preliminary Assessment of the Economic Viability of a Family of Very Large Transport Configurations. Technical Report AIAA-96-5516, AIAA, 1996.

[65] Intel. Moore's Law: Raising the Bar. *http://www.intel.com/technology/mooreslaw/index.htm*, 2005. [Date Accessed: June, 2006].

[66] Martino, J.P. A Review of Selected Recent Advances in Technological Forecasting. *Technological Forecasting & Social Change*, 70:719–733, 2003.

[67] Hibbeeler, R.C. *Engineering Mechanics—Dynamics.* Prentice Hall, Inc, Englewood Cliffs, NJ, seventh edition, 1995.

[68] Moran, M.J. and Shapiro, H.N. *Fundamentals of Engineering Thermodynamics.* John Wiley & Sons, New York, third edition, 1995.

[69] Poincaré, H. *The Foundations of Science; Science and Hypothesis, The Value of Science, Science and Method.* authorized translations by George Bruce Halsted 1913.

[70] Shigley, J.E. *Mechanical Engineering Design.* McGraw-Hill, New York, fifth edition, 1989.

[71] Mattingly, J.D., Heiser, W.H., and Daley, D.H. *Aircraft Engine Design.* AIAA Educations Series. AIAA, New York, 1987.

[72] Anderson, John D. *Aircraft Performance and Design.* WCB McGraw-Hill, Boston, 1999.

[73] Roth, B.A. *A Theoretical Treatment of Technical Risk in Modern Propulsion System Design.* PhD thesis, Georgia Institute of Technology, March 2000.

[74] Bejan A. *Advanced Engineering Thermodynamics.* John Wiley & Sons, New York, second edition, 1997.

[75] Ahern, J.E. *The Exergy Method of Energy Systems Analysis.* John Wiley & Sons, New York, 1980.

[76] Roth, B.A., McClure, E.M., and Danner, T.W. Implementation of Engine Loss Analysis Methods in the Numerical Propulsion System Simulation. Technical Report GT2005-68202, ASME, Reno-Tahoe, NV, June 2005.

[77] Bejan, A. *Entropy Generation Through Heat and Fluid Flow*. Wiley, New York, 1982.

[78] Roth, B.A. A Comparison of Thermodynamic Loss Models Suitable for Gas Turbine Propulsion: Theory and Taxonomy. Joint Propulsion Converence AIAA2000-3714, AIAA/SAE/ASME/ASEE, Huntsville, AL, July 2000.

[79] Moran, M.J. *Availability Analysis: A Guide to Efficient Energy Use*. Prentice Hall, Englewood Cliffs, NJ, 1982.

[80] Riggins, D.W. Evaluation of Performance Loss Methods for High-Speed Engines and Engine Components. *Journal of Propulsion and Power*, 13(2):296–304, March 1997.

[81] Roth, B.A. A Work Transfer Perspective of Propulsion System Performance. Technical Report AIAA-2004-4079, AIAA, Ft. Lauderdale, FL, July 2004.

[82] Roth, B.A. Work Transfer Analysis of Turbojet and Turbofan Engines. Technical Report AIAA-2004-4077, AIAA, Ft. Lauderdale, FL, July 2004.

[83] Roth, B. and de Luise, J. Lost Thrust Methodology for Gas Turbine Engine Performance. ASME, June 2005.

[84] Hayter, A.J. *Probability and Statistics for Engineers and Scientists*. PWS Publishing Company, Boston, 1996.

[85] Golberg, M.A. and Cho, H.A. *Introduction to Regression Analysis*. Computational Mechanics, Billerica, MA, 2004.

[86] Gross, J. *Linear Regression*. Springer, New York, 2003.

[87] Ratkowsky, D.A. *Handbook of Nonlinear Regression Models*. M. Dekker, New York, 1990.

[88] Decisioneering. *Crystal Ball risk analysis software & consulting services.* http://www.decisioneering.com/, 2005. [Date Accessed: May, 2006].

[89] SAS Institute. *JMP Software - Data Analysis - Statistics - Six Sigma - DOE.* http://www.jmp.com/, 2005. [Date Accessed: March, 2005].

[90] Kirby, M.R. and Mavris, D.N. Forecasting the Impact of Technology Infusion on Subsonic Transport Affordability. Technical Report 985576, SAE, 1998.

[91] Mavris, D.N. and DeLaurentis, D.A. A Stochastic Design Approach for Aircraft Affordability. Technical Report 98-6.1.3, ICAS, 1998.

[92] Mavris, D.N., Baker, A.P., and Schrage, D.P. Development of a Methodology for the Determination of Technical Feasibility and Viability of Affordable Rotorcraft Systems. Technical report, American Helicopter Society, Washington, D.C., May 1998.

[93] Mavris, D.N., Soban, D.S., and Largent, M.C. An Application of a Technology Impact Forecasting (TIF) Method to an Uninhabited Combat Aerial Vehicle. Technical Report 1999-01-5633, SAE, 1999.

[94] Younossie, O., Arena, M.V., Moore, R.M., Lorell, M., Mason, J., and Graser, J.C. . *Military Jet Engine Acquistion*. Rand, Arlington, VA, 2002.

[95] Peter, J.S. . *The History of Aircraft Gas Turbine Engine Devleopement in the United States ... A Tradition of Excellence*. the International Gas Turbine Institute of The American Society of Mechanical Engineers, Atlanta, GA, 1999.

[96] Sawyer, J.W. *Gas Turbine Engineering Handbook*. Gas Turbine Publications, Stamford, Connecticut, 1966.

[97] Gunston, B. *Jane's Aero-Engines*. Jane's Information Group Inc, Alexandria, VA, 2002.

[98] International Civil Aviation Organization. ICAO Engine Exhaust Emissions DataBank. *http://www.caa.co.uk/*, 2005. [Date Accessed: October, 2005].

[99] Joselzon, A. Aircraft Noise. San Diego, February 2002. Airport Noise Symposium.

[100] Hubbard, H. *Aeroacoustics of Flight Vehicles: Theory and Practice*. Acoustic Society of America, 1994.

[101] Dowling, A.P. and Ffowcs Williams, J.E. *Sound and Sources of Sound*. John Wiley & Sons, New York, 1983.

[102] Hill, P.B. and Peterson, C.R. *Mechanics and Thermodynamics of Propulsion*. Addison-Wesley, Reading, MA, 1965.

[103] Ahuja, K.K. Jet Noise Scaling from Lighthill's Theory. *Journal of Sound and Vibration*, 29, 1973.

[104] Mavris, D.N., Kirby, M.R.,, and Tai, J. FY04 VISTA technology assessmnet. Final report, NASA Grant Number NNL04AD06T, Task Order NAS 3-00179, 2004. Technical report, Aerospace System Design Laboratory, Georgia Institute of Technology, Atlanta, GA.

[105] Kambhatla, N. Dimension Reduction by Local Principal Component Analysis. *Neural Computation*, 9:1493–1516, October 1997.

[106] Crawford, C.M. *New Products Management*. Richard D. Irwin, Boston, fourth edition, 1994.

[107] Maidique, M.A. and Zirger, B.J. A Study of Success, and Failure in Product Innovation: the case of the US electronics industry. *IEEE Transactions on Engineering Management*, EM-31(4):192–203, 1984.

[108] Henderson, R.M. and Clark, K.B. Architectural Innovation: The Reconfiguration of Existing Product Technologies, and the Failure of Established Firms. *Journal of Economics*, 35:9–30, 1990.

[109] Abernathy, W.J. and Clark, K.B. Innovation. Mapping the Winds of Creative Destruction. *Research Policy*, 14(1):3–22, 1985.

[110] Tidd, J. Development of Novel Products Through Intraorganizational, and Interorganizational Networks: The Case of Home Automation. *Journal of Product Innovation Management*, 12:307–22, 1995.

[111] Rice, M.P., O'Connor, G.C., Peters, L.S., and Morone, J.G. . Managing Discontinuous Innovation. *Research Technology Management*, 41(3):52–8, 1998.

[112] Anderson, P. and Tushman, M.L. Technological Discontinuities and Dominant Designs: a cyclical model of technological change. *Administrative Science Quarterly*, 35:604–33, 1990.

[113] Robertson, T.S. The Process of Innovation and the Diffusion of Innovation. *Journal of Marketing*, 31:14–9, 1967.

[114] Yoon, E. and Lilien, G.L. New Industrial Product Performance: the effect of market characteristics and strategy. *Journal of Product Innovation Management*, 3:134–44, 1985.

[115] Moriarty, R.T. and Kosnik, T. High-Tech Concept, Continuity, and Change. *IEEE Engineering Management Review*, 3:25–35, 1990.

[116] Wheelwright, S.C. and Clark, K.B. *Revolutionizing Product Development*. Free Press, New York, 1992.

[117] Schmidt, J.B. and Calantone, R.J. Are Really New Product Development Projects Harder to Shut Down? *Journal of Product Innovation Management*, 15(2):111–23, 1998.

[118] Song, M.X. and Montoya-Weiss, M.M. Critical Development Activities for Really New Versus Incremental Products. *Journal of Product Innovation Management*, 15(2):124–35, 1998.

[119] Kleinschmidt, E.J. and Cooper, R.G. The Impact of Product Innovativeness on Performance. *Journal of Product Innovation Management*, 8:240–51, 1991.

[120] Rothwell, R. and Gardiner, P. Reinnovation and Robust Designs: producer and user benefits. *Journal of Marketing Management*, 3(3):372–87, 1988.

[121] Normann, R. Organizational Innovativness: product variation, and reorientation. *Administrative Science Quarterly*, 16:203–15, 1971.

[122] Grossman, J.B. The Supreme Court and Social Change: a preliminary inquiry. *American Behavioral Scientist*, 13:535–51, 1970.

[123] Meyers, P.W. and Tucker, F.G. Defining Roles for Logistics During Routine and Radical Technological Innovation. *Journal of Academy of Marketing Science*, 17(1):73–82, 1989.

[124] Freeman, C. Critical Survey: The Economics of Technical Change. *Journal of Economics*, 18(5):463–514, 1994.

[125] Chandy, R.K. and Tellis, G.J. The Incumbent's Curse: Incumbency, Size and Radical Product Innovation. *Journal of Marketing*, 64:1–17, 2000.

[126] Balachandra, R. and Friar, J.H. Factors in Success in R&D Projects and New Product Innovation: a contextual framework. *IEEE Transactions on Engineering Management*, 44:176–87, 1997.

[127] Atuahene-Gima, K. An Exploratory Analysis of the Impact of Market Orientation on New Product Performance: a contingency approach. *Journal of Product Innovation Management*, 12:275–93, 1995.

[128] Lee, M. and Na, D. Determinants of Technical Success in Product Development When Innovative Radicalness is Considered. *Journal of Product Innovation Management*, 11:62–8, 1994.

[129] Schumpeter, J.A. *The Theory of Economic Development.* Harvard University Press, Cambridge, 1934.

[130] Stobaugh, R. *Innovation, and Competition: the global managment of petrochemcial products.* Harvard Business School Press, Boston, 1988.

VITA

Travis Danner was born in Rockledge, Florida. He is the son of an Air Force pilot and grandson of an Air Force navigator. He spent his early childhood living on or near Air Force Bases and his teenage years working on his family's farm in East Tennessee. He studied mechanical and aerospace engineering at the University of Tennessee, Knoxville (BS, 2000, *summa cum laude*). He continued his education at Georgia Tech where he received a Master's Degree in Aerospace Engineering in December of 2001 and will receive his Doctorate in August of 2006.

Travis's professional interest is in the innovation, both invention and marketing, of renewable energy technologies. He is a co-founder of PetroGreen, LLC., which is currently focused on improving the economic viability of bio-fuels production.